VOL. 700 NOS. 1 + 2 12 MAY 1995
COMPLETE IN ONE ISSUE

3rd International Symposium on Capillary Electrophoresis York, 24–26 August 1994

JOURNAL OF CHROMATOGRAPHY A

INCLUDING ELECTROPHORESIS AND OTHER SEPARATION METHODS

ELSEVIER

JOURNAL OF CHROMATOGRAPHY A

INCLUDING ELECTROPHORESIS AND OTHER SEPARATION METHODS

Scope. The *Journal of Chromatography A* publishes papers on all aspects of **chromatography, electrophoresis** and related methods. Contributions consist mainly of research papers dealing with chromatographic theory, instrumental developments and their applications. In the *Symposium volumes*, which are under separate editorship, proceedings of symposia on chromatography, electrophoresis and related methods are published. *Journal of Chromatography B: Biomedical Applications* —This journal, which is under separate editorship, deals with the following aspects: developments in and applications of chromatographic and electrophoretic techniques related to clinical diagnosis or alterations during medical treatment; screening and profiling of body fluids or tissues related to the analysis of active substances and to metabolic disorders; drug level monitoring and pharmacokinetic studies; clinical toxicology; forensic medicine; veterinary medicine; occupational medicine; results from basic medical research with direct consequences in clinical practice.

Submission of Papers. The preferred medium of submission is on disk with accompanying manuscript (see *Electronic manuscripts* in the Instructions to Authors, which can be obtained from the publisher, Elsevier Science B.V., P.O. Box 330, 1000 AH Amsterdam, Netherlands). Manuscripts (in English; *four* copies are required) should be submitted to: Editorial Office of *Journal of Chromatography A*, P.O. Box 681, 1000 AR Amsterdam, Netherlands, Telefax (+31-20) 485 2304, or to: The Editor of *Journal of Chromatography B: Biomedical Applications*, P.O. Box 681, 1000 AR Amsterdam, Netherlands. Review articles are invited or proposed in writing to the Editors who welcome suggestions for subjects. An outline of the proposed review should first be forwarded to the Editors for preliminary discussion prior to preparation. Submission of an article is understood to imply that the article is original and unpublished and is not being considered for publication elsewhere. For copyright regulations, see below.

Publication information. *Journal of Chromatography A* (ISSN 0021-9673): for 1995 Vols. 683–714 are scheduled for publication. *Journal of Chromatography B: Biomedical Applications* (ISSN 0378-4347): for 1995 Vols. 663–674 are scheduled for publication. Subscription prices for *Journal of Chromatography A*, *Journal of Chromatography B: Biomedical Applications* or a combined subscription are available upon request from the publisher. Subscriptions are accepted on a prepaid basis only and are entered on a calendar year basis. Issues are sent by surface mail except to the following countries where air delivery via SAL is ensured: Argentina, Australia, Brazil, Canada, China, Hong Kong, India, Israel, Japan, Malaysia, Mexico, New Zealand, Pakistan, Singapore, South Africa, South Korea, Taiwan, Thailand, USA. For all other countries airmail rates are available upon request. Claims for missing issues must be made within six months of our publication (mailing) date. Please address all your requests regarding orders and subscription queries to: Elsevier Science B.V., Journal Department, P.O. Box 211, 1000 AE Amsterdam, Netherlands. Tel.: (+31-20) 485 3642; Fax: (+31-20) 485 3598. Customers in the USA and Canada wishing information on this and other Elsevier journals, please contact Journal Information Center, Elsevier Science Inc., 655 Avenue of the Americas, New York, NY 10010, USA, Tel. (+1-212) 633 3750, Telefax (+1-212) 633 3764.

Abstracts/Contents Lists published in Analytical Abstracts, Biochemical Abstracts, Biological Abstracts, Chemical Abstracts, Chemical Titles, Chromatography Abstracts, Current Awareness in Biological Sciences (CABS), Current Contents/Life Sciences, Current Contents/Physical, Chemical & Earth Sciences, Deep-Sea Research/Part B: Oceanographic Literature Review, Excerpta Medica, Index Medicus, Mass Spectrometry Bulletin, PASCAL-CNRS, Referativnyi Zhurnal, Research Alert and Science Citation Index.

US Mailing Notice. *Journal of Chromatography A* (ISSN 0021-9673) is published weekly (total 52 issues) by Elsevier Science B.V., (Sara Burgerhartstraat 25, P.O. Box 211, 1000 AE Amsterdam, Netherlands). Annual subscription price in the USA US$ 5389.00 (US$ price valid in North, Central and South America only) including air speed delivery. Second class postage paid at Jamaica, NY 11431. **USA POSTMASTERS**: Send address changes to *Journal of Chromatography A*, Publications Expediting, Inc., 200 Meacham Avenue, Elmont, NY 11003. Airfreight and mailing in the USA by Publications Expediting.

See inside back cover for Publication Schedule. Information for Authors and information on Advertisements.

0021-9673/95/$09.50

Printed in the Netherlands

JOURNAL OF CHROMATOGRAPHY A

VOL. 700 (1995)

JOURNAL OF CHROMATOGRAPHY A

INCLUDING ELECTROPHORESIS AND OTHER SEPARATION METHODS

ELSEVIER

Amsterdam – Lausanne – New York – Oxford – Shannon – Tokyo

0021-9673/95/$09.50

Printed in the Netherlands

SYMPOSIUM VOLUME

YORK MINSTER.

3rd INTERNATIONAL SYMPOSIUM ON CAPILLARY ELECTROPHORESIS

York (UK), 24–26 August 1994

Guest Editors

D.M. GOODALL
(York, UK)

T. THRELFALL
(York, UK)

VOL. 700, NOS. 1 + 2 JOURNAL OF CHROMATOGRAPHY A 12 MAY 1995

CONTENTS

(Abstracts/Contents Lists published in Analytical Abstracts, Biochemical Abstracts, Biological Abstracts, Chemical Abstracts, Chemical Titles, Chromatography Abstracts, Current Awareness in Biological Sciences (CABS), Current Contents/Life Sciences, Current Contents/Physical, Chemical & Earth Sciences, Deep-Sea Research/Part B: Oceanographic Literature Review, Excerpta Medica, Index Medicus, Mass Spectrometry Bulletin, PASCAL-CNRS, Referativnyi Zhurnal, Research Alert and Science Citation Index)

3RD INTERNATIONAL SYMPOSIUM ON CAPILLARY ELECTROPHORESIS, YORK, 24–26 AUGUST 1994

TECHNIQUES AND GENERAL

CHIRAL SEPARATIONS

AMINO ACIDS, PEPTIDES, PROTEINS

ELSEVIER

Journal of Chromatography A, 700 (1995) IX

JOURNAL OF CHROMATOGRAPHY A

Preface

The 3rd International Symposium on Capillary Electrophoresis, organised by the Chromatographic Society, the British Electrophoresis Society and the University of York, was held in York, 24–26 August, 1994.

The meeting took place at the University of York and was the first major event to be held in the new Exhibition Centre. The Welcome Reception and Buffet was held in the Victorian and Edwardian Streets of The Castle Museum whilst the Symposium Dinner was held in The Merchant Taylors' Hall; the guild and the hall both date back to the 14th Century. The delegates were thus introduced to the history of the City. Approximately 150 participants were present, 13 oral presentations and 71 posters were given and exhibits of capillary electrophoresis instrumentation and supplies were shown by 8 companies. The high quality of the presentations, the compact site for poster exhibition and lectures and the informal atmosphere of the meeting all contributed to the success of the symposium.

I should like to express my thanks to fellow members of the Scientific Committee: Dr. Chris Bevan (Glaxo Research and Development); Dr. Brian Clark (School of Pharmacy, University of Bradford), Dr. Michael Dunn (National Heart and Lung Institute), Professor Werner Kuhr (University of California, Riverside), Dr. David Lloyd (McGill University), Dr. David Perrett (St. Bartholomew's Medical College), and Dr. Stephen Wren (Zeneca Pharmaceuticals). Terry Threlfall and Jean Scott deserve special thanks for all their work as symposium manager and symposium secretary, respectively. I am also grateful to Professor Zdenek Deyl for organising and editing this volume.

Support for the symposium is gratefully acknowledged from the following companies: Beckman Instruments, Elsevier, Glaxo Research and Development, Wyeth Research (UK) and Zeneca.

We look forward to the 4th International Symposium on Capillary Electrophoresis, which will be held in York, 21–23 August, 1996.

York, UK DAVID M. GOODALL

SSDI 0021-9673(95)00424-6

ELSEVIER

Journal of Chromatography A, 700 (1995) 1–7

JOURNAL OF CHROMATOGRAPHY A

Appropriate calibration functions for capillary electrophoresis I. Precision and sensitivity using peak areas and heights

Hermann Wätzig

Institute of Pharmacy and Food Chemistry, University of Würzburg, Am Hubland, D-97074 Würzburg, Germany

Abstract

Calibration functions for CE can be calculated by using peak heights or areas. The relationship between peak heights and concentrations is non-linear, but can well be approximated by a parabolic function. The precision of peak heights is often better than of areas. However, the sensitivity of the calibration function decreases at higher concentrations. Thus calibration functions calculated by using areas lead to a better precision of the analytical result, which is estimated by the slope-normalized standard deviation.

1. Introduction

The use of capillary electrophoresis (CE) as a quantitative analytical technique is becoming more and more important [1–3]. Thus the choice of the appropriate calibration functions with respect to precision, accuracy and data collection shall be considered by using data sets of preceding works [4,5].

2. Experimental

The CE experiments were performed with P/ACE 2050 and 2100 systems (Beckman, Palo Alto, CA, USA).

The capillaries were from fused silica, their standard measure was 30 cm length (inlet to detector) × 50 mm I.D. Prior to their first use they were conditioned with 0.1 *M* NaOH for 30 min, heating to 50°C, and then equilibrated with running buffer for 40 min under the subsequent running conditions. Before each run the capillary was rinsed with the running buffer for 1 min. The thermostat was set to 25°C.

If not stated otherwise, chemicals were of analytical-reagent grade, supplied by Merck (Darmstadt, Germany).

Pyridine-2,4-dicarboxylic acid [5]: the wavelength of detection was 254 nm. It was injected by pressure, 5 s with 0.5 p.s.i. (=34.5 hPa). The separation voltage was 25 kV (33 μA, anode at the outlet buffer). Standard buffer citrate 60 m*M*, pH 3: 15 ml of a 60 m*M* (12.6084 g/l) solution of trisodium citrate (>99%; Riedel-de Haen) are filled up with a 60 mM solution (17.646 g/l) of citric acid to 100.0 ml.

N-Acetylcysteine [4]: the wavelength of detection was 214 nm. The samples were injected 4 s with 0.5 p.s.i. (=34.5 hPa). The separation potential was 20 kV. Borate buffer 90 m*M*, pH 8.55 with 5% polyethylenglycol 20000 (PEG; Hoechst, Germany; pharmacopoeia quality): 329 mg boric acid, 351 mg sodium tetraborate and 5000 mg PEG are dissolved in and diluted to 100.0 ml with HPLC-grade water (Millipore, Eschborn, Germany). Sample pretreatment:

0021-9673/95/$09.50
SSDI 0021-9673(95)00127-1

pharmaceutical formulations and standard substances were dissolved in degassed (ultrasonicated) HPLC-grade water. The solutions were immediately filled into sample vials and covered by a film of approximately 1 mm light mineral oil.

The program W_SA-statistics (see [6]) was partly used to evaluate the data sets shown in Figs. 1 and 2, and to calculate the data presented in Tables 1 and 2.

3. Results and discussion

The calibration data for N-acetylcysteine [4] and pyridine-2,4-dicarboxylic acid [5] are presented in Figs. 1 and 2, the corresponding electropherograms are shown in Figs. 3 and 4, respectively. In both cases the calibration function is a straight line, if corrected peak areas are used, but the function is curved when using peak heights. However, this curve can well be approximated by a parabola. This behavior of calibration functions is typical for CE.

When peak heights are used, the slope of the calibration function, that means its sensitivity, decreases at higher concentrations (Figs. 1 and 2, top). The standard deviation of analytical results [sdv(x)] is dependent on the standard deviation of measurements [sdv(y)], but also on the sensitivity of the calibration function (Fig. 5). This

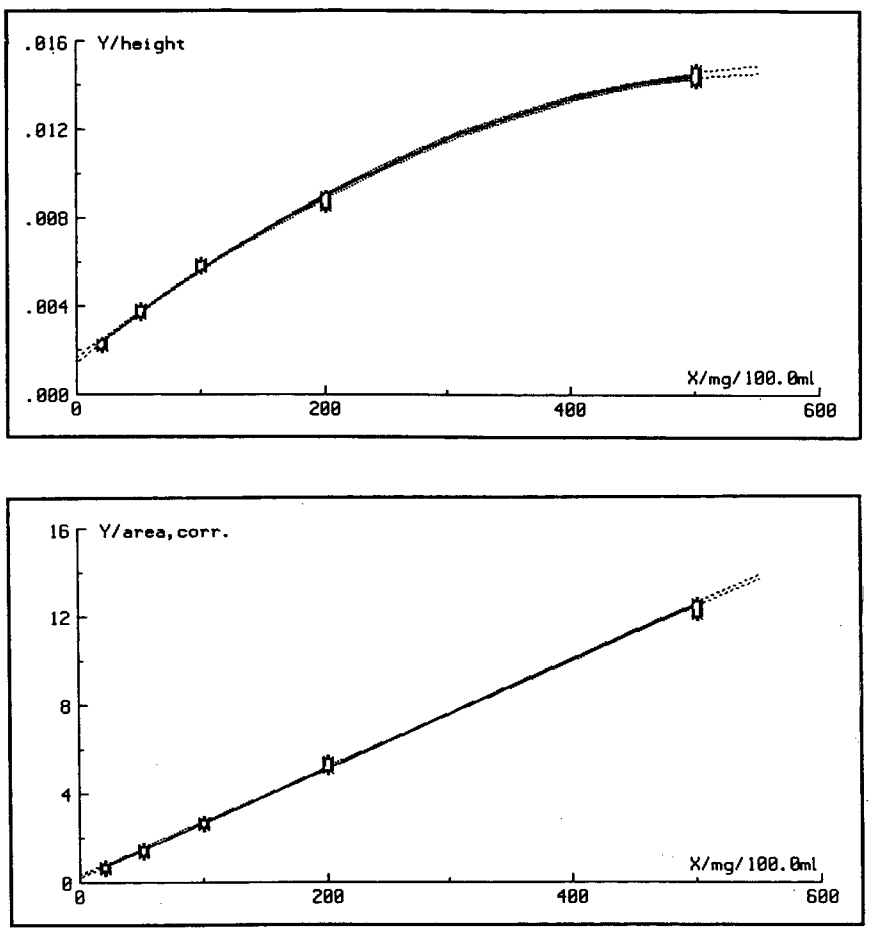

Fig. 1. Calibration functions of N-acetylcysteine ([4]; separation see Fig. 3). Peak heights (top) and corrected areas (bottom) were used. The data were taken from the same series, each concentration was measured eight times.

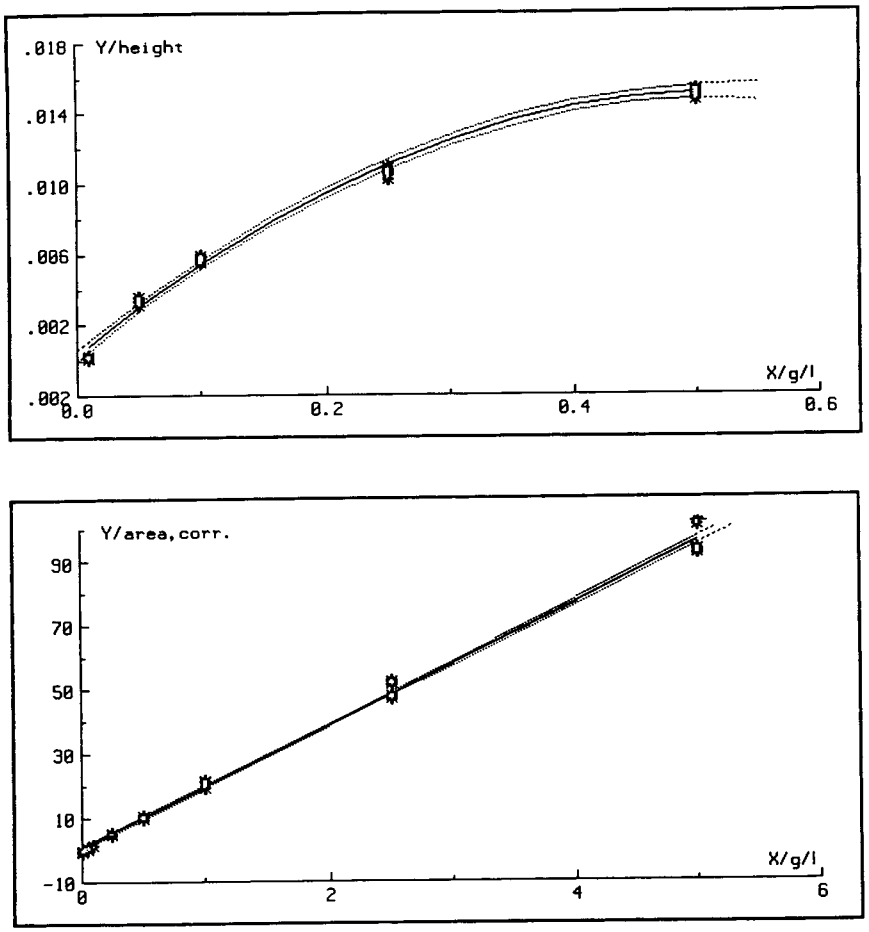

Fig. 2. Calibration functions of pyridine-2,4-dicarboxylic acid ([5]; separation see Fig. 4). Peak heights (top) and corrected areas (bottom) were used. The data was taken from the same series, each concentration was measured five times.

precision of the results, corresponding to sdv(x), can be calculated by error propagation of the reciprocal of the calibration function (see Appendix).

If possible, high sample concentrations should be used in CE to achieve optimal reproducibility [1,3,7]. However, at high sample concentrations the sensitivity of peak height calibrations is very low. Thus the relative standard deviation of the analytical result is much better, if peak area calibrations are used, although the standard deviation of peak heights may be lower (Tables 1 and 2). Therefore calibration functions using areas shall be preferred in most cases. There is only one exception: sometimes the determination of rather low sample concentrations cannot be avoided. In these cases the calibration curve of peak height may be sensitive enough, and the determination of peak heights may be more reproducible, because it is less influenced by integration errors than the determination of peak areas.

4. Conclusions

Peak areas shall be preferred to peak heights, when calibration functions are calculated in CE. These considerations are valid for other ana-

Table 1
Repeatability for the determination of N-acetylcysteine by CE.

	Concentration (mg/l)				
	205	513	1004	2010	5012
Peak height					
sdv(y) ($\times 10^{-5}$)	4.8	8.6	7.7	14.5	20.3
relsdv(y) (%)	2.1	2.2	1.3	1.6	1.4
dy/dx (10^{-6} l/mg)	4.3	4.1	3.7	3.0	0.7
sdv(x) (mg/l)	11.1	20.9	20.7	49.1	296.8
relsdv(x) (%)	5.40	4.08	2.06	2.44	5.92
Corrected peak area					
sdv(y)	0.05	0.055	0.036	0.104	0.168
relsdv(y) (%)	7.2	3.8	1.3	1.9	1.3
$dy/dx = a_1$ (10^{-3} l/mg)	2.4	2.4	2.4	2.4	2.4
sdv(x) (mg/l)	20.9	23.1	14.9	43.4	69.9
relsdv(x) (%)	10.2	4.5	1.5	2.2	1.4

Each concentration was measured eight times. The corresponding calibration functions are shown in Fig. 1, for calculations compare Appendix. rel = Relative.

Table 2
Repeatability for the determination of pyridine-2,4-dicarboxylic acid by CE.

	Concentration (mg/l)				
	10	50	100	250	500
Peak height					
sdv(y) ($\times 10^{-4}$)	0.5	1.7	1.5	2.9	2.1
relsdv(y) (%)	20.0	4.8	2.6	2.7	1.4
dy/dx (10^{-5} l/mg)	5.6	5.2	4.6	3.0	0.2
sdv(x) (mg/l)	0.9	3.3	3.3	9.7	105.0
relsdv(x) (%)	9.0	6.6	3.3	3.8	21.0
Corrected peak area					
sdv(y)	0.037	0.054	0.096	0.219	0.359
relsdv(y) (%)	48.9	5.9	4.8	3.9	3.4[a]
$dy/dx = a_1$ (10^{-3} l/mg)	21.6	21.6	21.6	21.6	21.6
sdv(x) (mg/l)	1.7	2.5	4.4	10.1	16.6
relsdv(x) (%)	17.0	5.0	4.4	4.0	3.3

Each concentration was measured five times. The corresponding calibration functions are shown in Fig. 2, for calculations compare Appendix and Table 1.
[a] Rather high sdv(y) compared to other measurement series.

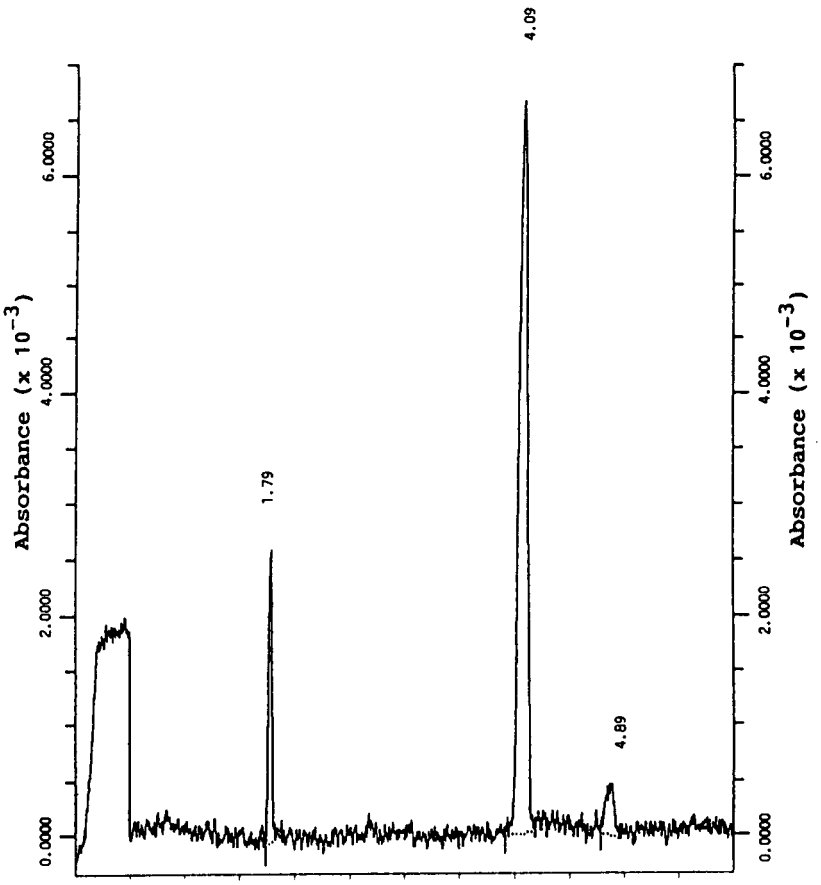

Fig. 3. Electropherogram of an aqueos solution of 1 g/l N-acetylcysteine. Migration order: acetanilide as marker of the endoosmotic flow: 1.79 min, N-acetylcysteine: 4.09 min, N,N-diacetylcystine: 4.89 min [4].

lytical techniques as well, if their characteristics of calibration and variance function are similar.

Appendix

Calculation of sdv(x)

The standard deviation of the analytical result is calculated by Eq. 1 [6,8,9]:

$$\mathrm{sdv}(x) = \frac{\mathrm{sdv}(y)}{\frac{\partial \mathrm{f}}{\partial x}} \sqrt{\frac{1}{n_\mathrm{a}} + \frac{1}{n_\mathrm{c}} + \frac{(x_\mathrm{a} - \bar{x}_\mathrm{c})^2}{S_{xx}}} \qquad (1)$$

where

$$S_{xx} = \sum_{i=1}^{n_\mathrm{c}} (x_i - \bar{x}_\mathrm{c})^2 \qquad (2)$$

and

$$x_\mathrm{a} = \frac{y_\mathrm{a} - \bar{y}_\mathrm{c}}{a_1} + \bar{x}_\mathrm{c} \qquad (3)$$

Thus x_a is the analytical result, estimated by the signal y_a. The value sdv(y) represents the standard deviation of the signal. $\partial \mathrm{f}/\partial x$ is the first derivative, that means the slope, of the calibration function f. The number n_a of measurements is used to obtain the mean y_a (n_a may

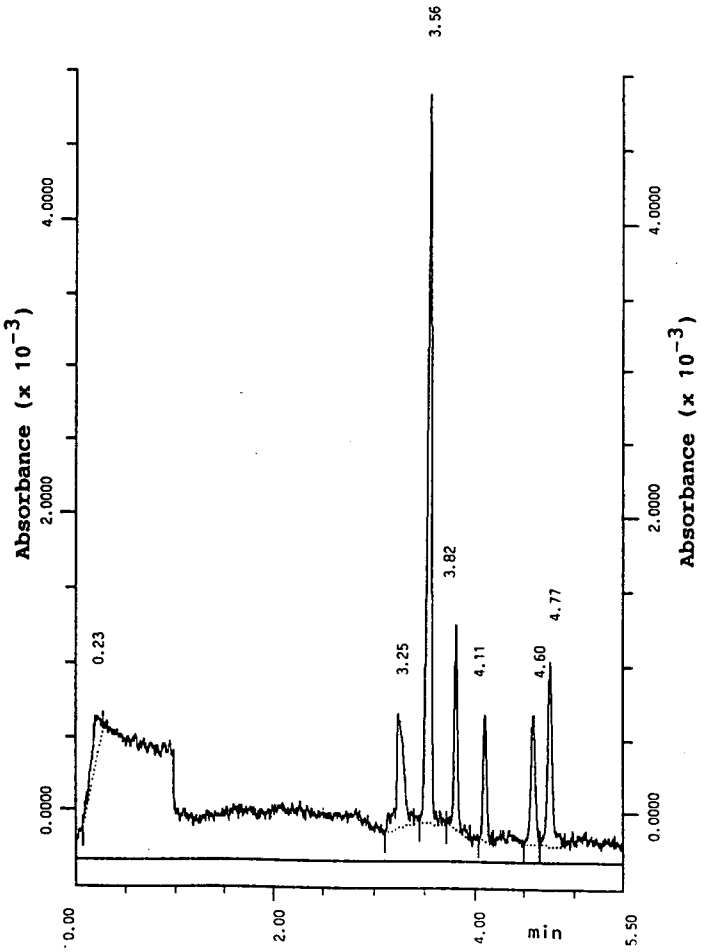

Fig. 4. Optimal separation of pyridine-dicarboxylic acids: citrate buffer pH 3.0, 60 m*M*. Sample concentration: 100 mg/l pyridine-2,4-dicarboxylic acid ($t_M = 3.56$ min), 20 mg/l for the added isomers. Elution order: pyridine-2,6; -2,4; -2,5; -2,3; -3,4 and -3,5-carboxylic acids [5].

equal 1), the number of measurements used to estimate the calibration function is called n_c.

A simplified formula (Eq. 4) may be used, because the value of the square root is close to unity and the same for calibrations using peak heights or areas. The relative standard deviation relsdv(x) is easily obtained from sdv(x) (Eq. 5):

$$\mathrm{sdv}(x) = \frac{\mathrm{sdv}(y)}{\frac{\partial \mathrm{f}}{\partial x}} \qquad (4)$$

$$\mathrm{relsdv}(x) = \frac{\mathrm{sdv}(x)}{x_a} \qquad (5)$$

The calculations for Table 1 are demonstrated in the following:

(1) Peak heights: the calibration function (Fig. 1) is:

$$\mathrm{f}(x) = a_0 + a_1 x + a_2 x^2$$

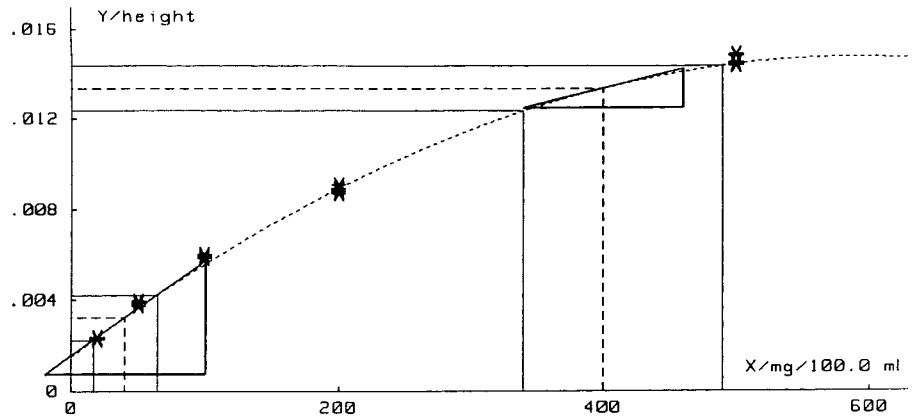

Fig. 5. The standard deviation of the analytical result [sdv(x)] is dependent on the standard deviation of the measurement [sdv(y)], but also on the sensitivity, that means the slope, of the calibration function. Same data as in Fig. 1 (top).

with $a_0 = 1.5 \cdot 10^{-3}$, $a_1 = 4.47 \cdot 10^{-6}$ l/mg and $a_2 = -3.78 \cdot 10^{-10}$ l^2/mg^2. Hence: $\partial f/\partial x = 4.47 \cdot 10^{-6}$ l/mg $- 7.56 \cdot 10^{-10}$ l^2/mg$^2 \cdot x$ for $x = 1004$ mg/l: $\partial f/\partial x = 3.714 \cdot 10^{-6}$ l/mg, thus:

$$\mathrm{sdv}(x) = \frac{\mathrm{sdv}(y)}{\frac{\partial f}{\partial x}} = \frac{7.67 \cdot 10^{-5}}{3.714 \cdot 10^{-6}\ \mathrm{l/mg}} = 20.65\ \mathrm{mg/l}$$

(2) Corrected peak areas: the calibration function is:

$$f(x) = a_0 + a_1 x$$

with $a_0 = 0.2686$ and $a_1 = 2.44 \cdot 10^{-3}$ l/mg. The first derivative is the slope of the calibration line, thus for $x = 1004$ mg/l:

$$\mathrm{sdv}(x) = \frac{\mathrm{sdv}(y)}{\frac{\partial f}{\partial x}} = \frac{3.63 \cdot 10^{-2}}{2.44 \cdot 10^{-3}\ \mathrm{l/mg}} = 14.87\ \mathrm{mg/l}.$$

Acknowledgements

The author wishes to thank Dr. C. Dette for his support.

References

[1] K.D. Altria, R.C. Harden, M. Hart, J. Hevizi, P.A. Hailey, J.V. Makwana and M.J. Portsmouth, *J. Chromatogr.*, 641 (1993) 147.
[2] J. Sadecka, J. Polonsky and H. Shintani, *Pharmazie*, 49 (1994) 631.
[3] H. Wätzig and C. Dette, *Pharmazie*, 49 (1994) 83.
[4] H. Wätzig and C. Dette, *Pharmazie*, 49 (1994) 656.
[5] H. Wätzig and C. Dette, *Pharmazie*, 48 (1993) 527.
[6] S. Ebel, *Würzburger Skripten zur Analytik, Reihe Statistik, Tl. 1-8*, Institut für Pharmazie und Lebensmittelchemie, Würzburg, 1992–1993.
[7] H. Wätzig and C. Dette, *J. Chromatogr.*, 636 (1993) 31.
[8] L. Sachs, *Angewandte Statistik*, Springer, Berlin, Heidelberg, 6th ed., 1984.
[9] J. Hartung, *Statistik*, Oldenbourg, Munich, 8th ed., 1991.

ELSEVIER

Journal of Chromatography A, 700 (1995) 9–20

JOURNAL OF CHROMATOGRAPHY A

Appropriate calibration functions for capillary electrophoresis II. Heteroscedasticity and its consequences

Knut Baumann[a], Hermann Wätzig[b,*]

[a]*Institute of Pharmacy, University of Berne, Baltzerstrasse 5, CH-3012 Berne, Switzerland*

[b]*Institute of Pharmacy and Food Chemistry, University of Würzburg, Am Hubland, D-97074 Würzburg, Germany*

Abstract

If ordinary least squares regression methods are to be used, the standard deviation of the signal should not depend on the sample concentration, but this is not true in CE. Results indicate, that the signal standard deviation is approximately proportional to the sample concentration. Therefore weighted least squares regression must be used, if the standard deviation within the concentration range differs by more than the factor 50. It is advised to use this regression method down to the factor 5, where the difference to ordinary least squares calculations is still significant. This is demonstrated by comparing experimental and simulated data. These considerations are valid for other analytical techniques as well, if their characteristics of calibration and variance function are similar.

1. Introduction

The use of capillary electrophoresis (CE) as a quantitative analytical technique is becoming more and more important [1–3]. Thus the choice of appropriate calibration functions must be considered. The importance of the sensitivity and its meaning for the precision was discussed in Part I [4]. The consequences of heteroscedasticity (dependence of the signal standard deviation on the sample concentration) shall be discussed by using data sets of preceding works [4,5] and simulations.

2. Experimental

The CE experiments were described in Part I [4] and [5].

2.1. Simulations

Each simulated data set consists of six equidistant blocks at position x_i. The values of x_i are given in the tables. Eight y values are determined for each block, leading to 48 data pairs. In a first step the y values are calculated by Eq. 1:

$$y_i = \alpha_0 + \alpha_1 x_i \quad (1)$$

Straight lines with a slope of $\alpha_1 = 1$ and an intercept of $\alpha_0 = 0$ were used for simplicity. In the second step normal distributed noise was added. Usually the standard deviation of this noise was chosen as 10% of the signal (Eq. 2):

$$y_i = y_i + 0.1 \cdot y_i \varepsilon_i \quad (2)$$

Here ε_i a normal distributed random variable with a standard deviation of 1 [6]. Thus ε_i can be positive or negative.

* Corresponding author.

0021-9673/95/$09.50
SSDI 0021-9673(95)00128-X

2.2. Weighted least squares algorithms

If the algorithm WLS/IV is used, the weighting factor w_i is defined as the inverse of the variance of y_i[var(y_i); Eq. 3]. In case of heteroscedasticity this variance depends on the position x_i of the data pair. Thus var(y_i) is defined as the variance of all y_i with identical x_i. Several data pairs with identical x_i must be available to estimate these weights [7–10].

$$w_i = \frac{1}{\mathrm{var}(y_i)} \tag{3}$$

The data of the weighted centroid ($\bar{x}_c$,$\bar{y}_c$) as well as of the slope a_1 are then obtained by the Eqs. 4–6:

$$\bar{x}_c = \frac{\sum_{i=1}^{n} w_i x_i}{\sum_{i=1}^{n} w_i} \tag{4}$$

$$\bar{y}_c = \frac{\sum_{i=1}^{n} w_i y_i}{\sum_{i=1}^{n} w_i} \tag{5}$$

$$a_1 = \frac{\sum w_i \sum w_i x_i y_i - \sum w_i x_i \sum w_i y_i}{\sum w_i \sum w_i x_i^2 - \left(\sum w_i x_i\right)^2} \tag{6}$$

The intercept a_0 can be calculated by Eq. 7:

$$a_0 = \bar{y}_c - a_1 \bar{x}_c \tag{7}$$

The further developed algorithm GLS/VFE [7,8] is outlined in the following:

(1) Start with a preliminary estimation of the regression parameters by OLS regression (Eqs. 4–6, all $w_i = 1$). Set variance parameter $\Theta = 0$.

(2) Calculate sdv(y):

$$\mathrm{var}(y) = \frac{1}{n} \cdot \sum_{i=1}^{n} \frac{[y_i - \hat{y}(x_i)]^2}{\hat{y}(x_i)^{2\Theta}} \tag{8}$$

Here $\hat{y}(x)$ is the linear regression function, thus

$$\hat{y}(x_i) = \bar{y}_c + a_1(x_i - \bar{x}_c) \tag{9}$$

The standard deviation sdv(y) is simply the square root of var(y).

(3) The pseudo-maximum likelihood L is estimated using Eq. 10 [11]:

$$L = -n \log[\mathrm{sdv}(y)] - \sum_{i=1}^{n} \log[\hat{y}(x_i)^{\Theta}] \tag{10}$$

L is maximized by variation of Θ in the range between −0.3 and 1.5. The step width begins with 0.01, the interval where the highest L are found is further examined in steps of 0.001. Note that sdv(y) depends on Θ. For each calculation sdv(y) is again calculated using Eq. 8.

(4) Calculate new weights (Eq. 11); use Θ of maximized L:

$$w_i = \frac{1}{\hat{y}(x_i)^{2\Theta}} \tag{11}$$

Note that GLS/VFE can estimate weights without having several data pairs (x_i,y_i) with identical x_i.

(5) Estimate new regression parameters by Eqs. 4–6 using the new weights. Estimate variance of this iteration step k by Eq. 12; this time the loss in the degrees of freedom is considered:

$$\mathrm{var}(y)_k = \frac{1}{n-2} \cdot \sum_{i=1}^{n} \frac{[y_i - \hat{y}(x_i)]^2}{\hat{y}(x_i)^{2\Theta}} \tag{12}$$

EXIT IF condition 13 holds true:

$$\frac{\mathrm{var}(y)_{k-1}}{\mathrm{var}(y)_k} < 1.05 \tag{13}$$

ELSE continue with step 2.

3. Results and discussion

3.1. The limitations of OLS regression for heteroscedastic CE calibration data

Calibration lines are usually calculated by ordinary least squares (OLS) regressions. Actually the use of OLS calculations should be restricted to cases, where the signal standard deviation is independent of the signal itself (homoscedasticity). A systematic error occurs, if heteroscedastic calibration data are evaluated by using OLS regressions. This error can be avoided by using weighted least squares (WLS) regressions [7,8,10–12], compare Experimental).

It is well known that calibration data are heteroscedastic in CE. This does not cause problems, if the concentration range is small. In this case statistical tests will fail to prove heteroscedasticity, and the systematic error will remain insignificant. If the expected concentration is rather well known, the use of the external standard evaluation is an interesting alternative [13].

However, there are cases where one wants to calibrate over a concentration range of one order of magnitude or more, e.g. if drug concentrations in urine or other body fluids shall be investigated. Here it is important to consider the magnitude of the systematic error that will occur by ignoring heteroscedasticity and using OLS estimations. Therefore calibration functions were calculated by using OLS and WLS for the same set of data. The results in Fig. 1 demonstrate that there is a clear difference between these methods. It is also well known from statistical theory that WLS gives the better estimation. However, the difference between the calibration functions still does not reveal the magnitude of the systematic error that is made by OLS regression. The line estimated by WLS could be a very good approximation of the true relationship. In this case the whole difference observed would be caused by the systematic error using OLS calculations. However, both lines are influenced by random error. Thus both deviate from the true relationship. If they deviate to different sides, the difference between them could become very large, although their deviation from the true relationship would be similar.

The true relationship is never known when experimental data are considered. Thus simulated sets of data must be used to clarify the amount of error made by OLS estimations. Here the true relationship is known by definition. The simulated data sets must be designed with similar properties like real CE calibration data.

3.2. Properties of CE calibration data

The linear relationship between sample concentration and peak area is well known in CE. However, although the dependence of the signal standard deviation on the sample concentration was recognized, this dependence was never systematically investigated. Thus the degree of heteroscedasticity for typical CE calibration data was unknown. The signal standard deviation is approximately proportional to the signal itself for the data set shown in Fig. 1 (Fig. 2). A

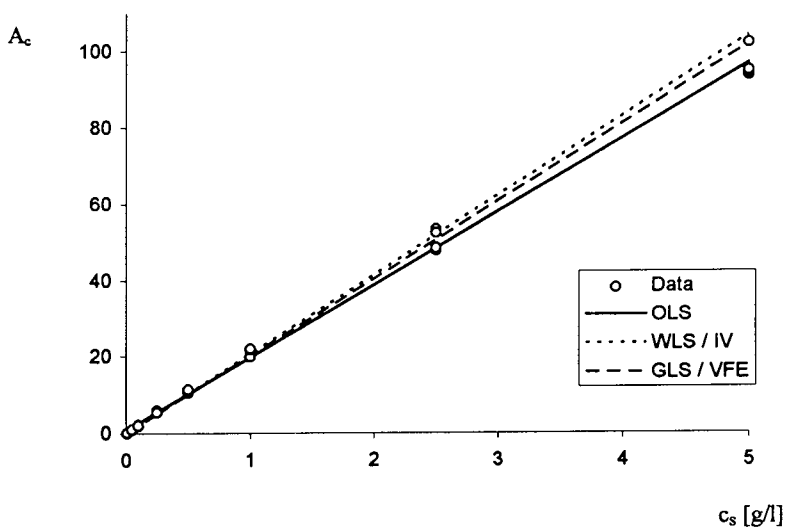

Fig. 1. Significant difference of regression lines, calculated using weighted least squares (GLS/VFE, WLS/IV) and ordinary least squares (OLS). Same data as in Fig. 2 of Part I [4] were used.

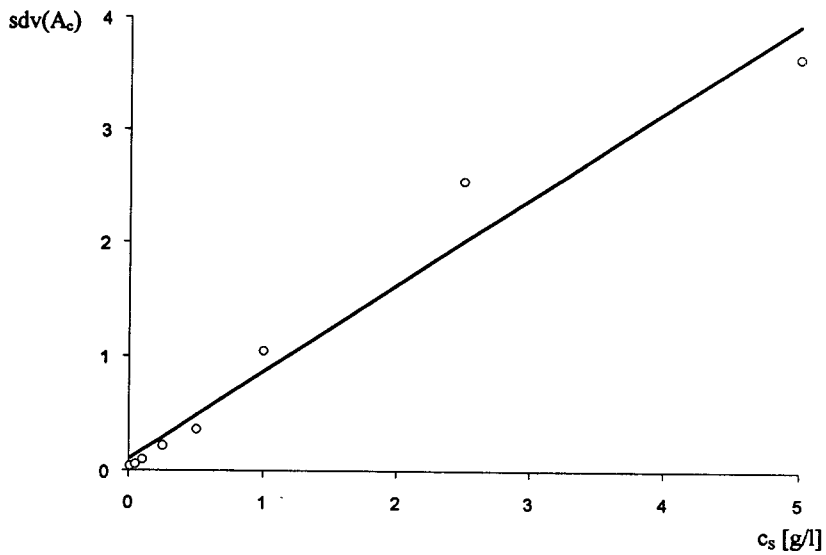

Fig. 2. Relationship between concentration and signal standard deviation for the data set presented in Fig. 1.

significant increase of the standard deviation with concentration was observed for other CE calibrations as well [5,14]. In these cases the standard deviation was a bit slower increasing than the signal, thus the relative standard deviation decreased with higher concentration.

The characteristics of the variance function are not only important for the following simulation experiments, but can also be used to estimate the contribution of different error sources to the total error in CE. Detection, integration, injection, dilution, weighting of substances and changing migration times from run to run are considered to be the main error sources in CE.

The error function for UV detection is well known [15–17]. After passing a minimum the detection error increases stronger than linear with the concentration (Eq. 14):

$$\text{relsdv}(A) = k \cdot \sqrt{1 + 10^{2A}} \qquad (14)$$

Here A is the absorbance. The constant factor k depends on the transmission of the reference solution and on its standard deviation.

The integration error of the considered data set can be neglected. The proper estimation of the baseline was visually controlled for all electropherograms. A few electropherograms at low concentrations had to be reintegrated.

The error is proportional to the sample concentration for injection, dilution and variation of migration times. For example, if a volume of 1 nl is injected with a standard deviation of 0.01 nl, the injected amount will be 1 ng and its standard deviation 10 pg, if a concentration of 1 g/l is injected, but only 10 pg with a standard deviation of 0.1 pg, if 10 mg/l are injected.

These errors, that are proportional to the concentration, seem to contribute the most to the total error. The detection error seems to have less influence.

There is another interesting consequence of this observed linearity of the variance function. The ratio of the standard deviations at the highest and the lowest concentration within the working range (R_{sdv}; Eq. 15) can be estimated from the ratio of the highest to the lowest concentration used for the calibration prior to the experiment. This is an important help to plan CE calibration experiments and evaluations.

$$R_{sdv} = \frac{sdv(y_{x=max})}{sdv(y_{x=min})} \quad (15)$$

3.3. Design of the simulation experiments

These simulations were designed to investigate the consequences of heteroscedasticity in general. Thus a linear functional relationship between x and y was simulated (Eq. 1). In CE x and y correspond to the sample concentration and the obtained signal, e.g. the peak area, respectively.

For simplicity the intercept α_0 was always chosen as 0, the slope α_1 as 1. Other parameters do not change the results. These are only influenced by the signal-to-noise ratio and the increase of the standard deviation with concentration.

The relationship between standard deviation $sdv(y)$ and x was also chosen linear for these simulations (Eq. 2). This was the strongest increase of the standard deviation so far observed in CE. The stronger this increase, the higher the systematic errors by using OLS. Thus these simulation demonstrate the systematic errors that must be expected in the worst case possible.

3.4. Performance of difference regression algorithms

The quality of a WLS regression depends on the knowledge about the variance function. The results are best, if the variances $var(y_i)$ are known. Thus the proper estimation of the variance function is very important. A number of different algorithms were designed for this purpose (reviewed in [7,8]). Mainly the two WLS algorithms WLS/IV and GLS/VFE were tested and compared to ordinary least squares (OLS) regression in this work.

Other algorithms, e.g. robust regression algorithms ([18,19]; cited in [20]), were considered in pilot studies. These algorithms also use weighting but to distinguish outliers from data belonging to the calibration set. They are very effective in doing this: their breakdown point is 50% outliers. These algorithms showed some slight advantages compared to OLS. However, they were by far inferior to the two mainly considered WLS algorithms. The calculation of robust regressions is very time-consuming. Thus it was decided not to include them in the main investigations.

The simple WLS/IV just uses inverse variances as weighting factors w_i (Eq. 3). The calculation of the regression parameters is analogous to OLS (Eqs. 4–6). However, the variance of a random sample is a disputable estimator for the variance of the whole set [11,12,21]. Even if the standard deviation is simulated as proportional to the signal, the standard deviation of a random sample corresponding to lower signals can be higher than at higher signals, caused by random errors. Thus the use of inverse variances as weighting factors can be misleading [8].

A further developed algorithm GLS/VFE (generalized least squares using variance function estimation) was recommended in preceding works [7,8]. The difficulty of estimating the variance is overcome by an iteration, where regression parameters and the variance function can be determined at the same time. The variance function is the dependence between signal y and the variance of the signal $var(y)$. This can often be expressed by Eq. 16.

$$var(y) = \sigma^2 y^{2\Theta} \quad (16)$$

Here σ^2 is the variance $var(y)$ at $y = 1$, and the variance parameter Θ represents the degree of heteroscedasticity. If Θ equals 0, then the variance is constant (homoscedasticity). If Θ equals 1, then the standard deviation of the signal is proportional to the signal itself. The algorithms WLS/IV and GLS/VFE were compared to WLS/SV (weighted least squares using simulated variances). Here the inverse of the known variances from the simulation procedure were used as weighting factors. The regression parameters were again calculated using Eqs. 4–6.

WLS/SV cannot be used in practice, because the true variance function is always unknown for experimental data. However, the error in es-

timating the simulated regression parameters is only caused by the random scatter of the simulation data, if this algorithm is used. The systematic error by erroneous estimation of the variances is avoided by using the true ones. Thus WLS/SV offers a possibility to recognize the amount of error which is caused by inprecise estimation of the variance function using other algorithms.

Some error measures were defined to quantify the systematic error that must be expected for the different algorithms in dependence on the ratio R_{sdv}. The mean squared error (MSE, Eq. 17) is a good measure for the average error that is caused by the estimation of the calibration function [7,11,12,22].

$$\mathrm{MSE} = \sum_{i=1}^{n} [(\alpha_0 + \alpha_1 x_i) - (a_0 + a_1 x_i)]^2 \qquad (17)$$

Here a_0 and a_1 are intercept and slope of the calibration function, α_0 and α_1 are the corresponding parameters of the simulated true function.

The true x values x_0 for a given y are known from the parameters of the simulated function (Eq. 18). The difference between the x value x_{estm} estimated using the calibration function (Eq. 19) and x_0 is a measure for the total error Err caused by the calibration function (Eq. 20, compare Fig. 3). This total error consists of the random error within the data pairs used for the calibration and the systematic error caused by incorrect weighting. Errors are considered at the lowest concentration (Err_{low}) and the highest concentration (Err_{hi}) used for the calibration.

$$x_0 = \frac{y - \alpha_0}{\alpha_1} \qquad (18)$$

$$x_{estm} = \frac{y - a_0}{a_1} \qquad (19)$$

$$\mathrm{Err} = \frac{|x_{estm} - x_0|}{x_0} \qquad (20)$$

The data in Table 1 show, that there is a big difference in performance between the different algorithms. The strongest distinction is observed for the systematic error at the lowest concentration, Err_{low}. This can be understood by looking at Fig. 4: if no weights are used, the data at high concentrations are given too much weight. Wrong estimations at high concentrations work like a lever and lead to a considerable systematic error at low concentrations.

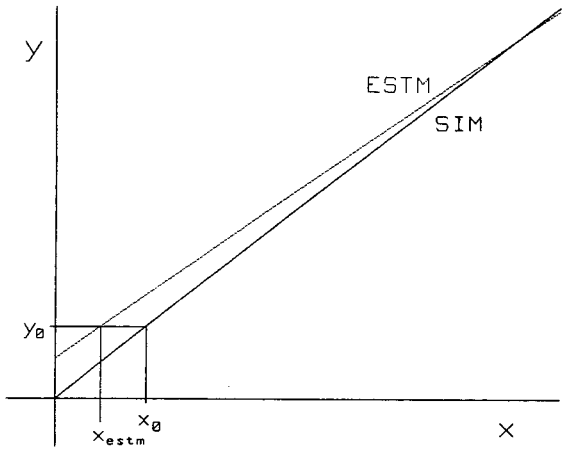

Fig. 3. Determination of the parameters x_0 (Eq. 18) and x_{estm} (Eq. 19), which are needed to estimate the error Err (Eq. 20) caused by the estimated calibration function ESTM at different x. The plain line represents the simulated function SIM. Especially at low x values the Err_{low} is strongly influenced by the error of the calibration function.

The error at low concentrations Err_{low} in dependence on R_{sdv} is the most important aspect of these investigations. The choice of the position of the x_i other than equidistant or of Θ other than 1 has only very minor effects [compare differences between sections (a) in Tables 1 and 2 as well as between sections (b) in Tables 1 and 2]. The results are independent of the signal-to-noise ratio [sdv(y)/y] used in the simulations.

This relationship between Err_{low} and R_{sdv} is presented in Table 3. If R_{sdv} equals 50, the error is increased by more than 10 fold, if OLS regression is used. Here the error caused by the wrong estimation of the calibration function is more than 3-fold compared to the random error at low concentrations [section (e) in Table 1, 0.33 compared to 0.1]. The error Err_{low} of OLS regressions is still more than 1.5-fold higher than of GLS/VFE, if R_{sdv} equals 5. The average error caused by the OLS estimation of the calibration

Table 1
Differences in errors for various R_{sdv}, if different regression algorithms are used

	Err_{low}	Err_{hi}	MSE
(a) $R_{sdv} = 2$, $x_i = 15, 18, 21, 24, 27, 30$			
WLS/SV	0.02321	0.01822	0.2067
GLS/VFE	0.02337	0.01840	0.2010
WLS/IV	0.02475	0.02001	0.2514
OLS	0.02456	0.01912	0.2235
Normalized to GLS/VFE			
WLS/SV	0.9929	0.9905	0.9865
GLS/VFE	1	1	1
WLS/IV	1.0587	1.0879	1.1997
OLS	1.0507	1.0395	1.0664
(b) $R_{sdv} = 3.16$, $x_i = 15.0, 21.5, 28.0, 34.4, 40.1, 47.4$			
WLS/SV	0.02487	0.01678	0.4071
GLS/VFE	0.02494	0.01690	0.4089
WLS/IV	0.02626	0.01844	0.4993
OLS	0.03071	0.01848	0.4852
Normalized to GLS/VFE			
WLS/SV	0.99972	0.9932	0.9957
GLS/VFE	1	1	1
WLS/IV	1.0533	1.0919	1.2210
OLS	1.2316	1.0934	1.1866
(c) $R_{sdv} = 5$, $x_i = 15, 27, 39, 51, 63, 75$			
WLS/SV	0.02621	0.01512	0.7823
GLS/VFE	0.02656	0.01533	0.7968
WLS/IV	0.02772	0.01693	0.9747
OLS	0.04187	0.01786	1.0560
Normalized to GLS/VFE			
WLS/SV	0.9870	0.9866	0.9818
GLS/VFE	1	1	1
WLS/IV	1.0435	1.1045	1.2232
OLS	1.5763	1.1652	1.3253
(d) $R_{sdv} = 10$, $x_i = 15, 42, 69, 96, 123, 150$			
WLS/SV	0.02774	0.01457	2.723
GLS/VFE	0.02780	0.01474	2.798
WLS/IV	0.02825	0.01625	3.426
OLS	0.07322	0.01787	4.081
Normalized to GLS/VFE			
WLS/SV	0.9980	0.9884	0.9733
GLS/VFE	1	1	1
WLS/IV	1.0163	1.1028	1.2245
OLS	2.6343	1.2123	1.4586
(e) $R_{sdv} = 50$, $x_i = 15, 162, 309, 459, 603, 750$			
WLS/SV	0.02841	0.01294	54.00
GLS/VFE	0.02841	0.01297	54.37
WLS/IV	0.02848	0.01447	68.47
OLS	0.33258	0.01740	95.10

(Continued on p. 16)

Table 1 (*continued*)

	Err_{low}	Err_{hi}	MSE
Normalized to GLS/VFE			
WLS/SV	1.0000	0.9976	0.9932
GLS/VFE	1	1	1
WLS/IV	1.0012	1.1150	1.2594
OLS	11.7056	1.3409	1.7492

Number of data sets simulated for each condition: 2000. Each set consists of six equidistant blocks x_i of y-values ($n = 48$ data pairs). First all y get the value of their x_i (corresponds to a straight line with $\alpha_0 = 0$ and $\alpha_1 = 1$), then normal distributed noise is added ([6]; see Experimental). The standard deviation sdv of the noise is 0.1 (10%) of the corresponding signal y. The noise is simulated proportional to signal, that means $\Theta = 1$.

function equals 0.0419 [section (c) in Table 1]. However, this error will be the double in a number of cases. Thus this error cannot be neglected compared to 0.1 random noise.

These investigations demonstrate the high performance of the algorithm GLS/VFE. The systematic errors caused by this algorithm are negligible, as can be seen from comparison to WLS/SV.

Table 4 offers a surprise in the first place. All regression parameters are the same, if only two concentrations are used for the calibration (2-point calibration). The systematic error by over-estimation of high concentrations using OLS cannot take place. Thus Err_{low} remains small, even if OLS is used. However, the use of a 2-point calibration for a concentration range of one order of magnitude or more causes problems, too. It must be validated, whether the method is really linear over some orders of magnitude, and the used statistical tests must be applicable in case of heteroscedasticity.

4. Conclusions

Weighted least squares regression (WLS) methods are superior to ordinary least squares (OLS) methods. If the ratio of standard deviations within the concentration range R_{sdv} exceeds 5, the additional error by using OLS cannot be neglected; if R_{sdv} exceeds 50, the use of WLS is mandatory. However, it is advisable to use WLS for smaller R_{sdv} as well. The difference between OLS and WLS is less, but was found significant down to an R_{sdv} of 3, which is consistent to previous results [7]. Moreover results can never get worse using WLS.

In CE the error is approximately linear to the concentration. Thus the expected R_{sdv} can be estimated from the ratio of the highest and the lowest concentration. Therefore it is possible to decide if WLS will be necessary before the calibration is started.

WLS is best if the weights are known. In this work two methods to estimate weighting factors were investigated. The further developed algorithm GLS/VFE [7,8] is beneficial compared to WLS/IV for a number of reasons. It is slightly better in estimating the true regression coefficients, and it can be applied to all possible sets of data, whilst WLS/IV needs several values y_i with identical x_i to calculate the weights. Moreover, it is not possible to estimate the variance function properly, if the simpler WLS/IV is used. Thus confidence intervals cannot be calculated correctly, and the uncertainty of the calibration function can only be roughly estimated. Therefore the error of the analytical result is less precisely obtained. GLS/VFE can be easily implemented and shall be used in all cases, if heteroscedasticity cannot be refused. The use of WLS/IV is still much better than using OLS regression in these cases.

The proper estimation of the variance function is still a challenge. Outliers can influence its estimation strongly. Other methods to estimate different models of variance functions, especially weighted robust methods, shall be the issue of future work.

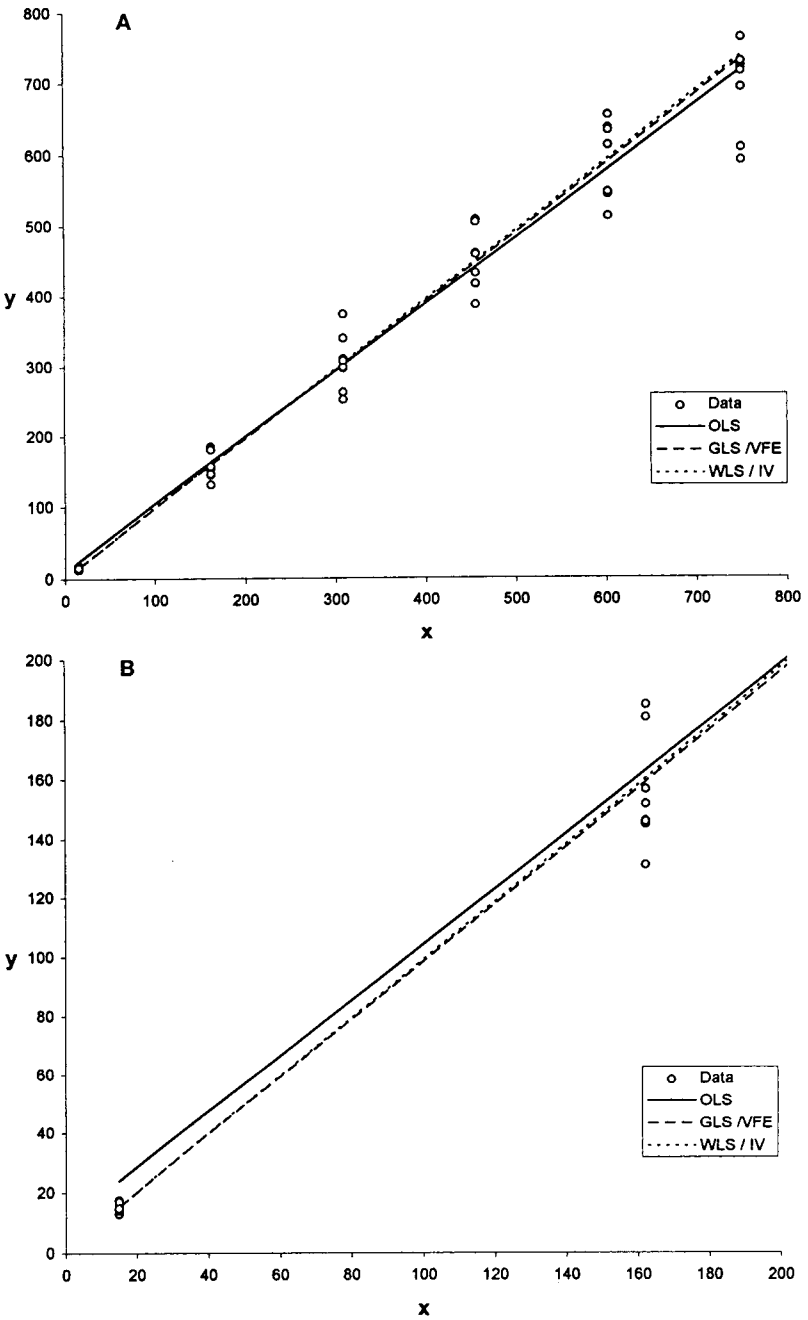

Fig. 4. Known linear functions were obtained by simulation. The signal standard deviation was chosen proportional to the signal [compare Experimental, same simulation parameters as for section (e) in Table 1]. In many simulations the data at high x values are strongly influenced by the random error. If no weighting factors are used, actually all data are equally weighted with the factor 1 (Eqs. 4–6). Thus the uncertain data at high concentration are given too much weight, if OLS is used (A). This leads to large deviations between OLS-estimated and simulated, thus true, functions at low x values. This is shown in (B), which is a magnification of (A). WLS algorithms provided a much better approximation. Over the whole range the lines estimated by WLS/IV, GLS/VFE and the simulated line ($\alpha_0 = 0$, α_1) can hardly be distinguished in this figure.

Table 2
Differences in errors for different regression algorithms for various R_{sdv}, if $\Theta \neq 1$; other conditions as in Table 1

	Err_{low}	Err_{hi}	MSE
(a) $R_{sdv} = 1.78$, $x_i = 15, 42, 69, 96, 123, 150$, $\Theta = 0.25$, that means the standard deviation of the noise at block x_i can be calculated as $sdv(x_i) = 0.1 \cdot x_i^{0.25}$			
WLS/SV	0.003005	0.000446	0.003355
GLS/VFE	0.003040	0.000447	0.003393
WLS/IV	0.003255	0.000490	0.004064
OLS	0.003182	0.000451	0.003515
Normalized to GLS/VFE			
WLS/SV	0.9884	0.9966	0.9886
GLS/VFE	1	1	1
WLS/IV	1.0707	1.0950	1.1976
OLS	1.0467	1.0087	1.0358
(b) $R_{sdv} = 3.16$, $x_i = 15, 42, 69, 96, 123, 150$. $\Theta = 0.5$, that means $sdv(x_i) = 0.1 \cdot x_i^{0.5}$			
WLS/SV	0.006536	0.001400	0.02893
GLS/VFE	0.006586	0.001410	0.02918
WLS/IV	0.006955	0.001553	0.03551
OLS	0.008366	0.001518	0.03378
Normalized to GLS/VFE			
WLS/SV	0.9924	0.9932	0.9915
GLS/VFE	1	1	1
WLS/IV	1.0560	1.1021	1.2171
OLS	1.2703	1.0778	1.1579

Possibly the use of 2-point calibrations is an interesting alternative to WLS regression. A systematic error is also avoided in our simulations. However, the use of 2-point calibrations over more than one order of magnitude sounds rather exotic for the practitioner. In the simulations considered the true function was strictly linear. If 2-point calibrations should be used, this must be true for the analytical method as well. Moreover, linearity has to be validated, which seems to be not trivial, especially in the heteroscedastic case. This another topic for further investigations.

Those considerations are valid for other ana-

Table 3
The difference in performance between the algorithms OLS and GLS/VFE is most pronounced for the total error caused by the calibration function at low x, Err_{low} (Eq. 20, Fig. 3); this error is considered as a function of the degree of heteroscedasticity, which is expressed as R_{sdv} (Eq. 15)

R_{sdv}	Normalized Err_{low} of OLS	Compare table
2	1.05	1a
3.16	1.23	1b
5	1.57	1c
10	2.63	1d
50	11.71	1e

The conditions of the simulations are described in Table 1.

Table 4
Two-point calibrations

	Err_{low}	Err_{hi}	MSE
WLS/SV	0.01626	0.01669	4.943
GLS/VFE	0.01626	0.01669	4.943
WLS/IV	0.01626	0.01669	4.943
OLS	0.01626	0.01669	4.943
Normalized to GLS/VFE			
WLS/SV	1.0000	1.0000	1.0000
GLS/VFE	1	1	1
WLS/IV	1.0000	1.0000	1.0000
OLS	1.0000	1.0000	1.0000

If 2-point calibrations are used, there is no additional error caused by heteroscedasticity. This is not surprising: a line is defined by two points, thus there is only one possibility. Systematic errors can only appear, if there are at least three x values: now one value can be given too much weight. Possibly the use of 2-point calibrations is an interesting alternative to WLS regression. However, linearity has to be validated, which seems to be not trivial, especially in the heteroscedastic case. Simulation conditions like in Table 1, but only two equidistant blocks x_i of 24 y values were simulated, $R_{sdv} = 10$, $x_i = 15, 150$.

lytical techniques as well, if their characteristics of calibration and variance function are similar.

Symbols and abbreviations

a_0	intercept of estimated regression line
a_1	slope of estimated regression line
α_0	intercept of simulated line
α_1	slope of simulated line
A	absorbance
A_c	corrected peak area
CE	capillary electrophoresis
c_s	sample concentration
ε_i	normal distributed random variable
Err_{hi}	total error caused by the calibration function at high x values
Err_{low}	total error caused by the calibration function at low x values
GLS/VFE	algorithm: generalized least squares using variance function estimations
k	iteration number
L	likelihood
MSE	mean squared error
n	number of data pairs per set
OLS	algorithm: ordinary least squares
relsdv	relative standard deviation
R_{sdv}	ratio of the standard deviations at the highest and the lowest concentration within the working range (Eq. 15)
σ^2	variance at y = 1
sdv	standard deviation
Θ	variance parameter
var	variance
w_i	weighting factor
WLS/IV	algorithm: weighted least squares using inverse variances
WLS/SV	algorithm: weighted least squares using simulated variances
x_0	true x at given y
$\bar{x}_c$	coordinate of the centroid
x_{estm}	x estimated by regression parameters a_0 and a_1 at given y
x_i	coordinate of simulated data pair; corresponds to sample concentration in CE
$\bar{y}_c$	coordinate of the centroid
y_i	coordinate of simulated data pair; corresponds to signal in CE
$\hat{y}(x)$	estimated regression function

Acknowledgements

The authors wish to thank Dr. T. Weekes for his helpful suggestions, him and Professor Dr. S. Ebel, C. Ehrensberger, V. Lukat and C. Oelsch for critically reading this manuscript, further-

more Dr. C. Dette for his support of the measurements.

References

[1] K.D. Altria, R.C. Harden, M. Hart, J. Hevizi, P.A. Hailey, J.V. Makwana and M.J. Portsmouth, *J. Chromatogr.*, 641 (1993) 147.
[2] J. Sadecka, J. Polonsky and H. Shintani, *Pharmazie*, 49 (1994) 631.
[3] H. Wätzig and C. Dette, *Pharmazie*, 49 (1994) 83.
[4] H. Wätzig, *J. Chromatogr.*, 700 (1995) 1.
[5] H. Wätzig and C. Dette, *Pharmazie*, 48 (1993) 527.
[6] W.H. Press, B.P. Flannery, S.A. Teukolsky and W.T. Vetterling, *Numerical Recipes in Pascal*, University Press, Cambridge, UK, 1992, p. 225.
[7] R.J. Carroll and D. Ruppert, *Transformation and Weighting in Regression*, Chapman & Hall, New York, 1988.
[8] M. Davidian and R.J. Carroll, *J. Am. Statistical Ass.*, 82 (1987) 1079.
[9] K. Doerffel and R. Hebisch, *Fresenius Z. Anal. Chem.*, 331 (1988) 510.
[10] J.N. Miller, *Analyst*, 116 (1991) 3.
[11] J. Hartung, *Statistik*, Oldenbourg, Munich, 8th ed., 1991.
[12] L. Sachs, *Angewandte Statistik*, Springer, Berlin, Heidelberg, 6th ed., 1984.
[13] H. Wätzig and C. Dette, *Pharmazie*, 49 (1994) 656.
[14] H. Wätzig and C. Dette, *J. Chromatogr.*, 636 (1993) 31.
[15] A. Ringbohm, *Fresenius Z. Anal. Chem.*, 115 (1939) 332.
[16] G. Kortüm, *Kolorimetrie, Photometrie und Spektrometrie*, Springer, Berlin, 1962.
[17] H.L. Pardue, T.E. Hewitt and M.J. Milano, *Clin. Chem.*, 20 (1974) 1028.
[18] A.F. Siegel, *Biometrika*, 69 (1982) 242.
[19] H. Oja, Stat. *Probab. Lett.*, 1 (1989) 327.
[20] P.J. Rousseeuw and A.M. Leroy, *Robust Regression and Outlier Detection*, Wiley, New York, 1987, pp. 65*ff* and 145*ff*.
[21] R.R. Williams, *Anal. Chem.*, 63 (1991) 1638.
[22] H. Martens and T. Naes, *Multivariate Calibration*, Wiley, Chichester, 1989.

ELSEVIER

Journal of Chromatography A, 700 (1995) 21–26

JOURNAL OF CHROMATOGRAPHY A

Influence of capillary dimensions on the performance of a coaxial capillary electrophoresis–electrospray mass spectrometry interface

L.W. Tetler[a,*], P.A. Cooper[a], B. Powell[b]

[a]*Michael Barber Centre for Mass Spectrometry, UMIST, PO Box 88, Manchester, M60 1QD, UK*

[b]*Zeneca Specialties, PO Box 42, Hexagon House, Blackley, Manchester, M9 3DA, UK*

Abstract

The dimensions of the capillaries used to construct a typical coaxial capillary electrophoresis–mass spectrometry (CE–MS) interface, i.e. the inner diameter, the outer diameter and the wall thickness, have been shown to affect the performance of the CE–MS system. The influence of these parameters has been investigated in both MS and MS–MS modes. The initial results indicate that by reducing all the sheath capillaries' dimensions and the CE capillary outer diameter, better operation and increased sensitivity can be achieved. The capillary arrangement which gives optimum sensitivity and stable operation has been suggested.

1. Introduction

Capillary electrophoresis–electrospray mass spectrometry (CE–MS), since its introduction in 1987 [1], has become an established technique in many research laboratories, mainly because of improvements made in interface design, stability and operation. Pioneering research in the late 1980's resulted in the emergence of two distinct types of CE–MS interface, the coaxial and the liquid junction. The liquid junction design was introduced by Minard et al. [2], using continuous flow fast atom bombardment, and by Henion and co-workers [3], using electrospray. A coaxial design was initially reported by Smith et al. [4] in 1988. Both interface designs have been shown to produce good data for a wide range of compounds, but subsequent research by Pleasance et al. [5] and our own investigations have tended to indicate that the coaxial arrangement is the more suitable of the two methods for interfacing with electrospray MS, offering robust and reproducible operation along with maintenance of both the CE and MS performance.

A typical coaxial interface (Fig. 1) comprises three concentric capillaries. The innermost capil-

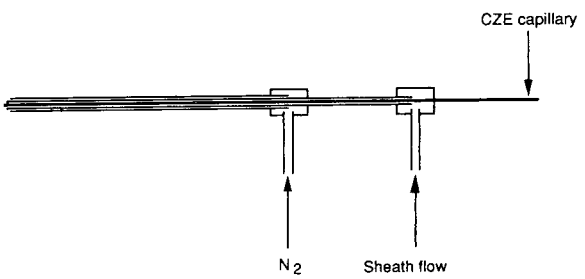

Fig. 1. A typical coaxial CE–MS interface.

* Corresponding author.

0021-9673/95/$09.50
SSDI 0021-9673(94)01171-0

lary (generally fused-silica) is used for electrophoresis with the middle capillary (usually stainless steel) providing a sheath flow of liquid, which is required for a number of reasons. First, the extra liquid compensates for the low flow emerging from the electrophoresis capillary. Secondly, it provides unbroken electrical contact between the electrospray needle and the CE capillary, thus defining the potential difference across the CE capillary. Thirdly, it allows the incorporation of solvents and/or reagents which can be used to stabilise the electrospray process or to perform post-separation sample or buffer modification. The outer capillary, also stainless steel, supplies a flow of nebulising gas which aids droplet formation during the electrospray process and also provides a certain amount of cooling for the CE capillary.

The dimensions of these capillaries, i.e. their inner diameter, outer diameter and hence wall thickness, are usually determined by availability and the current instrument requirements, but they will have an influence on the spray characteristics of the electrospray, the degree of mixing at the probe tip, the siphoning effect of the nebulising gas and the electrical environment that the cathode end of the electrophoresis capillary experiences. All these parameters will affect the sensitivity and performance of the system.

The durability of the electrophoresis capillary is an important factor that should be considered. Thinner walled fused-silica capillaries tend to become brittle and suffer from 'electrodrilling' processes when subjected to the high voltages used in capillary electrophoresis. Our experience is that a thicker walled capillary (75 μm I.D., 375 μm O.D.) can last up to 4–5 times longer than a thin walled capillary (75 μm I.D., 150 μm O.D.) before any evidence of arcing or breakage is noted.

We therefore decided to investigate various combinations of capillaries in order to find whether changing from thin to thick walled capillaries has an effect on performance and also to find the optimum capillary arrangement in terms of sensitivity, ease of optimisation and robustness. The initial results from our on-going research are reported here.

2. Experimental

The CE instrument was constructed in-house (Zeneca Specialties, Blackley, Manchester, UK) and utilised a 30 kV Brandenburg Power supply (Astec, Stourbridge, UK). The injection end of the CE capillary was housed within a perspex case which could be pressurised to enable pressure injections to be made or the capillary to be flushed. The sample and buffer reservoirs were situated on a rotating table, the height of which was adjustable, thus facilitating hydrostatic injections. The separation capillaries were all untreated fused-silica (Polymicro Technologies, Phoenix, AZ, USA), 1 m in length. The diameters of the capillaries are included in Fig. 2.

The sample used was an aqueous peptide mixture containing bradykinin ($M_r = 1064$), angiotensin I ($M_r = 1296$), angiotensin II ($M_r = 1040$) and substance P ($M_r = 1348$) at a concentration of 200 pmol/μl per component. Injections were performed hydrostatically at a height of 10 cm for 5 to 10 s (depending on the interface arrangement used). This corresponds to injection volumes of 6–12 nl.

The electrophoresis buffer was a mixture of formic acid–acetonitrile–water (5:50:45). The applied CE voltage was 30 kV, which resulted in a potential drop of 25 kV (250 V/cm) across the capillary (as the cathode end of the capillary was at the same voltage as the ionspray needle, i.e. 5 kV).

MS was accomplished using a PE Sciex API III instrument (Sciex, Toronto, Canada) operated in the ionspray configuration. The ionspray voltage and the orifice potential were maintained at 5 kV and 70 V, respectively. Nitrogen was used as both drying gas (1 l/min) and nebulising gas [0.8–1.8 l/min, 25–60 p.s.i. (172–414 kPa) depending upon the interface arrangement] and the source temperature was 60°C throughout.

MS spectra were acquired by scanning Q1 from 400 to 700 amu at a rate of 1.6 s/scan. MS–MS spectra were acquired using the RAD software, which allows an optimised set of MS–MS parameters to be used for individual components. Q1 was switched manually between precursor ions as the peaks were eluted and Q3 was scanned from 50 to 1350 amu. The collision

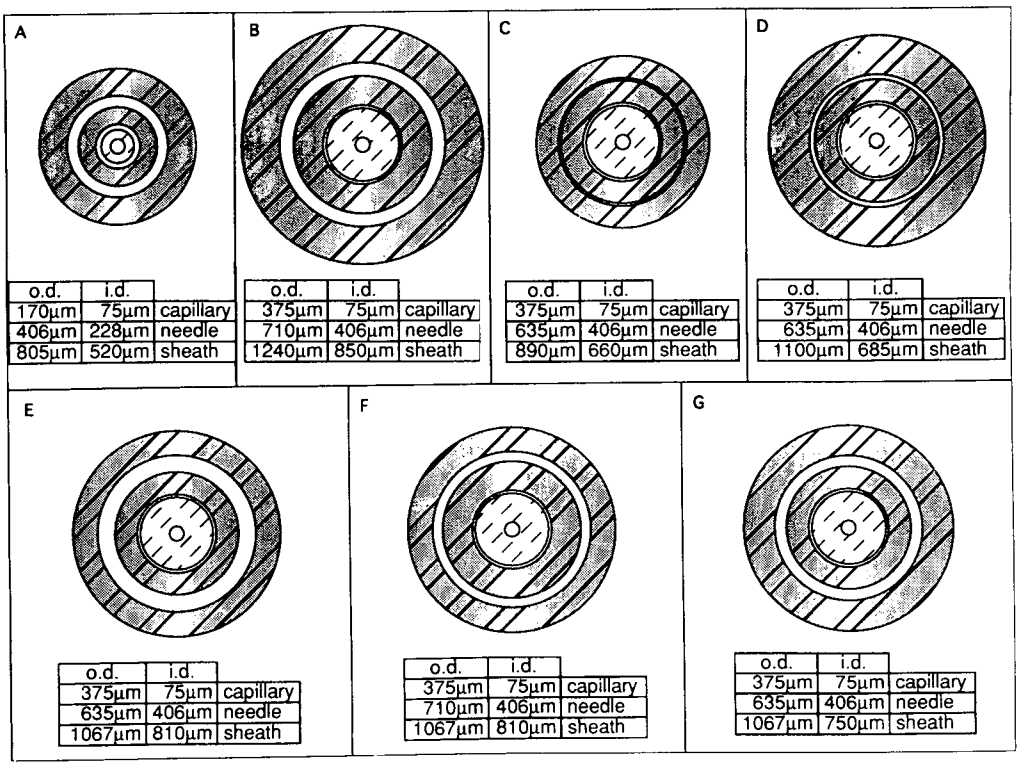

Fig. 2. Capillary combinations investigated.

gas employed was argon, at a collision gas thickness of 300×10^{13} atoms cm^{-2}.

The coaxial interface was operated with a sheath liquid comprising of a mixture of methanol–water (1:1) to which 0.1% v/v formic acid was added. The sheath liquid was delivered at a flow-rate of 8 μl/min by an Isco Model 1000 DM syringe pump (Isco, Lincoln, NE, USA).

The various capillary combinations considered in this study are shown drawn to scale in Fig. 2.

2.1. Chemicals

The peptides were purchased from Sigma (Poole, UK) and used without any further treatment. HPLC grade water, methanol and acetonitrile was obtained from Rathburn Chemicals (Walkerburn, UK). The Formic acid was supplied by Aldrich (Gillingham, UK).

3. Discussion

Our initial experiments were conducted using the original Sciex capillary dimensions which are reproduced in Fig. 2A. As expected, this arrangement resulted in a stable spray with good sensitivity, as reflected in the total ion chromatogram (TIC) of the peptide mixture (Fig. 3). However, this arrangement uses thin walled fused-silica CE capillaries which, as stated earlier, become brittle and break easily after prolonged application of high voltage. We therefore looked for capillary combinations which would allow the use of larger O.D. CE capillaries. The subsequent capillary combinations were chosen (depending upon availability) so that the ratios of the cross sectional areas of the three outlets (CE eluent, sheath flow and nebulising gas) formed a range around those of the original arrangement (Table 1). For these early experi-

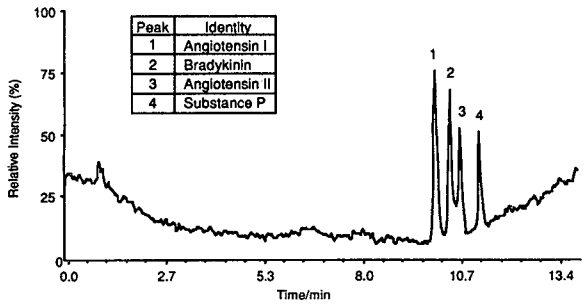

Fig. 3. CZE–MS TIC trace of the peptide mix using the original Sciex capillaries (arrangement A).

ments, the I.D. of the CE capillary was fixed at 75 μm in order to maintain sample loadings and separation parameters. Area 2 was chosen to be as small as possible. The only suitable size of capillary that was readily available had an I.D. of 406 μm. The next size up has an inner diameter of 510 μm which may have been usable, but the O.D. of this capillary meant that a larger outer capillary would have to be used and the O.D. of that capillary was too large to use with the standard 1/16 in. fittings.

The combinations shown in Figs. 2C and 2D were found to be unsuitable because of the tight fit of the middle capillary within the outer capillary. In the case of Fig. 2C, the capillaries were physically too tight to manoeuvre into position. The interface shown in Fig. 2D could be constructed without difficulty, but the closeness of the capillaries led to a restriction in the flow of nebulising gas. This meant working with very high pressures of nebulising gas, which made it very difficult to achieve stable electrospray conditions for any length of time, thus leading to fluctuation in the ion current and poor results.

The arrangements reproduced in Figs. 2B, 2E and 2F eventually all gave stable conditions but with varying degrees of difficulty. Table 2 is a comparison of the signals obtained with each of these arrangements and the Sciex original. The normalised values (relative to the largest signal for the particular peptide) are shown in parentheses and the overall relative sensitivity is shown in the final column. The ion currents have been calculated per mole of peptide. This compensates for differences in the composition between batches of the peptide mix. These discrepancies are reflected by the differences in relative peak heights in the TIC traces in Figs. 3, 4a and 5a.

It can be seen from Table 2 that capillary combination F gives the greatest sensitivity in terms of peptide ion current. However, this arrangement was more difficult to optimise and a stable spray could not always be achieved. This

Table 1
Cross sectional areas of the capillary combinations investigated

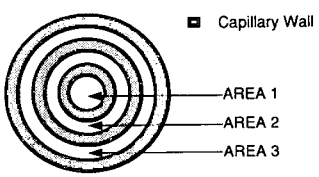

Capillary Arrangement (See Fig. 2)	Area (μm^2)	Area 2 (μm^2)	Area 3 (μm^2)	$\frac{\text{Area 3}}{\text{Area 2}}$	$\frac{\text{Area 2}}{\text{Area 1}}$
A	4416	18 121	82 868	4.1	4.6
B	4416	19 006	171 444	4.3	9.0
C	4416	19 006	25 414	4.3	1.3
D	4416	19 006	51 810	4.3	2.7
E	4416	19 006	198 507	4.3	10.4
F	4416	19 006	119 320	4.3	6.3
G	4416	19 006	125 031	4.3	6.6.

Table 2
Sensitivities of the capillary combinations investigated

Capillary arrangement (see Fig. 2)	Angiotensin I	Bradykinin	Angiotensin II	Substance P	Rel. sensitivity
A	326 000 (0.68)	214 000 (0.91)	184 000 (1.00)	75 000 (0.49)	0.8
B	300 000 (0.63)	188 000 (0.80)	135 000 (0.73)	48 000 (0.31)	0.7
E	256 000 (0.54)	226 000 (0.97)	113 000 (0.61)	145 000 (0.95)	0.7
F	476 000 (1.00)	234 000 (1.00)	131 000 (0.71)	153 000 (1.00)	1.0

Figures are ion current per mole of peptide.
Normalised value shown in brackets.

led to instability in the electrical contact at the probe tip, which caused the separation to be degraded and the baseline to fluctuate.

Arrangements B and E were less sensitive to changes in operating parameters and therefore optimisation was simpler and prolonged operation was attainable. The separation integrity was maintained when either of these arrangements was used.

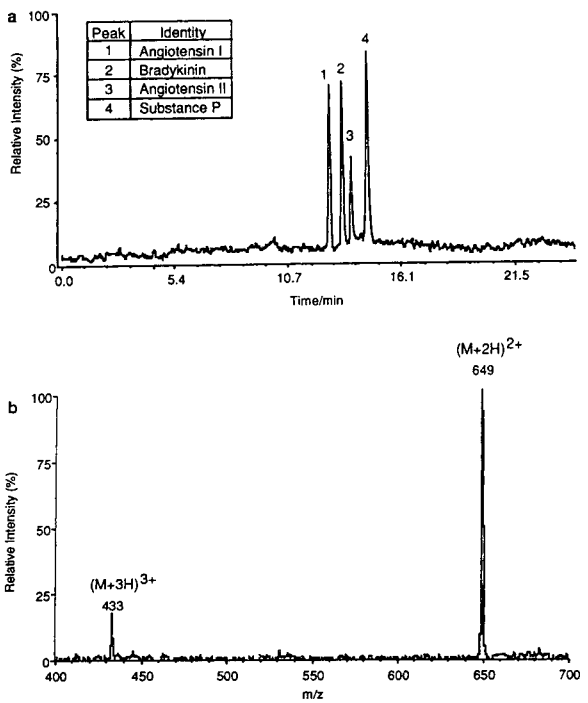

Fig. 4. (a) CE–MS TIC trace of the peptide mix using arrangement E. (b) ESI spectrum of angiotensin I, taken from peak 1 of Fig. 4a.

Fig. 4a is the TIC trace obtained from a CE–MS analysis using arrangement E. The spectrum of angiotensin I taken from the apex of the first peak is shown in Fig. 4b. To illustrate the performance of the system, CE–MS–MS experiments were performed and the TIC trace arising from interface B is reproduced in Fig. 5a. Fig. 5b is the product ion spectrum of angiotensin I taken from the first peak of the TIC.

Taking into account both sensitivity and the ease of optimisation and operation of the interfaces, the optimised capillary combination is suggested to have a surface area ratio which lies between those of arrangements F and B, and one such possibility is shown in Fig. 2G. As yet this combination has not been attempted because of the difficulty in obtaining the non-standard sized capillaries.

4. Conclusions

The dimensions of the capillaries in a coaxial capillary electrophoresis–electrospray mass spectrometry interface have been shown to affect the performance of the system in terms of both sensitivity and stability. These initial results suggest that a relationship exists between the ratio of the cross sectional areas of the outlet orifices between capillaries and the performance of the system, although further confirmation using different samples and buffer systems is

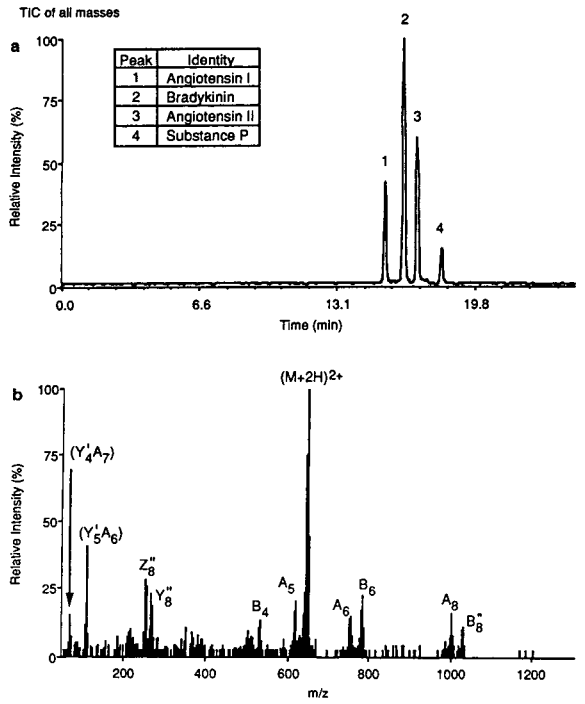

Fig. 5. (a) CE–MS–MS TIC trace from the peptide mix using arrangement B. (b) Product ion spectrum of angiotensin I, taken from peak 1 of Fig. 5a.

required. This relationship has led to the suggestion of an 'optimum' capillary arrangement. Currently we are unable to construct this interface as the stainless-steel capillary sizes required are non-standard and thus not readily available.

It has also been shown that it is possible to convert from thin to thick walled capillaries without any loss (indeed in some cases with a gain) in the performance of the system.

Acknowledgements

P.C. acknowledges the EPSRC and Zeneca Specialties (Blackley, Manchester, UK) for provision of funding for the project.

References

[1] J.A. Olivares, N.T. Nguyen, C.R. Yonker and R.D. Smith, *Anal. Chem.*, 59 (1987) 1230.

[2] R.D. Minard, D. Chinn-Fatt, P. Curry Jr. and A.G. Ewing, proceedings of the *36th ASMS conference on Mass Spectrometry and Allied Topics, San Francisco, CA, 1988*, p. 950.

[3] E.D. Lee, W. Muck, J.D. Henion and T.R. Covey, proceedings of the *36th ASMS conference on Mass Spectrometry and Allied Topics, San Francisco, CA, 1988*, p. 1085.

[4] R.D. Smith, C.J. Baringa and H.R. Udseth, *Anal. Chem.*, 60 (1988) 1948.

[5] S. Pleasance, P. Thibault and J. Kelly, *J. Chromatogr.*, 591 (1992) 325.

ELSEVIER

Journal of Chromatography A, 700 (1995) 27–33

JOURNAL OF CHROMATOGRAPHY A

Electrochromatography–electrospray mass spectrometry of textile dyes

G.A. Lord[a,b], D.B. Gordon[a,b,*], L.W. Tetler[b], C.M. Carr[c]

[a]*Department of Biological Sciences, Manchester Metropolitan University, Chester Street, Manchester M1 5GD, UK*
[b]*The Michael Barber Centre for Mass Spectrometry, UMIST, Manchester M60 1QD, UK*
[c]*Department of Textiles, UMIST, Manchester M60 1QD, UK*

Abstract

Electrochromatography with its high chromatographic performance has been coupled with electrospray mass spectrometry (MS) for the analysis of non-ionic disperse textile dyes. Electrochromatography offers an alternative to micellar electrokinetic capillary chromatography (MECC) for the analysis of uncharged compounds in conjunction with MS, since MECC generally relies on MS incompatible compounds for micelle formation. Overall, the technique of electrochromatography–MS should find application in many areas.

1. Introduction

Electrochromatography relies on the phenomenon of electroosmosis to effect solvent flow through packed fused-silica capillaries, with the advantage that a flat flow profile is produced in contrast to the parabolic Poisseuille flow of pressure driven systems, resulting in enhanced chromatographic performance. A further advantage is that flow is independent of particle diameter and it is possible to use very small particles, with no theoretical restriction on column length. Pretorius et al. [1] first demonstrated electrochromatography in 1974, and the technique was revived in 1981 by Jorgenson and Lukacs [2], but was not developed further until 1987 by Knox and Grant [3], which led to current interest in the technique. A recent report developed an idea of Knox and Grant on the use of a pressurised electrochromatography system to suppress bubble formation in the capillary, induced by Joule heating [4].

Electrochromatography capillaries are typically 25–100 cm long with 25–100 μm I.D., filled with reversed-phase packing material. Selectivity in electrochromatography is identical to that in conventional HPLC for neutral analytes but electrophoresis contributes for ionised species. The technique has particular advantages in coupling to mass spectrometry (MS), since narrower chromatographic peaks produce a higher mass flux, and in addition offers an alternative to micellar electrokinetic capillary chromatography (MECC) for the separation of neutral analytes. MECC generally relies on MS-incompatible

* Corresponding author. Address for correspondence: Department of Biological Sciences, Manchester Metropolitan University Chester Street, Manchester M1 5GD, UK.

0021-9673/95/$09.50
SSDI 0021-9673(95)00116-6

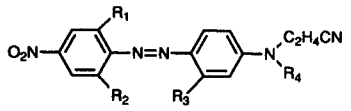

SERILENE YELLOW BROWN R-LS $R_1, R_2 = Cl\ R_3 = H\ R_4 = C_2H_4OOCMe$
SERILENE ORANGE 2RL $R_1, R_2, R_3 = H\ R_4 = C_2H_5$
SERILENE YELLOW BROWN G-LS $R_1, R_2 = Cl\ R_3 = H\ R_4 = C_2H_4OOCPh$
SERILENE DARK RED FL $R_1 = Cl\ R_2 = H\ R_3 = Me\ R_4 = C_2H_5$

Fig. 1. Structure of Serilene azo dyes.

quantities of compounds, typically anionic surfactants, for micelle formation. Initial work on the combination of electrochromatography with MS has been reported [5]. Combinations of both pressure driven and electroosmotically driven chromatography have been described, initially by Tsuda [6], who used pressure-driven flow in addition to electroosmosis, to suppress bubble formation. Later work by Verheij et al. [7] used the term pseudo-electrochromatography to distinguish the technique from pure electrically driven electrochromatography. This report was also concerned with the coupling of pseudo-electrochromatography to MS, and further work by the same group has recently been reported [8]. The flow profile in pseudo-electrochromatography approaches that in a pressure-driven system, resulting in a level of efficiency lying between electrochromatography and conventional HPLC, but biased towards the latter. However, since selectivity is based on both electrophoresis and partition, pseudo-electrochromatography does have particular advantages in coupling to MS for the separation of ionic compounds, owing to the lack of need for ion-pairing agents and buffer gradients, most of which are MS incompatible.

We report in this paper on the use of electrochromatography coupled with MS for the analysis of some non-ionic, water-insoluble, disperse textile dyes (azo and anthraquinone based with

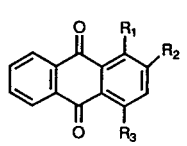

DISPERSOL BLUE BN $R_1 = NHCH_3\ R_2 = H\ R_3 = NHCH_2CH_2OH$
DISPERSOL RED B3B $R_1, R_3 = NH_2\ R_2 = OCH_3$
TERASIL BLUE 2R $R_1 = NH_2\ R_2 = H\ R_3 = NHPh$

Fig. 2. Structure of anthraquinone-based dyes.

structures shown in Figs. 1 and 2, respectively), particularly as an alternative to MECC. The combination of extremely efficient chromatography with the unrivalled specificity of MS results in a very powerful analytical technique. There are several areas where an efficient method for the analysis of dyes and related compounds is required, these include both the production of dyes and their use in textile dyeing, but also wider applicability such as environmental and forensic fields. In dye synthesis, side-reaction products are usually formed which may be economically wasteful and/or may be actively involved in the dyeing process. Degradation of dye when present on the textile is a further area of interest to the textile industry, and relates to a current interest of the authors, namely the analysis of dyes from textiles of archaeological significance [9]. The analysis of dyes and related compounds has been typically carried out by TLC, HPLC or GC, each technique having particular drawbacks, such as difficulties in quantitation with TLC, use of relatively large volumes of solvent in conventional HPLC and requirement for sample volatility in GC. More recently CE has been applied to dyestuff analysis following the pioneering work of Lee et al. in 1989 [10], who also coupled the technique to MS. Further work on CE–MS of dyestuffs by another group has also been recently reported [11]. These reports and others [12–14] concerned with CE alone, mostly involved the separation of charged species. However, following the work of Terabe et al. [15] on MECC, neutral species could also be analysed by CE techniques, as well as improving separation efficiency of some charged compounds. This technique has recently been applied to the analysis of both charged and neutral dyestuffs [14,16], including some disperse dyes, when acetonitrile was used as a co-solvent [16].

2. Experimental

2.1. Materials

All solvents used were of HPLC grade obtained from Rathburn, Walkerburn, UK, and

were filtered before use with the aid of vacuum through a 0.2-μm PTFE filter (Alltech Associates Applied Science, Carnforth, UK). Dyes were used as received: Serilene azo dyes were a gift from Yorkshire Chemicals, Leeds, UK; Dispersol red B3B, Dispersol blue BN and Terasil blue 2R were obtained from Zeneca, Manchester, UK. All other reagents from BDH, Poole, UK.

2.2. Preparation of capillary columns

The electrochromatography column consisted of uncoated fused-silica capillary (Polymicro Technologies, AZ, U.S.A.), 100 cm × 75 μm I.D. × 375 μm O.D., slurry packed with acetonitrile to a depth of 25 cm with 3-μm ODS-Hypersil (Shandon Scientific, Runcorn, UK), as described in detail elsewhere [5]. The progress of packing was observed through the capillary wall with the aid of a microscope, and when completed, the column was equilibrated with the mobile phase to be used for electrochromatography separations [acetonitrile–4 m*M* sodium tetraborate (80:20, v/v) adjusted to pH 8 with dilute sodium hydroxide solution].

The outlet end of the packed section of capillary was not fitted with a retaining frit, since when voltage was applied the negatively charged packing material would be pulled toward the inlet frit against the electroosmotic flow. Thus there is an absence of dead space, which is advantageous compared with conventional pressure-driven systems when a dead space often develops at the head of the column, and leads to a decline in chromatographic performance.

2.3. Chromatography

Electrochromatographic separations were performed using an Isco model 3140 electropherograph (Isco, Lincoln, NE, USA), which is designed primarily as a capillary electrophoresis instrument, but is equally suitable for electrochromatography.

Samples were dissolved in the eluent, and were applied to the column electrodynamically. Detection was by UV absorbance (210 nm) through a window in the capillary wall 30 cm from the inlet. A voltage of 30 kV was applied to the anode buffer solution into which the inlet end of the capillary was immersed. The outlet end of the capillary was linked to the mass spectrometer as described below.

2.4. Mass spectrometry

MS was carried out on VG Quattro quadrupole mass spectrometer fitted with an electrospray source (VG Biotech, Altrincham, U.K.), to which the electrochromatography capillary was linked via a co-axial interface-probe (VG Biotech) and is shown diagrammatically in Fig. 3. The interface comprises two concentric stainless-steel capillaries surrounding the inner electrochromatography capillary contained within a probe which is inserted into the instrument, and each is fitted into a separate tee-piece, as shown in the diagram. Methanol–water (1:1, v/v) containing 1% (v/v) acetic acid flowing at 10 μl/min was incorporated via the capillary at the first tee-piece, delivered by a Brownlee Microgradient syringe pump (Brownlee Labs., Santa Clara, CA, U.S.A.), to provide a "make-up" flow of liquid to compensate for the low flow-rate of electrochromatography. This was necessary for efficient operation of the electrospray process. The outer capillary supplied nitrogen gas via the second tee-piece to nebulize the liquid flow and

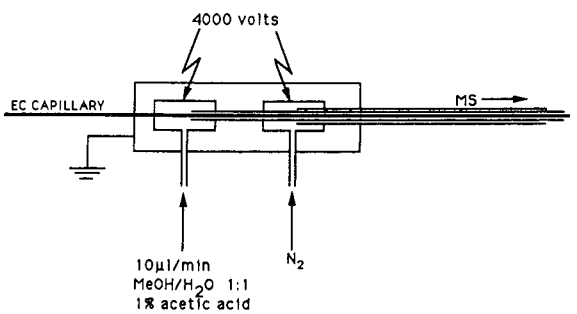

Fig. 3. Diagrammatic representation of co-axial electrochromatography (EC)–MS electrospray interface probe.

aid droplet formation. A voltage of 4 kV was applied to both stainless steel tee-pieces to provide high voltage at the probe tip for the electrospray process, and the interface is enclosed in an earthed box for operator safety. The tip of the electrospray probe at 4 kV acted as the cathode giving a net potential of 26 kV applied across the electrochromatography capillary.

MS acquisitions in positive mode were made using single ion monitoring of appropriate ions or scanning the appropriate mass range, and were initiated approximately 20 min after application of sample onto the column and commencement of elution.

3. Results and discussion

Fig. 4a is a UV chromatogram for the separation of a mixture of the four Serilene azo dyes shown in Fig. 1. Peaks 1 and 2 are just resolved, but using conventional HPLC with an analytical scale column, it was not possible to separate these compounds (data not shown), and electrochromatography-produced peaks which more closely approximated a Gaussian shape. Chromatographic performance was good, peak 4 for example, displays approximately 180 000 theoretical plates/m and a reduced plate height just below 2, although we have obtained reduced plate heights of near unity for weakly retained compounds in previous work [5]. However, a limiting factor on peak width narrowness is dictated by MS temporal requirements for full-scan data. Fig. 4b shows selected ion chromatograms of each dye, corresponding to the mass of the respective protonated molecule. Some loss of chromatographic resolution is apparent, particulary notable in the case of peaks 1 and 2, probably as a result of post detection window dispersion in the length of unpacked capillary necessary for MS coupling, and/or by a memory effect in the mass spectrometer. However, the specificity of MS obviates this problem by detection of the unique mass of each compound, and only fails when dealing with closely eluting isobaric compounds.

Fig. 5 displays selected ion chromatograms

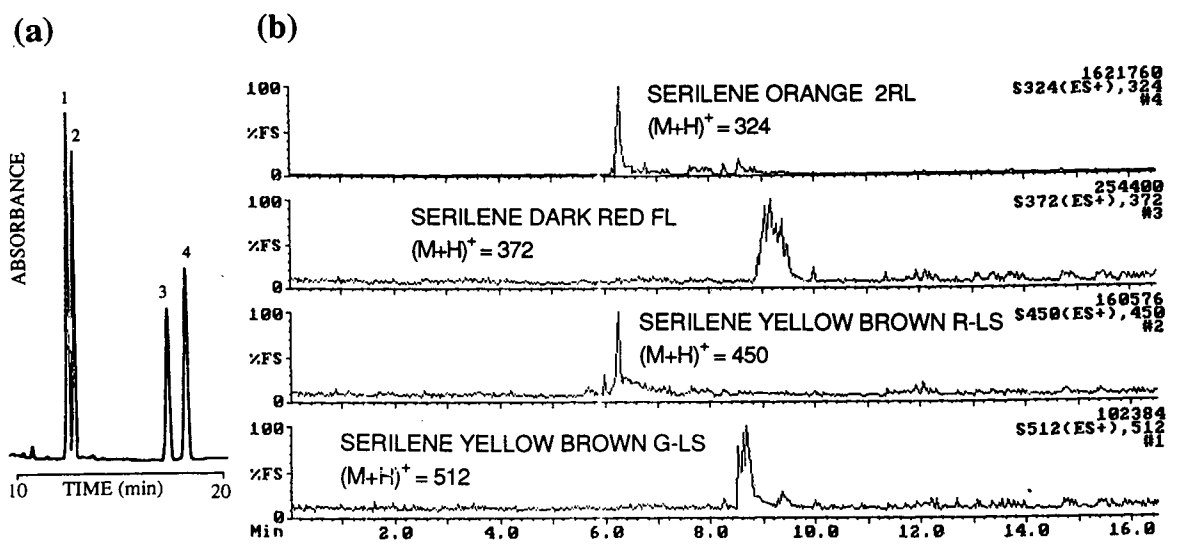

Fig. 4. On-line electrochromatography–MS separation of Serilene azo dyes, loading 100 pmol of each dye on-column. (a) UV chromatogram, peaks: 1 = Serilene yellow brown R-LS; 2 = Serilene orange 2 RL; 3 = Serilene yellow brown G-LS; 4 = Serilene dark red FL. (b) Selected ion chromatograms of $(M+H)^+$.

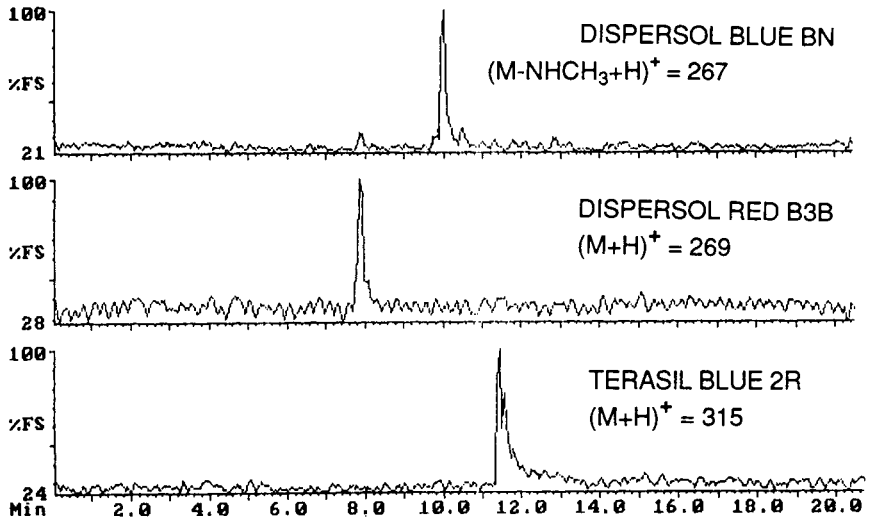

Fig. 5. Selected ion chromatograms from full-scan data for on-line electrochromatography–MS separation of anthraquinone based dyes, loading 100 pmol of each dye on-column.

from full scan data for the separation of the three anthraquinone based dyes: Dispersol blue BN, Dispersol red B3B and Terasil blue BN, demonstrating the ability to monitor fragment ions from full scan data. The lower two traces are chromatograms of intact protonated molecule ions selected from full-scan data, allowing inspection of the mass spectrum of each peak and this is further demonstrated in the next example. Fig. 6a is a UV chromatogram for the separation of one of the components in Fig. 5, Terasil blue 2R, at higher loading, in order to investigate the impurity peaks eluting before the main peak. Fig. 6b is a chromatogram of the total ion current, scanning mass range 200–600, and mirrors the UV chromatogram. Analysis of the spectra of the impurity peaks suggested that they were side reaction products arising from the synthesis of the dye. Fig. 6c shows a portion of the spectrum of the main component.

The combination of electrochromatography with MS has been shown to be a useful technique for the analysis of mixtures of neutral textile dyes, allowing identification of impurities in single dyes, and may offer wider application in the environmental and forensic areas. In addition several observations should be considered as well as the high chromatographic efficiency of the technique. These include no theoretical limitation on the use of very small particles and long column lengths, which may lead to the ability to separate previously intractable mixtures. The method offers the ability to deal with extremely small sample quantities, and there is the capability for higher loadings compared with conventional CE. Coupling of electrochromatography to MS gains advantage over the use of conventional detectors by virtue of the unrivalled specificity of mass analysis, and coupling is readily achieved owing to the compatibility of capillary flow rates with MS. Electrochromatography also obviates the major disadvantages of MECC with regard to MS, whilst retaining its virtues. Furthermore electrochromatography overcomes the difficulties encountered with open-capillary CE, where coupling to MS sources at high vacuum may result in vacuum-induced flow which degrades separation.

We are convinced that electrochromatography coupled to MS offers considerable advantages to many areas of interest, especially in the biological field.

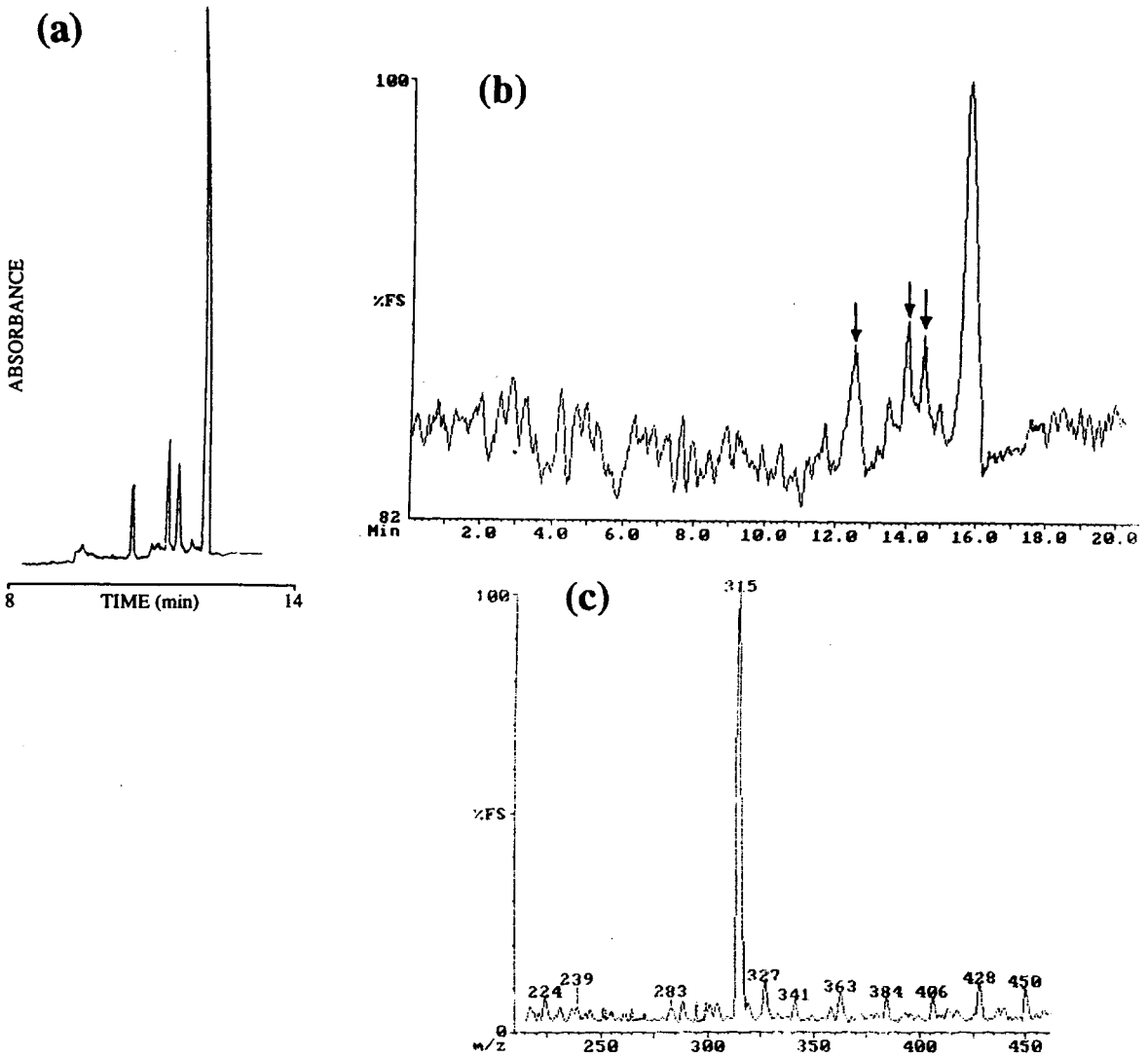

Fig. 6. On-line electrochromatography–MS separation of single dye (Terasil blue 2R) from mixture in Fig. 5, loading 1 nmol on-column, to investigate impurity peaks eluting prior to the main component as seen in (a) UV chromatogram, and arrowed in (b) full-scan total ion chromatogram. (c) Portion of mass spectrum of main component.

Acknowledgement

The authors thank Jones Chromatography, Hengoed, Mid-Glamorgan (UK) for loan of CE equipment and ICI Chemical and Polymers Ltd., Runcorn, Cheshire (UK) for loan of HPLC equipment.

References

[1] V. Pretorius, B.J. Hopkins and J.D. Schieke, *J. Chromatogr.*, 99 (1974) 23.
[2] J.W. Jorgenson and K.D. Lukacs, *J. Chromatogr.*, 218 (1981) 209.
[3] J.H. Knox and I.H. Grant, *Chromatographia*, 24 (1987) 135.

[4] N.W. Smith and M.B. Evans, *Chromatographia*, 38 (1994) 649.
[5] D.B. Gordon, G.A. Lord and D.S. Jones, *Rapid Commun. Mass Spectrom.*, 8 (1994) 544.
[6] T. Tsuda, *Anal. Chem.*, 59 (1987) 521.
[7] E.R. Verheij, U.R. Tjaden, W.M.A. Niessen and J. van der Greef, *J. Chromatogr.*, 554 (1991) 339.
[8] M. Hugener, A.P. Tinke, W.M.A. Niessen, U.R. Tjaden and J. van der Greef, *J. Chromatogr.*, 647 (1993) 375.
[9] G.A. Lord, D.B. Gordon and C.M. Carr, in preparation.
[10] E.D. Lee, W. Muck and J.D. Henion, *Biomed. Environ. Mass Spectrom.*, 18 (1989) 253.
[11] L.W. Tetler, P.A. Cooper and C.M. Carr, *Rapid Commun. Mass Spectrom.*, 8 (1994) 179.
[12] S.N. Croft and D.M. Lewis, *Dyes Pigments*, 18 (1992) 309.
[13] S.N. Croft and D. Hinks, *J. Soc. Dyers Colour.*, 108 (1992) 546.
[14] K.P. Evans and G.L. Beaumont, *J. Chromatogr.*, 636 (1993) 153.
[15] S. Terabe, K. Otsuka, K. Ichikawa, A. Tsuchiya and T. Ando, *Anal. Chem.*, 56 (1984) 111.
[16] S.M. Burkinshaw, D. Hinks and D.M. Lewis, *J. Chromatogr.*, 640 (1993) 413.

ELSEVIER

Journal of Chromatography A, 700 (1995) 35–42

JOURNAL OF CHROMATOGRAPHY A

Improving the UV detection sensitivity of condensed polyacrylamide gel-filled capillaries using non-flow buffer-filled capillaries as a detection cell

Yi Chen[1], Joachim-Volker Höltje*, Uli Schwarz

Max-Planck-Institut für Entwicklungsbiologie, Abteilung Biochemie, Spemannstrasse 35/II, D-72076 Tübingen, Germany

Abstract

Capillary coupling techniques are suggested for the connection of a non-flow buffer-filled capillary to gel-filled capillaries as a low-background detection cell. The UV detection sensitivity of the resulting capillaries is improved at least fivefold, as demonstrated by using polyamino acids as test samples. The detection sensitivity can be further improved by using a low-background running buffer. Several ways are suggested to overcome the problems of resolution decrease and baseline drift which were observed after coupling.

1. Introduction

Highly condensed polyacrylamide gel-filled capillaries are essential in the separation of polyamino acids [1] and oligosaccharides [2–4], but these capillaries yield very poor UV detection sensitivity because the gels show strong UV absorption which increases with decrease in the detection wavelength and increase in gel concentration. To improve the detection sensitivity, laser-induced fluorescence (LIF) methods have been suggested and demonstrated to be extremely sensitive [1–4]. However, the methods can only be used with samples that are fluorescent or can be labelled by fluorescent agents. In addition, the construction of the detector is expensive compared with UV detectors. It is therefore desirable to use UV detection as an inexpensive, universal detection method, but the background of the capillaries should be greatly reduced. The best way to reduce the background is to use a buffer-filled detection cell. Dovichi and co-workers [5,6] developed an off-line detection cell, a sheath flow cell, to improve further the detection sensitivity of LIF. It also seems possible to use a non-flow buffer-filled detection cell. This detection cell can be simply constructed by the capillary coupling technique, which is fairly frequently used in capillary free-solution electrophoresis.

In this paper, we discuss a method for the rapid connection of a low-background detection cell to gel-filled capillaries. The detection sensitivity and performance, including the problem

* Corresponding author.

[1] On leave from the Institute of Chemistry, Chinese Academy of Science, Beijing, China.

0021-9673/95/$09.50
SSDI 0021-9673(94)01137-0

of baseline drift, of the resulting capillaries were investigated using polyamino acids as test samples.

2. Experimental

2.1. Materials

Tricine [N-tris(hydroxymethyl)methylglycine], bicine [N,N-bis(2-hydroxyethyl)glycine], HEPES [N-(2-hydroxyethyl)-N′-(2-ethanesulfonic acid)], MES [2-(N-morpholino)ethanesulfonic acid], Bis-Tris [bis(2-hydroxyethyl)iminotris(hydroxymethyl)methane] and boric acid (biological buffers), γ-methacryloxypropyltrimethoxysilane, poly(Asp) [poly-(α,β)-D,L-aspartate sodium salt, M_r (average molecular mass detected by viscosity) = 6850], poly(Glu) [poly-L-glutamate sodium salt, M_r = 14 300] and poly(Lys) (poly-L-lysine, M_r = 3970) were purchased from Sigma (St. Louis, MO, USA). Acrylamide and Bis [N,N′-methylenebis(acrylamide)], electrophoretically pure, were obtained from Bio-Rad Labs. (Richmond, CA, USA). TEA (triethanolamine), Tris [tris(hydroxymethyl)aminomethane], TEMED (N,N,N′,N′-tetramethylethylenediamine), APS (Ammonium peroxodisulfate) and other chemicals were all of analytical-reagent grade from Merck (Darmstadt, Germany). All fused-silica capillaries were purchased from Composite Metal Services (Worcestershire, UK). Water purified with a Millipore Super Q system was used throughout.

2.2. Preparation of cross-linked gel-filled capillaries

All the capillaries with one-end immobilized cross-linked gels were prepared according to our previously developed method [7]. One end of a new capillary is dipped into a 0.5% (v/v) modification solution of γ-methacryloxypropyltrimethoxysilane in acetic acid–methanol (1:250) [5–8] until the solution reaches a height of 5 cm from the dipped end. The capillary is kept at room temperature for 10–20 min and then filled from the end without the silane solution with a degassed gelling solution [15–20%T + 5%C[1] prepared in 0.1 *M* tricine–0.05 *M* Tris containing 0.05% (v/v) TEMED and 0.05% (w/v) APS for the initiation of polymerization]. The polymerization is started from the silanized end of the capillary by dipping the tip in hot water of 50–70°C for about 1 min. The other end of the capillary is plugged into a sealed vial [7], which is then injected with 3–4 ml of ice-cooled water to build up pressure and also to slow the polymerization rate at this end. The capillary is hung vertically for about 4 h in a shockless and draught-free location at 15–25°C, with the pressurized end up and the heated end in water at 25–35°C. After hanging, about a 2-cm length of the cooled end of the capillary is cut off. The other (heated) end is checked under a microscope with fivefold magnification for possible voids, which should be cut off. The capillary is then stored at room temperature by dipping both ends into tricine–Tris buffer. When using these capillaries for electrophoresis, the end with the immobilized gel should be applied with a negative voltage to improve the running stability of the gels, that is, for the separation of anionic samples, the end of the capillaries with the gel not immobilized is used for sample injection, but for the separation of cationic samples, the immobilized end is used for sample injection.

2.3. Preparation of linear gel-filled capillaries

A new capillary is filled with the above-mentioned silane solution and kept for 20 min. This capillary is then continuously filled with a degassed 5%T solution containing 0.05% TEMED and 0.05% APS, using a water vacuum pump, until the solution stops flowing (30–60 min). The capillary is stored as described in Section 2.2.

[1] %T is the total grams of acrylamide and Bis in 100 ml of solution and %C is the grams of Bis in 100 g of the total monomers; in the case of linear gels, %C is neglected.

2.4. Coupling of buffer-filled capillaries with gel-filled capillaries

Coating the capillaries [8]

A capillary is sequentially washed with 1 *M* NaOH, water and methanol for 30 min each. The silane solution mentioned above is filled into the capillary, which is kept for 1 h. The silanized capillary is washed with methanol and water for 20 min each and then filled with 2%T + 3%C solution containing 0.1% TEMED and 0.1% APS. After 30 min of polymerization, the cross-linked gelling solution is replaced with 3.5%T linear gelling solution (containing the same amount of TEMED and APS), and the capillary is kept for at least 1 h. The coated capillary is washed with water for 20 min and dried with an air flow for more than 20 min using a water vacuum pump. The coated capillary can be stored at room temperature for 6 months.

Linearly coupled capillaries

There are two possibilities for connecting linearly a piece of buffer-filled capillary to a gel-filled capillary: (1) a buffer-filled capillary is simply connected to the outlet of a gel-filled capillary (Fig. 1A, type A); (2) the buffer-filled capillary is inserted between gel-filled capillaries (Fig. 1A, type B). To prepare such capillaries with an O.D. of 375 μm, connectors are needed. For easy manipulation, a wide connector of 1 cm × 0.53 mm I.D. cut from a coated, flexible capillary is used. There is hence a wide gap between the capillary and the connector, which should be sealed. It is crucial, during coupling, to prevent air bubbles from being introduced into the connector and other parts of the buffer-filled capillaries. To avoid bubbles, the connector and the detection capillary are filled with a newly degassed buffer and then immersed in the buffer just before coupling [Fig. 1C, (b) and (c)]. It is also important to fix the connected part of the capillaries, which can easily be achieved by coating the connected parts with a quick-drying glue (a cyanoacrylate with UHU Vertrieb, Bühl, Germany, was used). The detailed coupling steps are as follows.

(1) To form a sealing membrane, one end of the capillaries to be connected is carefully coated with Pattex (Henkel, Düsseldorf, Germany) and kept for about 5 min. If the capillary has been filled with a gel or a buffer, the end should be covered with a drop of buffer to prevent it from drying out [Fig. 1C, (a) 3]. If the capillary is

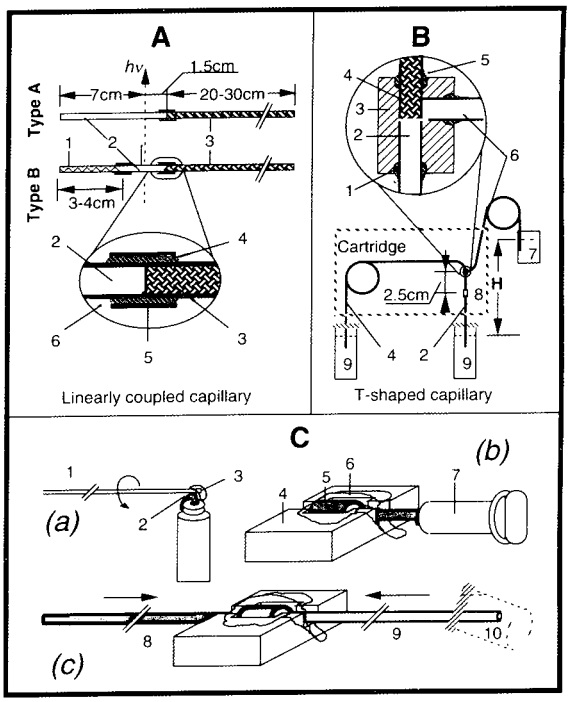

Fig. 1. (A) Structure of linearly coupled capillaries. 1 = Capillary filled with 5%T gel; 2 = buffer-filled capillary for detection; 3 = gel-filled capillary used for separation; 4 = Pattex (for sealing); 5 = connector; 6 = fixative. (B) Structure and the electrophoretic position of a T-shaped capillary. 1 = Pattex; 2 = detection capillary; 3 = connector; 4 = gel-filled capillary; 5 = fixative; 6 = buffer connection capillary (40 cm × 100 μm I.D.); 7 = buffer supply; 8 = detection window; 9 = electrode reservoirs. (C) Some important steps for connection of buffer-filled capillaries with gel-filled capillaries. (a) Coating the end of a gel- or buffer-filled capillary with Pattex; (b) holding and filling a connector; (c) a gel-filled capillary and a buffer-filled capillary are ready for plugging; the arrows show the plugging direction. 1 = Capillary; 2 = Pattex; 3 = buffer drop; 4 = holder made of glass or Perspex; 5 = connector; 6 = buffer (covering the connector totally); 7 = syringe; 8 = gel-filled capillary; 9 = buffer-filled capillary; 10 = sealed vial for filling, which can be removed just before the capillary is plugged into the connector.

empty, it is first coated with Pattex and then filled with a newly degassed buffer using a pressure method. We prefer to use a sealed vial [7]: the untreated end of the capillary is plugged into the sealed vial (with buffer), which is then pressurized by injection of 1–5 ml of air. The buffer is kept flowing until the coated end is immersed in a buffer or slipped into the connector [Fig. 1C, (c) 10].

(2) The connector is filled with the degassed buffer and immersed in the buffer. There are different ways to fill the connector and to protect or cover it with buffer. Fig. 1C, (b) shows a method used in our laboratory where the holder is made of glass or Perspex, with a chamfer for holding the connector. The buffer is injected into the connector until it flows out of the connector and covers the whole connector using a syringe or other tool.

(3) The Pattex-coated ends of the buffer-filled capillary and the gel-filled capillary are first plugged into the buffer outside the connector [the sealed vial at the end of the buffer-filled capillary, Fig. 1C, (c) 10, can now be taken off] and then plugged oppositely into the connector until the tips meet in the middle part of the connector. The connected capillaries are held manually, the buffer outside the connector is cleaned with filter-paper and the connected part is then coated with the quick-drying glue mentioned above. The fixative needs 2–5 min to dry out. It should be mentioned that the buffer used during coupling is generally 0.1 *M* tricine–0.05 *M* Tris. Some buffers, such as boric acid, dramatically decrease the adherence of the fixative.

(4) The detection window is opened at the buffer part, 1.5 cm from the tip of the separation gel (Fig. 1A). About 2 mm of the coating are manually removed using a scalpel and further cleaned with methanol.

T-shaped coupling

The construction and the electrophoretic position of a T-shaped capillary is shown in Fig. 1B. The connector (ca. $1.2 \times 0.7 \times 0.3$ cm) is made of Perspex with a T-tunnel of diameter 0.4 mm. Similarly to linear coupling, the connector is filled and covered with the degassed buffer and then mounted simultaneously with two pieces of buffer-filled capillaries and a piece of a gel-filled capillary. The capillary end is also coated with Pattex for sealing and the connected parts are fixed using the same quick-drying glue. The detection window is opened at the detection capillary, 2.5 cm from the gel tip (Fig. 1B, 8).

2.5. Electrophoresis

Before injection, all the capillaries were equilibrated with running buffer at 25°C and 200 V/cm for 60 min. When the running buffer was different from that used for the preparation of gelling solution (0.1 *M* tricine–0.05 *M* Tris), the capillaries were equilibrated with the running buffer for at least 2 h until the current became stable. The running buffer was renewed three times during equilibration, but during separation it was renewed after every run. Electrophoresis was performed using a Beckman P/ACE system 2100 controlled by an IBM SP/2 computer with System Gold software (version 7.0). The cartridges were laboratory-made so that different coupled capillaries could be mounted without breakage. The aperture mounted was 100×200 (axial direction) μm. The data sampling rate was 1 Hz and the rise time was 1 s. The sample was introduced into the capillary by dipping the injection end into the sample solution for 15–30 s (diffusion injection [9]). Because the response time of the software or the CE system requires 14 s to start a run (from the time of starting the method to the beginning of voltage application), the injection time should be least 14 s. Generally, the run should be started at the injection time minus 14 s after the capillary is dipped into the sample solution.

3. Results and discussion

3.1. Detection sensitivity

When using highly condensed gel-filled capillaries for the separation of polyamino acids, the optimum UV detection sensitivity is reached at

220 nm [1]. If the wavelength is shorter than 214 nm, no peaks can be detected. However, even at 220 nm, the sensitivity is very poor, as shown in Figs. 2A and 3A. In contrast, with a buffer-filled capillary as a detection cell, the coupled capillaries (types A and B) allow the use of a short-wavelength UV radiation for detection and a high detection sensitivity is obtained at 200 nm, which is the shortest wavelength available using our CE system. Both Figs. 2B and 3D show that, at 200 nm, the coupled capillaries (with the same bore as the detection cell) increase the peak height of poly(Asp) at least fivefold compared with the gel-filled capillaries at 220 nm (Figs. 2A and 3A). The sensitivity is further improved by coupling a wider capillary to the gel-filled capillaries (Fig. 2B–D), but at the cost of lower resolution. For maintaining the resolution, it is better to use a detection capillary slightly thinner than the separation capillary (Fig. 3C). If the detection capillary is too narrow, both the resolution and detection sensitivity will be reduced, as shown in Fig. 3B.

The detection sensitivity of the coupled capillaries also depends on running buffer, similarly

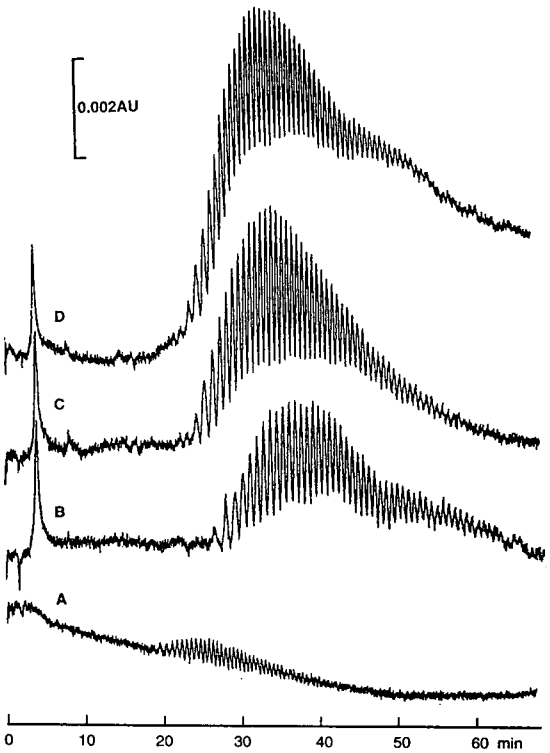

Fig. 2. Comparison of the detection sensitivity of a 15%T + 5%C gel-filled capillary (A) without detection cell and with (B–D) untreated buffer-filled detection cell (type A). A sample of poly(Asp) in water (50 mg/ml) was injected by diffusion into the capillary. Electrophoreses was performed at constant current (4.4 μA) and monitored at (A) 220 nm or (B–D) 200 nm. Detection cells were filled with 0.1 *M* tricine–0.05 *M* Tris. The following capillaries were used: (A) 30/37 cm (separation/total length) × 50 μm I.D.; (B) 32 cm × 50 μm I.D. (gel) + 8.5 cm × 50 μm I.D. (buffer); (C) 32 cm × 50 μm I.D. (gel) + 8.5 cm × 75 μm I.D. (buffer); (D) 32 cm × 50 μm I.D. (gel) + 8.5 cm × 100 μm I.D. (buffer).

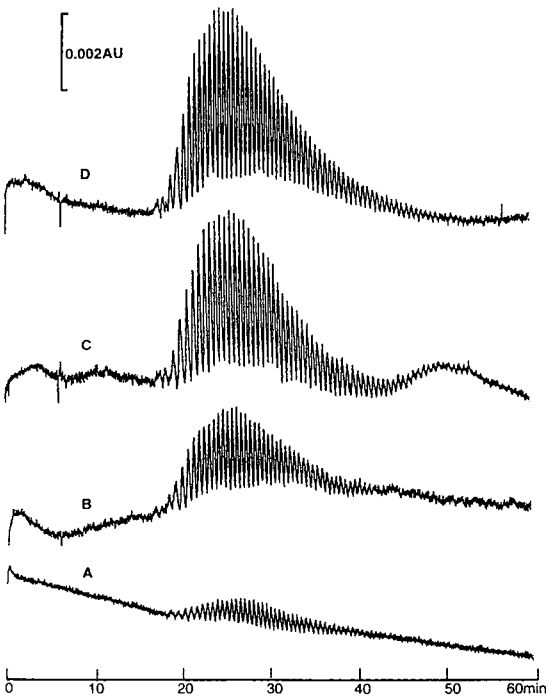

Fig. 3. Comparison of the detection sensitivity and performance of a 15%T + 5%C gel-filled capillary (A) without detection capillary and (B–D) with coated detection capillaries (type B). Electrophoresis was performed at 16 μA with the following capillaries: (A) 30/37 cm (separation/total length) × 100 μm I.D.; (B) 28.5 cm × 100 μm I.D. (gel) + 5.5 cm × 50 μm I.D. (buffer) + 3 cm × 100 μm I.D. (5%T gel); (C) 28.5 cm × 100 μm I.D. (gel) + 5.5 cm × 75 μm I.D. (buffer) + 3 cm × 100 μm I.D. (5%T gel); (D) 28.5 cm × 100 μm I.D. (gel) + 5.5 cm × 100 μm I.D. (buffer) + 3 cm × 100 μm I.D. (5%T gel). Other conditions as in Fig. 2.

to free-solution capillary electrophoresis. Fig. 4A, B, D and G show that the peak height of poly(Lys), which is positively charged, may be increased another fivefold when a low-background running buffer is used such as Bis-Tris–HCl or Bis-Tris–H_3PO_4. The overall improvement of the detection sensitivity is greater than one order of magnitude in this case.

3.2. Resolution

The resolution will be reduced after coupling since an interface and/or a dead volume exist inside the connected part. To improve the resolution, we first used the tube type A with an untreated (bare) capillary as the detection cell. For the separation of anionic samples, the bare detection capillaries will induce an electroosmotic sheath flow, that is, the buffer flows towards the gel end in the layer near the capillary wall and returns to the electrode reservoir from the centre of the tube. However, although the detection sensitivity is dramatically improved, the resolution losses are greater than 20% (Fig. 2B–D). The reasons are no clear. It seems that the interaction of the solutes with the capillary wall may account for this phenomenon because the baseline generally rises when or after the peaks emerge (see Fig. 2D). It is also possible that the electroosmotic sheath flow causes mixing of the separated peaks. We then turned to the tube type B with coated detection capillaries or non-flow detection cells. To decrease the influence of the interface and the dead volume, wider capillaries of 75–100 μm I.D. were used. Fig. 3B–D show that, after the detection capillary has been coated, the system peaks (before 10 min in both Figs. 2 and 3, which can be observed without the injection of samples) are greatly reduced, the separation time is similar to that with the gel-filled capillary and the resolution losses are less than 10%, depending on the bore of the detection capillaries. Some part of the resolution losses in Fig. 3B–D is caused by the shorter separation gels used.

Interestingly, the buffer distance between the gel tip and the detection window, ranging from 0.6 to 5 cm, only slightly influences the resolution (but influences the separation time). In the separation of poly(Lys) with the linearly coupled capillaries, we found that the running buffer greatly influenced the resolution. The use of tricine–Tris as a running buffer, which is an excellent buffer for the separation of anionic polyamino acids, yielded no or an extremely poor separation of the poly (Lys) (Fig. 4A and D), often accompanied by spikes, which implies that this buffer might induce aggregation of the sample. Some separation was observed when the Tris as the buffer was replaced with Bis-Tris (Fig. 4E) and the separation was improved by using Bis-Tris–MES buffer at pH 5.5–6.5 (compare Fig. 4E and F). Interestingly, the counter ions of the buffer (having opposite charge to the solutes) greatly affect the resolution of poly-(Lys). Fig. 4B and G show that chloride reduces the resolution whereas phosphate increases the resolution compared with MES (Fig. 4C and F). These phenomena mean that, when using the coupled capillaries for the separation of cationic polyamino acids, it is possible to improve the resolution by optimizing the running buffer and pH, but further investigations should be made.

In contrast, the pH (>7) and the components of running buffer have only a limited influence on the separation of anionic polyamino acids when using the coupled capillaries. Various organic buffers such as tricine, bicine, HEPES and MES with Tris, TEA or Bis-Tris as the counter ions yield similar resolutions of poly(Asp) and poly(Glu) (data not shown). However, some inorganic buffers such as borate yield no or very broad peaks of the anionic polyamino acids.

The simplest way to improve the separation is to increase the gel concentration (compare Fig. 4F and C), but the separation time will also be increased dramatically. For the separation of the above-mentioned polyamino acids, a gel of 20%T + 5%C is adequate.

3.3. Baseline drift

A problem in using linearly coupled capillaries is that the baseline drifts after the capillaries have been run for several hours. The drift may be greater than 0.01 absorbance per hour at 200

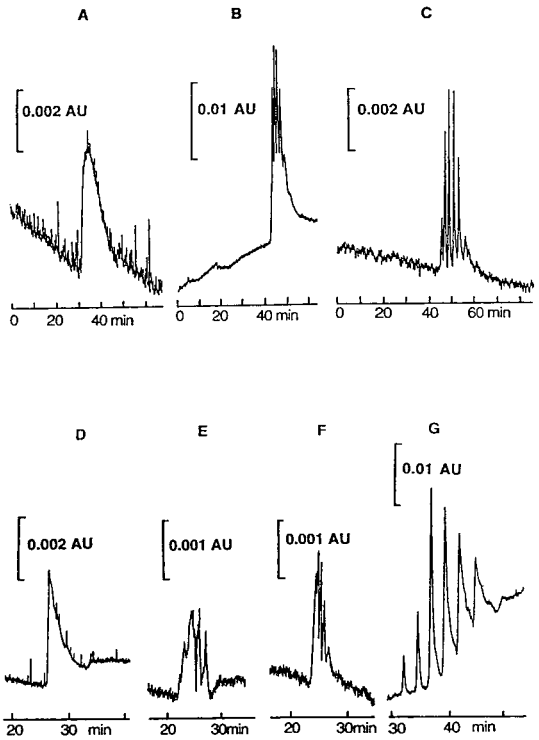

Fig. 4. Effects of pH and buffer composition on the detection sensitivity and resolution of poly(Lys) with a type B capillary. A sample of poly(Lys) in water (50 mg/ml) was injected by diffusion (15 s) into the capillaries and detection was effected at 200 nm. Different capillaries and running conditions were compared. (A) Capillary, 24 cm × 75 μm I.D. (20%T + 5%C gel) + 5.5 cm × 100 μm I.D. (buffer) + 3 cm × 100 μm I.D. (5%T gel); buffer, 0.1 *M* Tricine–Tris (pH 7.7); conditions, 5 kV/6.8 μA. (B) Capillary, 24 cm × 75 μm I.D. (20%T + 5%C gel) + 5.5 cm × 100 μm I.D. (buffer) + 3 cm × 100 μm I.D. (5%T gel); buffer, 0.1 *M* Bis-Tris–HCl (pH 6.0); conditions, 4.5 kV/12 μA. (C) Capillary, 24 cm × 75 μm I.D. (20%T + 5%C gel) + 5.5 cm × 100 μm I.D. (buffer) + 3 cm × 100 μm I.D. (5%T gel); buffer, 0.05 *M* Bis-Tris–0.1 *M* MES; conditions, 7 kV/8 μA. (D) Capillary, 30 cm × 75 μm I.D. (15%T + 5%C gel) + 5.5 cm × 75 μm I.D. (buffer) + 3 cm × 75 μm I.D. (5%T gel); buffer, 0.1 *M* tricine–Tris (pH 7.7); conditions, 6.5 kV/8.6 μA. (E) Capillary, 30 cm × 75 μm I.D. (15%T + 5%C gel) + 5.5 cm × 75 μm I.D. (buffer) + 3 cm × 75 μm I.D. (5%T gel); buffer, 0.1 *M* Bis-Tris–tricine (pH 7.7); conditions, 6.5 kV/ca. 3 μA. (F) Capillary, 30 cm × 75 μm I.D. (15%T + 5%C gel) + 5.5 cm × 75 μm I.D. (buffer) + 3 cm × 75 μm I.D. (5%T gel); buffer, 0.05 *M* Bis-Tris–0.1 *M* MES; conditions, 6 kV/7.7 μA. (G) Capillary, 30 cm × 75 μm I.D. (15%T + 5%C gel) + 5.5 cm × 75 μm I.D. (buffer) + 3 cm × 75 μm I.D. (5%T gel); buffer, 0.05 *M* Bis-Tris–H_3PO_4 (pH 6.0); conditions, 7 kV/12 μA.

nm. This phenomenon is possibly due to the unbalanced migration of the buffer ions from the gel to the buffer or vice versa, as the applied electric field across the capillaries is discontinuous. This can be demonstrated by using T-shaped capillaries. The T-shaped capillaries can suppress the unbalanced migration because of the buffer flow from the upper capillary (Fig 1B, 6) to the detection capillary (Fig. 1B, 2). Fig. 5 shows a comparison between T-shaped and linearly coupled capillaries. We found that the baseline stability of the T-shaped capillaries depended on the hydrodynamic height or the difference in the buffer levels between vial 7 and the electrode reservoir 9 (*H* in Fig. 1B). When *H* was between 0 and 2 cm, baseline drift occurred, but when *H* was greater than 10 cm, the baseline became stable. Unfortunately, although the coupled T-shaped capillaries can stabilize the baseline by increasing the value of *H*, the detection sensitivity is dramatically reduced because the separated bands will be diluted when they pass through the detection capillary. To maintain a moderate detection sensitivity, the gel-filled capillary should be at least as wide as 75 μm I.D. and *H* should be less than 15 cm. If *H* is between 10 and 15 cm, the detection sensitivity of the T-shaped capillary is reduced to about 50% compared with the linearly coupled capillary. The peak height shown in Fig. 5B is higher than that in Fig. 5A. The reasons are that, first, the

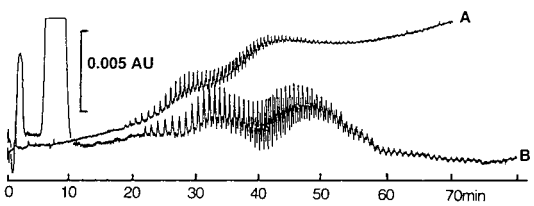

Fig. 5. Comparison of the baselines with differently coupled capillaries. A sample of (A) 50 or (B) 100 mg/ml of poly(Glu) in water was injected by diffusion (30 s) into the capillary coupled to a 0.1 *M* tricine–0.05 *M* Tris buffer-filled detection cell. Detection was effected at 200 nm. (A) Linearly coupled capillary (type A), 30 cm × 50 μm I.D. (15%T + 5%C gel), with 8.5 cm × 50 μm I.D. detection capillary; conditions, 6 kV/ca. 4 μA. (B) T-shaped capillary, 30 cm × 100 μm I.D. (15%T + 5%C gel), with 9.5 cm × 100 μm I.D. detection capillary; conditions, 6 kV/ca. 15.5 μA.

capillary used to obtain Fig. 5B is wider than that for Fig. 5A, and second, the sample concentration in Fig. 5B is higher than that in Fig. 5A. Another problem in using the T-shaped capillary is that bubbles accumulate very easily inside the connector, disrupting the separation. The capillaries should be re-coupled in this case.

The baseline drift of the linearly coupled capillaries also depends on the running buffers, samples and detection wavelengths. The baseline drift at 220 nm is about 60% less than that at 200 nm. When the detection wavelength is set at 280 or 254 nm, the baseline becomes fairly stable. For the separation of poly(Lys), Bis-Tris–MES buffer yields a fairly stable baseline, but if the MES is replaced with phosphate or chloride, the baseline drifts positively (Fig. 4C–B and F–D). In the analysis of anionic polyamino acids with tricine–Tris as the running buffer, the baseline drifts positively but can be suppressed by replacing Tris with TEA. The baseline can further be stabilized if the detection capillary is inserted between gels (tube type B). Hence, the general approaches for overcoming the problem of baseline drift include (1) using a type B capillary and replacing the detection capillary when the baseline begins to drift substantially; the replacement or re-coupling takes about 10–15 min if the coated detection capillaries are at hand and a gel-filled capillary allows more than ten re-couplings; (2) carefully selecting the components of the running buffer; (3) using a longer detection wavelength whenever possible. In addition, an electronic approach is to subtract a baseline obtained just before or after the separation from the electropherograms. This is possible by using the System Gold software.

Acknowledgement

We thank Victoria Kastner for improving the English of the manuscript. The financial support of the Alexander von Humboldt foundation is gratefully acknowledged by Y. C.

References

[1] V. Dolnik and M. Novotny, *Anal. Chem.*, 65 (1993) 563–567.
[2] J. Liu, O. Shirota and M. Novotny, *J. Chromatogr.*, 559 (1991) 223–235.
[3] J. Liu, O. Shirota and M. Novotny, *Anal. Chem.*, 64 (1992) 973–975.
[4] J. Liu, V. Dolnik, Y.-Z. Hsieh and M. Novotny, *Anal. Chem.*, 64 (1992) 1328–1336.
[5] D.Y. Chen, H.P. Swerdlow, H.R. Harke, J.Z. Zhang and N.J. Dovichi, *J. Chromatogr.*, 559 (1991) 237–246.
[6] M.-J. Rocheleau and N.J. Dovichi, *J. Microcol. Sep.*, 4 (1992) 449–453.
[7] Y. Chen, J.-V. Höltje and U. Schwarz, *J. Chromatogr. A*, 680 (1994) 63–71.
[8] S. Hjertén, *J. Chromatogr.*, 347 (1985) 191–198.
[9] Y. Chen and A. Zhu, *Sepu (Chin. J. Chromatogr.)*, 7 (1990) 5–10.

ELSEVIER

Journal of Chromatography A, 700 (1995) 43–49

JOURNAL OF CHROMATOGRAPHY A

Enantiomeric resolution of chiral imidazole derivatives using capillary electrophoresis with cyclodextrin-type buffer modifiers

Bezhan Chankvetadze[1], Gabriele Endresz, Gottfried Blaschke*

Department of Pharmaceutical Chemistry, University of Münster, Hittorfstrasse 58–62, 48149 Münster, Germany

Abstract

Enantiomeric resolutions of some chiral pharmaceuticals containing the imidazole (1,3-diazole) moiety were carried out using capillary electrophoresis. Various native cyclodextrins (α-, β- and γ-cyclodextrin) and derivatized cyclodextrins (hydroxypropyl-, and sulfobutyl ether-β-cyclodextrin) were used as chiral buffer modifiers. The effects of the cavity size, the structure and the charge of the selectors on the chiral recognition ability were evaluated. The influence of the type and concentration of the organic modifier on the separation of miconazole enantiomers and the pH of the run buffer on the separation of enilconazole enantiomers was also studied.

1. Introduction

Many imidazole derivatives are widely used or recommended for pharmaceutical use as antimycotics (clotrimazole, miconazole, enilconazole, etc.), antineoplastic agents (dacarbazine), antiepileptics (nafimidon, denzimol) cytostatics (erbulozol), thromboxane synthetase inhibitors (dazoxiben), etc. [1]. Some of the pharmaceutically used imidazole derivatives contain a chiral carbon atom and therefore exist as racemic mixtures of the enantiomers. Substantial differences in pharmacokinetic, pharmacodynamic and toxic properties between the enantiomers of many chiral drugs are well established [2,3].

A prerequisite for the accurate study of stereoselective effects of the action of chiral drugs is the development of a versatile and accurate method for the resolution of enantiomers. Capillary electrophoresis (CE) meets this requirement and has been rapidly established as the method of choice for enantiomeric analysis during the last few years [4–13]. The application of new types of chiral selectors with higher efficiency is of primary importance in this area at present.

The chiral resolution of some racemic imidazole and triazole derivatives using CE has been reported recently [5–8], but no systematic study has yet been performed. This study was conducted in order to evaluate systematically the resolution of chiral drugs containing an imidazole moiety by CE. The effects of the concentration of the chiral selector and the organic modifier and the pH of the run buffer on the enantioseparation were studied.

* Corresponding author.

[1] Permanent address: Department of Chemistry, Tbilisi State University, Chavchavadze Ave. 1, 380028 Tbilisi, Georgia.

0021-9673/95/$09.50
SSDI 0021-9673(94)01065-X

2. Experimental

2.1. Equipment

A Grom 100 capillary electrophoresis system (Grom, Herrenberg, Germany), equipped with a Linear Instruments (Reno, NV, USA) UVIS 200 detector and a HP 3396 A integrator (Hewlett-Packard, Avondale, PA, USA), was used with an untreated fused-silica capillary (Grom) of total length 61 cm and effective length 44 cm × 50 μm I.D. The electric field was 400 V/cm and the temperature was 21 ± 1°C. The samples were introduced hydrostatically (10 cm) at the anodic end of the capillary during 5 s. The detection of the solutes was carried out at 210 nm. The anode and cathode buffers had the same pH and molarity as the run buffer but contained no chiral selectors.

2.2. Chemicals and reagents

The racemic drugs (Fig. 1) were gifts from the manufacturers. SBE-β-CD (degree of substitution ca. 3.14, $M_r = 1684$) was a kind gift from Professor J.F. Stobaugh and Professor V.J. Stella (Center for Drug Delivery Research, University of Kansas, Lawrence, KS, USA).

α-, β-, γ- and HP-β-CD were obtained from Wacker Chemie (Munich, Germany), analytical-reagent grade KH_2PO_4, Na_2HPO_4, H_3PO_4 and NaOH from Merck (Darmstadt, Germany) and HPLC-grade methanol, acetonitrile and 2-propanol from J.T. Baker (Deventer, Netherlands).

2.3. Preparation of solutions buffer and sample solutions

Stock standard solutions of 50 m*M* KH_2PO_4 and 50 m*M* Na_2HPO_4 were prepared in doubly distilled, deionized water. The pH was adjusted with 0.5 *M* H_3PO_4 or 0.5 *M* NaOH. The run buffers were prepared accordingly after the addition of appropriate amounts of the chiral selectors. All solutions were filtered and degassed by sonication before use. Stock standard solutions of 1 mg/ml of the racemic drugs were prepared, stored at 4°C and diluted to 60 μg/ml before use.

3. Results and discussion

3.1. Effect of the type of chiral selector on chiral recognition

The structures of eight representative members of chiral imidazole derivatives are shown in Fig. 1. The results of the resolution of these derivatives by CE using five native and derivatized cyclodextrins as chiral selectors are summarized in Table 1. The effect of the cavity size is obvious. Apparently α-CD does not bind at least stereoselectively with any of the imidazole derivatives studied. In contrast, the enantiomers of most of them are resolved using γ- and β-CD and also with uncharged (HP-β-CD) and charged (SBE-β-CD) derivatives. HP-β-CD seems to have better chiral recognition abilities than the native cyclodextrins. Thus, enantiomers of miconazole (**4**) and econazole (**5**) could not be resolved using native α-, β- or γ-CD, whereas the enantiomers of these drugs were baseline resolved using HP-β-CD. The chiral selector SBE-β-CD seems to be exceptionally effective and gives baseline separations for most of the racemic compounds in the concentration range 0.1–1.0 m*M* in the run buffer. In Table 1 the decisive role of hydrophobic forces in selectand–selector interactions is demonstrated. In particular, a hydrophobic phenyl moiety is absent in the ornidazole molecule (**2**) and, moreover, a hydrophilic hydroxy group is present. As a result, the enantiomers of this compound could not be resolved using any of the chiral selectors used.

3.2. Effect of concentration of chiral selector on the resolution of enantiomers

The concentration dependence of the enantiomeric resolution (R_s) was studied with racemic enilconazole (**5**) as an example. It seems noteworthy that nearly the same resolution (R_s) and selectivity (α) were achieved with chiral selector concentrations varying in range 0.07–12.5 m*M* depending on their type (Fig. 2).

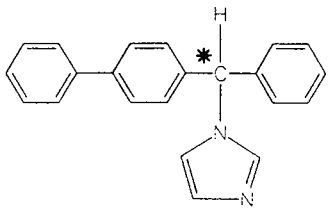

Bifonazole (1)

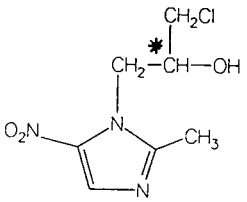

Ornidazole (2)

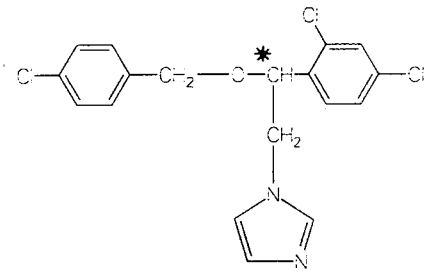

Econazole (3)

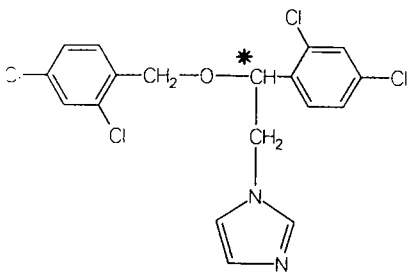

Miconazole (4)

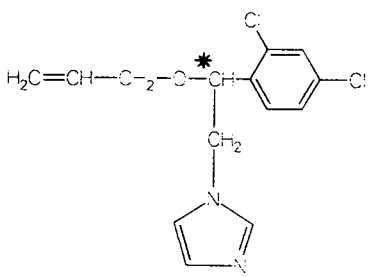

Enilconazole (5)

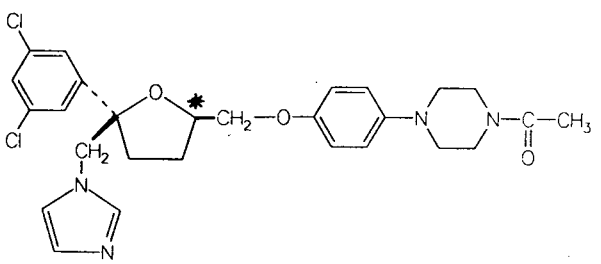

Ketoconazole (6)

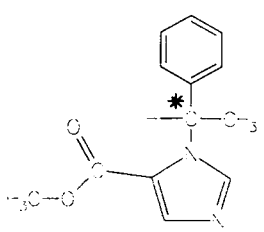

Metomidate (7)

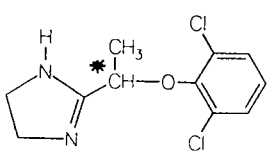

Lofexidine (8)

Fig. 1. Structures of the racemic drugs.

Table 1
Chiral separation of imidazole derivatives

Compound	50 m*M* α-CD–10% MeOH		20 m*M* β-CD–10% MeOH		50 m*M* γ-CD–10% MeOH		20 m*M* HP-β-CD–10% MeOH		0.1 m*M* SBE-β-CD–20% MeOH		1 m*M* SBE-β-CD–0% MeOH	
	t_1/t_2	R_s	t_1/t_2	R_s	t_1/t_2	R_s	t_1/t_2	R_s	t_1/t_2	R_s	t_1/t_2	R_s
Bifonazole	14.86	–[a]	13.59	–[a]	16.95	–[a]	16.90	–[a]	15.20/15.33	1.01	–	
Econazole	16.78	–[a]	15.39	–[a]	18.30	–[a]	15.80/16.10	1.60	12.92/13.69	2.46	–	
Enilconazole	14.97	–[a]	11.96/12.30	1.92	12.69/13.16	2.87	12.33/13.19	6.75	7.80/8.10	2.34	–	
Ketoconazole	14.35	–[a]	11.16/11.25	0.61	14.87/14.96	0.67	13.71	–[a]	12.01[b]/12.62[b]	1.66[b]	–	
Lofexidine	9.01	–[a]	10.44/10.59	1.47	11.33/12.01	5.10	9.16/9.40	2.72	6.21	–[a]	8.80/9.09	1.03
Metomidate	10.68	–[a]	9.76/10.17	2.79	13.61/14.46	5.85	12.35/12.81	3.45	8.85	–[a]	9.03/9.26	2.21
Miconazole	17.19	–[a]	15.06	–[a]	20.20	–[a]	15.46/15.74	1.55	12.41/13.07	1.44	–	
Ornidazole	30.07	–[a]	34.00	–[a]	32.00	–[a]	30.80	–[a]	19.17	–[a]	–	

[a] No enantioseparation.
[b] 0.1 m*M* SBE-β-CD–40% MeOH.

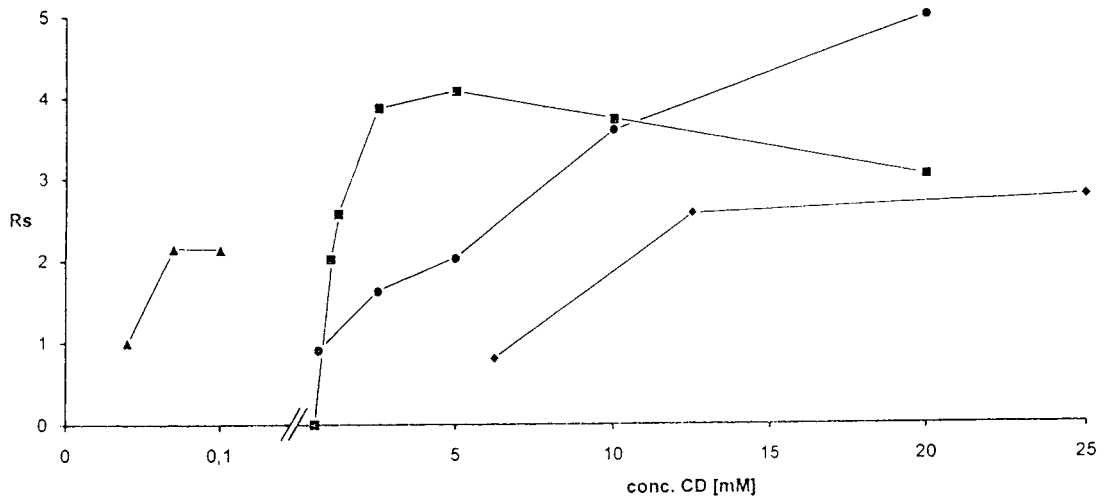

Fig. 2. Plot of resolution (R_s) of enilconazole (**5**) enantiomers vs. concentration of the various cyclodextrins in the run buffer. Conditions: 50 m*M* phosphate buffer (pH 3.0); 400 V/cm; detection at 210 nm. ■ = β-CD; ● = HP-β-CD; ◆ = γ-CD; ▲ = SBE-β-CD.

3.3. pH dependence of the separation of enilconazole

Enilconazole (**5**) seems to be protonated at a pH lower than ca. 6.0–7.0, hence the separation of its enantiomers seems not to be possible at pH > 7 using uncharged cyclodextrins as chiral buffer modifiers. Fig. 3 shows the chiral separation of enilconazole with a run buffer containing various amount of SBE-β-CD and β-CD

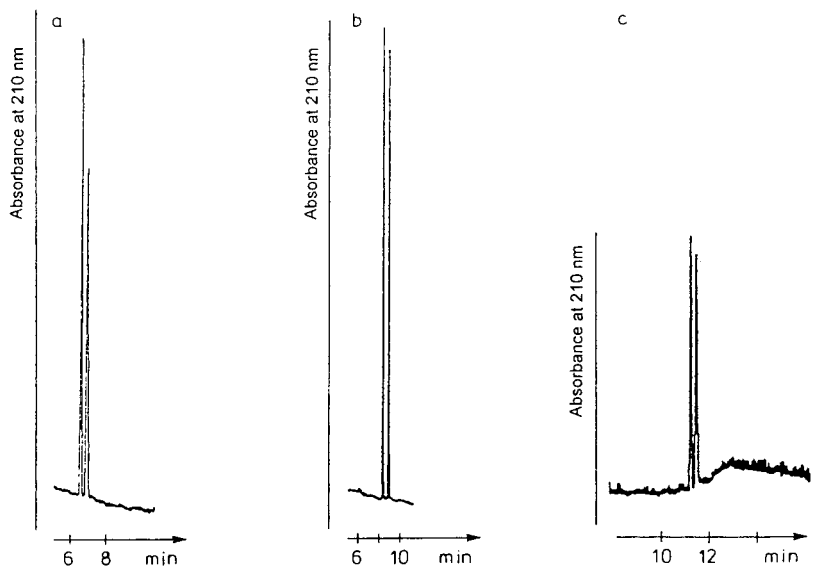

Fig. 3. Separation of enilconazole (**5**) enantiomers. Conditions: 50 m*M* phosphate buffer; detection at 210 nm; (a) pH 3.0, 0.1 m*M* SBE-β-CD–10% methanol, 400 V/cm; (b) pH 3.0, 2.5 m*M* β-CD–10% methanol, 400 V/cm; (c) pH 9.0, 1.0 m*M* SBE-β-CD–10% methanol, 200 V/cm.

in acidic (pH 3.0) and alkaline (pH 9.0) media. Both chiral selectors discriminate between enilconazole enantiomers at pH 3.0, but the amount of SBE-β-CD needed is markedly smaller than that of β-CD. At pH 9.0 a run buffer containing 1 m*M* SBE-β-CD permits adequate enantioseparation, whereas β-CD concentrations as high as 20 m*M* do not show any sign of enantioseparation with buffer of the same pH.

3.4. *Effect of organic modifier on selectivity and peak resolution*

The influence of the concentration of the organic modifier in enantioseparations was also studied. The important role of organic modifiers in CE enantioseparation was first reported by Fanali [4]. It has been considered that the organic modifier can have two roles: (a) improving the solubility of chiral substances and (b) decreasing the affinity of chiral compounds for the hydrophobic cavity of chiral selectors. The former factor diminishes the interaction of substances with the capillary wall and leads to decreased peak broadening whereas the latter needs to be optimized as decreasing the selectand–selector interactions also improves the peak shape but sometimes is accompanied by a substantial loss of selectivity.

Fig. 4 shows the dependence of the peak resolution on the content of organic modifier in the run buffer. There is always one optimum concentration of the organic modifier for chiral resolution. This is to be expected as the result of above-mentioned two opposite effects: increase in efficiency (N) and decrease in selectivity (α) with increase in the concentration of organic modifier. The effect with 2-propanol seems to be most pronounced.

4. Conclusions

The enantiomeric resolution of racemic imidazole derivatives was performed using high-performance CE with various cyclodextrin-type chiral selectors in the run buffer. The effects of the cavity size, the structure and the charge of the chiral selector were studied. The influence of the type and concentration of the organic modifier on the separation of the miconazole enantiomers and of the pH of the run buffer on the separation of enilconazole enantiomers was also investigated. α-CD does not exhibit a chiral recognition ability for the imidazole derivatives studied. HP-

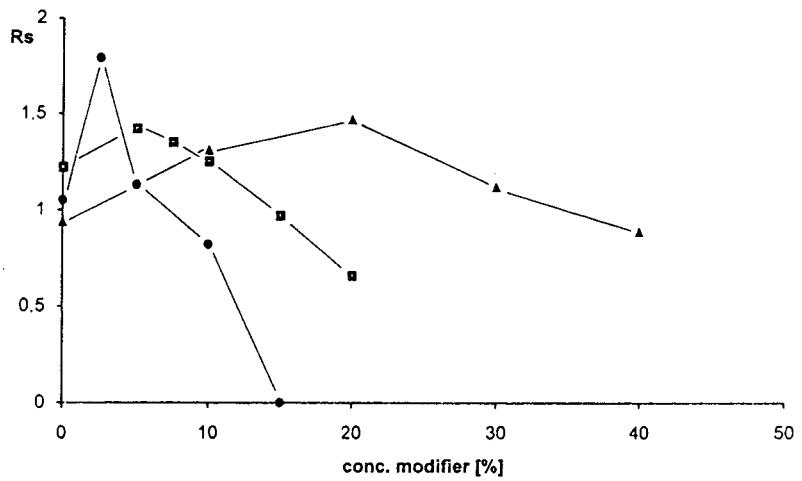

Fig. 4. Plot of resolution (R_s) of miconazole (**4**) enantiomers vs. concentration of various organic modifiers in the run buffer. Conditions: 50 m*M* phosphate buffer (pH 3.0); 0.1 m*M* SBE-β-CD; 400 V/cm; detection at 210 nm. ▲ = Methanol; □ = acetonitrile; ○ = 2-propanol.

β-CD shows better chiral recognition ability than the native CDs. The negatively charged SBE-β-CD seems to be the most efficient chiral selector.

Acknowledgements

The authors thank the Heinrich-Hertz-Stiftung for a stipend (B.C.), the Deutsche Forschungsgemeinschaft for financial support and Professors J.F. Stobaugh and V.J. Stella (University of Kansas, Lawrence, KS, USA) for a sample of SBE-β-CD.

References

[1] J.E.F. Reynolds (Editor), *Martindale, The Extra Pharmacopoeia*, The Pharmaceutical Press, London, 30th ed., 1993, pp. 315, 368, 523 and 917.
[2] E.J. Ariëns, W. Soudijn and P.B.M.W.M. Timmermans, *Stereochemistry and Biological Activity of Drugs*, Blackwell, Oxford, 1983.
[3] I.W. Wainer (Editor), *Drug Stereochemistry*, Marcel Dekker, New York, 2nd ed., 1993.
[4] S. Fanali, *J. Chromatogr.*, 545 (1991) 437.
[5] M. Heuermann and G. Blaschke, *J. Chromatogr.*, 648 (1993) 505.
[6] R. Futura and T. Doi, *J. Chromatogr. A*, 676 (1994) 431.
[7] S.G. Penn, D.M. Goodall and J.S. Loran, *J. Chromatogr.*, 636 (1993) 149.
[8] S.G. Penn, E.T. Bergström, D.M. Goodall and J.S. Loran, *Anal. Chem.*, 66 (1994) 2866.
[9] N.W.H. Nielen, *Anal. Chem.*, 65 (1993) 885.
[10] J.M. Dethy, S. De Broux, M. Lesne, J. Longstreth and P. Gilbert, *J. Chromatogr. B*, 654 (1994) 121.
[11] Y.Y. Rawjee and G. Vigh, *Anal. Chem.*, 66 (1994) 619.
[12] C. Quang and M.G. Khaledi, *J. High Resolut. Chromatogr.*, 17 (1994) 99.
[13] B. Chankvetadze, G. Endresz and G. Blaschke, *Electrophoresis*, 15 (1994) 804.

ELSEVIER

Journal of Chromatography A, 700 (1995) 51–58

JOURNAL OF CHROMATOGRAPHY A

Resolution of the enantiomers of oxamniquine by capillary electrophoresis and high-performance liquid chromatography with cyclodextrins and heparin as chiral selectors

Adel M. Abushoffa, Brian J. Clark*

Pharmaceutical Chemistry, School of Pharmacy, University of Bradford, Bradford BD7 1DP, UK

Abstract

The methods of separation of the enantiomers of the chiral drug oxamniquine are compared, between HPLC with either cyclodextrins and their related derivatives as chiral selectors in the mobile phase or immobilised in a chiral stationary phase (as Cyclobond I and II) and between capillary zone electrophoresis (CZE) where the cyclodextrins are added to the buffer solution. The HPLC experiments, which included structured method optimisation were largely unsuccessful in resolving the enantiomers, with the exception of when a Chiral-AGP protein stationary phase was introduced into the programme. However although this chiral stationary phase provided baseline resolution of the enantiomers the stability of the method was suspect to small changes in the pH (0.2 units). In contrast the CZE method developed for both cyclodextrins and their derivatives gave good resolution of the enantiomers and method stability (R.S.D. $< 1\%$, $n = 10$ on precision). The basis of the interaction mechanism between selector and selectand was shown as a 1:2 relationship of cyclodextrin to analyte by NMR. In addition the polysaccharide, heparin was investigated as a chiral additive and excellent resolution of the oxamniquine was achieved with 3 m*M* heparin in 50 m*M* sodium dihydrogenphosphate (pH 3.0) as buffer in CZE, which also gave a stable procedure. This method allowed the detection of each of the enantiomers in the presence of the other down to 0.23% (m/m). The overall composition of the heparin material from different sources can however be slightly variable and this can result in small differences in resolution capability.

1. Introduction

Capillary electrophoresis (CE) utilised in a free solution or micellar electrokinetic mode with a chiral selector introduced into the run buffer, has been shown to be particularly useful for the resolution of the enantiomers of chiral drugs [1]. Currently the most powerful method is through the use of cyclodextrins and their related derivatives as selectors in either CE mode, although the introduction of proteins [2] and crown ethers has been considered [3]. By this former mode, a wide range of chiral drugs have been separated for assay in pharmaceutical preparations and biological fluids often with resolution or improved resolution over the cognate procedure with mobile phase additives or the requisite chiral stationary phase in HPLC. This contrast in resolution between CE incorporating cyclic oligosaccharides and HPLC, is considered to be due to the many different contributions to the stability equilibrium and includes differences in the effects from the operational variables on the selector-selectand binding. Although the

* Corresponding author.

0021-9673/95/$09.50
SSDI 0021-9673(95)00111-5

primary mechanisms of interaction may involve: inclusion within the cyclodextrin cavity relative to the hydrophobicity, size and shape of the analyte, multiple hydrogen bonding and other attractive and repulsive interactions which are similar in both cases. In a number of examples, however, it has been shown with these techniques and particularly in CE, that the interactions are not always concentrated around the inclusion into the cyclodextrin cavity, but it is possible that multiple complexation or the formation of diamers or triamers of either the selector or selectand in situ may complex more predominantly through interactions such as hydrogen bonding, and other attractive and repulsive effects. The accumulation of these parameters therefore combines to provide enantioselective equilibria differences in CE over those cognate separations in HPLC which are often manifest as improved resolution. In pharmaceutical analysis it is also important in method development, to consider the operational improvements of CE relative to HPLC, such as the ease of method development and optimisation through the experimental programme [4] together with generally better peak efficiency, which all go together to raise CE firmly alongside HPLC as a suitable method for examination of chiral drugs.

Both the conventional α-, β- and γ-cyclodextrins and the relatively large number of mainly alkylated derivatised cyclodextrins, which now include neutral and charged materials [5] were initially used where solubility limits in cyclodextrin concentration precluded the attainment of an optimised enantiomer resolution. However it was quickly shown that these alkylated derivatives gave the capability of achieving differences in resolution over the original cyclodextrin materials [6]. This is particularly when an extended structural addition is made to the β-cyclodextrin, such as in the formation of hydroxypropyl- and hydroxyethyl-β-cyclodextrin. In addition with the derivatives, the degree of substitution of the secondary hydroxyls (known as the RS value) on the cyclodextrin cavity can lead to marked differences in the observed enantiomeric resolutions as shown by Valko et al. [7].

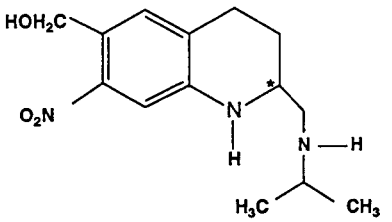

Fig. 1. Structure of oxamniquine.

In this study it was proposed to examine methods by HPLC and CE for resolution of the antischistosmiasis drug oxamniquine (Fig. 1), which is marketed in Africa and Brazil as a racemic mixture in the pharmaceutical preparation. In the case of developed HPLC methods, questions would be asked about the ruggedness of these methods for assay of the drug. Comparisons would then be made between HPLC and CE when conventional cyclodextrins and their derivatives were included within the electrolyte solution. In optimisation of the methods further, consideration would be given to the nature of the chiral selector and its ability to give a stable robust procedure for assay of the drug as a racemic mixture and as the enantiopure component. For this extension, the linear polysaccharide heparin (Fig. 2) [8] would be examined and its performance against the cyclodextrins assessed.

2. Experimental

2.1. Materials

β-Cyclodextrin was obtained from Sigma (St. Louis, MO, USA) and heparin from Sigma and Lancaster Synthesis (Morecambe, UK) and hydroxypropyl-β-cyclodextrin from Aldrich (Steinheim, Germany). Buffer materials and other general chemicals were purchased from either BDH (Poole, UK) or Hopkin and Williams (Chadwell Heath, UK).

Oxamniquine and its individual enantiomers

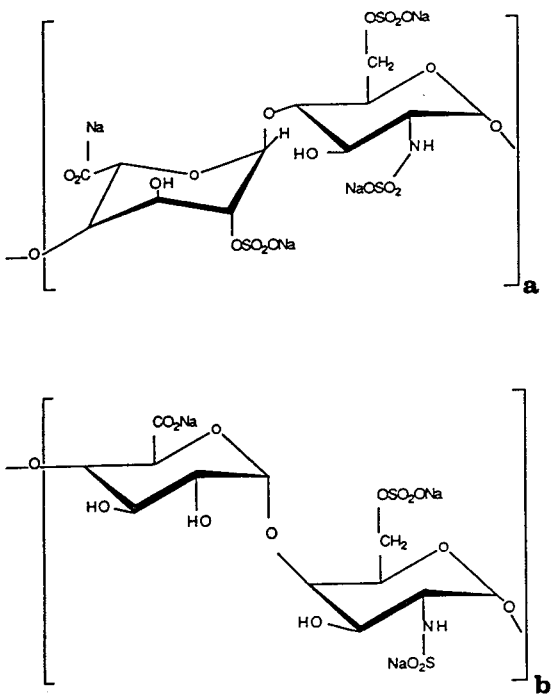

Fig. 2. Structure of heparin, showing the two forms which can vary in their proportions in heparin samples from different sources [8]. The composition of a + b is in the range 8–15 molecules in samples from different sources.

were kindly supplied by Pfizer (Pfizer Central Research, Sandwich, UK). For initial method development experiments racemic oxamniquine and the individual enantiomers were prepared at about 60 μg/ml in methanol–water (60:40, v/v) with each sample solution filtered through a 0.22-μm filter before use.

2.2. Apparatus

HPLC system

This consisted of a ConstaMetric 3000 dual reciprocating pump (LDC, Riviera Beach, FL, USA) and a Pye Unicam PU 4020 variable-wavelength UV detector (wavelength 246 nm) (ATI-Unicam, Cambridge, UK) with data manipulation through a Hewlett-Packard HP3394A computing integrator (Waldbronn, Germany). The sample was introduced through a Rheodyne 7125 injection valve, fitted with a 20-μl loop.

For mobile phase additive experiments the achiral stationary phase was either 5-μm C_{18}-Hypersil or SAS-Hypersil packed onto a 100 × 4.6 mm stainless-steel column (Shandon Scientific, Runcorn, UK).

For experiments with chiral stationary phases 100 × 4.6 mm Cyclobond I and II cyclodextrin phases (Astec, Whippany, NJ, USA) and a 100 × 4.6 mm Chiral-AGP column packing material was examined (ChromTech, Norsborg, Stockholm, Sweden). A range of mobile phases were used of variable composition, but the optimum for the assays on the Chiral-AGP column packing was: propan-2-ol–10 m*M* sodium dihydrogenphospate + 0.1 *M* sodium chloride pH 5.85 (99.5:0.5, v/v). All mobile phases were filtered through a 0.45-μm Durapore filter (Millipore, Molsheim, France) and degassed by ultrasonication under reduced pressure prior to use.

Capillary electrophoresis system

The instrument was an Applied Biosystems Model 270A (Warrington, UK) and the data was manipulated on a Model HP3396A integrator.

The uncoated fused-silica capillary was 710 × 0.05 mm I.D. (500 mm to the detector) (Chrompack, London, UK). Again a range of buffer compositions were used. But the injection time of 2 s (7 nl, hydrodynamic vacuum injection at the anode), temperature 30°C, applied voltage 15 or 20 kV and detection wavelength 246 nm were kept constant throughout the development experiments.

In order to establish reproducible, robust results, the capillary was conditioned and rinsed in a set procedure at the beginning and end of each day. For the initial capillary conditioning, a new capillary was washed for 2 h with 1 *M* sodium hydroxide, 1 h with double distilled water and then 30 min with run buffer (all solutions were initially filtered through a 0.22-μm filter). Each day the capillary was washed for 40 min with 1 *M* sodium hydroxide, water for 15 min prior to use and between runs with 0.1 *M* sodium hydroxide (2 min) and run buffer (3 min).

3. Results and discussion

The initial HPLC experiments involved β-cyclodextrin (5 m*M*) or hydroxypropyl-β-cyclodextrin (20 m*M*) introduced into the mobile phase on the C_{18} or SAS-Hypersil achiral stationary phase and the use of a Cyclobond I or II chiral stationary phase with a mobile phase of acetonitrile–water. Stepwise optimisation of the mobile phase was attempted in each case, but no appreciable resolution of the chiral oxamniquine drug was achieved with either of the chiral selector additives or the chiral stationary phases. This lack of success was slightly unexpected as the structure of oxamniquine suggests inclusion of the aromatic moiety (with the possibility of the nitro and alcohol groups passing through the hydrophobic cavity) and the likelihood of N–H hydrogen bonding. However, the retention time data for oxamniquine in the presence of the chiral selector was different from that in the same mobile phase without the cyclodextrin, indicating selector interaction but similarity in equilibrium constant binding and/or the rate of migration is faster than the achievement of differences in binding equilibrium [9].

As an extension to the HPLC work further examination of the oxamniquine structure indicated that the cyclic ring nitrogen and hydrogen bonding groups could show favourable interactions on a protein based chiral stationary phase and a number of experiments were carried out to examine the best conditions for separation. The range of recommended operating parameters for the Chiral-AGP stationary phase are slightly limited but a suitable range of mobile phase conditions was found for examination through a modified simplex, structured optimisation procedure. The starting conditions were: pH 4.0–7.0 and propan-2-ol concentration of 0.2–1.4%(v/v) with a 10 m*M* sodium dihydrogenphosphate buffer. After 12 experiments the global optimum was reached where the mobile phase was: propan-2-ol–10 m*M* sodium dihydrogenphosphate (0.5:99.5, v/v) (pH 5.85), although the chromatographic peak shape was slightly broad. But the addition of 0.1 *M* sodium chloride caused a sharpening of the peaks. However when this simplex was viewed as the three-dimensional response surface, it was clear that small changes in the pH would cause large differences in the enantiomeric resolution (Fig. 3). This would result in a very unstable operating basis on which to carry out regular assays on racemic oxamniquine as the bulk drug and the tablet pharmaceutical preparation [10] (differences as small as 0.2 pH units led to relatively large losses in resolution) and therefore although baseline resolution of the racemic oxamniquine was achieved the lack of ruggedness in the assay suggested further study was necessary.

The picture was completely different when CE

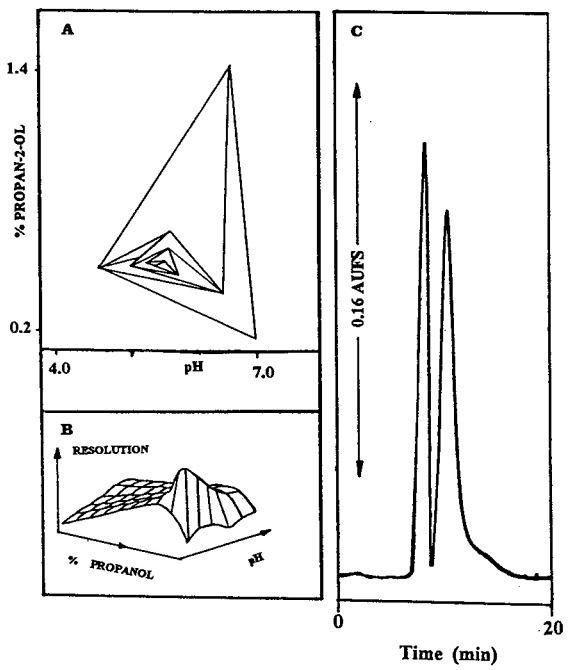

Fig. 3. Basis of the optimisation experiments for the resolution of oxamniquine (60 mg/ml) on the Chiral-AGP stationary phase. (A) Optimisation experiments based on the modified simplex procedure using a two-variable design; (B) three-dimensional response surface from the simplex procedure, indicating the steepness of the pH and propan-2-ol responses; (C) optimum chromatographic separation of the oxamniquine enantiomers from the structured optimum procedure. The conditions were: 100 × 4.6 mm stainless-steel column packed with 5-μm Chiral-AGP, the optimised mobile phase was propan-2-ol–10 m*M* NaH_2PO_4 + 0.1 *M* NaCl (0.5:99.5, v/v), pH 5.85. Flow-rate was 1.0 ml/min and the detection wavelength 246 nm.

was used in the buffer/chiral selector additive mode of capillary zone electrophoresis (CZE) with β-cyclodextrin and quite rapidly good resolution of the oxamniquine enantiomers was achieved. From this further fine tuning of the enantiomer separation was carried out along with a pH study to check method stability. These experiments gave the enantioseparation shown in Fig. 4, where the electrolyte consisted of 50 m*M* disodium hydrogenphosphate (pH 12.0) containing 25 m*M* β-cyclodextrin.

In order to describe the chiral resolution in free solution CE a number of theoretical models have been suggested. These have attempted to take into account the effects of diffusion band broadening [11], electroosmotic mobility and equilibration selector–analyte binding [12,13]. In addition the operating conditions of applied potential, electrolyte pH [14] and organic buffer additive [15] have been included in these ideal models. The importance of cyclodextrin concentration was discussed by Wren and Rowe [16] and the resolution given here followed their theoretical work with an optimum concentration reached in terms of resolution and effective reduced band broadening at 25 m*M* β-cyclodextrin (a limit of 30 m*M* β-cyclodextrin was reached before solubility was problematic). It is possible, by taking into account all these influences to suggest that the differences in observed resolution in CE over HPLC are linked directly to the many different factors influencing the electrophoretic mobility difference. As regards the sites of molecular interaction between the cyclodextrin and the oxamniquine it has been shown in early NMR studies that a 1:2 relationship of cyclodextrin to analyte is occurring and this aspect is currently being more fully studied along with the examination of the competitive binding equilibria for the HPLC and CE data. Through the 1:2 molecular interactions it is possible that the oxamniquine diamer comes closely into contact with the secondary hydroxyls on the rim of the cyclodextrin cavity and because of steric effects the higher competition factor in the selector–enantiomer binding leads to a difference in the enantiomeric mobility.

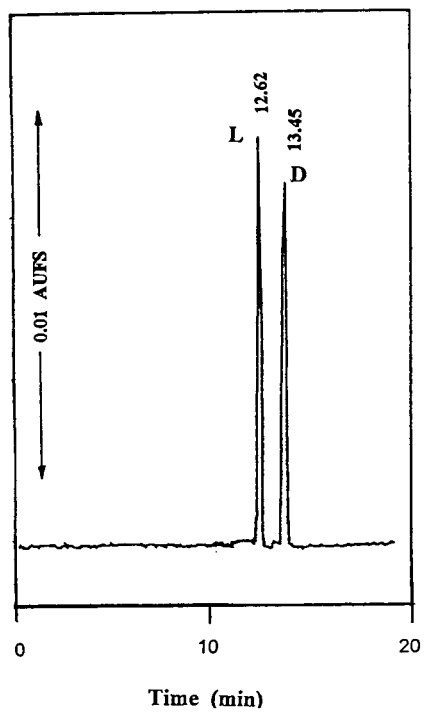

Fig. 4. Resolution of the enantiomers of oxamniquine by capillary zone electrophoresis with β-cyclodextrin in the electrolyte. The operating conditions were, applied voltage of 15 kV, temperature 30°C, wavelength 246 nm and buffer, 50 m*M* disodium hydrogenphosphate containing 25 m*M* β-cyclodextrin pH 12.0.

In examining the resolution of the oxamniquine enantiomers it is interesting to note that the migration order differs between the β-cyclodextrin and the hydroxypropyl-β-cyclodextrin (RS = 0.9), which may be a function of the differential interaction due to the alkyl spacer on the extended hydroxypropyl arm, over the conventional β-cyclodextrin.

Method stability in both these cases was very good as demonstrated in Table 1, where migration times and peak height (peak areas) gave values of R.S.D. < 1%. This was also the position on examining method ruggedness on a day to day basis. In this case stability under varying buffer pH changes was much better (changes of ±1 pH unit gave only small changes in resolution between the enantiomers) than in HPLC with the protein chiral stationary phases.

These data suggest that the method would be

Table 1
Repeatability of migration times and peak height values for oxamniquine (60 μg/ml, $n = 10$) by CZE with β-cyclodextrin (25 m*M*) in the buffer solution

	Migration time (min)		Peak height	
	Peak I	Peak II	Peak I (L)	Peak II (D)
Mean	12.49	13.34	28156	21505
S.D.	0.116	0.106	430.91	304.14
R.S.D. (%)	0.93	0.80	0.97 (1.53)[a]	0.73 (1.41)[a]

For experimental details: see text.
[a] Values of peak height are normalised and the untreated values are given in parentheses.

suitable for determination of the individual enantiomers in the bulk drug and the pharmaceutical tablet preparation (Vansil, Pfizer), where the drug is present in the racemic form and this is currently being completed.

In conjunction with these method development CE experiments using cyclodextrins, the chiral selector has also been considered and polysaccharides have been examined. Of these heparin, a mucopolysaccharide (extracted from bovine lung tissue and intestinal mucosa of pigs and cattle), was shown to be particularly successful in the resolution of the enantiomers of oxamniquine.

This polysaccharide (Fig. 2) is a linear sugar molecule, but with some degree of helical structure around the α-1,4 links within the molecule and as it has a relatively large number of sulphate groups present then the molecule has a strong anionic charge. Previously, the resolution of a small number of chiral chemicals has been achieved [17], but very little consideration has been given to the separation or chiral drugs [18].

In this case the oxamniquine was resolved with a very large resolution factor, in a buffer of 50 m*M* sodium dihydrogenphosphate (pH 3.0) containing 3 m*M* heparin (Fig. 5A). As with the cyclodextrin assays the method gave very stable results (method repeatability around a R.S.D. of 1%, $n = 10$) under small changes in buffer composition, and therefore it is also suggested that the procedure could be used for assay of oxamniquine in bulk drug and pharmaceutical preparation. There is a slight drawback, however, to the regular use of heparin in chiral drug assays, in that the material is heterogeneous and thus heparin from different sources can give small changes in resolution due to the variable composition of the disaccharide and trisaccharide residues. This is illustrated in the material examined in this programme from different biochemical suppliers, where the effects of variable chain length and composition have been shown to provide a difference in the degree of resolution experienced with oxamniquine (Fig. 5B).

Nevertheless it was possible to show that if oxamniquine was to be marketed as either the pure D- or L- enantiomer for related substance analysis or if a check on chiral inversion was required after pharmaceutical formulation, they could be detected in the presence of one enantiomer in the other, down to 0.23% (m/m), although for reproducible results one source of heparin is recommended for use in the electrolyte solution.

In all these experiments to obtain acceptable method validation values, it was important to condition and regularly wash the fused-silica capillary at start up, between runs and at the end of the day.

4. Conclusions

This particular example of resolution of oxamniquine with cyclodextrins demonstrates the usefulness of CE as a tool to resolve chiral drugs and illustrates its advantages over HPLC in this case. The findings in this programme are backed up generally in the literature, where it is clear

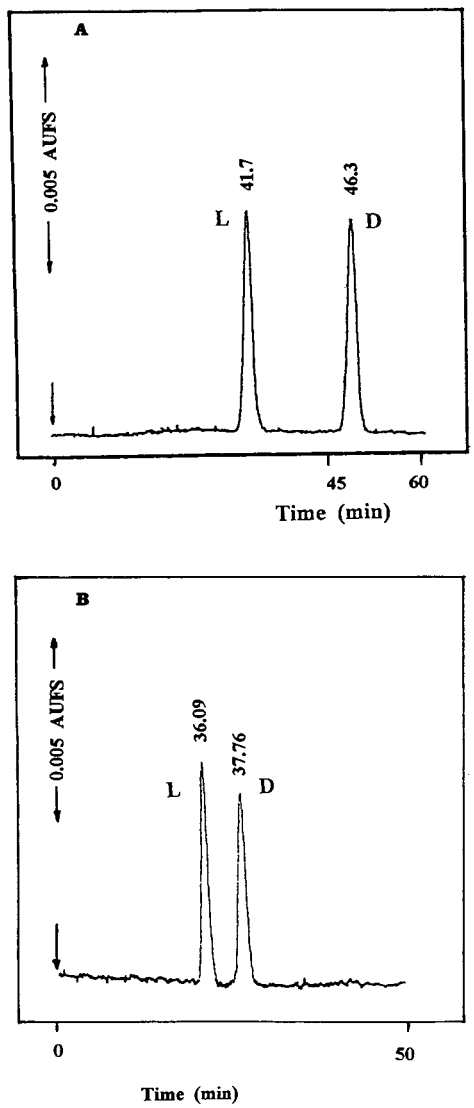

Fig. 5. Resolution of the enantiomers of oxamniquine by capillary zone electrophoresis with heparin in the electrolyte solution. (A) Resolution achieved with an electrolyte solution of 50 m*M* sodium dihydrogenphosphate (pH 3.0) + 3 m*M* heparin (from Sigma), an applied voltage of 20 kV, temperature 30°C and detection wavelength of 246 nm. (B) Resolution under the same conditions, but with 3 m*M* heparin from Lancaster Synthesis.

that in many instances the analyst has found that CE in capillary zone and micellar mode with chiral selectors added to the buffer solution, gives better resolution and more rapid method development over HPLC. The method was shown to be stable and robust over a period and could be applied to the assay in a pharmaceutical preparation. This was also the case with the method developed around heparin which as a newly suggested additive for chiral separation of drugs, gives very impressive resolution of oxamniquine. However the analyst would have to be careful with use of the additive on a regular basis, unless the variation in the composition of the heparin from different sources, which leads to differences in resolution of the chiral compound of interest, could be resolved.

Acknowledgement

The authors would like to acknowledge the Libyan Secretary for Higher Education and Scientific Research (SHESR) for sponsoring the work of A. A.

References

[1] T. Ward, *Anal. Chem.*, 66 (1994) 633 A.
[2] S. Birmbaum and S. Nilsson, *Anal. Chem.*, 64 (1992) 2872.
[3] R. Kuhn, F. Stoecklin and F. Erni, *Chromatographia*, 33 (1992) 32.
[4] B.J. Clark, P. Barker and T. Large, *J. Pharm. Biomed. Anal.*, 10 (1992) 723.
[5] T. Schmitt and H. Engelhardt, *Chromatographia*, 37 (1993) 475.
[6] M. Novotny, H. Soini and M. Stefansson, *Anal. Chem.*, 66 (1994) 646A.
[7] I.E. Valko, H.A.H. Billiet, J. Frank and K.C.A.M. Luyben, *J. Chromatogr. A*, 678 (1994) 139.
[8] J. Kiss, in V.V. Kakkar and D.P. Thomas (Editors), *Heparin; Chemistry and Clinical Usage*, Academic Press, London, 1976, p. 3.
[9] M.M. Rogan, K.D. Altria and D.M. Goodall, *Chirality*, 6 (1994) 25.
[10] A.F. Fell, T.A.G. Noctor, J.E. Mama and B.J. Clark, *J. Chromatogr.*, 434 (1988) 377.
[11] J.H. Park and T.H. Nah, *J. Chem. Soc., Perkin Trans. 2*, (1994) 1359.
[12] S.A.C. Wren, *J. Chromatogr.*, 636 (1993) 57.
[13] S.G. Penn, E.T. Bergstrom and D.M. Goodall, *Anal. Chem.*, 66 (1994) 2866.
[14] Y.Y. Rawjee and G. Vigh, *Anal. Chem.*, 66 (1994) 619.

[15] S.A.C. Wren and R.C. Rowe, *J. Chromatogr.*, 609 (1992) 363.
[16] S.A.C. Wren and R.C. Rowe, *J. Chromatogr.*, 603 (1992) 235.
[17] J.B.L. Damm and G.T. Overklift, *J. Chromatogr. A*, 678 (1994) 151.
[18] A.M. Stalcup and N. Hgyei, *Anal. Chem.*, 66 (1994) 3054.

ELSEVIER

Journal of Chromatography A, 700 (1995) 59–67

JOURNAL OF CHROMATOGRAPHY A

Systematic approach to treatment of enantiomeric separations in capillary electrophoresis and liquid chromatography II. A study of the enantiomeric separation of fluoxetine and norfluoxetine

Stavroula Piperaki[a], Sharron G. Penn[b], David M. Goodall[b,*]

[a]*Department of Pharmacy, Division of Pharmaceutical Chemistry, University of Athens, Panepistimiopoli Zografou, GR-15771 Athens, Greece*

[b]*Department of Chemistry, University of York, Heslington, York, YO1 5DD, UK*

Abstract

A systematic approach to enantiomeric separations in capillary electrophoresis (CE) and liquid chromatography (LC) with chiral mobile phase additives (MPA) or a chiral stationary phase (CSP) is used in the study of fluoxetine and norfluoxetine with cyclodextrins as chiral selectors. Binding constants and selectivities are determined under the same experimental conditions (mobile phase, buffer composition). Good agreement is found between results from the three techniques. The role of the buffer salt is investigated by comparison of binding constants obtained with triethylammonium and sodium acetate buffers.

Investigation of the effects of derivatisation of the selector in CE and LC with MPA demonstrates the appropriate choice of cyclodextrin type for use in LC. By studying the influence of organic modifier content on separation parameters, CE can predict a useful solvent working range for a CSP.

1. Introduction

The different pharmacological behaviour of drug enantiomers has become increasingly important due to the fact that they are often readily discriminated by biological systems and may have different toxicological, pharmacokinetic and pharmacodynamic profiles. The growing awareness in this field has resulted in an increased demand for suitable methods to determine the stereoisomeric composition of a drug. Generally enantiomers are only distinguishable in a chiral environment, thus the separation methods are based on interaction of enantiomeric solutes with an optically-active compound used as a chiral selector.

In liquid chromatography (LC) the direct separation and determination of the enantiomers is performed using either a chiral stationary phase (CSP) or by the addition of a chiral mobile phase additive (MPA) [1,2]. There has recently been a dramatic growth in the use of capillary electrophoresis (CE) with chiral MPAs for the separation and analysis of enantiomers [3,4]. Benefits of CE include speed of separations, high efficiencies and resolution, low running costs

* Corresponding author.

0021-9673/95/$09.50
SSDI 0021-9673(95)00113-1

relative to LC, and robust assays for bulk drugs [5].

We have recently initiated development of a systematic approach to the treatment of enantiomeric separations which brings together information from CE and LC using the same selector as MPA or CSP [6]. By formulating theory and applying this to systems where analytes, selector and buffer composition are the same, our aim is to link the two key separation techniques of CE and LC. This should allow the substantial body of knowledge in reversed-phase LC to be used in a rational way to guide method development in CE. In addition, rapid and inexpensive CE experiments could be used in method development for LC, which remains the method of choice for analyses where low detection limits are required, and for preparative enantioseparations.

In our previous paper (Part I, [6]), equations are given for the optimum determination of binding constants and selectivity for selector–selectand complexes involving enantiomeric analytes in CE and LC with MPAs. LC separations of enantiomers with CSPs and MPAs are categorised in one of four ways according to the nature of the stationary and mobile phase equilibria involved. A quantitative comparison is given of CE and LC separations of dansyl derivatives of glutamate and leucine with β-cyclodextrin (β-CD) as selector. In the present paper we apply this general treatment to the separations of enantiomers of fluoxetine and norfluoxetine, for which LC separations using a β-CD CSP have previously been optimised [7].

Fluoxetine is an important antidepressant drug for the treatment of unipolar mental depression. Both fluoxetine (FL) {(±)-N-methyl-3-phenyl-[α,α,α-trifluoro-*p*-tolyl-oxyl]-propylamine hydrochloride} and its N-desmethylated metabolite norfluoxetine (NR) (Fig. 1) enhance serotoninergic neurotransmission through selective inhibition of presynaptic serotonin reuptake [8]. The enantiomers of FL exhibit their selective 5-hydroxytryptamine (5-HT) uptake inhibition with about equal potencies [9]. However, many differences have been reported in the literature regarding their pharmacological properties, as

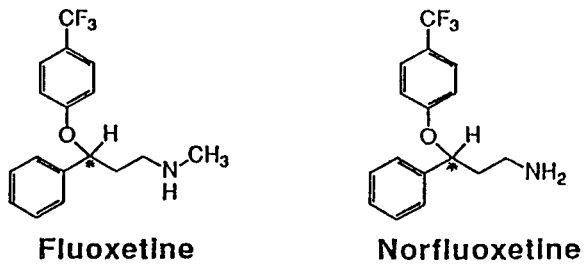

Fluoxetine Norfluoxetine

Fig. 1. Structures of fluoxetine and norfluoxetine.

well as those of NR [9,10], necessitating the development of new analytical methods permitting the chiral separation of these compounds.

The aims of this paper are (i) to study binding with selector in the mobile phase under the conditions used for the optimised CSP separation, (ii) to systematically investigate the role of the mobile phase, salt concentration and solvent composition, and (iii) to compare binding and separations with native and derivatised β-CDs.

We did not set out to achieve the best possible chiral separation of FL and NR in both CE and LC, but rather to investigate the ability to form links between the two techniques. Optimisation of the separation of FL enantiomers by CE has been previously investigated by Soini et al. [11], who found that a buffer containing 10 m*M* methyl-β-cyclodextrin, 30 m*M* Tris, pH 2.8, 0.1% methylhydroxycellulose gave excellent results.

2. Theory

Whilst a full explanation of the theory can be found in our previous paper [6], a brief summary is given here. Building on the treatment given by Sybilska et al. [12], we catagorise four cases for chiral discrimination in LC.

Case 1. Chiral mobile phase additives and achiral stationary phase. All discrimination in the mobile phase. *Case 2.* Chiral mobile phase additives partially bound to achiral stationary phase. Discrimination in both mobile and stationary phase. *Case 3.* Dynamically coated chiral stationary phase. All discrimination in the

stationary phase. *Case 4.* Covalently bonded chiral stationary phase. All discrimination in the stationary phase.

Case 1 is analogous to CE with mobile phase additives, and therefore an identical rational separation strategy applies for optimising the selector concentration in the two techniques. In this case, k', the capacity factor versus C, the concentration of the free selector, is a binding curve analogous to the CE binding curve of mobility, μ, vs. C, with equations for the curves [6,13]

CE:

$$KC = \frac{\mu_0 - \mu}{\mu - \mu_\infty}$$

LC:

$$KC = \frac{k'_0 - k'}{k' - k'_\infty}$$

When using chiral MPAs in CE or a case 1 LC chiral separation, optimum mobility or retention time difference occurs when $\bar{K}C = 1$, where $\bar{K}$ is the average binding constant defined as $(K_1K_2)^{1/2}$. In all our papers selectivity, α, is given by the ratio of binding constants for the enantiomers, K_2/K_1, in order to have the same definition when using CSPs and MPAs. Some authors in the CE field have equated chiral selectivity, α, to the mobility ratio μ_1/μ_2 [14]. This is inappropriate for a thermodynamic analysis, since α from this definition is a concentration-dependent quantity.

The non-linear least squares method we use for data fitting [13,15] is superior to methods previously adopted [12] in that by using the primary data all the points are weighted equally, without excess emphasis being placed on points at high selector concentration as is the case when using inverse data methods [16]. This is particularly beneficial when dealing with very strongly bound analytes. Cases 3 and 4 assume that all binding to the stationary phase occurs at identical chiral selector sites. The ratio of the capacity factors for the enantiomers, k'_2/k'_1, is equal to K_2/K_1. Individual binding constants cannot be obtained directly from LC without knowledge of phase ratios. Case 2 is intermediate between case 1 and cases 3 and 4.

3. Experimental

3.1. Capillary electrophoresis

Methyl-β-cyclodextrin was a gift from Wacker Chemicals (Halifax, UK), sulphobutyl-β-cyclodextrin was a gift from Jones Chromatography (Hengoed, UK). Fluoxetine and norfluoxetine were gifts from Eli Lilly, and were in the form of hydrochloride salts. All other materials were from Aldrich (Gillingham, UK).

Capillary electrophoresis experiments were carried out on an automated CE system (P/ACE 2100, Beckman, High Wycombe, UK), thermostatted at 25°C. The fused-silica separation capillary had an internal diameter of 50 μm, a total length of 57 cm and a length from inlet to detector of 50 cm. A voltage of 20 kV was normally used for the separation, with on-capillary UV detection at 230 nm. The run buffer (unless otherwise stated) was prepared by titrating a 1% (w/w) triethylamine solution with dropwise addition of glacial acetic acid, until the desired pH was achieved. Organic modifiers were added as required, and cyclodextrin added in varying amounts. Samples were dissolved in run buffer at the concentrations stated and prepared fresh each day. The samples were loaded with a 1 s pressure injection (corresponding to 1 nl). Each experiment was run in duplicate, with mesityl oxide as the neutral marker. Relative viscosity was determined from the ratio of the currents I, and I_0 at [cyclodextrin] = 0 mM, with and without cyclodextrin in the run buffer; $I_0/I = \eta/\eta_0$ [13].

3.2. Liquid chromatography

All solvents were of HPLC grade and were purchased from Tech-Line (Athens, Greece). Triethylamine and glacial acetic acid were of analytical grade and were purchased from Aldrich. The LC system consisted of a pump (Waters, Model 501), an injector (Rheodyne,

Model 7125) with a 5-μl loop and a spectrophotofluorimeter detector (Perkin Elmer, Model LS30) with an 8-μl flow cell. Detection was accomplished at an excitation wavelength of 235 nm and an emission wavelength of 315 nm. The chromatograms were obtained using an integrator (Hewlett Packard, Model HP3394A). For the MPA work a phenyl column (100 × 4.6 mm I.D., Hellamco, Athens, Greece) was used. For the CSP work a Cyclobond I column (Spherisorb-phenyl S5, 250 × 4.6 mm I.D., Advanced Separation Technologies) was used, with a flow-rate of 0.4 ml min^{-1} (10% acetonitrile mobile phase composition) and 0.8 ml min^{-1} (20% acetonitrile mobile phase composition). When not in use both these columns were stored in methanol. The void volume of each column was determined by injecting 5 μl of pure methanol. All experiments were performed at room temperature. The mobile phase was prepared as for the CE experiments, filtered and degassed under vacuum using a Millipore system. The stock solutions of FL and NR were prepared at 1 mg ml^{-1} and kept in amber-coloured bottles in a refrigerator and made fresh each week. Working standard solutions of 1 μg ml^{-1} were prepared fresh every day in mobile phase. Typically a volume of 5 μl of each solution was injected.

4. Results and discussion

4.1. Comparison of binding constant data from CE and LC

Previous experiments [7] optimised a set of conditions for the simultaneous LC separation of FL and NR enantiomers using a Cyclobond I CSP with a 1% (w/v) triethylammonium acetate ($Et_3NH^+Ac^-$) buffer, pH 5.5, containing 10% acetonitrile (MeCN). This stationary phase is composed of β-CD bonded on 5 μm spherical silica beads. The tether to the β-CD is an ether linkage between a surface silanol group and one or two of the primary hydroxyl groups on the β-CD [17]. An LC separation using β-CD as a MPA was investigated using the same buffer conditions and an achiral reversed-phase phenyl LC column. By varying the β-CD concentration it is possible to obtain a plot of k' vs. [β-CD], and hence to obtain a binding constant for the FL–β-CD complex as discussed in the theory section. A CE experiment was carried out again using identical buffer conditions, with β-CD as a MPA, and a plot of mobility, μ, vs. [β-CD] gave the binding constant for the FL–β-CD complex.

The separation of FL in $Et_3NH^+Ac^-$ buffer with 10% MeCN is shown in Fig. 2, using LC

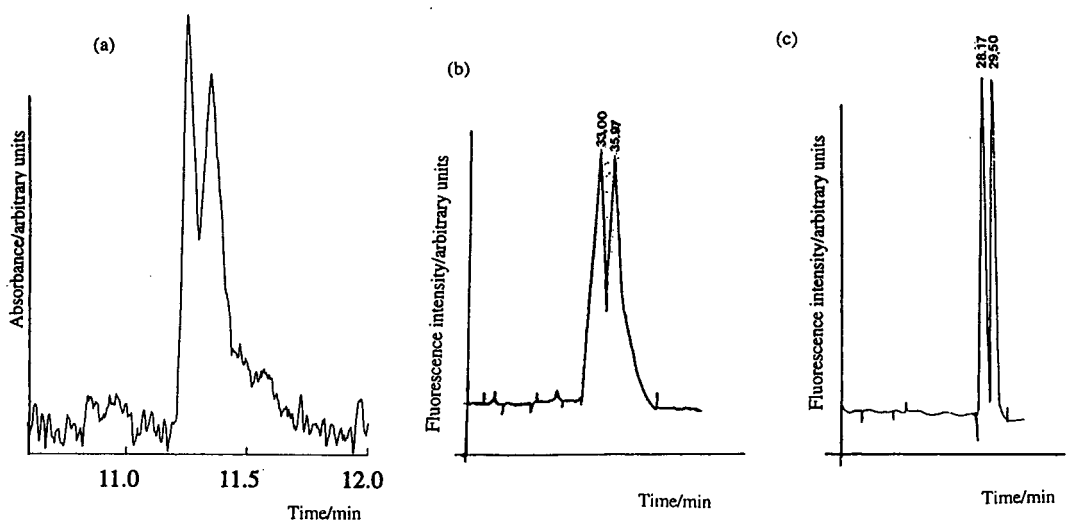

Fig. 2. Separations of fluoxetine enantiomers using (a) CE with 1 m*M* β-CD added to buffer, (b) LC with 1 m*M* β-CD added to mobile phase and (c) LC with a Cyclobond I CSP. Buffer conditions 1% triethylammonium acetate, pH 5.5, 10% acetonitrile. Other conditions as described in Experimental section.

Table 1
Comparison of enantiomeric separation parameters for fluoxetine and norfluoxetine with β-CD using (i) LC with CSP, (ii) LC with MPA and (iii) CE

Technique	Parameter	Fluoxetine	Norfluoxetine
(i) LC with CSP	k'_S	18.9	16.2
	k'_R	20.1	17.1
	α	1.06	1.05
	R_s	0.87	0.98
(ii) LC with MPA	K_S	$1147 \pm 51\ M^{-1}$	$1206 \pm 37\ M^{-1}$ [a]
	K_R	$1268 \pm 46\ M^{-1}$	
	α	1.11	–
	R_s	0.57	–
(iii) CE	K_S	$1078 \pm 61\ M^{-1}$	$991 \pm 26\ M^{-1}$
	K_R	$1144 \pm 65\ M^{-1}$	$1043 \pm 27\ M^{-1}$
	α	1.06	1.05
	R_s	0.62	0.68

Buffer composition: pH 5.5, 1% triethylammonium acetate, 10% MeCN.
[a] Unresolved.

with CSP, LC with β-CD as MPA, and CE with β-CD as buffer additive. Table 1 compares binding constant, selectivity and resolution values from all three methods. As mentioned in the Theory section the binding constants obtained by CE and LC with a MPA should be identical. The binding constants from LC with MPA and CE were found to be in good agreement, with differences outside the error limits probably attributable to temperature differences. The LC experiments were carried out at ambient temperature (25–27°C), and the CE experiments were carried out using an instrument setting of 25.0°C.

Excellent agreement is seen between selectively measured by CE and LC with CSP, $\alpha = 1.06$ for FL and 1.05 for NR respectively. This implies that there is no hindrance to binding to the CSP arising from steric effects of the tether to the surface silanol groups. Resolution in the NR case was insufficient to provide selectivity data. Table 1 shows that highest resolution is obtained using LC with the CSP.

Assignments of peaks were made by spiking with an excess of one enantiomer. In CE, the first migrating enantiomer was confirmed as the (+)-(*S*)-enantiomer, this being the weaker binding of the two. In LC with CSP the (+)-(*S*)-enantiomer was also confirmed as the first eluting enantiomer, this being the least retained on the column, and hence having the lowest value of k'. In LC with MPA the (+)-(*S*)-enantiomer has the higher k' values, since the β-CD pulls more of the stronger binding (−)-(*R*)-enantiomer into the mobile phase.

4.2. Effect of LC buffer additives in CE separations

When transferring buffer conditions between LC and CE care must be taken to understand the nature of the buffer solutions. In LC the use of $Et_3NH^+Ac^-$ at a relatively high concentration of 0.1% to 1% is necessary in order to give a dynamic coating to unreacted silanol groups and thus avoid peak broadening and tailing [18]. Previous work using cyclohexanol has shown that large organic additives in the buffer may compete for the cyclodextrin cavity [13]. This complexation will cause the apparent binding constant to decrease, and hence the optimum [β-CD] to achieve chiral resolution to be increased. Therefore the role of the LC buffer in the CE experiment was investigated by using sodium acetate (Na^+Ac^-) in place of $Et_3NH^+Ac^-$.

The 1% $Et_3NH^+Ac^-$ buffer used in the LC experiments has an ionic composition of 100 m*M* and its action as a buffer at pH 5.5 is due to the

presence of CH_3COOH and CH_3COO^-, and not due to the Et_3NH^+ cation: the pK_a of Et_3NH^+ is 10.8. Many CE experiments use concentrations of buffer very much less than 100 m*M*. The CE chiral separation of FL was repeated with 10% MeCN using a 50-m*M* Na^+Ac^- buffer at pH 5.5 as a replacement for the $Et_3NH^+Ac^-$ buffer. The electroosmotic flow (EOF) in the absence of β-CD was $0.99 \cdot 10^{-8}$ $m^2V^{-1}s^{-1}$ for the 100-m*M* $Et_3NH^+Ac^-$ buffer, and $3.08 \cdot 10^{-8}$ m^2 V^{-1} s^{-1} for the 50-m*M* Na^+Ac^- buffer. Several groups [19,20] have also observed a decrease in EOF with $Et_3NH^+Ac^-$ buffer systems. 10 m*M* $Et_3NH^+Ac^-$ in a water–methanol (85:15) system has been reported to reverse the EOF [20]. This was attributed to the Et_3NH^+ cation binding to the capillary wall and changing the sign of the charge at the Stern layer. Whilst we observe a substantial decrease in the EOF in the 100-m*M* $Et_3NH^+Ac^-$ water–acetonitrile (90:10) buffer, no flow reversal was found. The dependence of EOF magnitude and direction on the Et_3NH^+ concentration, organic modifier type and concentration is therefore complex. Since a high ionic concentration helps to reduce electromigration dispersion and the low EOF and positive coating of the walls is beneficial for resolution and peak shape of positively charged analytes, the 100-m*M* $Et_3NH^+Ac^-$ buffer should in principle be better than the 50-m*M* Na^+Ac^- buffer for separation of the cationic species FL and NR. Fig. 3 shows the comparison of the CE chiral separation of FL in the $Et_3NH^+Ac^-$ buffer and the Na^+Ac^- buffer, both containing 1 m*M* β-CD. The migration time of FL is longer in the 100 m*M* $Et_3NH^+Ac^-$ buffer, the resolution is greater, whilst the peak shape is poorer.

Calculation of the binding constants in the sodium acetate buffer system for FL gave $\bar{K} = 760 \pm 95\ M^{-1}$ with $\alpha = 1.04$, and $\bar{K}$ for NR equal to $840 \pm 105\ M^{-1}$ with $\alpha = 1.02$. If the buffer in the CE capillary was not interacting with the analyte–selector complex we should expect to see identical binding constants and selectivity, with changes limited to EOF and resolution [13]. This is clearly not the case; comparison of data in Table 2 shows that the values of the binding

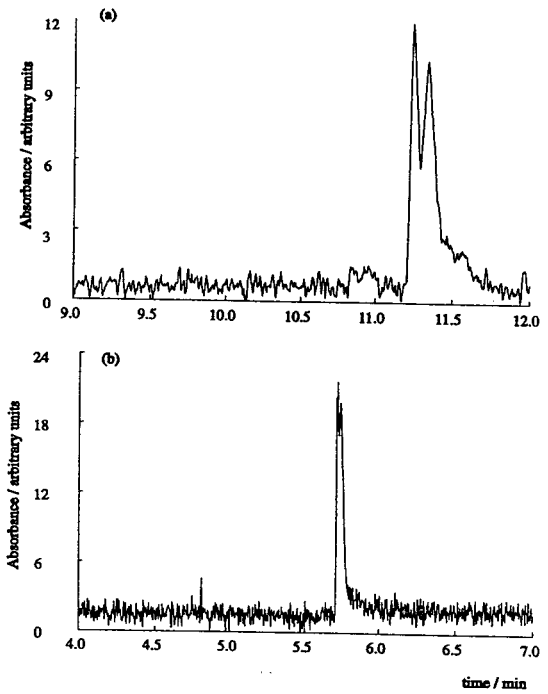

Fig. 3. Separation of FL enantiomers by CE in (a) 1% triethylammonium acetate buffer, pH 5.5, 1 m*M* β-CD, 10% acetonitrile, (b) 50 m*M* sodium acetate buffer, pH 5.5, 1 m*M* β-CD, 10% acetonitrile. Other conditions as described in Experimental section.

constants in the Na^+Ac^- buffer are 20–30% less than in the $Et_3NH^+Ac^-$ buffer. α values are also systematically lower. Li and Lloyd [20] report the formation of a ternary complex between amino acids, $Et_3NH^+Ac^-$, and β-CD. The differences measured here in binding constant and selectivity may also be due to ternary complex formation, and further experiments are underway to clarify the nature of any possible binding of $Et_3NH^+Ac^-$ to β-CD.

Differences in ionic strength between the two buffers cannot account for the observed differences in binding constant. Correction to $\bar{K}$ for non-ideality using Debye–Hückel theory gives values of the average thermodynamic equilibrium constant, K^0, for the enantiomers [13,21]. When this is done there is still a substantial difference between K^0 values derived from the

Table 2
Comparison of binding constant data in triethylammonium acetate and sodium acetate buffer solution, with correction for non-ideality

	Fluoxetine		Norfluoxetine	
	Na^+Ac^- (50 mM)	$Et_3N^+Ac^-$ (100 mM)	Na^+Ac^- (50 mM)	$Et_3N^+Ac^-$ (100 mM)
$\bar{K}(M^{-1})$	760	1111	840	1017
K^0	794	1182	878	1082

two buffers, and this applies to both FL and NR. Table 2 shows the measured values of $\bar{K}$ and the corrected values of K^0 for both FL and NR.

4.3. *Effect of derivatised cyclodextrins in CE and LC*

Derivatised cyclodextrins are often used to enhance selectivity of chiral separations using CE. We have investigated the variation in binding constant with the use of methylated-β-CD (Me-β-CD) and hydroxypropyl-β-CD (HP-β-CD). Table 3 shows the variation in binding constant for FL with chiral selector, in CE and LC with MPA. As in previous sections identical conditions for buffer composition were used in CE and LC. Binding constants from the two techniques are again seen to be in good agreement. FL–HP-β-CD is seen to have a very low binding constant in comparison with FL–β-CD. Since hydroxypropylation introduces bulky groups at the cavity rim, these might sterically interfere with FL inclusion into the cavity. The binding constants with Me-β-CD are about 10% lower than with the native β-CD. The most significant difference between these two cyclodextrins however, lies in the selectivity, α, which is considerably lower for Me-β-CD than the native β-CD and HP-β-CD, and thus leads to worse resolution [13].

The use of charged cyclodextrins in chiral separations by CE can expand the resolution window in comparison with neutral cyclodextrins, and can also strengthen binding when the cyclodextrin and analyte have opposite charges [22]. We investigated the use of sulphobutyl-β-CD, a negatively charged cyclodextrin, for the separation of the positive charged FL. The electropherogram in Fig. 4 shows baseline separation of the enantiomers, obtained using reverse polarity, under identical buffer conditions as in

Table 3
Variation of binding constant with chiral selector in CE and LC with MPA

Selector	$K_S(M^{-1})$	$K_R(M^{-1})$	α	R_s
CE				
HP-β-CD	307 ± 14	326 ± 15	1.06	0.59
Me-β-CD	995 ± 20	1019 ± 21	1.02	0.32
β-CD	1078 ± 65	1144 ± 65	1.06	0.62
SB-β-CD^-	–	–	–	1.71
LC with MPA				
HP-β-CD	363 ± 27	398 ± 30	1.10	0.41

Conditions: pH 5.5, 1% $Et_3N^+Ac^-$ buffer, 10% MeCN.

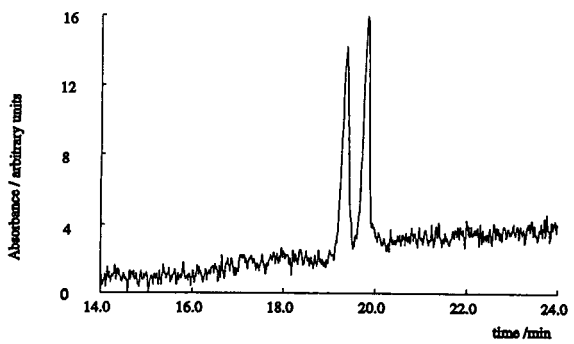

Fig. 4. Separation of fluoxetine enantiomers by CE, using 7.5 m*M* sulphobutyl-β-cyclodextrin as a buffer additive. Other conditions as described in Experimental section.

Table 3. A resolution of 1.71 was obtained, the highest value for all the selectors investigated.

4.4. *Effect of organic modifiers in CE and LC*

The effect of variation of MeCN concentration was studied using the three techniques. Data for FL is given in Table 4 for the binding constants, capacity factors, selectivity and resolution obtained using 20% MeCN. Satisfactory agreement between binding constants from LC with MPA and CE is seen. Upon addition of organic modifier there is a decrease in binding constant. This is similar to observations with another cationic species, tioconazole [13]. Theory suggests that the action of the organic modifier is to increase the affinity of the analyte for the mobile phase, with no change to selectivity. Comparison of data for LC with MPA and CE in Tables 1 and 4 shows that this is the case. Using the LC with a CSP resolution is essentially lost in going from 10% to 20% acetonitrile. Although two peaks could be observed, the separation between the peak maxima was insufficient to give meaningful values of R_s and α. The higher flow-rate used with 20% acetonitrile may in part explain the loss of resolution, since R_s has previously been shown to decrease with increasing flow-rate in inclusion chromatography on a Cyclobond I column [7]. The decrease in the binding constant with increase in organic modifier concentration is graphically demonstrated in Fig. 5 where the binding curves at 10% and 20% MeCN are overlaid. These solution phase results would suggest, following the ideas in the Theory section, that k' should decrease by a factor of 7.5 and the capacity factor should be insufficient to give any chiral resolution when comparing K in 10% and 20% acetonitrile. Whilst k' does not appear to scale linearly with binding constant, information from CE can still be used as a guide for method development in LC.

Table 4
Comparison of enantiomeric separation parameters for fluoxetine and norfluoxetine with β-CD using (i) LC with CSP, (ii) LC with MPA and (iii) CE

Technique	Parameter	Fluoxetine
(i) LC with CSP	k'_S	13.24
	k'_R	13.58
	α	–
	R_s	<0.5
(ii) LC with MPA	K_S	$124 \pm 4\ M^{-1}$
	K_R	$135 \pm 4\ M^{-1}$
	α	1.09
	R_s	0.52
(iii) CE	K_S	$143 \pm 7\ M^{-1}$
	K_R	$152 \pm 8\ M^{-1}$
	α	1.06
	R_s	0.68

Buffer composition: pH 5.5, 1% triethylammonium acetate, 20% MeCN.

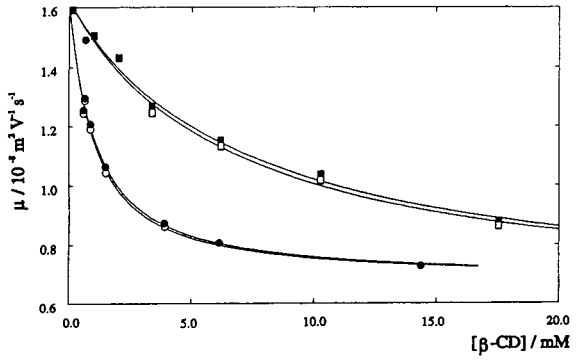

Fig. 5. Binding curves from CE for fluoxetine enantiomers comparing 90:10 (circles) and 80:20 (squares) water–acetonitrile buffer, where open symbols are the (*R*)-enantiomers and closed symbols are the (*S*)-enantiomers. Conditions as described in Experimental section.

5. Conclusion

The same binding processes are shown to occur in CE and LC, and binding constants and selectivities measured with cyclodextrin selectors in both CE and LC with mobile phase additives are shown to be in good agreement. Using an aqueous triethylammonium acetate buffer–acetonitrile (90:10) as solvent, chiral resolution was obtained using both mobile phase additive and chiral stationary phase techniques. Increasing the organic modifier content to 20% decreased binding constants as expected, and gave insufficient resolution using the CSP. A benefit of CE can be seen here, in the prediction of a useful solvent working range for a CSP. A range of solvent compositions could be screened quickly using CE, without the need to extensively use the CSP column, and thus extend column life time.

Acknowledgements

We would like to thank the SERC and Pfizer Central Research for a CASE award (SGP), and the British Council for travel support (SP).

References

[1] S.G. Allenmark, *Chromatographic Enantioseparations*, Ellis Horwood, Chichester, 1988.
[2] D. Sybilska and J. Zukowski, in A.M. Krstulovic (Editor), *Chiral separations by HPLC –Applications to Pharmaceutical Compounds*, Ellis Horwood, Chichester, 1989, Ch 7.
[3] M.M. Rogan, K.D. Altria and D.M. Goodall, *Chirality*, 6 (1994) 25.
[4] S. Terabe, K. Otsuka and S. Nishi, *J. Chromatogr. A*, 666 (1994) 295.
[5] K.D. Altria, R.C. Harden, M. Hart, J. Hevizi, P.A. Hailey, J.V. Makwana and M.J. Portsmouth, *J. Chromatogr.*, 641 (1993) 147.
[6] S.G. Penn, G. Liu, E.T. Bergström, D.M. Goodall and J.S. Loran, *J. Chromatogr. A*, 680 (1994) 147.
[7] S. Piperaki and M. Parissi-Poulou, *Chirality*, 5 (1993) 258.
[8] R.F. Bergström, L. Lemberger, N.A. Farid and R.L. Wolen, *Br. J. Psychiat.*, 153 (1988) 47.
[9] D.T. Wong, R.W. Fuller and D.W. Robertson, *Acta Pharm. Nord.*, 2 (1990) 171.
[10] R.W. Fuller, D.T. Wong and D.W. Robertson, *Med. Res. Rev.*, 11 (1990) 17.
[11] H. Soini, M. Riekkola and M.V. Novotny, *J. Chromatogr.*, 608 (1992) 265.
[12] D. Sybilska, J. Zukowski and J. Bojarski, *J. Liq. Chromatogr.*, 9 (1986) 591.
[13] S.G. Penn, E.T. Bergström, D.M. Goodall and J.S. Loran, *Anal. Chem.*, 66 (1994) 2866.
[14] S.A.C. Wren and R.C. Rowe, *J. Chromatogr.*, 603 (1992) 235.
[15] S.G. Penn, E.T. Bergström, G. Liu, I. Knights, A. Ruddick and D.M. Goodall, *J. Phys. Chem.*, in press.
[16] W.B. Person, *J. Am. Chem. Soc.*, 87 (1965) 167.
[17] R.D. Armstrong, T.J. Ward, N. Pattabiraman, C. Benz and D.W. Armstrong, *J. Chromatogr.*, 414 (1987) 192.
[18] T.J. Ward and D.W. Armstrong, *J. Liq. Chromatogr.*, 9 (1986) 407.
[19] I. Bechet, P. Paques, M. Fillet, P. Hubert and J. Crommen, *Electrophoresis*, 15 (1994) 818.
[20] S. Li and D.K. Lloyd, *J. Chromatogr. A*, 666 (1994) 321.
[21] M.A. Survay, D.M. Goodall, S.A.C. Wren and R.C. Rowe, *J. Chromatogr. A*, in press.
[22] B. Chankvetadze, G. Endresz and G. Blaschke, *Electrophoresis*, 9 (1994) 407.

ELSEVIER

Journal of Chromatography A, 700 (1995) 69–72

JOURNAL OF CHROMATOGRAPHY A

Separation and identification of the *Z* and *E* isomers of 2-(3-pentenyl)pyridine by capillary electrophoresis and nuclear magnetic resonance spectroscopy

Andrew G. McKillop[a], Roger M. Smith[a,*], Raymond C. Rowe[b], Stephen A.C. Wren[b]

[a]*Department of Chemistry, Loughborough University of Technology, Loughborough, Leics. LE11 3TU, UK*
[b]*Zeneca Pharmaceuticals, Hurdsfield Industrial Estate, Macclesfield, Cheshire, SK10 2NA, UK*

Abstract

A mixture of the *Z* and *E* isomers of 2-(3-pentenyl)pyridine has been separated with baseline resolution by capillary electrophoresis. Using molecular modelling it was proposed that the smaller more rapidly migrating peak would be the *Z* isomer. This agreed with a 38:62 (*Z*/*E*) composition by nuclear magnetic resonance spectroscopy. The sample was also investigated by gas chromatography coupled to mass spectrometry.

1. Introduction

Capillary electrophoresis (CE) is rapidly developing as a complementary technique to high-performance liquid chromatography (HPLC) for the separation of small molecules [1]. Since CE is based on different physicochemical properties than HPLC, different performance characteristics are obtained, such as higher efficiencies and rapid times of separation. Together with low consumption of buffer and small sample requirements, it is clear that CE is an attractive method of separation for the pharmaceutical industry.

Separation in CE depends on the movement of the analyte ions in the applied electrical field. The electrophoretic mobility, μ, of a particle is defined as the steady state velocity per unit field strength, $\mu = q/f$, where q is the charge on the analyte and f is the frictional coefficient of the analyte. Thus, the principal parameters that can influence separation are the charge on the analyte, q, and the factors which influence the frictional coefficient, f, which are the size of the analyte and also the shape of the analyte ion.

Rowe et al. [2] have investigated the influence of size/shape on the separation of the monosubstituted alkyl pyridines. The separation of positional isomers was achieved and various molecular descriptors were investigated to predict the mobility of the analytes. Chadwick and Hsieh [3] have also reported the separation of the alkenes, fumaric acid, maleic acid, all *trans*-retinoic acid and 13-*cis*-retinoic acid. Differences in mobility were ascribed to differences in shape of the alkenes, which were regarded as spheres with different hydrodynamic radii.

Quantitative impurity content determination by CE has been shown to be of comparable precision to HPLC by Altria [4,5]. It was shown that the analytes must have the same UV chro-

* Corresponding author.

0021-9673/95/$09.50
SSDI 0021-9673(95)00069-0

mophores or correction factors applied, and that peak areas must be normalised by migration time in order to correct for the effect of analytes spending different residence times in the portion of the capillary that acts as the detection cell, because of the different mobilities.

In this study a mixture of the *Z* and *E* isomers of 2-(3-pentenyl)pyridine were investigated as model compounds, and the relative abundance of each isomer was determined by CE and compared to the nuclear magnetic resonance (NMR) spectrum of the sample. The sample of 2-(3-pentenyl)pyridine was also investigated by gas chromatography coupled to mass spectrometry (GC–MS).

2. Experimental

2.1. Chemicals

The sample of 2-(3-pentenyl)pyridine was used as received from Aldrich (Poole, UK) and was a mixture of the *Z* and *E* isomers. ^{1}H NMR spectra were run in deuterated chloroform on a 250 MHz AC250 Brüker NMR spectrometer. The sample of 2-(3-pentenyl)pyridine as a dilute solution in dichloromethane was also analysed using GC–MS on a Fisons GC 8000 gas chromatograph coupled to MD 800 mass spectrometer using a DB 5 ms column isothermally at 100°C. Molecular modelling measurements were made using Nemesis Sampler (Oxford Molecular).

2.2. Capillary electrophoresis

Work was carried out on a P/ACE 2050 system (Beckman Instruments, High Wycombe, UK) using a fused-silica capillary of 57 cm (50 cm to detector) × 75 μm I.D. Samples were loaded by a 2-s pressure injection at the anode and separated using a voltage of 15 kV. The external temperature of the capillary was thermostated at 25°C. The capillary was rinsed between each injection with a rinse cycle of sodium hydroxide (0.1 *M*, 2 min) and running buffer (3 mins). The peaks were detected at 254 nm using a 2 Hz collection rate. Electrophoretic separations were performed in a phosphate buffer (40 m*M*) prepared from orthophosphoric acid (BDH, Poole, UK) and adjusted to pH 2.5 with lithium hydroxide (1 *M*; FSA, Loughborough, UK).

3. Results and discussion

2-(3-Pentenyl)pyridine is marketed as a mixture of isomers and in a solution at pH of 2.5 these can readily be separated by CE in 11 mins (Fig. 1). Little method development was required, as 2-(3-pentenyl)pyridine was fully protonated under these conditions. However, it was not possible to directly assign structures to the peaks in the electropherogram but as electrophoretic mobility increases with decreasing size of the analyte it should be possible to use molecular modelling to predict the migration order of the isomers. When the lengths of the side chains were calculated, it was found from a molecular modelling package that the *E* isomer was fully extended with a length from the *ortho*-hydrogen on the pyridine ring to the end of the sidechain of 10.2 Å. The corresponding measurement for the *Z* isomer was 9.2 Å (Fig. 2). Thus the smaller peaks at 10.11 min was predicted to correspond to the *Z* isomer and the second larger peak at 10.31 min to the *E* isomer. These assignments agreed with the expected ratio of the isomers based on the greater thermodynamic stability of the *E* isomer.

In order to quantify the proportion of the two isomers, the absorbance of the analytes are required. Because of the similarity of the chromophore it was expected that the spectra would be effectively identical and this was confirmed using a CE system equipped with a diode array detector. Both peaks gave identical spectra with a maximum absorbance at 265 nm. It was also necessary to correct the peak areas by division by their migration times, in order to take account of the unequal residence time of the analytes in the detection window. Using this correction, the mean proportions over six runs was 40.9% for the minor isomer and 59.1% for

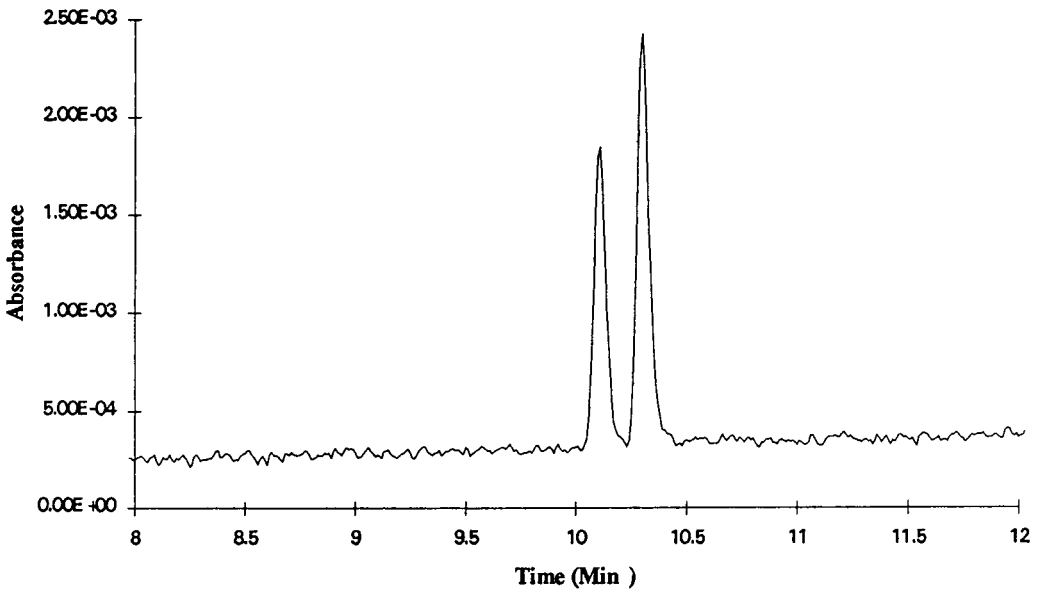

Fig. 1. Electropherogram showing the separation of (*Z*)- and (*E*)-2-(3-pentenyl)pyridine.

the major isomer with a standard deviation of 0.9%. The precision of these measurements is in agreement with the work of Altria [5], who reported precisions of 1–2% relative standard deviations.

Confirmation of the assignment of the isomers can be obtained by using 1H NMR spectroscopy to independently determine the proportion of the isomers. The shifts of the terminal methyl groups adjacent to the double bonds are different for the *Z* and *E* isomers, and each are split due to the adjacent protons. Coupling across the double bond was also observed, which split each methyl signal into a doublet of doublets and can be used to identify the isomers (Fig. 3). The larger peaks showed a long-range coupling of 1.1 Hz and were therefore assigned to the *E* isomer, whereas the small peaks had a coupling of 0.6 Mz typical of a *Z* isomer. It was also predicted that the methyl group in the *Z* isomer would be more shielded than in the *E* isomer, thus it would occur at a higher field as was observed. The heights of the two methyl signals were compared to give relative concentrations of each isomer in the sample, giving a percentage of (*Z*)-2-(3-pentenyl)pyridine of 38% and (*E*)-2-(3-pentenyl)pyridine of 62% in agreement with the CE assignments.

In order to ensure that the two peaks were isomers and not homologues or other derivatives a sample of 2-(3-pentenyl)pyridine was also investigated by GC–MS. At 100°C under isothermal conditions, major peaks were obtained at 16.0 and 17.1 mins, which had identical mass spectra with molecular ions (*m/z* 147), which correspond to 2-(3-pentenyl)pyridines. A minor impurity was also present. The proportions of the major peaks differed from those observed by the other techniques which was attributed to thermal equilibration of the isomers.

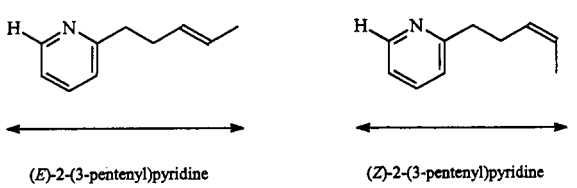

Fig. 2. Structures of (*Z*)- and (*E*)-2-(3-pentenyl)pyridine.

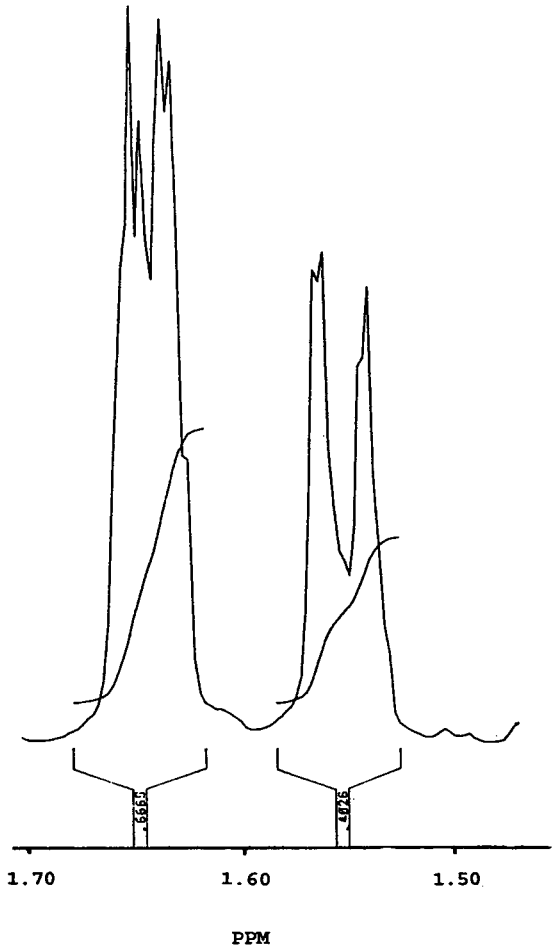

Fig. 3. Expanded methyl signals in the NMR spectrum of 2-(3-pentenyl)pyridine.

4. Conclusions

The *Z* and *E* isomers of 2-(3-pentenyl)pyridine can be separated according to their shape by CE. By considering the shape of the molecules, it was possible to predict the order of migration which was subsequently confirmed by NMR spectroscopy.

References

[1] C.W. Demarest, E.A. Monnot-Chase, J. Jiu and R. Weinburger, in P.D. Grossman and J.C. Colburn (Editors), *Capillary Electrophoresis – Theory and Practice*, Academic Press, San Diego, CA, 1992, Ch. 11, p. 301.
[2] R.C. Rowe, S.A.C. Wren and A.G. McKillop, *Electrophoresis*, 15 (1994) 635.
[3] R.R. Chadwick and J.C. Hsieh, *Anal. Chem.*, 63 (1991) 2377.
[4] K.D. Altria, *Chromatographia*, 35 (1993) 177.
[5] K.D. Altria, *LC · GC Int.*, 6 (1993) 616.

ELSEVIER

Journal of Chromatography A, 700 (1995) 73–80

JOURNAL OF CHROMATOGRAPHY A

Determination of tryptophan and kynurenine in brain microdialysis samples by capillary electrophoresis with electrochemical detection

Michael A. Malone[a,1], Hong Zuo[a], Susan M. Lunte[a,*], Malcolm R. Smyth[b]

[a]*Center for Bioanalytical Research, University of Kansas, Lawrence, KS 66047, USA*

[b]*School of Chemical Sciences, Dublin City University, Dublin, Ireland*

Abstract

Capillary electrophoresis with electrochemical detection (CEEC) is evaluated for the determination of tryptophan and kynurenine in microdialysis samples obtained from rat brain. These compounds were separated from all other electroactive metabolites of tryptophan. Limits of detection for both compounds were in the low attomole range. The response was linear for kynurenine between 4.9 and 980 fmol injected with a correlation coefficient of 0.9992 ($n = 12$). The system was evaluated for monitoring tryptophan and kynurenine in the extracellular fluid of the rat brain following systemic administration of tryptophan.

1. Introduction

Microdialysis is a sampling technique which allows continuous monitoring of substances from the extracellular space of tissue and organs with minimal perturbation of the physiological system [1,2]. An advantage of microdialysis sampling is that samples are protein-free and are therefore amenable to direct injection into the analytical system. In microdialysis, recovery of analyte through the probe increases with decreasing flow-rate; therefore, rates of 1 μl/min or less are typically employed. In order to obtain the best temporal resolution in microdialysis, highly sensitive techniques capable of analyzing small sample volumes are required.

Capillary electrophoresis (CE) is a highly efficient technique for the separation of charged analytes [3]. The integration of microelectrochemical detectors with capillary electrophoresis results in a highly efficient and sensitive system capable of analyzing ultrasmall sample volumes. The utility of capillary electrophoresis–electrochemistry (CEEC) has been demonstrated in the past for easily oxidizable compounds [4–6] and more recently for easily reducible compounds [7]. The latest advances in this field were recently reviewed by Ewing et al. [8]. CEEC has been employed for the analysis of amino acids and L-DOPA in microdialysis samples obtained from brain and blood, respectively [9,10].

In recent years there has been a surge of interest in the kynurenine pathway [11,12]. This pathway gives rise to a set of metabolites which account for approximately 90% of tryptophan metabolism in mammals. One of these,

* Corresponding author.

[1] Present address: Ciba-Geigy Ltd., Basel CH 4002, Switzerland.

0021-9673/95/$09.50
SSDI 0021-9673(94)01191-5

kynurenic acid, is believed to act as a non-selective antagonist of excitatory amino acid receptors and to attenuate the neuronal excitation induced by agonists of N-methyl-D-aspartate (NMDA). Basal levels of kynurenic acid have been reported to be in the low n*M* range in the extracellular fluid (ECF) of rats and slightly higher in humans [13,14]. It has been shown that kynurenic acid cannot cross the blood–brain barrier and, therefore, all kynurenic acid present in brain tissue is generated from kynurenine. Approximately 60% of kynurenine enters the central nervous system through the blood–brain barrier; the remaining 40% is synthesized directly in the brain from L-tryptophan [15].

The purpose of the present work was to evaluate the use of CEEC for the determination of compounds of the kynurenine pathway in brain microdialysis samples. The method was used to monitor both tryptophan and kynurenine in the brain following intraperitoneal (i.p.) administration of tryptophan.

2. Experimental

2.1. Reagents

Tryptophan, kynurenine, kynurenic acid, anthranilic acid, 3-hydroxykynurenine, 3-hydroxyanthranilic acid, 5-hydroxyanthranilic acid, and xanthurenic acid were all purchased from Sigma (St. Louis, MO, USA) and used as received. All solutions were prepared in NANOpure water (Sybron-Barnstead, Boston, MA, USA) and passed through a membrane filter (0.2 μm pore size) before use. The CE separation buffer consisted of 20 m*M* sodium borate (pH 9) unless otherwise indicated. If a higher pH were required, the solution was adjusted with sodium hydroxide. All stock solutions were prepared daily in water and stored at 4°C.

2.2. Apparatus

The CEEC system and the construction of the Nafion decoupler which allows on-column electrochemical detection have been described elsewhere [16]. Electrophoresis was driven by a high voltage supply (Spellman Electronics, Plainview, NY, USA). Polyimide-coated fused-silica capillaries (360 μm O.D., 50 μm I.D.) were obtained from Polymicro Technologies (Phoenix, AZ, USA) and capillary lengths 70–90 cm were used. Sample introduction was accomplished using a laboratory-built pressure injection system. The injection volume was calculated to be 9.8 nl using the continuous fill mode by recording the time required for the sample to reach the detector. A Spectra-Physics (Data Jet) integrator (San Jose, CA, USA) was used for data acquisition.

Cylindrical carbon fiber microelectrodes were constructed using 33 μm diameter fibers (AVCO Specialty Products, Lowell, MA, USA). The fiber was bonded to a length of copper wire using silver epoxy (Ted Pella, Redding, CA, USA). Capillary tubes were pulled to a narrow tip with a Liste-Medical Model 3A vertical pipette puller (Greenvale, NY, USA). The carbon fiber was then inserted through the capillary until it protruded ca. 0.5 cm from the tip. UV-cure-glue (UVEXS, Sunnyvale, CA, USA) was applied to the tip at the junction of the capillary and the carbon fiber. The fiber was drawn back until the desired length (150–300 μm) protruded and sealed with Black and Decker thermogrip glue to fix the copper connecting wire in place.

2.3. Cyclic voltammetry

All cyclic voltammetry experiments were carried out using a Model CySY-1 computerized electrochemical analyzer (Cypress Systems, Lawrence, KS, USA). A three-electrode cell consisting of a carbon fiber or glassy carbon working electrode, a Ag/AgCl reference electrode and a platinum auxiliary electrode was used. All cyclic voltammograms were carried out in 20 m*M* sodium borate buffer (pH 9) using a scan rate of 100 mV s^{-1}.

2.4. Microdialysis

Male Sprague-Dawley rats (290–400 g) were anesthetized with urethane (1.5 g/kg i.p.) and maintained under anesthesia during the entire

experiment. The rats were placed in a stereotaxic frame on a heating pad at 37°C. CMA/12 3-mm dialysis probes (Bioanalytical Systems, West Lafayette, IN, USA) were implanted in the hippocampus of the rat brain at the coordinates 4.8 mm posterior to bregma, 4.8 mm lateral to the midline and 5.8 mm ventral to the skull surface.

The microdialysis probes were perfused with artificial cerebrospinal fluid (ACSF) (120 m*M* NaCl, 20 m*M* $NaHCO_3$, 3 m*M* KCl, 1.2 m*M* $CaCl_2$, 1.0 m*M* $MgCl_2$ and 0.25 m*M* $NaHPO_4$) at a flow-rate of 250 nl/min. Probes were calibrated in vitro by placing them in a standard mixture of the tryptophan metabolites. The dialysates were collected and analyzed every 15 min and the relative recovery was calculated for each compound. All dialysates were directly injected into the CEEC system.

2.5. Tryptophan loading studies

Tryptophan (100 mg/kg i.p.) was systemically administered to rats. Baseline fractions were collected beginning ca. 3 h after probe implantation. At least four 15-min fractions were collected before any manipulation was attempted. Microdialysates were collected for 6 h following administration of tryptophan.

3. Results and discussion

3.1. Cyclic voltammetry

Cyclic voltammograms of tryptophan and its metabolites were obtained using both glassy carbon and carbon fiber electrodes. As can be seen from Table 1, the tryptophan metabolites exhibited a wide range of half-wave potentials. Kynurenic acid exhibited a very high oxidation potential (+ 1015 mV), and, in fact, was previously reported to be non-electroactive [17]. On the other hand, 3-hydroxykynurenine, 3-hydroxyanthranilic acid and 5-hydroxyanthranilic acid all exhibited very low oxidation potentials (as low as + 100, + 160 and +95 mV, respectively).

Table 1
The half-wave potentials of the tryptophan metabolites using a glassy carbon electrode

Compound	Half-wave potential(s) (mV) (vs. Ag/AgCl)
Tryptophan	590
Kynurenine	760
3-Hydroxykynurenine	100
Anthranilic acid	690
3-Hydroxyanthranilic acid	160 and 830
5-Hydroxyanthranilic acid	95
Kynurenic acid	1015
Xanthurenic acid	460

Experimental conditions given in Fig. 1.

One important consideration when using CEEC with a carbon fiber microelectrode is that the background current increases significantly at potentials above + 950 mV. Fig. 1 compares electropherograms obtained at + 900 and + 1000 mV. No response is obtained for kynurenic acid (Fig. 1A) at + 900 mV. At + 1000 mV kynurenic acid was detectable; however, an appreciable change in the quality of the baseline is evident (Fig. 1B). This large increase in background and baseline drift significantly decreases the *S/N* and makes it impossible to detect kynurenic acid at physiologically relevant levels in brain microdialysis samples. Since we were interested in the levels of the kynurenic acid precursors tryptophan and kynurenine in microdialysis samples, all subsequent studies employed a working potential of + 900 mV.

3.2. Separation optimization

Separation of all the compounds involved in the kynurenine pathway by CE was investigated. Initially, a 10 m*M* MES buffer at pH 7 was employed. However, both tryptophan and kynurenine migrated with the system (neutral) peak at this pH. If the buffer were changed to 10 m*M* sodium borate at pH 9, tryptophan and kynurenine were resolved from the system peak. Resolution could be further improved by increasing the ionic strength to 20 m*M*. Under these conditions, all the tryptophan metabolites were

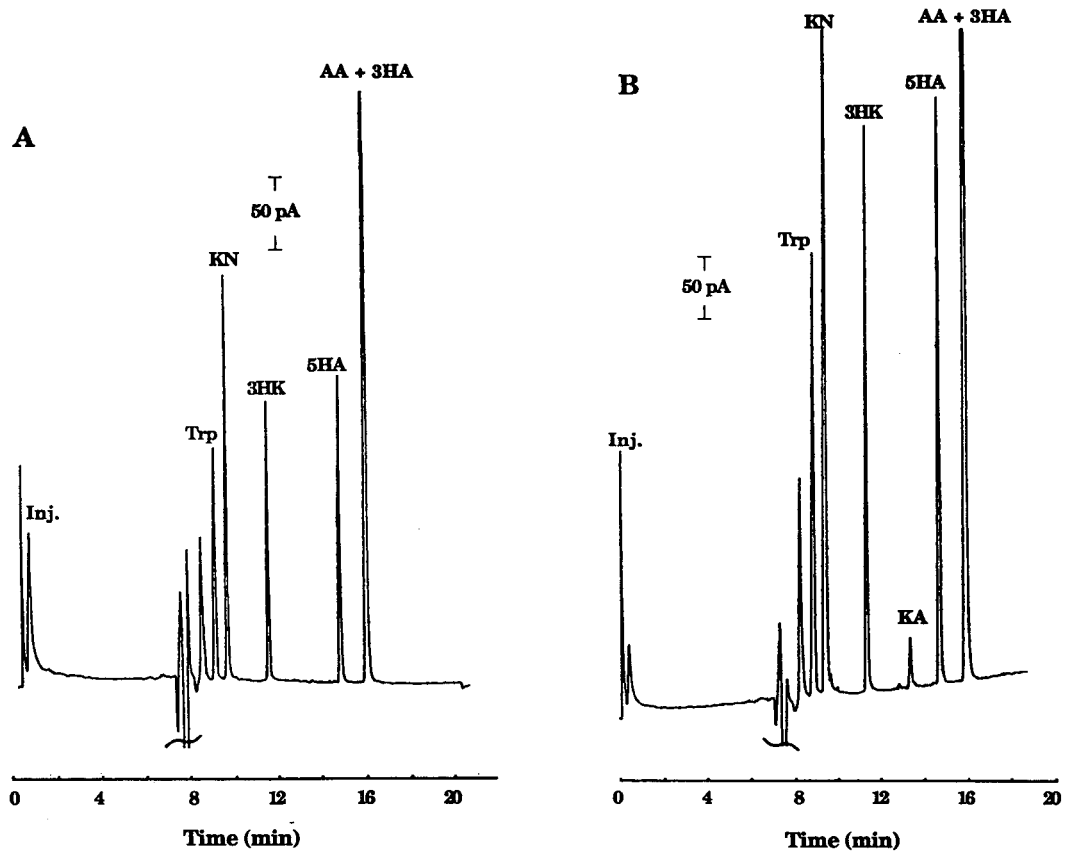

Fig. 1. Electropherograms of a standard mixture of tryptophan metabolites containing 1 μM each of tryptophan (Trp); kynurenine (KN); 3-hydroxykynurenine (3HK); anthranilic acid (AA); 3-hydroxyanthranilic acid (3HA); 5-hydroxyanthranilic acid (5HA) and 2 μM kynurenic acid (KA). Working potential of; (A) + 900 mV and; (B) + 1000 mV were applied. Separation conditions: 20 mM borate buffer, pH 9; capillary length, 80 cm, 50 μm I.D.; 20 kV.

resolved except anthranilic acid and 3-hydroxyanthranilic acid, which comigrated. These two compounds could be resolved at pH 9.6, but the overall separation efficiency was decreased. Xanthurenic acid exhibited an extremely long migration time at pH 9 due to its large negative electrophoretic mobility. Therefore, it is not shown in the electropherogram. A comparison of the separation at pH 9 and 9.6 is shown in Fig. 2.

3.3. Analytical characterization

Because kynurenine is important as a precursor to kynurenic acid, it was decided to use pH 9 for the separation of tryptophan and kynurenine in microdialysis samples. The limits of detection for all of the relevant tryptophan metabolites were determined at a detector potential of + 900 mV. A summary of the results is presented in Table 2. Very low limits of detection (LOD), generally in the attomole region, were obtained for most compounds. The LOD for kynurenic acid (determined at 1000 mV) was ca. 100 × higher than for the other compounds. As mentioned previously, this is a function of the higher baseline noise at the higher oxidation potential. In addition, + 1000 mV is not yet at the current-limiting plateau for kynurenic acid, so the response is not optimal.

The system was also evaluated for linearity and reproducibility. The detector response for kynurenine was linear between 0.5 and 100 μM

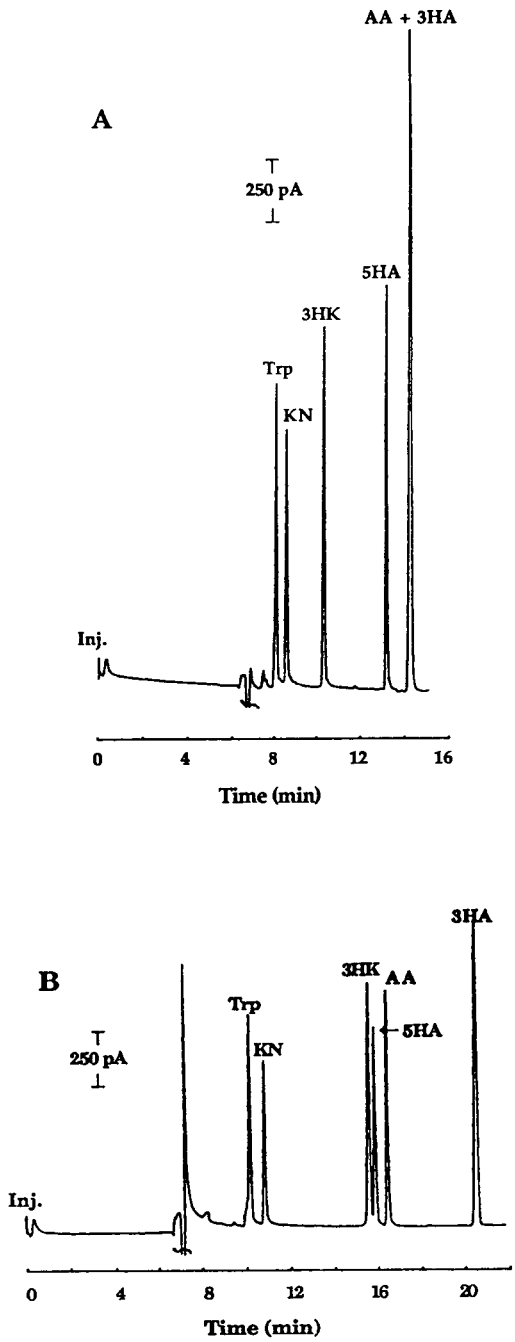

Fig. 2. Electropherograms of a standard mixture of tryptophan metabolites containing 5 μM each of Trp, KN, 3HK, AA, 3HA and 5HA. The electropherograms were run in a 20 mM sodium borate buffer at: (A) pH 9; and (B) pH 9.6. A working potential of +900 mV was used. All other conditions as in Fig. 1.

Table 2
Concentration and mass limits of detection of the tryptophan metabolites using CEEC

Compound	Concentration limit detection (nM)	Mass limit of detection (amol)
Tryptophan	4.8	46.0
Kynurenine	3.1	30.0
3-Hydroxykynurenine	0.4	4.2
Anthranilic acid	3.3	32.6
3-Hydroxyanthranilic acid	6.0	58.8
5-Hydroxyanthranilic acid	0.2	1.8
Kynurenic acid	22.2	218
Xanthurenic acid	0.6	5.9

(equivalent to 4.9–980 fmol injected) with a slope of 0.22 μM/nA and a regression coefficient of 0.9992 ($n = 12$). The reproducibility was determined by making repetitive injections of 10 μM (98 fmol injected) kynurenine. The R.S.D. was 4.54% ($n = 11$). No electrochemical activation of the carbon fiber was performed between injections since no passivation of the carbon fiber was evident following continuous use. However, electrochemical activation of the carbon fiber was necessary prior to initial use. Failure to do this resulted in slower electrode kinetics, which was evident in the cyclic voltammetric studies.

3.4. Analysis of rat brain dialysate using CEEC

In order to evaluate this method for monitoring tryptophan metabolites of the kynurenine pathway, the effect of intraperitoneal administration of tryptophan on the concentration of kynurenine in the ECF of the rat brain hippocampus was studied. In these studies, a very slow perfusion flow-rate of 250 nl/min was employed, resulting in high recovery values for tryptophan (72.5%, $n = 5$). This is much higher than the previously reported recovery of 19% using a perfusion flow-rate of 2 μl/min and LC analysis [18]. Recovery values for the other metabolites were also higher: kynurenine, 83.8%; 3-hydroxykynurenine, 43.2%; 5-hydroxykynurenine, 34.8%; and anthranilic acid, 62.4%.

It was found that immediately upon implantation of the microdialysis probe, the level of endogenous substances in the perfusate was high. Therefore, the probe was perfused for a period of at least 3 h prior to sampling, after which fractions were collected for an additional hour at 15-min intervals. Once the levels were determined to be steady, 100 mg/kg of tryptophan was administered i.p. The microdialysis experiment was continued for a period of 6 h.

Fig. 3 compares an electropherogram of dialysate samples collected (A) before tryptophan loading and (B) near the maximum ECF concentration of tryptophan. The increase of tryptophan and, subsequently, kynurenine in the ECF is clearly illustrated. It was found that the tryptophan concentration increased three- to four-fold following loading, and reached a maximum concentration of 2–3 μM ($n = 3$) at ca. 90 min after administration (indicated by arrow). This can be seen from Fig. 4A. The primary metabolite, kynurenine, reached a maximum concentration of 1.3 μM ($n = 3$) approximately 60 min after the maximum was reached for tryptophan, as can be seen in Fig. 4B.

Tryptophan and kynurenine were identified based on comigration with an authentic standard. The peaks are somewhat broader in the electropherograms of the microdialysate samples than in the electropherograms of the standards due to the discrepancy in ionic strength and pH between the dialysate samples (pH 7, 120 mM) and the run buffer (pH 9, 20 mM). Voltammetric characterization was also used to verify the identity of the kynurenine peak. This was accom-

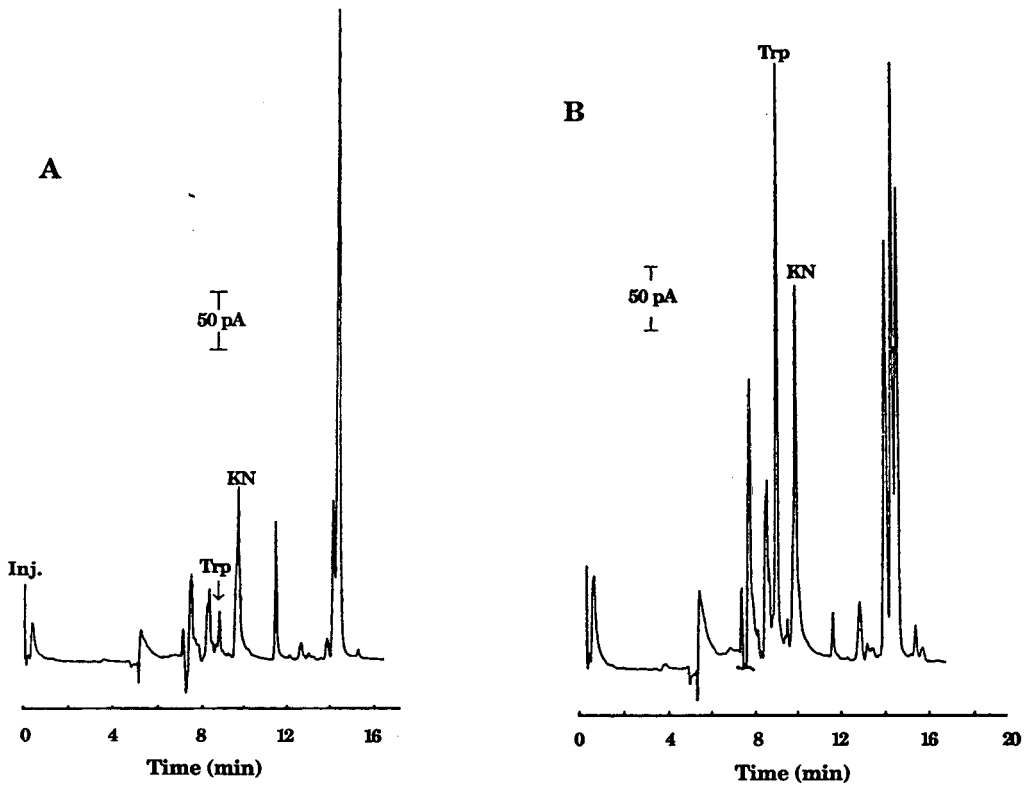

Fig. 3. Electropherograms of in vivo microdialysis samples taken from the hippocampus region of the brain of an anesthetized rat. (A) Dialysate sample taken before tryptophan administration; and (B) dialysate sample taken after tryptophan administration (100 mg/kg i.p.) near the maximum ECF concentration of Trp. The figure demonstrates the increase in both Trp and KN concentrations. Working potential = + 900 mV. Other conditions as in Fig. 1.

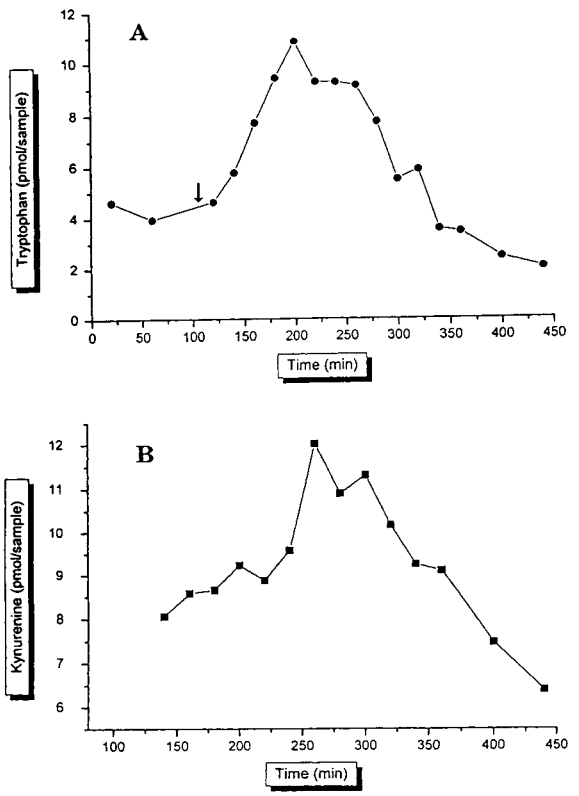

Fig. 4. A plot of ECF concentration vs. time for (A) tryptophan and (B) kynurenine for a tryptophan-loading experiment (100 mg/kg i.p.). The arrow indicates the time of Trp loading. Working potential + 900 mV. All other conditions as in Fig. 1.

plished by calculating the current ratio of + 800/ + 850 mV. The ratios were 0.65 and 0.62 for the sample and standard, respectively. In this particular set of experiments, the other tryptophan metabolites were not quantitated. However, it can be seen in Fig. 4B that the levels of 5-hydroxyanthranilic acid and 3-hydroxyanthranilic acid also increased.

4. Conclusions

In this report we have demonstrated the use of CEEC for monitoring in vivo microdialysis samples for kynurenine and tryptophan. The high sensitivity and low volume requirements of this technique make it possible to monitor these compounds with good temporal resolution and high recoveries. Future studies will focus on the development of improved methods for the separation and detection of the other tryptophan metabolites as well as alternative methods of detection for kynurenic acid.

Acknowledgments

The support of this work by Bioanalytical Systems, The Kansas Technology Enterprise Corporation and the National Science Foundation via grant EHR 92-55223 is gratefully acknowledged. The authors thank Nancy Harmony for editorial assistance in the preparation of the manuscript.

References

[1] C.E. Lunte, D.O. Scott and P.T. Kissinger, *Anal. Chem.*, 63 (1991) 773A.
[2] T.E. Robinson and J.B. Justice, Jr. (Editors), *Microdialysis in the Neurosciences*, Elsevier, Amsterdam, 1992.
[3] J.W. Jorgenson and K.D. Lukacs, *Anal. Chem.*, 53 (1981) 1298.
[4] R.A. Wallingford and A.G. Ewing, *Anal. Chem.*, 61 (1989) 98.
[5] P.D. Curry, G.E. Engstrom-Silverman and A.G. Ewing, *Electroanalysis*, 3 (1991) 358.
[6] S.M. Lunte and T.J. O'Shea, *Electrophoresis*, 15 (1994) 79.
[7] M.A. Malone, P.L. Weber, M.R. Smyth and S.M. Lunte, *Anal. Chem.*, in press.
[8] A.G. Ewing, J.M. Mesaros and P.F. Gavin, *Anal. Chem.*, 66 (1994) 527A.
[9] T.J. O'Shea, P.L. Weber, B.P. Brammel, C.E. Lunte, S.M. Lunte and M.R. Smyth, *J. Chromatogr.*, 608 (1992) 189.
[10] T.J. O'Shea, M. Telting-Diaz, S.M. Lunte, C.E. Lunte and M.R. Smyth, *Electroanalysis*, 4 (1992) 463.
[11] R. Schwarcz, F. Du, W. Schmidt, W.A. Turski, J.B.P. Gramsbergen, E. Okuno and R.C. Roberts, *Ann. N.Y. Acad. Sci.*, 648 (1992) 140.
[12] R. Schwarcz, *Biochem. Soc. Trans.*, 21 (1993) 77.
[13] P. Russi, M. Alesiami, G. Lombardi, P. Davolio, R. Pellicciari and F. Moroni, *J. Neurochem.*, 59 (1992) 2076.
[14] K.J. Swartz, M.J. During, A. Freese and M.F. Beal, *J. Neurosci.*, 10 (1990) 2965.

[15] E.M. Gal and A.D. Sherman, *Neurochem. Res.*, 30 (1980) 223.
[16] T.J. O'Shea, R.D. Greenhagen, S.M. Lunte, C.E. Lunte, M.R. Smyth, D.M. Radzik and N. Watanabe, *J. Chromatogr.*, 593 (1992) 305.
[17] A.J. Elderfield, R.J.W. Truscott, I.E.T. Ganon and G.M. Schier, *J. Chromatogr.*, 495 (1989) 71.
[18] A.-K. Collin and U. Ungerstedt, *Microdialysis, Users Guide*, Carnegie Medicin, Stockholm, 4th ed., 1988.

ELSEVIER

Journal of Chromatography A, 700 (1995) 81–87

JOURNAL OF CHROMATOGRAPHY A

Analysis of glutamate in striatal microdialysates using capillary electrophoresis and laser-induced fluorescence detection

L.A. Dawson*, J.M. Stow, C.T. Dourish, C. Routledge

Wyeth Research UK, Taplow, Maidenhead, Berks. SL6 0PH, UK

Abstract

High-performance liquid chromatography (HPLC) with electrochemical detection has been used routinely to analyse the neurochemical constituents of brain microdialysates. However, conventional HPLC analysis requires large injection volumes and hence lengthy dialysis sampling times. Capillary electrophoresis (CE) is a rapid high-resolution separation technique with the ability to routinely handle very small sample volumes. If CE is coupled to a high-sensitivity detection system, such as laser-induced fluorescence (LIF), it becomes a powerful and rapid separation technique for the analysis of small-volume microdialysis samples.

These preliminary studies report reduced separation times for the excitatory amino acid glutamate, prederivatised with naphthalene 2,3-dialdehyde, and demonstrate its detection within small-volume brain microdialysis samples. The limit of detection for this system was 10^{-8} *M*.

Characterisation of striatal microdialysis samples comprised infusions of Ca^{2+}-free artificial cerebrospinal fluid (aCSF) and Tetrodotoxin (TTx) (10 m*M*) to demonstrate that the detected transmitter is of neuronal origin and released in a calcium-dependent manner.

Removal of calcium from aCSF resulted in a decrease in glutamate in dialysis samples. Glutamate release significantly decreased ($p < 0.05$) to ca. 40% of preinfusion control levels after 60 min and this level was maintained throughout the sampling period. These data suggest that glutamate release is, to some degree, a calcium-dependent process. TTx infusion (10 μM) produced a significant ($p < 0.05$) reduction in glutamate release to ca. 10% of preinfusion levels. It would therefore appear that glutamate release is dependent on neuronal activity. In summary, we have demonstrated the establishment of CE–LIF and microdialysis for the measurement of glutamate.

1. Introduction

The excitatory amino acids are quantitatively one of the most important group of neurotransmitters in the brain with ubiquitous occurrence and universal neuronal excitatory properties [1]. Glutamate is one of these amino acids with such characteristics. Glutamate is involved in various metabolic functions, is released from neurones in response to neuronal stimulation and is subsequently taken up by both neurones and glia [2]. Recently glutamate has been implicated in the pathogenesis of neurological and psychiatric disorders such as Alzheimers disease [3], Parkinson's disease [4] and schizophrenia [5]. The rapid and sensitive in vivo monitoring of excitatory amino acids, in particular glutamate, in response to potential neuroactive molecules is therefore of particular interest in the search for possible treatments for these conditions. Brain mi-

* Corresponding author.

0021-9673/95/$09.50
SSDI 0021-9673(94)01138-9

crodialysis [6] is a technique which can monitor in vivo changes in release of many neurotransmitters such as dopamine [7], serotonin [8] and amino acids [9].

Analysis of the neurochemical constituents of brain microdialysates has conventionally used high-performance liquid chromatography (HPLC) with electrochemical detection. However, conventional HPLC analysis requires large injection volumes and hence lengthy dialysis sampling times. Capillary electrophoresis (CE) is a rapid high-resolution separation technique with the ability to routinely handle very small sample volumes (typically 1–5 nl). If CE is coupled to a high-sensitivity detection system, such as laser-induced fluorescence (LIF), it becomes a powerful technique for the analysis of small-volume microdialysis samples.

We now report a rapid and sensitive method for the analysis and detection of glutamate in rat striatal dialysates by CE–LIF.

2. Experimental

2.1. Chemicals

All chemicals were analytical grade and purchased from BDH (Poole, UK). Tetrodotoxin was purchased from Sigma (Poole, UK). Naphthalene 2,3-dialdehyde (NDA) was purchased from Aldrich (Poole, UK).

2.2. Microdialysis

Animals

Male Sprague–Dawley rats (280–350 g Charles River) were used in all experiments. All animals were group housed in cages with food and water available ad libitum. Following surgery the animals were singly housed in Plexiglass cages (30 cm^2) with food and water available ad libitum.

Surgical procedure

Following induction of anaesthesia with gaseous administration of halothane (5%) (Fluothane, Zeneca, Macclesfield, UK) the animals were secured in a stereotaxic frame with ear and incisor bars. Anaesthesia was maintained by continuous administration of halothane (1–2%). A microdialysis guide cannula (CMA/Microdialysis, Sweden) was implanted and cemented to the skull using dental acrylic. Coordinates for the striatum were taken according to Paxinos and Watson [10]: RC, 0.4; L, 3.7 (reference point taken from bregma); V, 2.8 mm from the dura. The wound was sutured and the animals left to recover for 24 h.

Microdialysis procedure

The dialysis probe (4 mm × 0.5 mm O.D.) (CMA/Microdialysis) was implanted via the guide cannula into the striatum of the unrestrained rat 24 h post surgery and was perfused with artificial cerebrospinal fluid (aCSF) (NaCl 125 m*M*, KCl 3.0 m*M*, $MgSO_4$ 0.75 m*M* and $CaCl_2$ 1.2 m*M*, pH 7.4) at a flow-rate of 0.5 μl/min. A 3-h stabilisation period was allowed following probe implantation after which time dialysis sampling was carried out by a modification of the method of Routledge et al. [11]; 20-min samples were collected throughout the experimental period. Five preinfusion control samples were collected and all subsequent values were expressed as a percentage of the preinfusion control level. Characterisation studies comprised continuous infusions of either Ca^{2+}-free aCSF (NaCl 125 m*M*, KCl 3.0 m*M* and $MgSO_4$ 0.75 m*M*, pH 7.4) or Tetrodotoxin (TTx) (10 μM in aCSF).

2.3. Capillary electrophoresis

Apparatus

All analyses were performed on a Beckman P/ACE 2050 with He–Cd LIF (442 nm) (Omnichrome, CA, USA). Separations were performed in fused-silica capillaries (47 cm × 375 μm O.D. × 50 μm I.D.) (Composite Metal Services, Hallow, Worcester, UK) with an applied voltage of 0.64 kV/cm. Sample was applied to the capillary via a high-pressure injection system. Data were collected and integrated using Xchrom (VG Data Systems, Altrincham, UK).

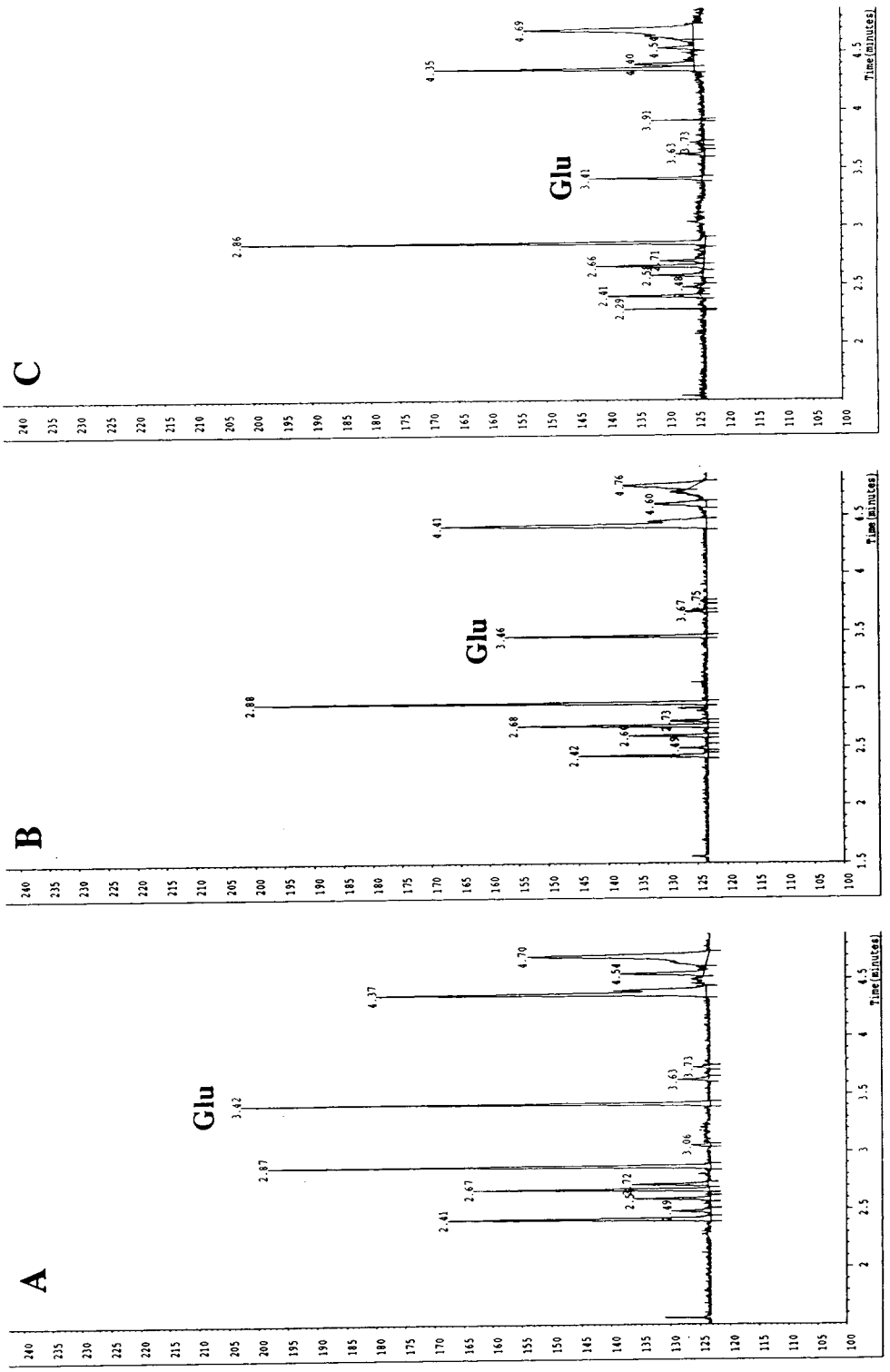

Fig. 1. Electropherograms demonstrating decreasing glutamate in response to infusions of Ca^{2+}-free aCSF. (A) Preinfusion control sample, (B) 100 min post infusion, (C) 280 min post infusion.

Separation procedure

Separations used 30 m*M* sodium carbonate with 20 m*M* sodium dodecyl sulphate (SDS) pH 9.5 (pH using 1 *M* NaOH). Total run time was 5 min. The capillary was rinsed with 0.1 *M* NaOH (2 min) and running buffer (2 min) between analyses.

Derivatisation procedure

All samples were prederivatised with NDA by a modification of the method of Hernandez et al. [12]. Dialysate or standard samples (10 μl) were mixed with 50 m*M* boric acid buffer pH 9.5, 10 m*M* sodium cyanide and 30 m*M* NDA in methanol (1:5:2:1) and left to stand for 5 min at room temperature before analysis.

Analysis of data

Results were analysed by ANOVA followed by post hoc analysis where appropriate using the Super ANOVA software application (Abacus Concepts, Berkeley, CA, USA) on an Apple Macintosh PC.

3. Results

Samples were analysed by micellar electrokinetic capillary chromatography (MECC) and separation conditions were optimised to produce high resolution of the excitatory amino acid glutamate and as many of the other dialysate constituents as possible. Reproducibility was good with separations of glutamate maintained with as little as a 1% variation in retention time (3.26 ± 0.01 min). Standard calibrations revealed a linear relationship between concentration and peak area over the concentration range 10^{-6}–10^{-8} *M* for derivatised glutamate (slope $= 5.6 \cdot 10^{7}$ and correlation coefficient = 1). The limit of detection for glutamate was 50 amol on capillary which corresponds to a concentration of 10^{-8} *M*.

The average recovery of the probe, for glutamate, was calculated to be $18.5 \pm 1.4\%$. Basal levels of glutamate within dialysates, ranged between 1 and 10 μM.

Infusions of Ca^{2+}-free aCSF resulted in a decrease in glutamate concentrations in dialysis samples (Fig. 1). Glutamate release showed a significant decrease ($p < 0.05$) to 40% of preinfusion control levels 60 min post infusion and this reduced level was maintained throughout the sampling period (Fig. 2).

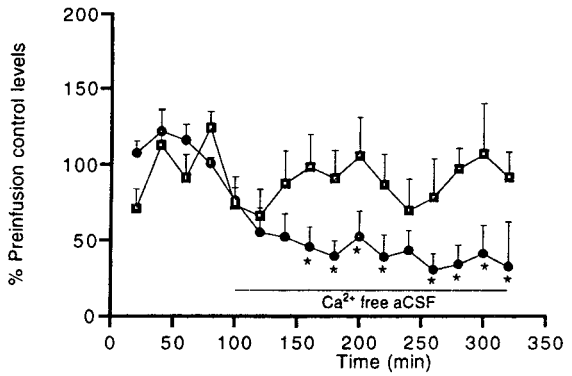

Fig. 2. Effects of Ca^{2+}-free aCSF infusion on striatal glutamate release. □ = Vehicle controls; ○ = Ca^{2+}-free aCSF treatment. Data are expressed as the mean ± standard error of the mean (SEM) for $n = 6$ animals. * demonstrates statistical significance ($p < 0.05$) from vehicle controls.

Infusions of TTx (10 μM) also resulted in a significantly ($p < 0.05$) decreased glutamate in dialysis samples (Fig. 3), reaching a maximum of 10% of preinfusion control levels (Fig. 4).

4. Discussion

These data demonstrate that separation and detection of glutamate in brain microdialysate samples is possible using CE–LIF. The linearity of the derivatisation and detection appears to be effective to a minimum of 10^{-8} *M* glutamate (amol levels on capillary) and the reproducibility of this system also appears to be excellent; since basal levels are well within the limit of detection the routine analysis of glutamate using this system is now possible. Also the 5 min run time is an improvement on conventional HPLC analyses using *o*-phthalaldehyde (OPA) derivatisation [13].

Ca^{2+} dependence and tetrodotoxin sensitivity are regarded as fundamental criteria for determining the neuronal origin and mechanisms of

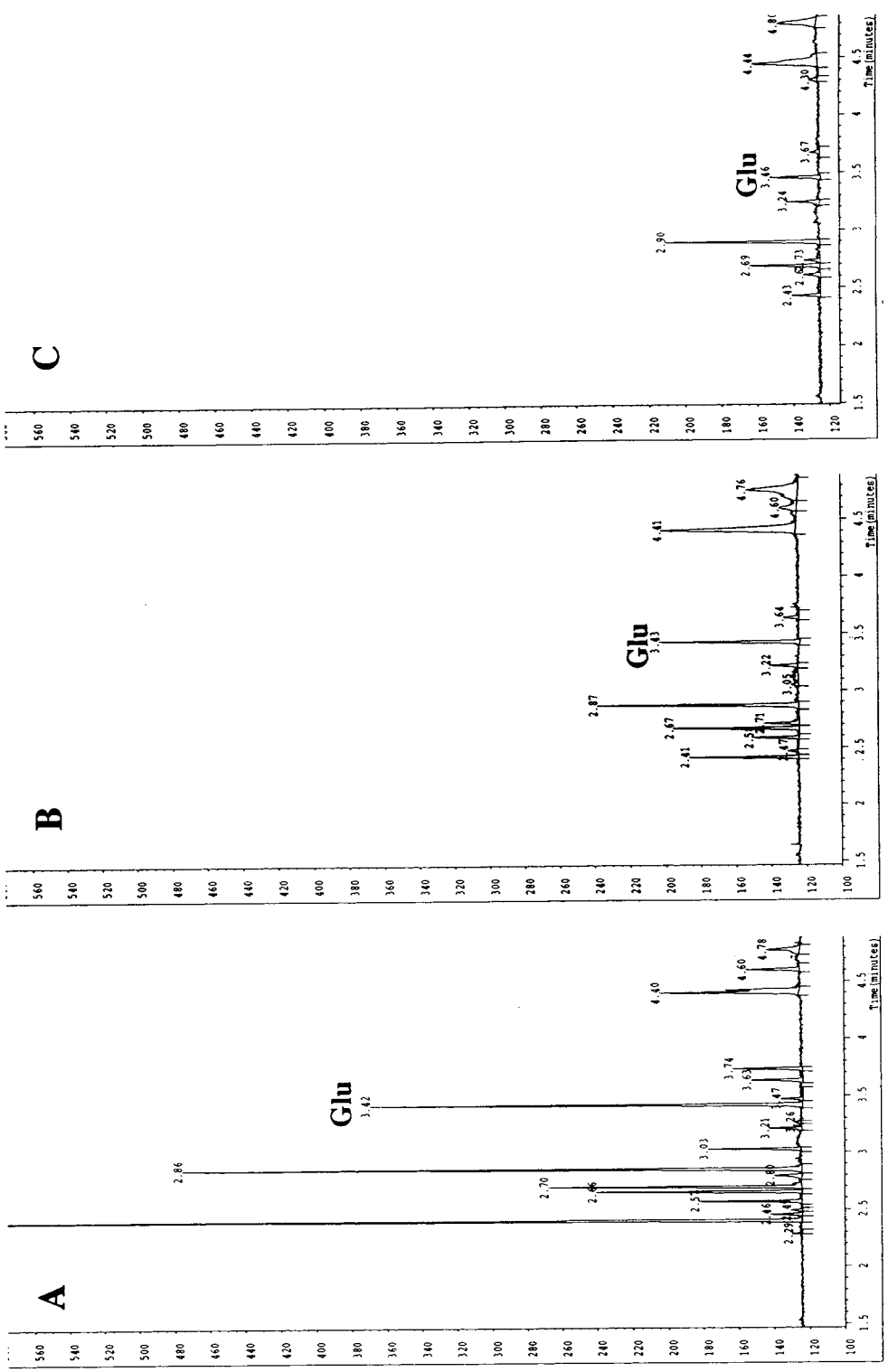

Fig. 3. Electropherograms demonstrating decreasing glutamate in response to infusions of TTx. (A) Preinfusion control sample, (B) 100 min post infusion, (C) 280 min post infusion.

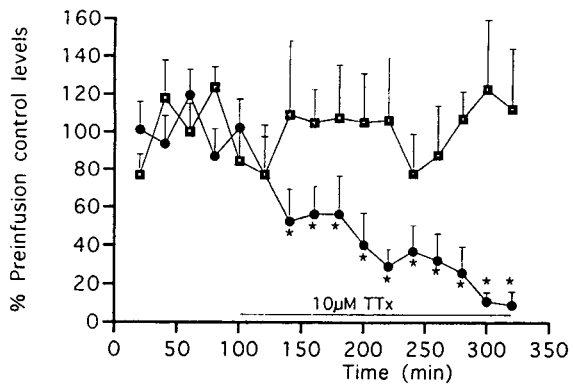

Fig. 4. Effects of TTx infusion on striatal glutamate release. □ = Vehicle controls; ○ = TTx treatment. Data are expressed as the mean ± SEM for $n = 6$ animals. * demonstrates statistical significance ($p < 0.05$) from vehicle controls.

release of neurotransmitters and therefore these are the standard manipulations frequently used to characterise microdialysis studies [14].

Removal of calcium from the infused aCSF resulted in a decrease in glutamate in dialysis samples suggesting that glutamate release is, to some degree, a calcium-dependent process. It is known that non-synaptically released pools of glutamate exist throughout the brain and the size of these pools may vary; thus it would be predicted that all sampled glutamate may not necessarily be released in a Ca^{2+}-dependent manner [15]. Therefore, in the present study 40% of the glutamate sampled from the striatum may have been from non-synaptically released sources or released by a Ca^{2+}-independent mechanism. Although separation was optimised for glutamate other unknown components were detected (retention times 2.41, 2.49, 2.59, 2.68, 2.72, 3.64, 4.54 min) (Figs. 1 and 3). These components show similar decreases in response to the Ca^{2+}-free aCSF suggesting that many of these molecules are released by a Ca^{2+}-dependent mechanism.

TTx is a Na^+ channel blocker which prevents neuronal impulse flow and consequently neurotransmitter release. Infusions of TTx resulted in a marked and significant decrease in glutamate levels; these data suggest that glutamate release in the striatum is dependent on neuronal activity. TTx, like Ca^{2+}-free aCSF infusions, induced decreases in many of the other components observed from electropherograms and it appears likely that these molecules may be other amino acids (e.g. aspartate, glycine, taurine and serine) and monoamine neurotransmitters (e.g. dopamine and noradrenaline).

In summary, we have demonstrated the establishment of CE–LIF and microdialysis for the measurement of glutamate. The present study utilised these techniques for the analysis and characterisation of glutamate release from the striatum of the freely moving rat. Decreases in dialysate glutamate concentrations following infusions of Ca^{2+}-free aCSF and TTx demonstrated that release is mainly from neuronal sources and that both Ca^{2+}-dependent and -independent mechanisms of release may be involved. The main advantage of CE–LIF is its ability to assay small sample volumes within a short analysis time making it very suitable for use with microdialysis. This technique has the potential to measure not only amino acids but many other constituents of brain dialysates, and to monitor these molecules simultaneously in response to drugs and other stimuli.

References

[1] F. Fonnum, *J. Neurochem.*, 42 (1984) 1–11.
[2] L. Hertz, L. Peng, N. Westerguard, M. Yudkoff and A. Schousboe, in A. Schousboe, N.H. Diemer and H. Kofod (Editors), *Alfred Benzon Symposium 32, Drug Research Related to Neuroactive Amino Acids*, Munsgaard, Copenhagen, 1992, pp. 30–48.
[3] J.T. Greenamyre and A.B. Young, *Neurobiol. Aging* 10 (1989) 593–602.
[4] J.T. Greenamyre, *J. Neural Transm.*, 91 (1993) 255–269.
[5] M. Carlsson and D. Carlsson, *Trends Neurosci.*, 13 (1990) 272–277.
[6] U. Ungerstedt and A. Hallstrom, *Life Sci.*, 7 (1987) 861–864.
[7] A. Imperato and G. Di Chiara, *J. Neurosci.*, 5 (1985) 297–306.
[8] T. Sharp and S. Hjorth, *J. Neurosci. Methods*, 34 (1990) 83–90.
[9] U. Tossman and U. Ungerstedt, *Acta Physiol. Scand .*, 128 (1986) 9–14.

[10] G. Paxinos and C. Watson, *The Rat Brain in Stereotaxic Coordinates*. Academic Press, New York, 1986.
[11] C. Routledge, J. Gurling, I.K Wright and C. T. Dourish, *Eur. J. Pharm.*, 239 (1993) 195–202.
[12] L. Hernandez, J. Escalona, P. Verdeguer and N.A. Guzman, *J. Liq. Chromatogr.*, 16 (1993) 2151–2160.
[13] H.L. Rowley, K.F. Martin and C.A. Marsden, *Br. J. Pharmacol.*, 111 (1994) 210P.
[14] G. Di Chiara, *Trends Pharmacol. Sci.*, 11 (1990) 116–121.
[15] V. Adam-Vizi, *J. Neurochem.*, 58 (1992) 395–404.

ELSEVIER

Journal of Chromatography A, 700 (1995) 89–94

JOURNAL OF CHROMATOGRAPHY A

Separation of r-hirudin from similar substances by capillary electrophoresis

C. Dette, H. Wätzig*

Institute of Pharmacy and Food Chemistry, University of Würzburg, Am Hubland, D-97074 Würzburg, Germany

Abstract

The thrombin inhibitor r-hirudin is a peptide of 65 amino acids and with a p*I* of 4.4. Capillary electrophoresis (CE) was used to separate r-hirudin from seven closely related substances which may be found as by-products or from degradation. Possibly two of these substances differ only in an isoaspartyl instead of an aspartyl binding. A baseline separation was possible with an acetate buffer (pH 4.4, 60 m*M*) containing 0.3% (m/m) PEG 20 000 and 0.1 m*M* Zn^{2+}. The possibilities to prevent wall adsorption are discussed.

1. Introduction

The peptide hirudin (Fig. 1) is a potent and specific thrombin inhibitor for anticoagulant therapy. Hirudin is used for post-operative venous thrombosis or prophylaxis of arterial thrombosis. It is applied subcutaneously or intravenously.

Natural hirudin is a peptide consisting of 65 amino acids (relative molecular mass ca. 7000) with an isoelectric point (p*I*) of about 4.4 (Fig. 1). The hydrophilic C-terminus is remarkable rich in acidic amino acids, which are printed bold in Fig. 1, including a tyrosin-O-sulfonate in position 63 in about 30% of the natural hirudin forms. The acidic C-terminus, three disulfide bridges and lysin in position 47 are essential for the therapeutical effects [1].

The natural source are the salivary glands of the bloodsucking leech (*Hirudo medicinalis*). A single leech contains about 10 μg of hirudin. Thus 1000 leeches will be necessary for one daily dosage, which is too much for a sufficient production of hirudin. More substance is available for medical research and treatment since the production of r-hirudin is possible by gene technology.

If synthezised proteins or polypeptides are used therapeutically, purity evaluation and characterization of minor impurities are important aspects for quality control. The structural differences between r-hirudin and the degradation products are minor. The purpose of this study was to examine whether r-hirudin can be separated from seven closely related artificial substances which may be found as by-products or after degradation of the product. Although all the seven substances will probably have the same effects as r-hirudin, a purity control gives information about the quality of the preparation process.

The isoforms of artificial r-hirudin are not sulfonated in position 63. Different variations exist, e.g. the two valines at the N-terminal are

* Corresponding author.

0021-9673/95/$09.50
SSDI 0021-9673(94)01261-X

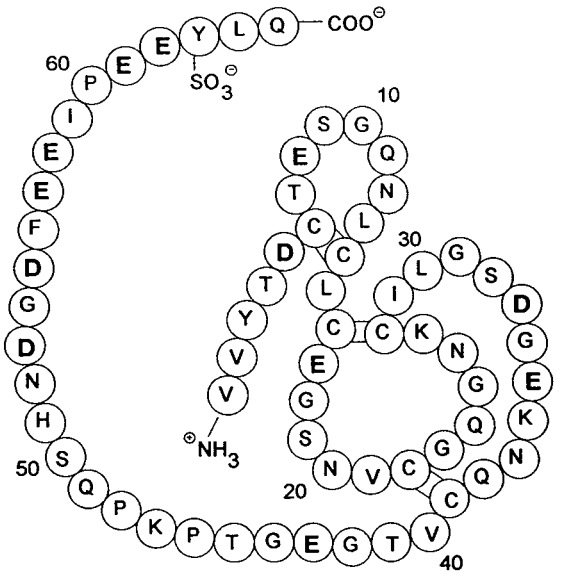

Fig. 1. Primary structure of natural hirudin, acids printed bold. C = Cys = Cysteine; D = Asp = aspartic acid; E = Glu = glutamic acid; F = Phe = phenylalanine; G = Gly = glycine; H = His = histidine; K = Lys = lysine; L = Leu = leucine; N = Asn = asparagine; P = Pro = proline; Q = Gln = glutamine; S = Ser = serine; T = Thr = threonine; V = Val = valine; Y = Tyr = tyrosine.

exchanged for variation 1 (r-HV1). Additionally two aspartic acids (Asp) in positions 33 and 53 are exchanged to asparagine (Asn) for variation 2 (r-HV2). Both show the same anticoagulant activity as native hirudin [2].

r-Hirudin (r-HH) and the seven analogous substances (aS1–aS7) all consist of 65 amino acids. r-HH under investigation could be r-HV1 or r-HV2. Structural information about the analogous substances was not available. However, they were characterized by their behavior in ion-exchange chromatography (IEC). Structural differences of possible variations to r-HV1 or r-HV2 are described. They are mainly caused by deamidation and isomerisation of Asn. Geiger and Clarke [3] explained that Asn–Gly structures easily undergo deamidation. First a succinimide (= imido binding) is built followed by hydrolysis to aspartyl or isoaspartyl in a ratio of 1:3 (Fig. 2). The succinimide is stable and can be isolated. Thus for r-HV2 seven similar products are possible [4]. More drastic conditions are necessary to form succinimide bindings from Asp–Gly structures [5]. Additionally deamidation of Asn^{52} [4] or O-phosphorylation, e.g. at Thr^{45} [6], are possible. Combinations of deamidation, isomerisation and phosphorylation lead to a variety of slightly different r-hirudin derivatives.

Capillary electrophoresis (CE) is chosen to separate these closely related proteins. Lüdi and Gassmann [7] and Paulus and Gassmann [8] separated r-hirudin from degradation products which consist of one or two amino acids less. Buffers are used of pH > 6, including several modifiers, e.g. N-[tris(hydroxymethyl)methyl]-glycine (Tricine), ethylendiaminetetraacetate (EDTA) or diaminobutane. These separation conditions were tested, but their selectivity was not sufficient to separate hirudin and the seven analogous compounds under investigation. Therefore another method was developed by optimizing the pH first.

2. Experimental

A Beckman P/ACE 2000 system was used, equipped with an UV detector operated at 214 nm. The electrophoretic experiments were performed in uncoated fused-silica capillaries with 300 mm effective length to the detector (370 mm total length) and 50 μm I.D. (Polymicro, Phoenix, AZ, USA) with 25 kV (25–26 μA) as applied voltage at a constant temperature of 25°C. The injection time was 4 s with 34.5 kPa (= 0.5 p.s.i.). The coated capillary was CElect-H2 with 600 mm effective length to the detector (670 mm total length) and 50 μm I.D. (Supelco Deutschland, Bad Homburg, Germany). If not stated otherwise, chemicals were of analytical-reagent grade, supplied by Merck (Darmstadt, Germany). The standard 60 m*M* acetate buffer, pH 4.4 with 0.3% polyethyleneglycol 20 000 (PEG 20 000; Hoechst, Frankfurt, Germany, pharmacopoeia quality) and 0.1 m*M* $ZnCl_2$ was prepared by dissolving 4.12 ml 1 *M* acetic acid, 154.4 mg sodium acetate, 300.0 mg PEG 20000

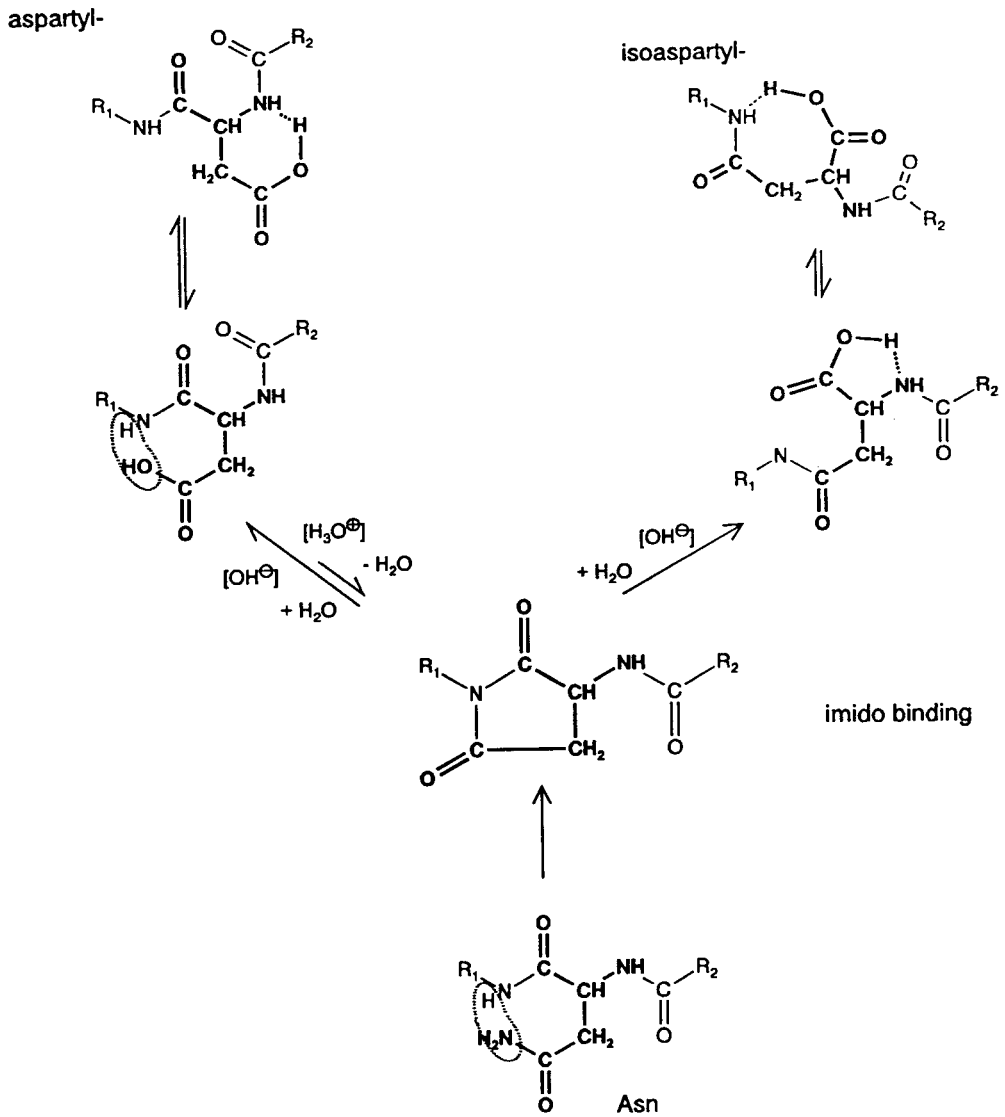

Fig. 2. Scheme of the formation of succinimide and isoaspartyl starting with aspartyl (printed bold), according to Refs. [3] and [4].

and 1.4 mg $ZnCl_2$ to 100.0 ml with HPLC-grade water (Millipore, Eschborn, Germany). r-Hirudin and related substances were kindly given by Hoechst. Usually about 1.8 mg/ml of the main compound and 0.4–1.2 mg/ml of the related substances were solved in HPLC-grade water.

3. Results and discussion

3.1. Method development

In general the method development in CE should start with optimizing the pH [9]. Usually the best pH is close to the pK_a of the compounds

involved, because there the differences of the charge/mass ratio are maximized. Using different acetate buffer the best results were found with 60 m*M* at pH 4.4 (Fig. 3), although the selectivity was still uncomplete.

The modifiers used in the literature [7,8] were now adapted to enhance selectivity. EDTA will complex all metal cations, so the proteins will be in their native conformations. The addition of a definite amount of metal cations, e.g. Zn^{2+} or Mg^{2+} will cause the opposite effects, defined protein–cation complexes. The mobility and thus the selectivity is changed by formation of complexes with Zn^{2+} or Mg^{2+}. While EDTA and Mg^{2+} give hardly, if any, improvement, Zn^{2+} slightly improved the separation.

Modifiers to manipulate the endoosmotic flow (EOF) were tried next to enhance efficiency. Tricine, also added in increasing amounts (up to 0.2 m*M*), showed no effects. Diaminobutane also gave no improvement and was worse to handle with. The addition of PEG with a relative molecular mass of 20 000 led to an optimal separation of hirudin and analogues (Fig. 4). However, shifting migration times show that adsorption still takes place.

3.2. Migration order

The resultant migration order (aS4, r-HH, aS1, aS2, aS3, aS5, aS7 and aS6, Fig. 4) and the structural differences described above should lead to some remarks about the possible structures of the r-hirudins analogous. All substances are negatively charged, so they migrate slower than the EOF. The longer they stay on the capillary the smaller is their gross mobility and the higher their electrophoretic mobility (μ_{ep}). A higher μ_{ep} means a higher charge/mass ratio. From migration order it should be expected that aS4 has the smallest, aS6 the greatest negative charge with the remaining products having intermediate charge. The same results were obtained by characterisation with preparative IEC.

aS4 (migration time 4.42 min, Fig. 4) is less negatively charged than r-HH, because it is migrating before r-HH (4.92 min, Fig. 4). A succinimide means for r-HV1 one negative charge less and a reduction of 18 ($=H_2O$) in relative molecular mass. Probably aS4 has one or two succinimide bindings.

The other substances are more negatively charged than r-HH. Three groups can be distinguished. Slightly more negative substances are possible because of one or two isoaspartyl bindings instead of an Asn. Isoaspartyl should be more acidic because of the better possibility for aspartyl to build intramolecular hydrogen bonds.

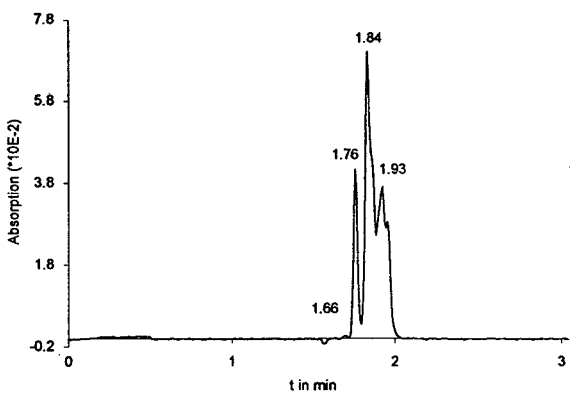

Fig. 3. Mixture of r-hirudin and seven related substances separated by an acetate buffer 60 m*M*, pH 4.4, 300 mm × 50 μm I.D. capillary, 25 kV (26 μA), 25°C. It was not possible to identify the peaks.

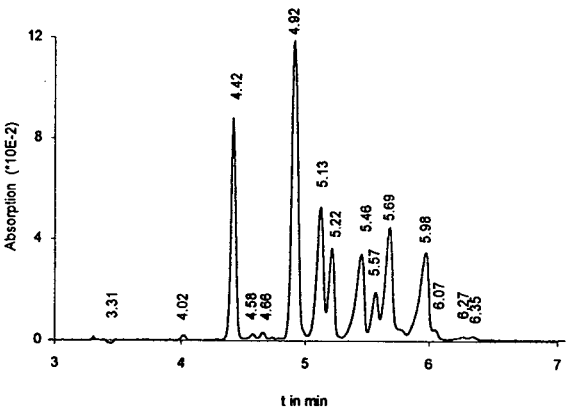

Fig. 4. Mixture of r-hirudin and seven related substances with an acetate buffer 60 m*M*, pH 4.4 + 0.3% PEG 20 000 + 0.1 m*M* Zn^{2+}; other conditions as in Fig. 3. Migration order: aS4 (migration time 4.42 min), r-HH (4.92 min), aS1 (5.13 min), aS2 (5.22 min), aS3 (5.46 min), aS5 (5.57 min), aS7 (5.69 min), aS6 (5.98 min); peaks at 4.02, 4.58, 4.66, 6.07, 6.27 and 6.35 min are unknown substances, probably degradation products from the reference substances.

Table 1
Migration times and electrophoretic mobilities of r-hirudin, seven analogous substances and acetanilide as the neutral marker in 15 consecutive runs

	EOF	aS4	r-HH	aS1	aS2	aS3	aS5	aS7	aS6
Migration times (min)									
	3.48	4.42	4.92	5.13	5.22	5.46	5.57	5.69	5.98
	3.46	4.4	4.9	5.11	5.2	5.44	5.55	5.67	5.96
	3.49	4.44	4.94	5.15	5.25	5.49	5.61	5.72	6.02
	3.5	4.45	4.95	5.17	5.26	5.5	5.62	5.74	6.03
	3.5	4.47	4.98	5.2	5.3	5.54	5.66	5.78	6.08
	3.53	4.49	5	5.23	5.32	5.57	5.69	5.8	6.11
	3.88	5.1	5.77	6.07	6.2	6.54	6.7	6.86	7.29
	3.85	5.06	5.72	6.02	6.11	6.47	6.64	6.79	7.22
	3.86	5.06	5.73	6.02	6.15	6.48	6.64	6.79	7.22
	3.86	5.07	5.73	6.03	6.15	6.49	6.65	6.8	7.23
	3.96	5.23	5.95	6.26	6.4	6.77	6.94	7.11	7.58
	3.93	5.18	5.88	6.19	6.33	6.69	6.86	7.02	7.48
	3.92	5.18	5.88	6.19	6.33	6.68	6.86	7.02	7.48
	3.93	5.19	5.89	6.2	6.34	6.7	6.87	7.03	7.49
	3.94	5.19	5.9	6.21	6.35	6.7	6.88	7.04	7.5
Mean	3.74	4.86	5.48	5.75	5.86	6.17	6.32	6.46	6.84
S.D.	0.21	0.36	0.45	0.5	0.52	0.57	0.6	0.62	0.7
R.S.D. (%)	5.61	7.41	8.21	8.7	8.87	9.24	9.49	9.6	10.23
Increase (%)	12.4	16.02	18.11	19.05	19.53	20.39	21.04	21.21	22.55
Electrophoretic mobilities ($cm^2\ kV^{-1}\ min^{-1}$)									
	0.00	−2.71	−3.73	−4.10	−4.25	−4.63	−4.79	4.96	−5.33
	0.00	−2.74	−3.77	−4.14	−4.29	−4.67	−4.83	−5.00	−5.38
	0.00	−2.72	−3.73	−4.10	−4.26	−4.63	−4.81	−4.96	−5.35
	0.00	−2.71	−3.72	−4.10	−4.24	−4.61	−4.79	−4.95	−5.32
	0.00	−2.75	−3.77	−4.15	−4.31	−4.67	−4.84	−5.00	−5.38
	0.00	−2.69	−3.70	−4.09	−4.23	−4.61	−4.77	−4.92	−5.31
	0.00	−2.74	−3.75	−4.13	−4.28	−4.65	−4.82	−4.97	−5.35
	0.00	−2.76	−3.77	−4.16	−4.27	−4.67	−4.85	−4.99	−5.38
	0.00	−2.73	−3.75	−4.13	−4.28	−4.65	−4.82	−4.96	−5.35
	0.00	−2.75	−3.75	−4.14	−4.28	−4.66	−4.83	−4.97	−5.36
	0.00	−2.72	−3.75	−4.12	−4.27	−4.65	−4.81	−4.97	−5.35
	0.00	−2.73	−3.75	−4.12	−4.28	−4.66	−4.83	−4.97	−5.36
	0.00	−2.76	−3.78	−4.15	−4.31	−4.68	−4.85	−5.00	−5.39
	0.00	−2.74	−3.76	−4.14	−4.29	−4.67	−4.83	−4.98	−5.37
	0.00	−2.71	−3.74	−4.12	−4.28	−4.64	−4.82	−4.96	−5.35
Mean	0	−2.73	−3.75	4.13	4.28	4.65	4.82	4.97	−5.36
S.D.	0	0.02	0.02	0.02	0.02	0.02	0.02	−0.02	−0.02
R.S.D. (%)	0	0.73	0.53	0.48	0.47	0.43	0.41	0.4	0.37

Separation conditions as in Fig. 4. The capillary was not washed with NaOH between runs. The R.S.D. of the migration times is high. The reason is a significant trend, which can be recognized by looking at the percental increase (difference between the first and last value divided by their mean). This trend is caused by adsorption at the capillary wall, which decreases the EOF. The electrophoretic mobility during the series is free of trends, the corresponding R.S.D. is only about 0.5%.

A strong increase in negative charge is possible because of deamidation, much more negatively charged substances are formed by phosphorylation or more than one deamidation or isomerisation.

3.3. Adsorption

The theoretical plate number of the main peak in Fig. 4 is about $N = 38\,000$. This is far below the obtained efficiency in other separations. In addition the migration time of consecutive separations shifts and the separation itself is not stable without prewashing the capillary with 0.1 *M* NaOH. These facts indicate adsorption. Migration times of the EOF and the substances increased during consecutive runs, if the capillary was not washed with NaOH between runs. However, μ_{ep} of the investigated compounds remained constant (Table 1). Moreover, peak tailing was not observed (Fig. 4). Both facts indicate that no chromatography-like process takes place, i.e. the adsorption is very strong.

Several possibilities are described to prevent adsorption. In this case the change of pH to an acidic [10] or basic [11] pH is not possible because the selectivity would be lost. Both high-ionic-strength buffers (0.2 *M* K_2SO_4) [12] and dynamic coating with cetyltrimethylammonium bromide (CTAB) [13] reduced the EOF so strongly that a switch of polarity became necessary. The separations achieved were worse in these cases. The use of coated capillaries was unsuccessful, too. Although the same amount was injected, UV absorption was insufficient. Probably the coating material shows an own absorption at the used detection wavelength. Nevertheless, it was not possible to prevent adsorption during the separation.

The only possibility to hold the migration times nearly constant is to wash the capillary with 0.1 *M* NaOH for a longer time (> 30 min) before each run.

Acknowledgements

We thank Beckman Instruments, especially Dr. C. Nutzhorn, for the loan of the instrument and the support of our measurements, and Hoechst for the reference substances.

References

[1] P. Walsmann, *Folia Haematol. (Leipzig)*, 116 (1989) 821.
[2] F. Markwardt, *Haemostasis*, 21 (1991) 11.
[3] T. Geiger and S. Clarke, *J. Biol. Chem.*, 262 (1987) 785.
[4] A. Tuong, M. Maftouh, C. Ponthus, O. Whitechurch, C. Roitsch and C. Picard, *Biochemistry*, 31 (1992) 8291.
[5] R. Bischoff, P. Lepage, M. Jaquinod, G. Cauet, M. Acker-Klein, D. Clesse, M. Laporte, A. Bayol, A. Van Dorsselaer and C. Roitsch, *Biochemistry*, 32 (1993) 725.
[6] M. Coulet, B. Domon, H. Grossenbacher, C. Guenat, W. Märki, D. Müller and W.J. Richter, *J. Mol. Struct.*, 292 (1993) 89.
[7] H. Lüdi and E. Gassmann, *Anal. Chim. Acta*, 213 (1988) 215.
[8] A. Paulus and E. Gassmann, *Applications DS-752*, Beckman, Palo Alto, CA, 1989.
[9] H. Wätzig and C. Dette, *Pharmazie*, 49 (1994) 83.
[10] R.M. McCormick, *Anal. Chem.*, 60 (1988) 2322.
[11] H.H. Lauer and D. McManigill, *Anal. Chem.*, 58 (1986) 166.
[12] J. Green and J. Jorgenson, *J. Chromatogr.*, 478 (1989) 63.
[13] J. Wiktorowicz and J. Colburn, *Electrophoresis*, 11 (1990) 769.

ELSEVIER

Journal of Chromatography A, 700 (1995) 95–103

JOURNAL OF CHROMATOGRAPHY A

Analysis of metallothionein isoforms by capillary electrophoresis: optimisation of protein separation conditions using micellar electrokinetic capillary chromatography

John H. Beattie[a,*], Mark P. Richards[b]

[a]*Division of Biochemical Sciences, Rowett Research Institute, Bucksburn, Aberdeen, AB2 9SB, Scotland*
[b]*USDA, Agricultural Research Service, Growth Biology Laboratory, Beltsville, MD 20705-2350, USA*

Abstract

Capillary electrophoresis (CE) techniques have been successfully applied to the separation of metallothionein (MT) isoforms and have proved to be rapid, practical and economical. Study of a variety of different electrolytes and capillaries has shown that electrolyte buffer composition and capillary wall surface modifications can have considerable influence on isoform separation and resolution. Ionic surfactants such as sodium dodecyl sulphate (SDS) form micelles at elevated concentrations and the partitioning of molecules between the hydrophobic micelle phase and the aqueous phase and their resulting migration in an electric field is the basis of the technique known as micellar electrokinetic capillary chromatography (MECC). In the present work, we have used sheep and rabbit MT to optimise MECC conditions for analysis of MT isoforms. Capillaries of 57 cm gave much better separations than shorter columns although analysis times were increased to about 12 min. Changing the buffer and SDS concentration or the pH affected the selectivity of isoform separation and up to 5 isoforms in sheep MT and 6 in rabbit MT were completely or partially resolved. Comparing different diameter capillaries we conclude that 25 μm I.D. columns give better separations than 50 or 75 μm I.D. columns although sensitivity is reduced by a factor of about 3 and 5, respectively. Using our MECC conditions, columns coated with C_1 or C_{18} hydrophobic material were not found to be useful in improving MT separation or resolution although further evaluation of these columns is in progress. Analysis of sheep liver extracts using optimised conditions showed the expression of at least 4 MT isoforms in response to Zn injection and 3 of these forms were evident in extracts from untreated sheep. We therefore conclude that MECC is a suitable method for MT isoform analysis.

1. Introduction

Capillary electrophoresis (CE) has been successfully applied to the study of peptides and proteins [1–5] including metalloproteins [6]. Several different CE techniques have been applied to the separation of metallothionein (MT), a 61 amino acid metalloprotein with 20 conserved cysteine residues binding 7 divalent transition metal atoms such as zinc in a 2-domain structure [7]. In many species, MT is composed of a family of protein isoforms which code from different genes and have distinctive characteristics through substitution of as little as 1 amino acid or up to 15 residues. Separations of purified mammalian MT at neutral/alkaline pH by polyacrylamide gel electrophoresis [8] or capillary zone electrophoresis (CZE) in uncoated silica capillaries [9–11]

* Corresponding author.

0021-9673/95/$09.50
SSDI 0021-9673(94)01167-2

reveal 2 charge-distinct classes of isoforms, namely MT-1 and MT-2. The differences in charge at this pH range arise largely from substitutions involving acidic residues and MT-2 forms are more negatively charged than MT-1 forms. These proteins are induced by a wide variety of different factors including metals, cytokines and steroids [12,13] but due to limitations in available analytical techniques such as HPLC, routine study of individual isoform expression and tissue concentration has not been practicable.

The binding of metals to MT isoforms is crucial in stabilising the protein secondary structure and so metal dissociation during acidification gives rise to conformational changes. At the same time, the protein charge changes as the pH decreases below the p*I* of MT (3.8–4.4) and isoforms which co-migrate at neutral or alkaline pH can be resolved by CZE at pH 2.5 [14,15]. Unfortunately, decreasing pH also diminishes UV absorbance, which is the usual method of detecting components separated by CE, and hence sensitivity is reduced. We have therefore investigated alternative electrolyte chemistry and capillaries with different surface modifications for use at higher pH.

Capillaries with polyamine coatings reverse the electroosmotic flow (EOF) and their use with phosphate buffers at neutral pH has achieved the complete separation of 4 rabbit MT isoforms [16]. The use of neutral hydrophilic polyacrylamide-coated capillaries, in which the EOF is abolished and separation occurs by electromigration only, also encouraged the separation of different isoforms [15]. The capacity of both the polyamine and neutral coated capillaries to separate MT isoforms was found to be highly dependent on the concentration, pH and chemical nature of the buffer used as the electrolyte.

We have also investigated the application of micellar electrokinetic capillary chromatography (MECC) to the separation of MT isoforms and showed that the anionic surfactant SDS in borate buffer at pH 8.4 was suitable for resolving additional isoforms of MT-1 and MT-2 [17]. MECC does not require specialised capillaries and is a robust CE technique. The principle of MECC involves partitioning of analytes, according to their hydrophobicity, into the micellar phase which is highly charged and therefore migrates rapidly in an electric field [18]. MECC techniques were first developed by Terabe and co-workers [19,20] and a range of anionic and cationic surfactants and modifiers have been used to manipulate the selective partitioning and separation of analytes [21,22] including closely related large peptides [23]. Although the mass limit for MECC is reportedly $M_r < 5000$ [22], MT isoforms, which have metal-saturated mass values of about M_r 6500, are sufficiently influenced by the surfactant to separate during migration.

Our aim in this study was to evaluate the electrolyte and capillary conditions for MECC in order to optimise the separation of MT isoforms in purified proteins and in tissue extracts. Our preliminary investigation of various anionic, zwitterionic and cationic surfactants indicated that SDS was of greatest potential for MT isoform separation (unpublished observations). Additives which modify analyte partitioning into micelles such as methanol and urea were found to be deleterious to isoform separation and borate appeared to be better than phosphate as an MECC electrolyte buffer. Therefore our efforts to optimise the electrolyte have concentrated on modifying borate buffer concentration and pH and also SDS levels. The affinity of some types of protein to bare silica during separation is known to cause poor resolution with uncoated capillaries and the use of hydrophobic coatings in combination with MECC conditions significantly reduces the influence of the column wall [24]. Such coatings also decrease the EOF and both resolution and migration reproducibility of components separated in the capillary are improved [25]. In the case of C_1 coated capillaries, a greater proportion of the silanol groups are shielded than with the C_{18} coated capillaries and thus the reduction in EOF as compared to bare silica is reported by the manufacturer to be 47.4 and 34.4%, respectively, for the columns used in this study. Although there is no indication from previous work that MT isoforms interact with bare silica capillary walls, we investigated the utility of hydrophobic capillaries in enhancing

MT separation by EOF manipulation during MECC separations.

2. Experimental

2.1. Metallothionein samples

Sheep MT-1 and MT-2 were purified from the liver of a Zn-injected grey face ewe using standard chromatographic procedures [26] whereas rabbit Cd,ZnMT (containing MT-1 and MT-2) was obtained from a commercial source (Sigma Chemical, Poole, UK). In order to test the application of the technique to tissue extracts, samples of liver from sheep were processed using a 2-step solvent extraction method based on that of Hidalgo et al. [27] but using ethanol–acetonitrile for protein precipitation. The solvent, (ethanol–acetonitrile, 1:3, v/v) was slowly added, while vortexing, to a 33% (w/v) homogenate of liver in water (usually 1 g liver + 2 ml water) using 15 ml polypropylene tubes and after centrifugation (10 000 *g* for 5 min), the concentration of solvent in the supernatant was increased to 80%. The precipitate was collected by centrifugation at 10 000 *g* for 5 min, re-suspended in 100 μl water, centrifuged in eppendorf tubes, and the supernatant was analysed for MT.

2.2. Instrument and separation conditions

Separations were performed using a P/ACE 5000 system (Beckman Instruments, High Wycombe, UK). For studies on the influence of capillary diameter and length and electrolyte modifications, capillary cartridges with 100 × 800 μm windows were fitted with polyimide-coated fused-silica capillaries, 27, 37 and 57 cm in total length (20, 30 and 50 cm from inlet to detector window, respectively) and 25, 50 or 75 μm I.D./375 μm O.D. (Composite Metal Services Ltd., Hallow, UK). For evaluation of surface modified hydrophobic capillaries, C_1 (H50) and C_{18} (H250) columns (57 cm total length, 50 μm I.D. and 363 μm O.D.; Supelco, Poole, UK) and uncoated columns of the same length (50 μm I.D., 375 μm O.D.) were fitted in cartridges with 100 × 200 μm windows. The hydrophobic capillaries were conditioned for 2 h prior to use for protein separation, as described in the manufacturers' instructions. Detection with the larger window cartridges was made using a diode array detector monitoring at 200 nm and scanning between 190 and 340 nm whereas a fixed wavelength (200 nm) UV detector was used for cartridges with smaller windows. Separations were performed at 10–25 kV (anode, inlet; cathode, outlet) and the temperature of the capillary was maintained at 25°C by means of circulating coolant. Borate–SDS buffers were made by adjusting the pH of boric acid and SDS using NaOH (all high purity or AristaR reagents, BDH, Poole, UK). Unless otherwise stated, sample introduction by low pressure injection (0.5 p.s.i., $3.45 \cdot 10^3$ Pa) was 1, 3 and 10 sec. for 75, 50 and 25 μm I.D. capillaries respectively.

3. Results and discussion

Since previous work indicated the potential application of MECC to MT isoform quantification [17], we have systematically evaluated a range of separation conditions using sheep and rabbit MT isoforms. The separation of sheep MT-1 + MT-2 by MECC using borate buffer concentrations up to 300 m*M* and SDS levels up to 100 m*M* showed 3 main components labelled a, c and e in Figs. 1 and 2. By separation of MT-1 (Fig. 4) and MT-2 (data not shown) individually, components a and c were shown to be MT-1 isoforms whereas component e was an MT-2 form. Additional minor components b and d were also evident and were shown to be MT-1 forms (Fig. 4). Multiple functional MT genes have been identified in sheep [28] and electrospray mass spectra of the proteins to 1 mass accuracy have demonstrated that many, if not all of these genes are translated in response to metal induction [29]. Flow injection mass spectra recorded at acid and neutral pH have shown that all of these components bind up to 7 atoms of Cd or Zn per molecule. As regards sheep MT-1 therefore, we have shown that the components separated by various CE techniques using a wide

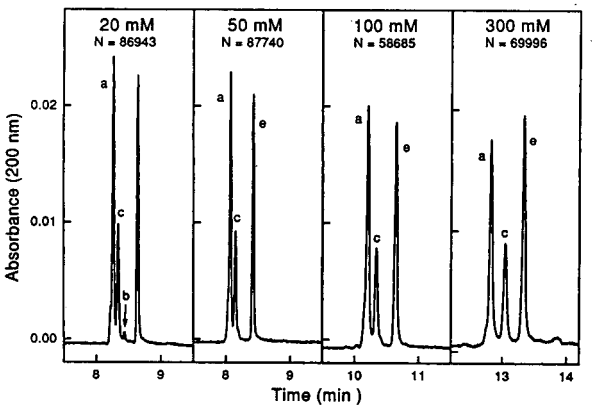

Fig. 1. The effect of increasing sodium borate concentration at pH 8.4 on the separation of sheep MT-1 + MT-2 (1 mg of each isoform/ml water) by MECC at 10 kV. A 57 cm × 75 μm I.D. uncoated capillary was used and SDS concentration was maintained at 75 m*M*. Components a, b and c are MT-1 forms whereas component e is MT-2. The separation efficiency was determined by calculating the number of theoretical plates (*N*).

variety of different CZE and MECC conditions are isoforms of metallothionein rather than contaminants or aggregation/degradation products.

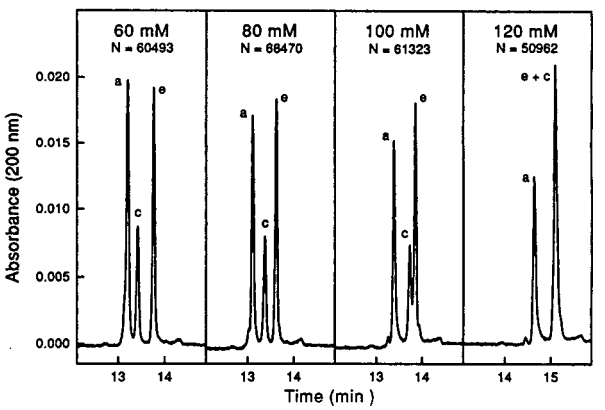

Fig. 2. The effect of increasing SDS concentration on the separation of sheep MT-1 + MT-2 (1 mg of each isoform/ml water) by MECC at 10 kV. A 57 cm × 75 μm I.D. uncoated capillary was used and sodium borate concentration was maintained at 300 m*M* with a pH of 8.4. Components a and c are MT-1 forms whereas component e is MT-2. The separation efficiency was determined by calculating the number of theoretical plates (*N*).

According to the relative abundance of the isoforms detected by mass spectrometry of the purified sheep MT-1 protein, we believe that component a in all MECC separations is MT-1a and that component c is MT-1c, in accordance with the nomenclature designated by Peterson et al. [28] who sequenced the corresponding genes. Component b and d are as yet unidentified but the mass spectra suggest the presence of an unacetylated form of MT-1a and a small amount of MT-1b. The amino acid substitutions which distinguish MT-1a from MT-1c are pro (MT-1a) to ser (MT-1c) at residue 8, gly to ser at residue 11 and val to ile at residue 49. In the case of MT-1b, the difference from MT-1a is even less significant with a single substitution of gly (MT-1a) to ser (MT-1b) at residue 10.

3.1. Electrolyte optimisation

When maintaining a constant SDS concentration of 75 m*M* and varying the buffer concentration, separation of c from a was best achieved using a borate level of 300 m*M* although separation efficiency expressed as the number of theoretical plates (*N*) calculated from Eq. (1), where t is the migration time and σ is the peak width at half peak height [30], was found to be optimal at 50 m*M* (Fig. 1).

$$N = (t/\sigma)^2 \quad (1)$$

Changing the SDS concentration while maintaining the buffer level at 300 m*M* showed the best separation of a, c and e and the optimum peak resolution at 80 m*M* (Fig. 2). The importance of selecting the correct separation conditions for MT isoforms is illustrated by the tendency of c (MT-1c) to co-migrate with a (MT-1a) under standard CZE conditions [14] and to co-migrate with e (MT-2) under MECC conditions using higher SDS levels (Fig. 2).

The electrolyte pH had a profound effect on rabbit MT isoform separation pattern (Fig. 3) which contrasted with the lack of pH influence on sheep MT isoform migration order (data not shown). The MECC of rabbit MT using 100 m*M* borate and 75 m*M* SDS at pH 8.4 was the same

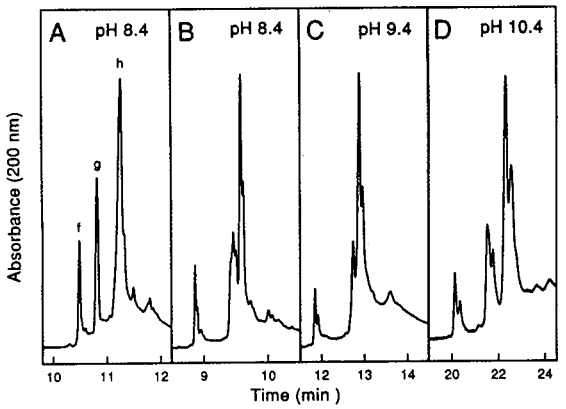

Fig. 3. The effect of pH on the separation of rabbit MT isoforms (1 mg MT/ml water) by MECC at 10 kV and 100 m*M* borate–75 m*M* SDS, pH 8.4 (A) or 20 kV and 500 m*M* borate–100 m*M* SDS at pH 8.4 (B), 9.4 (C) or 10.4 (D). Separations were performed in 57 cm × 25 μm I.D. capillaries and components f and g are MT-1 forms whereas h contains MT-2 forms.

as we have obtained previously [17] and the components labelled f and g are isoforms with a similar net charge to MT-1 whereas component h contains only MT-2 forms. These 3 components were evident at pH 10.4 but 3 further forms were also partially resolved and the separation was a mirror image of that obtained using polyamine coated capillaries and electrolyte buffered at pH 7 [16]. The heterogeneity of rabbit MT confirms other observations using RP-HPLC [31], CZE with uncoated capillaries at low pH [14,15], and CZE with neutral-coated capillaries [15].

The resolution of sheep MT-1 separations in particular, but also that of rabbit MT at 500 m*M* borate–100 m*M* SDS pH 10.4 was reduced, which may have been due to the increased ionic concentration differential between the sample matrix (water) and the electrolyte. We routinely inject samples prepared in water to enhance resolution by stacking and this has proved to be successful for many separation conditions. However, it is thought that the electrolyte:sample concentration differential should be in the order of 10 for optimal stacking effect [32] and it may therefore be possible to improve these separations by increasing the sample ionic strength.

3.2. Capillary optimisation

In order to evaluate the separation of sheep MT-1 in different diameter capillaries, buffer conditions (200 m*M* borate, 125 m*M* SDS, pH 8.4) were selected to enhance isoform separation. It should however be noted that the isoform c in Fig. 4 would co-migrate with MT-2 under these conditions. New 57 cm capillaries of all 3 sizes were conditioned by purging with NaOH, water and buffer for exactly the same time, taking into account the different flow rates through each capillary. Injections using low pressure of 1.2, 3 and 10 s duration were made for 75, 50 and 25 μm I.D. capillaries, respectively, so that an equivalent length of plug was introduced. Separations were performed at 10 kV and, as expected, migration time deceased with increasing capillary diameter. These electrophoresis conditions using new capillaries resolved the minor components labelled b and d in all 3 columns although separation was marginally superior with the 25 μm I.D. (Fig. 4). Of greater significance was the considerable difference in sensitivity which was a factor of approximately 5 × higher in the 75 μm I.D. column than the 25 μm I.D. capillary. Thus from the point of view of a potential assay for MT-1a, MT-1c and MT-

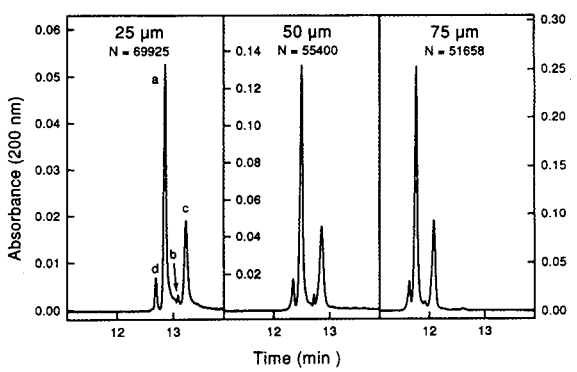

Fig. 4. The influence of capillary diameter on the separation and resolution of sheep MT-1 isoforms (1 mg MT-1/ml water) by MECC at 10 kV in uncoated 57 cm capillaries with 200 m*M* borate–125 m*M* SDS, pH 8.4 electrolyte. The separation efficiency was determined by calculating the number of theoretical plates (*N*).

2, the advantage of enhanced sensitivity using wider columns outweighs the slight loss in resolution. However in compromising on resolution, the assumption that components b and d would not contribute greatly to the peak area of MT-1a under any circumstances may be questionable. In any case, metabolic studies of these components may be of specific interest and the solution to this problem lies in the development or utilisation of more sensitive methods of detection.

One advantage normally associated with the use of smaller diameter capillaries is the ability to use high ionic strength buffers, which enhance resolution, without exceeding the capacity for Joule heat dissipation during electrophoresis [21], which on the P/ACE system is about 0.05 W/cm. However, due to the relatively low conductance of sodium borate and SDS, high concentrations can be used in 57 cm × 75 μm I.D. capillaries without exceeding this limit. The power generated in all separations presented here was <0.02 W/cm and usually <0.01 W/cm. Nevertheless, small increases in resolution and migration time as found, for example, with capillaries of decreasing I.D. (Fig. 4) may be due to more efficient cooling of the narrower bore columns.

On examining the influence of column length using new 25 μm I.D. capillaries and a 500 m*M* borate–100 m*M* SDS buffer pH 8.4 and 10 kV potential, it was clear that increasing column length was beneficial to isoform separation (Fig. 5). This is to be expected since a longer residence time on the column will enhance separation of closely related compounds. The CZE of MT-1 in 500 m*M* borate buffer without SDS using a 57 cm × 25 μm I.D. capillary at 25 kV partially separated components a and c and this electropherogram was similar in profile to the MECC separation of MT-1 in the 27 cm capillary.

The surface modified hydrophobic capillaries were of no obvious advantage for MT separation using our MECC conditions although we have not made extensive evaluation of these columns with a wide range of electrolyte composition, concentration and pH. The electropherograms

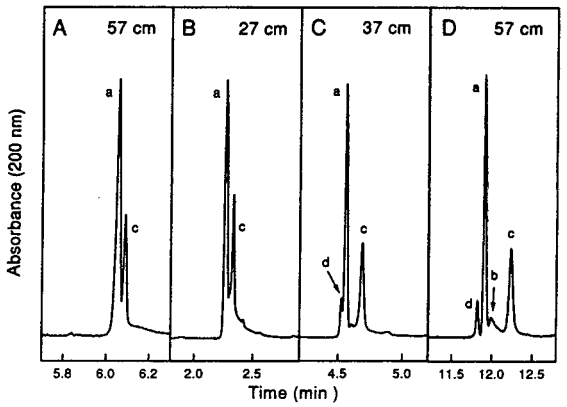

Fig. 5. The influence of capillary length on the separation and resolution of sheep MT-1 isoforms (1 mg MT-1/ml water) by MECC in uncoated 25 μm I.D. capillaries using 500 m*M* borate–100 m*M* SDS, pH 8.4 electrolyte (B–D) and a potential of 10 kV. MECC separations are compared with CZE at 25 kV and 500 m*M* borate buffer, pH 8.4 using a 57 cm × 25 μm I.D. uncoated capillary (A).

for sheep MT-1 using the coated and uncoated capillaries were similar to those in Fig. 4. Separation efficiency (N) of the MT-1 in the C_1 and C_{18} capillaries was reduced by 0.64 and 0.52 and migration time increased by 1.12 and 1.20, respectively, compared to those in an uncoated column of the same length and I.D. The decrease in EOF observed due to the coating was less than that reported by the manufacturer. However, we used elevated SDS concentrations and the reduction in EOF due to shielding of silanol groups may have been partly counteracted by increased association of the surfactant with the hydrophobic coating, thus exposing more negatively charged detergent sulphate groups to assist in the generation of EOF. Lowering the borate and SDS concentrations to 50 and 10 m*M*, respectively, as used in other protein separation studies [24] resulted in the further deterioration of the MT-1 separation (data not shown). As expected, separations of MT performed in the absence of SDS using a C_{18} capillary gave no absorbance peaks since the protein was entirely adsorbed onto the capillary wall. Separations using electrolytes containing 5% acetonitrile or 10 m*M* SDS were sufficient to prevent adsorption of sheep MT-1 but did not

resolve any of the composite isoforms (data not shown). Attempts to find concentrations of solvent or surfactant which enhanced competitive interaction with the capillary wall but prevented adsorption yielded poorly resolved peaks and better separations may be obtained using capillaries packed with C_{18} material [33].

3.3. Tissue extract analysis using optimised MECC conditions

Our experiences with analysing tissue extracts by various CE techniques has been largely favourable although sample preparation is of crucial importance. We have used solvents to precipitate contaminant proteins because MT is relatively soluble at concentrations where many proteins denature or precipitate. Residual solvent in the extract is also compatible with CE analysis and we have injected MT samples containing as much as 50% acetonitrile without significantly affecting the isoform separation (unpublished observations). Because only nanolitres of sample can be injected onto a column, sensitivity is limited by the degree to which extracts can be concentrated into small volumes.

As a compromise between isoform separation, resolution and detection sensitivity, a buffer of 300 m*M* borate–85 m*M* SDS pH 8.4, a 75 μm I.D. capillary and a potential of 10 kV was used for MECC of these extracts. Isoforms a, c and e in the purified protein separations were identified in extracts from both untreated and Zn-treated sheep although there was considerable induction of all 3 forms in the latter extract (Fig. 6). Isoform d was detected only in the extract from the Zn-injected sheep. Spectral scans of these components in standards and Zn-induced extracts revealed spectra characteristic of MT, with no absorbance at 280 nm due to the absence of aromatic amino acids and a slight shoulder at 230 nm indicating the presence of Zn-mercaptide charge transfer bonds (Fig. 7) [34].

3.4. Conclusions

We have demonstrated the significant influence of capillary column length, pH, buffer and SDS concentration on the separation and resolution of MT isoforms. With the development of more sensitive detectors, it would be appropriate to analyse these isoforms using long, small diameter uncoated capillaries in combination with high ionic strength sodium borate buffers, the pH and SDS level being adjusted from 8.4 to 10.4 and from 70 to 125 m*M*, respectively, to suit the separation of particular MT samples. In the

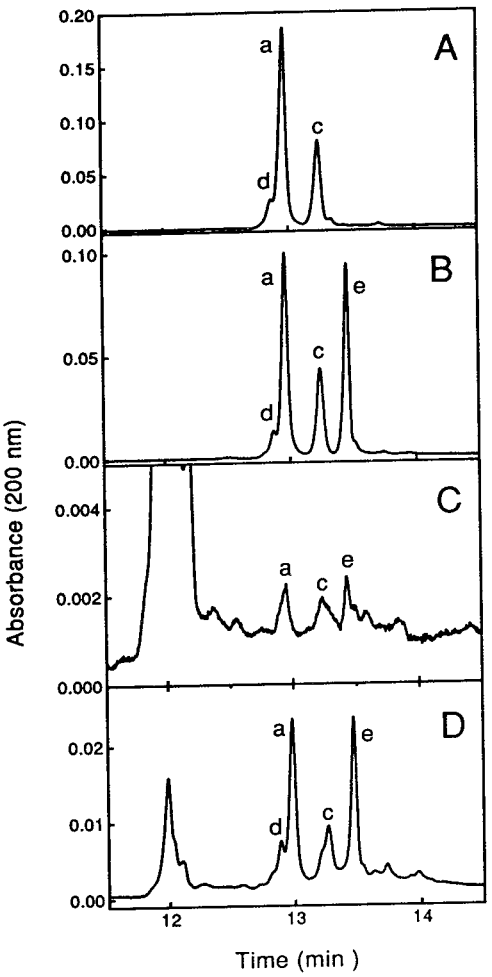

Fig. 6. The separation of MT isoforms in liver extracts from untreated (C) and Zn-injected (D) sheep. Comparison is made with separations of purified MT-1 (A) and MT-1 + MT-2 (B) using identical conditions: 300 m*M* borate–85 m*M* SDS, pH 8.4, at 10 kV using a 57 cm × 75 μm I.D. uncoated capillary. Components a, c and d are MT-1 forms whereas component e is MT-2.

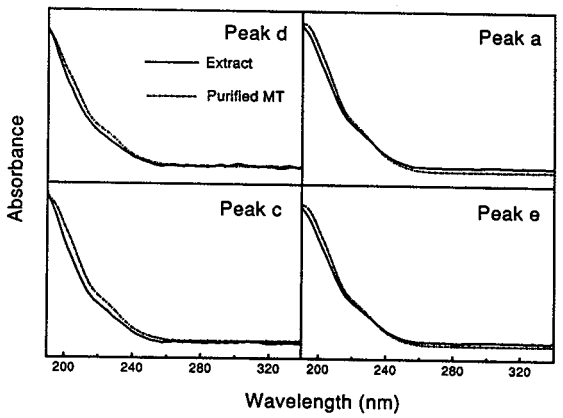

Fig. 7. UV absorbance spectra of the peaks labelled a, c, d and e of the MT-1 + MT-2 purified protein separation and the liver extract from Zn-induced sheep shown in Fig. 6. Scans between 190 and 340 nm were obtained 4 times a second using a diode array detector and the scan at each peak apex is presented.

case of sheep MT, the pH should be around 8.4 and SDS concentration in the range 80–90 m*M*. In contrast, the best separations of rabbit MT were obtained at pH 10.4 and SDS concentrations of 100 m*M*. As regards the electrical potential applied to the capillary, the best separations were obtained when micelle migration rate was low and therefore isoform migration times longer, namely at about 10–20 kV. MT isoforms could be detected even in untreated sheep liver and so using the conditions developed in this study, MECC has practical application to the analysis of MT in tissue extracts.

Comparing MECC with other CE techniques for MT analysis, we conclude that MECC with SDS at alkaline pH and CZE at acid pH, both in untreated fused-silica capillaries, are the most robust, practical and cost-effective methods which have been investigated. The method of choice depends on the intended application since the 2 methods are to some degree complementary. Using a UV detector, MECC gives better sensitivity for MT due to additional absorbance from intact mercaptide bonds and CZE using high concentration phosphate, low pH buffer electrolytes and narrow bore capillaries often yields better resolution. The selection of technique may also depend on the organism from which the MT sample is obtained. Isoforms of, for example, horse kidney MT are better separated by CZE [15] whereas sheep MT isoforms are better separated using MECC conditions. The relative merits of these and other CE methods are further discussed in a separate article [35].

Acknowledgements

The authors would like to thank Dr. I. Bremner for his critical review of the manuscript. This work was funded by the Scottish Office Agriculture and Fisheries Department, UK.

References

[1] M.J. Gordon, K.J. Lee, A.A. Arias and R.N. Zare, *Anal. Chem.*, 63 (1991) 69.
[2] K.J. Lee and G.S. Heo, *J. Chromatogr.*, 559 (1991) 317.
[3] V.J. Hilser, G.D. Worosila and S.E. Rudnick, *J. Chromatogr.*, 630 (1993) 329.
[4] R. Lausch, T. Scheper, O.W. Reif, J. Schlosser, J. Fleischer and R. Freitag, *J. Chromatogr. A.*, 654 (1993) 190.
[5] E. Yildiz, G. Grubler, S. Horger, H. Zimmermann, H. Echner, S. Stoeva and W. Voelter, *Electrophoresis*, 13 (1992) 683.
[6] M.P. Richards and J.H. Beattie, *J. Cap. Elec.*, 1 (1995) 196.
[7] J.H.R. Kägi, in K.T. Suzuki, N. Imura and M. Kimura (Editors), *Metallothionein III*, Birkhäuser Verlag, Basel, 1993, p. 29.
[8] C.C. McCormick and L.Y. Lin, *Methods Enzymol.*, 205 (1991) 71.
[9] J.H. Beattie, M.P. Richards and R. Self, *J. Chromatogr.*, 632 (1993) 127.
[10] M.P. Richards, J.H. Beattie and R. Self, *J. Liq. Chromatogr.*, 16 (1993) 2113.
[11] G. Liu, W. Wang and X. Shan, *J. Chromatogr. B*, 653 (1994) 41.
[12] I. Bremner and J.H. Beattie, *Ann. Rev. Nutr.*, 10 (1990) 63.
[13] I. Bremner and J.H. Beattie, *Proc. Nutr. Soc.*, (1995) in press.
[14] M.P. Richards and J.H. Beattie, *J Chromatogr*, 648 (1993) 459.

[15] M.P. Richards and P.J. Aagaard, *J. Cap. Elec.*, 1 (1994) 90.
[16] M.P. Richards, *J. Chromatogr. A*, 457 (1994) 345.
[17] J.H. Beattie and M.P. Richards, *J. Chromatogr. A*, 664 (1994) 129.
[18] C. Zhang, Z. Sun and D. Ling, *J. Chromatogr. A*, 655 (1993) 309.
[19] S. Terabe, K. Otsuka, K. Ichikawa, A. Tsuchiya and T. Ando, *Anal. Chem.*, 56 (1984) 111.
[20] S. Terabe, K. Otsuka and T. Ando, *Anal. Chem.*, 57 (1985) 834.
[21] S.F.Y. Li, *Capillary Electrophoresis*, Elsevier, Amsterdam, 1992, p. 201.
[22] S. Terabe, *Micellar Electrokinetic Chromatography*, Beckman Instruments Inc., Fullerton, CA, 1992.
[23] S. Terabe, *J. Pharm. Biomed. Anal.*, 10 (1992) 705.
[24] M.A. Strege and A.L. Lagu, *Anal. Biochem.*, 210 (1993) 402.
[25] X.W. Yao, D. Wu and F.E. Regnier, *J. Chromatogr.*, 636 (1993) 21.
[26] R.K. Mehra and I. Bremner, *Biochem. J.*, 227 (1985) 903.
[27] J. Hidalgo, M. Giralt, J.S. Garvey and A. Armario, *Am. J. Physiol.*, 254 (1988) E71.
[28] M.G. Peterson, F. Hannan and J.F.B. Mercer, *Eur. J. Biochem.*, 174 (1988) 417.
[29] J.H. Beattie, J.A. Lomax, M.P. Richards, R. Self, R. Pesch and H. Münster, *Proceedings of the 42nd Conference of the American Society for Mass Spectrometry, Chicago, IL, May–June 1994*, ASMS, Santa Fe, NM, 1994, p. 667.
[30] J.W. Jorgenson and Lukacs K.DeA., *Anal. Chem.*, 53 (1981) 1298.
[31] M. Wan, P.E. Hunziker and J.H.R. Kagi, *Biochem. J.*, 292 (1993) 609.
[32] S.F.Y. Li, *Capillary Electrophoresis*, Elsevier, Amsterdam, 1992, p. 31.
[33] J. Bullock, *J. Chromatogr.*, 633 (1993) 235.
[34] M. Vašák, *Meth. Enzymol.*, 205 (1991) 41.
[35] M.P. Richards and J.H. Beattie, *J. Chromatogr. A*, (1995), in press.

ELSEVIER

Journal of Chromatography A, 700 (1995) 105–110

JOURNAL OF CHROMATOGRAPHY A

Separation of β-lactoglobulin A, B and C variants of bovine whey using capillary zone electrophoresis

Geoff R. Paterson, Jeremy P. Hill, Don E. Otter*

Food Science Section, New Zealand Dairy Research Institute, Private Bag 11029, Palmerston North, New Zealand

Abstract

β-Lactoglobulin is a whey protein that affects milk composition and product functionality and which can be present in up to eight genetic variant forms. A free zone capillary electrophoresis method has been developed to separate and identify the β-lactoglobulin A, B and C variants. Three buffer systems [borate, 2-(N-morpholino)-ethanesulphonic acid (MES) and bis(2-hydroxyethyl)imino-tris(hydroxymethyl)methane (Bistris)] were examined over a range of pH values and with the addition of the separation buffer modifiers Tween 20 and/or ethanolamine. The most successful combination of these was 50 m*M* MES at pH 8.0 with the addition of 0.1% Tween 20 which clearly resolved the three variants from both each other and from the other whey proteins even though the MES buffer was acting well outside its pK_a range (pH 5.3–7.3). The retention times and identification of the individual variants were verified by spiking with commercially purified β-lactoglobulin A and B proteins and a β-lactoglobulin AC whey. The method was then used to phenotype β-lactoglobulin in a sample population of New Zealand Jersey cows.

1. Introduction

Genetic variants of the major milk proteins [α_{s1}-, β- and κ-casein and β-lactoglobulin (β-Lg)] are present in the milk produced by New Zealand cows with β-Lg, the major whey protein, present in up to eight variant forms [1]. Although β-Lg A and β-Lg B are the most prevalent variants, the C variant has been observed in some populations of the Jersey breed at frequencies between 0.01 and 0.11 [2–4]. The presence of this variant may affect the milk composition and functional properties of the milk and milk products [5,6]. There are two amino acid differences (Asp-64 and Val-118 are substituted by Gly and Ala, respectively) between the A and B variants, three between the A and C but only one (Gln-59 to His) between the B and C [7,8] (Fig. 1).

In a previous study [9] no C variants were detected in New Zealand Jersey cows using native, non-reducing polyacrylamide gel electrophoresis. DEAE–cellulose ion-exchange chromatography [8], starch gel electrophoresis [10] and chromatofocusing with a Pharmacia polybuffer exchanger column [11] have also been used to separate the three variants but are not practical for phenotyping large cow populations. The A and B variants of β-Lg have also been separated by capillary electrophoresis [12–14] although separation of the C variant has not been reported.

* Corresponding author.

0021-9673/95/$09.50
SSDI 0021-9673(95)00054-2

Position	57	58	59	60	61	62	63	64	65	66 ...	116	117	118	119	120
Variant															
A	Leu	Leu	Gln	Lys	Trp	Gln	Asn	Asp	Glu	Cys ...	Ser	Leu	Val	Cys	Gln
B	Leu	Leu	Gln	Lys	Trp	Gln	Asn	Gly	Glu	Cys ...	Ser	Leu	Ala	Cys	Gln
C	Leu	Leu	His	Lys	Trp	Gln	Asn	Gly	Glu	Cys ...	Ser	Leu	Ala	Cys	Gln

Fig. 1. Amino acid sequence of β-Lg variants (total: 162 amino acids). Differences in amino acid sequence are shaded.

In the present study a capillary electrophoresis method to separate the A, B and C variants of β-Lg has been developed and was then used for the β-Lg phenotyping of a large sample of New Zealand dairy cattle.

2. Experimental

2.1. Chemicals

Sodium tetraborate (borate), 2-(N-morpholino)ethanesulphonic acid (MES), ethanolamine (EA) and polyoxyethylene (20)-sorbitan monolaurate (Tween 20) were obtained from BDH Chemicals (Poole, UK) and bis(2-hydroxyethyl)imino-tris(hydroxymethyl)methane (Bis-tris) from Sigma (St. Louis, MO, USA). Commercially purified whey proteins (whey protein standards): α-lactalbumin (α-Lac), β-Lg A, β-Lg B and bovine serum albumin (BSA) were supplied by Sigma. Freeze dried whey phenotypic for the β-Lg variants A and C (AC whey) was gratefully received from Mary Christian of the Department of Agriculture, Ellinbank, Victoria, Australia. All reagents were of Analar grade or better and water was purified by reverse osmosis followed by deionization (Milli-Q, Millipore, MA, USA).

2.2. Whey samples

Individual whey samples were prepared from 258 Jersey cows by acid precipitation of casein at pH 4.6 using HCl. The casein was removed by centrifugation and the whey was filtered (0.45 μm) to remove any residual casein precipitate and fat.

2.3. Capillary electrophoresis

Capillary zone electrophoresis (CZE) was performed on an Applied Biosystems 270A-HT CE system (Foster City, CA, USA) using a PE Nelson 900 series interface and a PE Nelson TurboChrom 3.3 software package (Cupertino, CA, USA) for data acquisition and analysis, respectively. The uncoated capillary (72 cm total length, 50 cm effective length and 50 μm internal diameter) was supplied by Applied Biosystems. Samples were injected at the anode using vacuum (17 kPa) for 10 s during method development and 4 s for the whey samples. The separation voltage was 20 kV with detection at 215 nm. Between the injections the capillary was flushed for 2 min (68 kPa) consecutively with 0.1 *M* NaOH, Milli-Q water and buffer to retain separation reproducibility.

3. Results and discussion

AC whey spiked with β-Lg B was initially separated using a 50 m*M* sodium borate buffer at pH 9.0 containing 0.1% EA and 0.1% Tween 20 (Fig. 2) as this buffer system had been used previously to successfully separate α-Lac, β-Lg A, β-Lg B and BSA (unpublished results). The

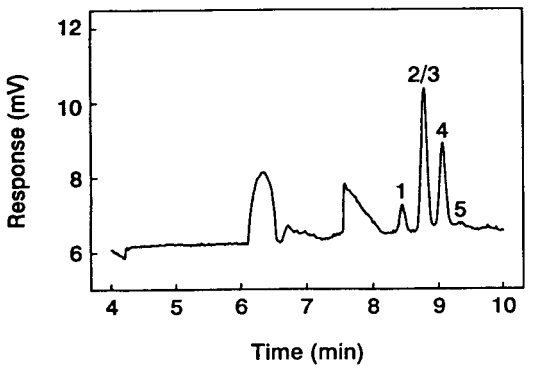

Fig. 2. Initial separation of AC whey and β-Lg B. AC whey and β-Lg B were prepared at 0.2 mg/ml and 0.04 mg/ml in Milli-Q water, respectively. The separation buffer was 50 m*M* sodium borate, pH 9.0, containing 0.1% ethanolamine and 0.1% Tween 20. Peaks: 1 = α-Lac; 2 = β-Lg C; 3 = β-Lg B; 4 = β-Lg A; 5 = BSA; S = air spike.

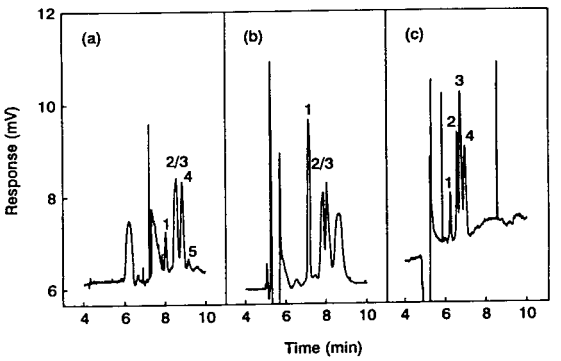

Fig. 3. Effect of buffer on separation of AC whey and β-Lg B. Samples and peaks as in Fig. 2. Buffers: (a) 50 m*M* sodium borate, pH 8.5, containing 0.1% ethanolamine and 0.1% Tween 20; (b) 50 m*M* Bistris, pH 7.0; (c) 50 m*M* MES, pH 8.0.

elution order of the whey proteins was α-Lac, β-Lg B, β-Lg A and BSA. Under these conditions, however, β-Lg C co-eluted with β-Lg B.

A number of different buffers at different pH values and in the presence of the separation buffer modifiers EA and Tween 20 were surveyed to determine the optimal conditions for the separation of β-Lg B and β-Lg C. Buffer pH values were kept above pH 6.0 to increase protonation of the proteins and to thus affect a better separation due to an increased mobility of the β-Lg C.

Fig. 3 shows that of the three buffers investigated 50 m*M* MES at pH 8.0 resulted in the best separation of the three β-Lg variants. There was a slight separation of β-Lg B and β-Lg C with the sodium borate buffer at pH 8.5 which suggested the complete separation may have been achieved at a lower pH. This was also observed with Bistris buffer at pH 7.0 although in this instance there was also a broad unidentified peak at approximately 10 min.

The MES buffer system was then made up at a number of different pH values (Fig. 4) to determine the optimum pH for separation of the β-Lg variants. Although the pK_a of MES buffer is 6.3 a pH range between 6.0 and 8.5 was investigated based on the results highlighted in Fig. 3. The best resolution of the three β-Lg variants occurred at pH 8.0 although at pH 7.5 there was partial separation of the C and B variants and almost baseline resolution between these and the A variant. Below pH 7.0 there was

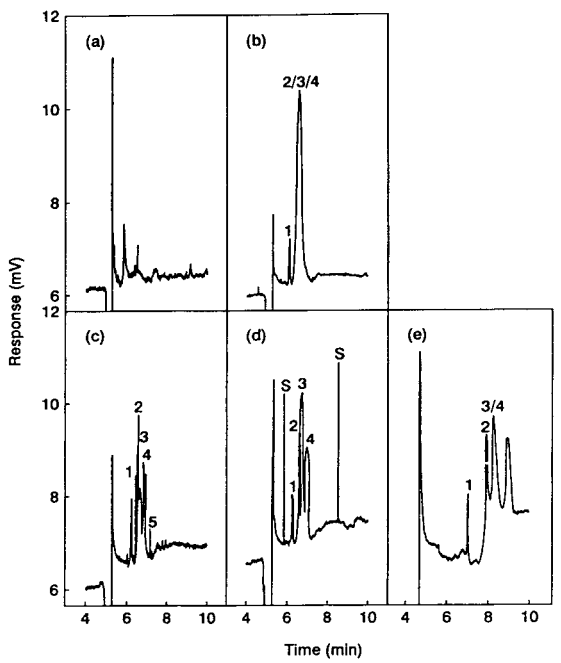

Fig. 4. Effect of buffer pH on separation of AC whey and β-Lg B. Samples and peaks as in Fig. 2. Buffer: 50 m*M* MES. pH: (a) 6.0; (b) 7.0; (c) 7.5; (d) 8.0; (e) 8.5.

no separation of the β-Lg variants whilst at pH 8.5 the B and A variants were not resolved.

The electrolyte modifiers Tween 20 and EA were then added to the MES buffer in an attempt to further enhance the separation of the β-Lg variants by suppressing protein capillary wall interactions [15]. Fig. 5 shows that both Tween 20 and Tween 20 plus EA resulted in more highly resolved peaks with excellent, near-baseline separation of all three β-Lg variants. A 50 m*M* MES buffer, pH 8.0, containing 0.1% Tween 20 was selected as the most appropriate separation buffer for the separation of β-Lg A, B and C variants in whey.

Positive identification of the peaks obtained from the AC whey by CZE was achieved by spiking the whey with individual whey protein standards (Fig. 6). α-Lac co-migrated with the first protein peak, β-Lg B with the third and β-Lg A with the fourth. Thus by implication β-Lg C was assigned to peak 2. The last minor peak coeluted with a BSA standard (data not shown). In subsequent phenotyping the α-Lac peak was used as an internal marker to correct for peak shifting caused by ion depletion of the cathodal buffer.

The separation method described above was then used to identify the β-Lg phenotypes of a sample population of 258 New Zealand Jersey cows. Examples of the phenotype identification are highlighted in Fig. 7. The frequencies of the different β-Lg phenotypes in the New Zealand Jersey cow population phenotyped is shown in

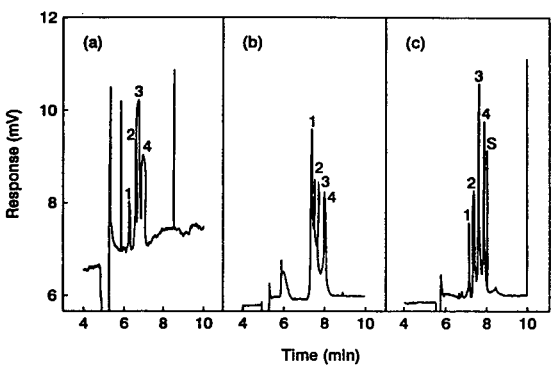

Fig. 5. Effect of separation buffer modifiers on separation of AC whey and β-Lg B. Samples and peaks as in Fig. 2. Buffer: 50 m*M* MES, pH 8.0. Modifier: (a) none; (b) 0.1% Tween 20; (c) 0.1% Tween 20 plus 0.1% ethanolamine.

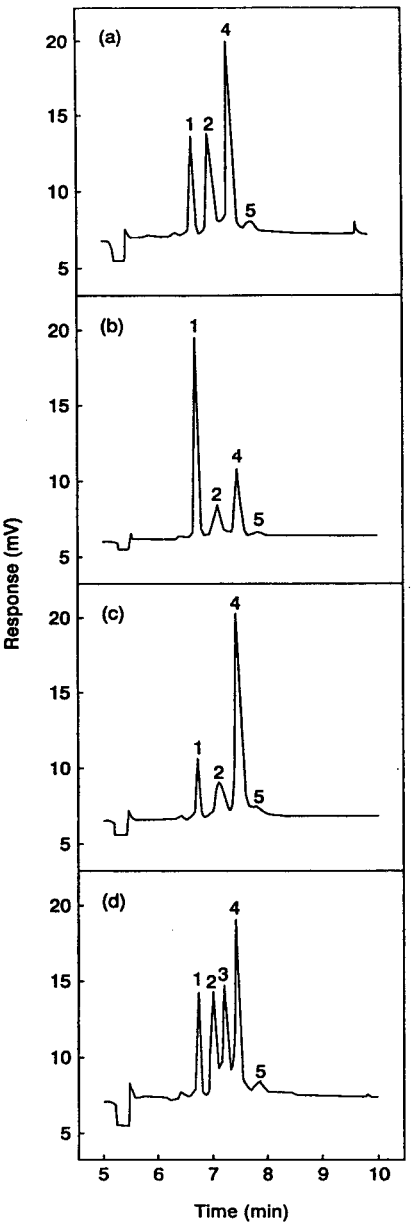

Fig. 6. Verification of AC whey CE peaks by spiking with whey standards. AC whey was prepared at 0.2 mg/ml in Milli-Q water. Individual whey standards were added to the AC whey at 0.14 mg/ml as follows: (a) none; (b) α-Lac; (c) β-Lg A; (d) β-Lg B. Peaks are as in Fig. 2.

Table 1. The A and B alleles were observed in approximately equivalent ratios whilst the C allele had a low frequency of 0.03. No β-Lg CC phenotypes were observed in the sample population.

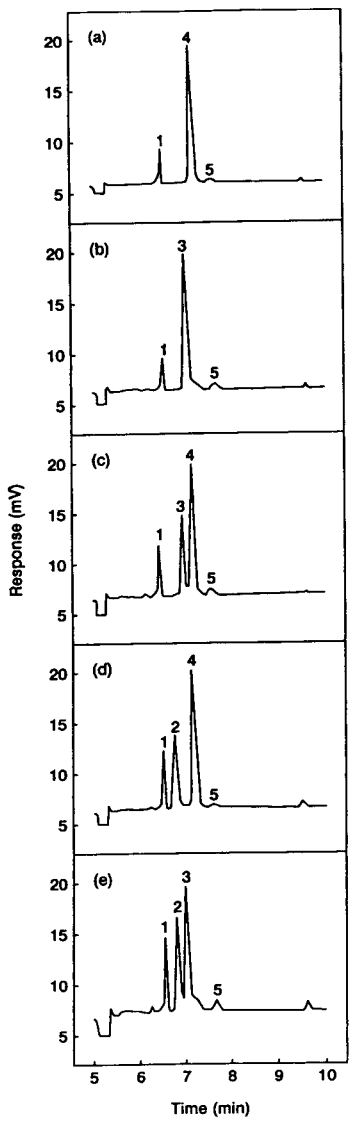

Fig. 7. Electropherograms of whey from individual Jersey cows of different phenotypes. Whey samples were prepared as detailed in Experimental. Electropherograms were aligned using the α-Lac internal standard. The phenotypes are: (a) AA; (b) BB; (c) AB; (d) AC; (e) BC. Peaks are as in Fig. 2.

Table 1
Frequencies of β-Lg phenotypes

Phenotype	Frequency of phenotype
AA	0.225
BB	0.244
AB	0.473
AC	0.023
BC	0.035

Whey samples were collected and analysed as in Experimental. The buffer system was 50 m*M* MES, pH 8.0, containing 0.1% Tween 20.

4. Conclusions

A capillary electrophoretic method based on zone electrophoresis has been developed to separate the β-Lg variants A, B and C in bovine whey. The separation was achieved by exploiting the charge differences that can occur between the variants at certain pH values as a consequence of variant amino acid substitutions. MES buffer (50 m*M*, pH 8.0) gave the best separation of the buffer systems analysed at a pH which was outside its useful pK_a range. The addition of the separation buffer modifier Tween 20 at 0.1% enhanced the resolution of the separation.

In the sample population studied β-Lg C variant containing phenotypes were found to be present at a frequency of approximately 0.06.

References

[1] P.F. Fox, in P.F. Fox (Editor), *Developments in Dairy Chemistry, Vol. 4*, Elsevier Applied Science, London, 1989, p. 31.
[2] R. Aschaffenburg and J. Drewry, *Nature*, 176 (1955) 218.
[3] A.-M. Bech and K. Rotvig Kristiansen, *J. Dairy Res.*, 57 (1990) 53.
[4] D.M. McLean, E.R.B. Graham and R.W. Ponzoni, *J. Dairy Res.*, 51 (1984) 531.
[5] R. McL Whitney, in N.P. Wong (Editor), *Fundamentals of Dairy Chemistry*, VNR Press, New York, 1988, p. 81.
[6] R.L. Motion and J.P. Hill, Brief Communication of the *XXIV International Dairy Congress, Melbourne 18–22 September 1994*, Australian National Committee of the International Dairy Federation, Glen Iris, p 122.

[7] K. Bell, H.E. McKenzie and D.C. Shaw, *Biochim. Biophy. Acta*, 154 (1968) 284.
[8] E.B. Kalan, R. Greenberg and M. Walter, *Biochem. J.*, 14 (1965) 991.
[9] J.P. Hill, *J. Dairy Sci.*, 76 (1993) 281.
[10] K. Bell, *Nature*, 195 (1962) 705.
[11] R.J. Pearce and R.M. Shanley, *Aust. J. Dairy Technol.*, 36 (1981) 110.
[12] F.-T.A. Chen, *Beckman Technical Information*, D5-818 (1991) 1.
[13] F.-T.A. Chen and J.H. Zang, *J. Assoc. Off. Anal. Chem. Int.*, 75 (1992) 905.
[14] H.H. Lauer and D. McManigill, *Trends Anal. Chem.*, 5 (1986) 11.
[15] F.Y.S. Li, *Capillary Electrophoresis — Principles, Practice and Applications*, Elsevier, Amsterdam, 1992.

ELSEVIER

Journal of Chromatography A, 700 (1995) 111–123

JOURNAL OF CHROMATOGRAPHY A

Comparison of capillary electrophoresis with traditional methods to analyse bovine whey proteins

Nicki M. Kinghorn, Carmen S. Norris, Geoff R. Paterson, Don E. Otter*

Food Science Section, New Zealand Dairy Research Institute, Private Bag 11029, Palmerston North, New Zealand

Abstract

The separation of the four major whey proteins by sodium dodecyl sulphate (SDS)–capillary gel electrophoresis (CGE) is described. Whilst commercially purified whey proteins could be analysed using the recommended protocol, the more complex nature of an acid whey and a reconstituted whey protein concentrate (WPC) powder necessitated considerable refinement of the CGE sample buffer. Individual whey proteins in the acid whey and WPC samples were then also separated and quantitated using capillary zone electrophoresis, polyacrylamide gel electrophoresis (PAGE) and HPLC methods and the results were compared. The values obtained for α-lactalbumin (α-Lac) and β-lactoglobulin (β-Lg) were consistent throughout the various methods, although size-exclusion HPLC, SDS-PAGE and SDS-CGE could not separate the two β-Lg variants or the glycosylated form of α-Lac from the β-Lg. There was considerable variation in the values for the bovine serum albumin and immunoglobulin determined by the different methods and it was concluded that none of the methods could satisfactorily quantitate all four whey proteins.

1. Introduction

For humans bovine milk is an excellent source of essential nutritional components. These include proteins, present at 3–3.5% (w/v) of which the whey proteins comprise 0.5–0.7% (w/v) [1]. Whey proteins are classified as milk proteins which are soluble at pH 4.6 and 20°C and include β-lactoglobulin (β-Lg), α-lactalbumin (α-Lac), bovine serum albumin (BSA) and immunoglobulins (Ig) [2]. Also present are the minor proteins lactoferrin (LF), lactoperoxidase, proteose-peptone components (PP), glycomacropeptide and protein components of the milk fat globular membrane [3]. The four major whey proteins represent a diverse group of globular proteins and their properties are listed in Table 1.

The analysis of the whey proteins has traditionally been performed by polyacrylamide gel electrophoresis (PAGE) [native and sodium dodecyl sulphate (SDS)] and HPLC which provide information on purity, molecular mass and microheterogeneity. These methods have been extensively discussed in a number of recent reviews [4,5]. The advent of capillary electrophoresis has resulted in the development of similar techniques but in a capillary format which can be quicker, automated with on-line detection and which require very small sample and buffer volumes [6]. To date, capillary zone electrophoresis (CZE) has predominantly been used to separate the whey proteins. Most research has centered on the separation of only α-Lac and the

* Corresponding author.

0021-9673/95/$09.50
SSDI 0021-9673(95)00117-4

Table 1
Physical properties of the whey proteins[a]

Whey protein	Molecular mass	p*I*	Concentration in whey (mg/ml)	Total whey protein (%)
Major				
β-Lg	18 300	5.4	2.0–3.0	50
α-Lac	14 200	4.4	0.6–1.7	12
BSA	66 000	5.1	0.2–0.4	5
IgG	150 000	5.5–8.3	0.5–1.8	10
Minor				
LF	80 000	7.5	0.1	1
PP	4000–40 000	–	1.4	23

[a] See Refs. [1,2].

two variants of β-Lg (A and B) in uncoated [7] and coated [8,9] capillaries, although Otte et al. [10] have used uncoated capillaries and low pH buffers to separate the four major whey proteins.

In the present study a capillary gel electrophoresis (CGE) method has been developed to analyse whey proteins. This method and a recently developed CZE method [11] have then been used in conjunction with a number of traditional analytical techniques to quantitate the four major whey proteins in a liquid whey sample and a reconstituted whey protein concentrate (WPC) powder. The results were then compared and the suitability of using just one of these techniques to quantitate all the whey proteins is discussed.

2. Experimental

2.1. Materials

All buffers and reagents were of Analar grade or better. The commercially purified whey proteins α-Lac, β-Lg A, β-Lg B, BSA and IgG were supplied by Sigma (St. Louis, MO, USA). These are referred to in the text as the whey protein standards. Water was purified by reverse osmosis followed by deionization (Milli-Q, Millipore, Bedford, MA, USA).

2.2. Whey and WPC samples

Acid whey, prepared by the acid precipitation of casein from skim milk at pH 4.6, and WPC, prepared by ultrafiltration/difiltration, evaporation and spray drying acid whey, were obtained from a New Zealand commercial whey processing site. A liquid sample of WPC was also obtained immediately prior to evaporation and drying.

2.3. α-Lactalbumin and glycosylated-α-lactalbumin samples

An α-Lac/glycosylated-α-Lac (glyco-α-Lac) preparation was made using the method of Mailliart and Ribadeau-Dumas [12]. The final preparation was essentially free of β-Lg but contained some BSA and IgG. Glyco-α-Lac was produced from the sample above by separating the α-Lac from the glyco-α-Lac using a size-exclusion HPLC column (Beckman Ultraspherogel-SEC 3000). The glyco-α-Lac eluted before the α-Lac and, although there was a small amount of overlap between the two peaks, fractions were collected so as to avoid this overlap.

2.4. Deglycosylation of glyco-α-Lac

PNGase F (New England Biolabs, Beverly, MA, USA) was used to cleave the N-linked carbohydrate moiety from the asparagine residue in glyco-α-Lac. A volume of 50 μl of a 2-mg/ml solution of glyco-α-Lac was mixed with 10 μl of Biolabs 10x denaturing buffer and 19 μl of Milli-Q water. The protein in the glyco-α-Lac sample was then denatured by heating to 100°C for 10 min. After cooling, 10 μl of Biolabs reaction

buffer, 10 μl of 10x NP-40 (Biolabs) and 1 μl Biolabs PNGaseF enzyme were added and incubated at 37°C for 1 h. Following this deglycosylation step the sample was analysed by SDS and native PAGE.

2.5. Ultrafiltration/diafiltration of whey sample

A 5-ml sample of acid whey was ultrafiltered to 0.5 ml in an Amicon Micro-UF System (Model 8MC, Beverly, MA, USA) using a 1000 nominal molecular mass cut-off polysulphone membrane. This was then diafiltered with two 4.5-ml volumes of sample buffer before the volume was made up to the original 5 ml with CGE sample buffer.

2.6. Capillary electrophoresis

CE was performed on an Applied Biosystems 270A-HT CE system (Foster City, CA, USA) using a PE Nelson 900 series interface and a PE Nelson Turbo Chrom 3.3 software package (Cupertino, CA, USA) for data acquisition and handling, respectively.

2.7. HPLC

The HPLC system consisted of two pumps (Waters Model 6000A), an automatic injector (Waters WISP 7108), a Waters 490 absorbance detector and a Waters Millenium 2010 data acquisition and manipulation system. Prior to use all buffers were filtered (0.45 μm cellulose acetate, Millipore) and degassed. All samples were filtered (0.45 μm Sunvial nylon/polypropylene filter).

2.8. Capillary gel electrophoresis

A ProSort SDS-Protein Analysis Kit (Applied Biosystems) was used for CGE. The manufacturer's protocol was followed, except the reduced sample buffer was 2% SDS–5% 2-mercaptoethanol (2ME) and the non-reduced sample buffer was 2% SDS. The following whey protein concentrations were used to construct standard curves: α-Lac, 0.05–0.24 mg/ml; β-Lg A and β-Lg B, 0.09–0.45 mg/ml; BSA, 0.03–0.13 mg/ml and IgG, 0.02–0.10 mg/ml. Acid whey and WPC were prepared at a 1:9 dilution and 1 mg/ml respectively.

2.9. Capillary zone electrophoresis

CZE was performed as described by Kinghorn *et al.* [11] using an uncoated capillary (72 cm total length, 50 cm effective length and 50 μm I.D.), a 10-m*M* phosphate, pH 7.4 sample buffer and a 150-m*M* sodium borate, pH 8.5, plus 0.05% Tween 20 separation buffer. Whey protein standards, acid whey and WPC were prepared in sample buffer as described above (Section 2.8).

2.10. Size-exclusion HPLC

A Beckman Ultraspherogel-SEC 3000 column (300 × 7.5 mm I.D., 5 μm bead diameter, Beckman, Fullerton, CA, USA) connected in series with a Beckman Ultraspherogel guard column (40 × 7.5 mm I.D., 5 μm bead diameter) were used to separate the whey proteins. The flow-rate was 1 ml/min using a buffer of 0.05 *M* sodium sulphate–0.02 *M* sodium dihydrogen orthophosphate, pH 6.8. Proteins were detected by absorbance at 280 nm and the total run time was 16 min. Whey protein standards (α-Lac, β-Lg A, β-Lg B, BSA and IgG) in the range 2–40 μg were used to construct standard curves. The acid whey was diluted 1:6 in sample buffer and the WPC made up to 2 mg/ml in Milli-Q water.

2.11. Ion-exchange HPLC

The anion-exchange column MonoQ (Pharmacia, Uppsala, Sweden) was used for the ion-exchange chromatography. Samples were introduced on to the column in buffer A (20 m*M* piperazine and 1 m*M* $CaCl_2$, pH 5.5) and eluted with a gradient of buffer B (Buffer A plus 1 *M* NaCl) according to the method of Humphrey and Newsome [13]. Detection was by absorbance at 214 nm and 280 nm with a total run time of 28 min. The whey protein standards, whey and WPC were prepared as described above (Section 2.10), except IgG was not included in the whey

protein standard as this protein does not bind to the MonoQ column.

2.12. IgG affinity HPLC

Bovine IgG was measured by affinity HPLC on a Pharmacia Hi-Trap Protein G column. Samples were injected on to the column in buffer A (50 m*M* sodium dihydrogen phosphate, pH 6.5) and eluted with a gradient of buffer B (50 m*M* glycine, pH 2.5) according to the protocol described in Table 2. Proteins were detected by absorbance at 280 nm with a 7-min total run time. A standard curve was constructed using 4–40 μg bovine IgG. Whey was diluted 1:5 and WPC was prepared at 2 mg/ml in buffer A.

2.13. Native PAGE

Native, non-denaturing polyacrylamide gels were prepared according to Andrews [14] with a 4% stacking gel and a 15% separating gel. The resolving gel buffer was 0.375 *M* Tris–HCl (pH 8.8), the stacking gel buffer was 0.125 *M* Tris–HCl (pH 6.8) and the reservoir buffer was 0.025 *M* Tris–0.192 *M* glycine (pH 8.8). Slab gels of 0.75 mm were prepared and run using the Mini Protean II apparatus (Bio-Rad Labs., Richmond, CA, USA). Protein staining was performed with 0.05% Coomassie Brilliant Blue R-250 (Bio-Rad Labs.) in 25% isopropanol, 10% glacial acetic acid for 1 h.

Destaining was with 10% isopropanol, 10% glacial acetic acid for 2 h. Protein bands were quantitated using a laser scanning computing densitometer (Molecular Dynamics Model 300A, Sunnyvale, CA, USA). Volumes of 10 μl of either whey protein standards (α-Lac, β-Lg A, β-Lg B: 0.04–0.22 mg/ml; BSA and IgG: 0.02–0.12 mg/ml), acid whey (1:9 dilution in sample buffer) or WPC (1 mg/ml) were loaded on to each lane.

2.14. SDS-PAGE

The procedure of Laemmli [15] was employed for SDS-PAGE using a 4% stacking gel and a 15% separating gel. Protein staining, destaining and quantitation was as described above (Section 2.13). Standard concentrations were: α-Lac (0.04–0.23 mg/ml), β-Lac, (0.09–0.46 mg/ml); BSA (0.02–0.12 mg/ml) and IgG (0.02–0.12 mg/ml) with 10 μl being loaded. Acid whey and WPC were prepared in sample buffer at a 1:9 dilution and at 1 mg/ml, respectively.

3. Results and discussion

3.1. Capillary gel electrophoresis

The separation and quantification of the whey standards and whey samples by capillary gel electrophoresis are shown in Fig. 1. Although a commercial kit (ProSort SDS-Protein Analysis Kit, Applied Biosystems) was used, a number of modifications were required before satisfactory results were obtained. The recommended sample buffer (0.28% SDS–1% 2ME) resulted in excellent resolution of the whey protein standards with the exception of the two β-Lg variants which migrated as a single peak (results not

Table 2
Gradient conditions for protein G affinity HPLC

Time (min)	Flow-rate (ml/min)	A (%)	B (%)	Gradient
0	1.0	100	0	–
0.5	1.0	100	0	–
1.0	2.0	100	0	Linear
1.5	2.0	0	100	–
4.0	2.0	0	100	Linear
5.0	1.0	100	0	–
7.0	1.0	100	0	–

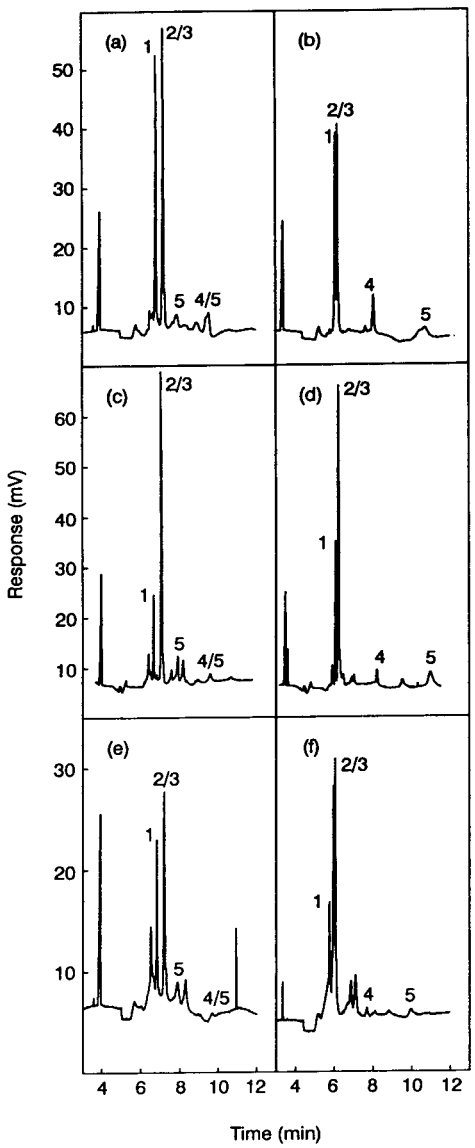

Fig. 1. Capillary gel electrophoresis of whey protein standards, acid whey and WPC was performed under reduced (a), (c) and (e), and non-reduced (b), (d) and (f) conditions respectively. Electrophoresis was performed as described in the Experimental section. Peaks: 1 = α-Lac; 2 = β-Lg A; 3 = β-Lg B; 4 = BSA; 5 = IgG.

shown). When this system was used with the acid whey sample, however, a white precipitate formed. After this precipitate was removed from the sample by centrifugation and filtration the subsequent whey protein values were considerably lower than expected from the results of other techniques. This precipitate was probably a sodium or potassium-dodecyl sulphate complex which on aggregation also precipitated out some of the whey protein.

A sample of whey was ultrafiltered and diafiltered against the sample buffer to decrease both its potassium ion concentration and its overall ionic strength. Table 3 shows that after this treatment the values for both α-Lac and β-Lg were restored to the expected levels as ascertained by SDS-PAGE.

Another possible reason for the low values for α-Lac and β-Lg in the acid whey samples was that if the initial ionic strength of the whey was higher than that of the whey protein standards then less whey would be introduced on to the capillary by the electrokinetic injection. This effect would presumably have been negated by the ultrafiltration/diafiltration step and may be circumvented by using vacuum injection.

As the use of ultrafiltration/diafiltration is not practical when assaying large numbers of samples, the sample buffer conditions were therefore modified to prevent the formation of this precipitate. A sample buffer of 2% SDS, containing either 5% 2ME for a reduced system or no 2ME for a non-reduced system, together with an 1:6–1:10 dilution of the whey sample was selected to prevent any precipitate formation. Under these conditions, the reduced and non-reduced buffer systems produced different separation profiles for the whey protein standards (Fig. 1a and b).

Using the reducing buffer baseline separation of α-Lac and β-Lg was achieved but the BSA and IgG peaks were not as well defined. The disulphide bonds in the IgG protein were disrupted resulting in peaks corresponding to the heavy and light chain subunits. The heavy chain subunit peak overlapped with the BSA peak. When the BSA and IgG standards were loaded at lower concentrations to mimic the protein ratios observed in whey quantification of the two proteins was very difficult.

In the non-reduced buffer systems, BSA and IgG were more highly resolved and gave discrete peaks. Unexpectedly, however, there was de-

Table 3
Effect of whey sample ultrafiltration/diafiltration (UF/DF) on analysis by capillary gel electrophoresis

Sample	α-Lac (mg/ml)	β-Lg (mg/ml)
Acid whey	0.32	1.28
Retenate after UF/DF	0.52	3.17
Permeate after UF/DF	0	0
Analysis by SDS-PAGE	0.50	3.10

Sample preparation and methods used were as described in the Experimental section.

creased separation between the α-Lac and β-Lg peaks. When run under non-reducing conditions β-Lg would be expected to be in the dimer form and hence have a higher apparent molecular mass (approximately 36 600, cf. 18 300 for the monomer) which would result in greater separation from α-Lac. The reason for this anomalous behaviour is not presently known.

An electrophoretic pattern similar to that observed for the whey protein standards was obtained when the acid whey was separated using the buffer system described above (Fig. 1c and d). There were also a number of other peaks present which were most probably low-molecular-mass proteose peptone fractions and small amounts of casein protein. One problem with these buffer systems, however, was that at the whey sample dilution required to prevent precipitation, the levels of both BSA and IgG were close to the detection limits, which made quantification of these proteins difficult.

With WPC (Fig. 1e and f), although the general electrophoretic protein pattern was similar to that obtained with the whey protein standards, there were a number of differences. Whilst the α-Lac levels were similar to those measured in the corresponding whey sample the α-Lac–β-Lg protein ratio was considerably higher which implied that there was a loss of β-Lg material during the processing of the whey to WPC. This loss could be accounted for by an increase in other 215 nm-absorbing material which took the form of an extra peak eluting before α-Lac at approximately 6.5 min with the reduced buffer and 6.0 min with the non-reduced buffer, and two extra peaks eluting after the β-Lg peak. This latter material was assumed to be denatured and aggregated β-Lg as any β-Lg polymerisation would have been dissociated by the SDS and reducing buffers.

There was also a considerable amount of background material eluting under the α-Lac–β-Lg peaks which made quantification difficult. This material may be Amadori rearrangement products of the α-Lac and β-Lg proteins which could be produced during evaporation and drying [16].

3.2. Capillary zone electrophoresis

The separation of the whey proteins in the three samples by CZE is shown in Fig. 2. As described previously [11] there was excellent resolution of the whey protein standards (Fig. 2) although baseline separation was not achieved between the two variants of β-Lg and BSA. There was also high resolution of the different

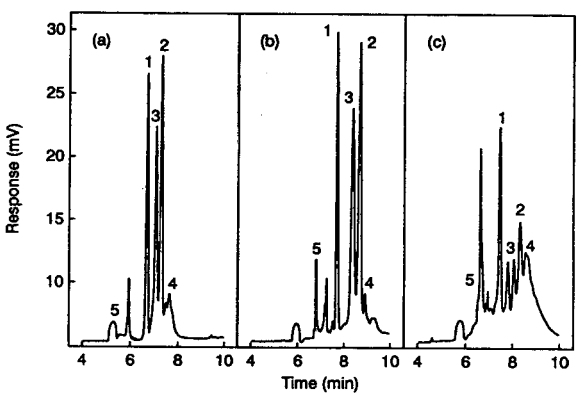

Fig. 2. Capillary zone electrophoresis of (a) whey protein standards, (b) acid whey, (c) WPC. Conditions for capillary electrophoresis as in Experimental. Peaks as described in Fig. 1.

whey proteins with the acid whey sample (Fig. 2b) although in this instance there were also a number of other minor peaks between IgG and α-Lac and β-LgA and BSA, respectively. There was a change in the retention times with the acid whey sample which was presumed to be caused by whey matrix effects (minerals, ionic strength, pH, ions, and lactose) on the electroosmotic force and/or on the protein–capillary wall interactions. These factors all contributed to making quantitation of the BSA peak more difficult. A whey sample was spiked with BSA standard to verify the position of the BSA peak (data not shown).

The separation of the whey proteins in WPC by CZE (Fig. 2c) proved to be more difficult with an extra peak overlapping the IgG peak, the loss of resolution of the β-Lg variant peaks, the emergence of additional peaks adjacent to the β-Lg peaks, and a subsequent lack of resolution of the BSA peak from these additional peaks. These changes were attributed to heat-induced chemical modifications in the protein structure during the evaporation/drying stage of processing as discussed in the previous section. This was verified by comparing the electropherograms of WPC immediately prior to evaporation and drying but after ultrafiltration and diafiltration (Fig. 3a) to the final dried WPC powder (Fig. 3b). Although the WPC before drying was highly concentrated it still had a protein peak profile similar to both the whey protein standards and the whey sample. There was, however, a loss of resolution of the β-Lg peaks by the evaporation stage of processing. This was presumed to be due to the partial polymerisation of the β-Lg molecules which was brought about by their high concentration. This polymerisation was even more evident after drying (Fig. 3b) with the increased change in the peak profile presumed to be due to a combination of the high protein concentration, high temperature (above 65–70°C) and possible high pH (above pH 7) experienced by the sample during evaporation and drying. The poor resolution and unknown/unverified peaks made quantification very difficult and methods to overcome this problem are currently being investigated.

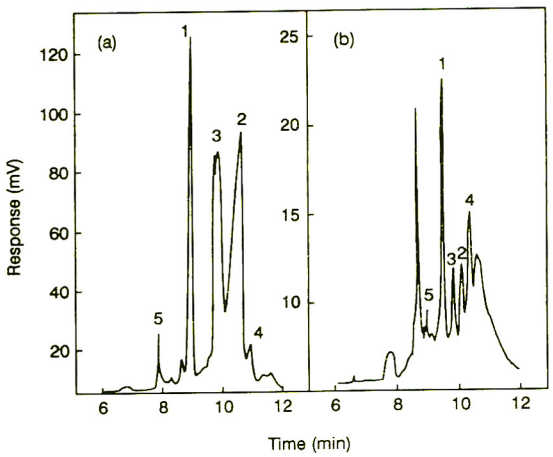

Fig. 3. Capillary zone electrophoresis of WPC (a) before and (b) after drying. Conditions for capillary electrophoresis as described in the Experimental section. Peaks as in Fig. 1. Concentrated WPC prior to drying was diluted 1:100 in sample buffer.

3.3. Native PAGE

The separation of whey protein standards, an acid whey and a WPC by native PAGE is shown in Fig. 4. The separation is based on both the charge and size of the different whey proteins such that the two main β-Lg variants (A and B) are separated and that α-Lac runs above these two β-Lg bands even though it has a smaller molecular mass.

BSA migrates as a well defined band although if there are any caseins present in the sample, these run as a broad smear which covers the BSA band. The high molecular mass of the IgG proteins restricted their entry into the gel such that they appear as a band at the interface between the stacking and running gels and are therefore difficult to quantitate. There may also be other high-molecular-mass material at this interface.

The acid whey (Fig. 4, lane 3) and WPC (Fig. 4, lane 4) samples show similar band patterns to the whey protein standards (Fig. 4, lanes 1, 2, 5 and 6) although the bands in the WPC were not as sharp. In both samples the BSA band was considerably weaker than the α-Lac and β-Lg

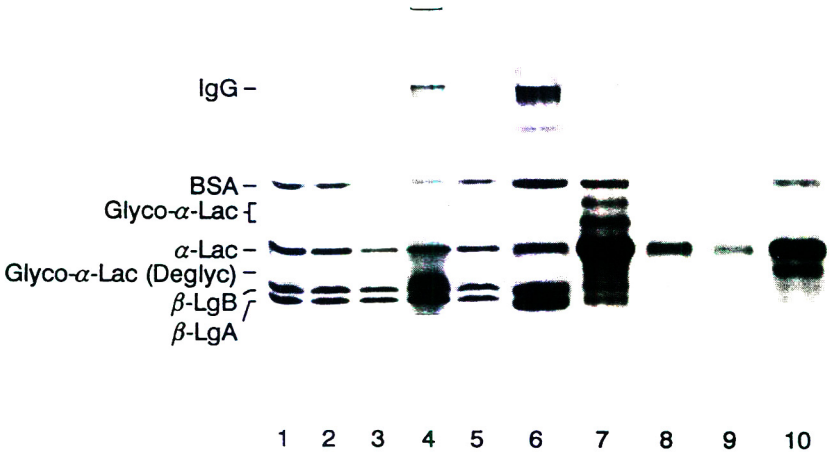

Fig. 4. Native PAGE of whey standards and samples. Gels were run and samples prepared as in Experimental. Lanes 1, 2, 5, 6 = whey protein standards; 3 = acid whey; 4 = WPC; 7 = α-Lac/glyco-α-Lac preparation; 10 = deglycosylated α-Lac/glyco-α-Lac preparation. The whey protein standards are identified on the left.

bands due to its lower concentration and the IgG appeared as a smear centered around the stacking/running gel interface. There was also considerable distortion of the β-Lg bands in the WPC sample. Whilst this sample had a high protein loading on the gel the most probable reason for the anomalous behaviour was chemical modifications of the β-Lg protein during the WPC processing as previously discussed. There was also some WPC protein material which did not enter the stacking gel from the sample well. This high-molecular-mass material was assumed to be aggregates produced during the WPC processing.

In addition to the four major whey proteins there are also a number of minor bands. These include two bands between α-Lac and BSA which have been identified as two species of glycosylated α-Lac. This was verified by the analysis of an α-Lac/glyco-α-Lac preparation (Fig. 4, lane 7) and is in agreement with the results of Hopper and McKenzie [17]. After deglycosylation of the α-Lac/glyco-α-Lac sample (Fig. 4, lane 10) the two glyco-α-Lac bands disappeared and were replaced by one band which ran just below the α-Lac band. The deglycosylated α-Lac was presumed to have a different migration pattern to α-Lac because when the carbohydrate moiety is cleaved from the Asn side chain in an N-linked glycoprotein the amino group is also removed to convert the Asn to an Asp. The concomitant change in the overall charge of the α-Lac molecule is reflected in the faster relative migration.

3.4. SDS-PAGE

The electrophoresis patterns of the whey protein standards, the acid whey and the WPC samples after separation by reduced SDS-PAGE are shown in Fig. 5. As this technique separates proteins by molecular mass differences only, the two β-Lg variants co-migrate as a single band above α-Lac. The presence of the reducing agent 2-Mercaptoethanol results in the cleavage of the disulphide bonds in IgG into its heavy and light chains which run just below BSA and above β-Lg, respectively. This method results in good separation of the whey protein standards (Fig. 5, lanes 1, 2, 5, 6 and 9) although both the heavy

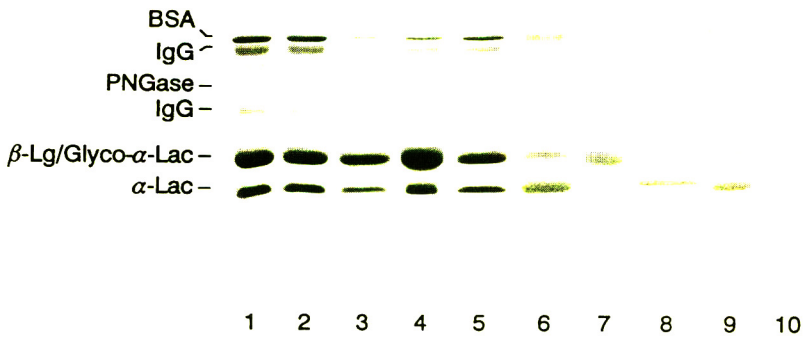

Fig. 5. SDS-PAGE of whey standards and samples. Gels were run and samples prepared as in Experimental. Lanes 1,2,5,6 and 9 = whey protein standards; 3 = acid whey; 4 = WPC; 7 = purified glyco-α-Lac; 8 = deglycosylated glyco-α-Lac; and 10 = PNGase F. The whey protein standards and PNGase F bands are identified on the left.

and light chains of IgG are reasonably diffuse making quantification more difficult.

The acid whey (Fig. 5, lane 3) and the WPC sample (Fig. 5, lane 4) displayed similar protein band profiles to the whey protein standards with the exception of the light chain of IgG which occurred as a series of smeared bands running just below the IgG light chain standard. There were also a number of light bands above the IgG light chain which were assumed to be casein protein and also some higher molecular mass material which ran above the BSA band. In the WPC sample the β-Lg band did not have the same distortion problem as observed with the native gel. This was probably because any small changes, e.g. deamidation, would not significantly alter the molecular mass.

An α-Lac/glyco-α-Lac preparation was separated by SDS-PAGE to determine where glyco-α-Lac runs using this system (Fig. 5, lane 7). The glyco-α-Lac co-migrated with the β-Lg which, on quantification, would result in an overestimate of the amount of β-Lg and an underestimate of the amount of α-Lac. When this sample was deglycosylated (Fig. 5, lane 8) the α-Lac band increased and the β-Lg/glyco-α-Lac band decreased. The deglycosylated bands were more diffuse on electrophoresis due to the different buffers used in the enzymatic deglycosylation with PNGase F. A band corresponding to this protein was also observed (Fig. 5, lane 10).

3.5. PAGE Limitations

Whey proteins in both whey and WPC samples can be measured by PAGE methods subject to the following criteria. Native PAGE can be used to determine levels of α-Lac, β-Lg A and β-Lg B as there is no interference by glyco-α-Lac though the α-Lac level may be low if glyco-α-Lac is not also measured. BSA can also be quantitated providing caseins are not present. IgG proteins can not be quantitated. SDS-PAGE can be used to quantitate BSA and IgG (using the heavy chain) but the presence of glyco-α-Lac should be considered when determining α-Lac and β-Lg levels. Whilst reduced SDS-PAGE measures total protein the native PAGE only measures undenatured, non-aggregated protein.

The accuracy of both PAGE methods is dependent on staining/destaining protocols and on reproducible densitometry. Differences of up to 10% have been observed between individuals quantitating the same protein bands on any given gel (unpublished results).

3.6. Size-exclusion HPLC

Fig. 6 shows the separation of whey proteins by size-exclusion HPLC. Whilst there was near baseline separation for the whey protein standards (Fig. 6a), with the whey and WPC samples (Fig. 6b and c) the resolution between the β-Lg A/B and α-Lac peaks was not as good. This was due to: (i) the high concentration of β-Lg required to enable simultaneous identification and quantification of the BSA and IgG proteins; (ii) the high extinction coefficient of α-Lac which enlarged that peak, and; (iii) the presence of glyco-α-Lac in the whey and WPC samples which migrated as a shoulder on the trailing edge of the β-Lg A/B peak.

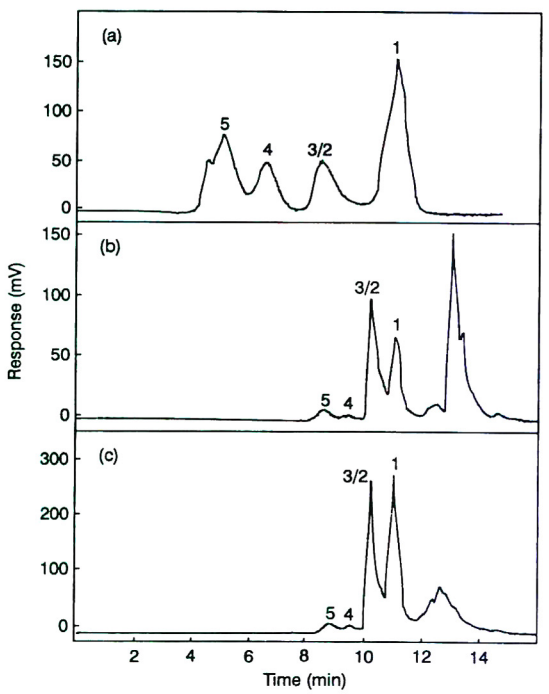

Fig. 6. Size-exclusion HPLC of (a) whey protein standards, (b) acid whey, (c) WPC. Conditions for chromatography as in Experimental.

This lack of resolution could not be readily overcome by using a higher sample dilution as the β-Lg A/B retention time was dependent on its concentration such that the retention time increased with decreasing β-Lg A/B concentration [18]. These factors need to be considered when quantifying β-Lg and α-Lac.

Other characteristics of size-exclusion HPLC included the co-migration of the A and B variants of β-Lg due to their similar molecular masses and the appearance of two peaks within the IgG standard. As observed previously with CGE there was also a number of lower molecular mass peaks in the whey and WPC samples. These were presumed to be attributable to the presence of the proteose-peptone fraction, orotic acid and hippuric acid [19]. Lastly, if there are any casein proteins present in the sample these co-migrate with the BSA and IgG peaks in the form of an ill-defined peak making quantification of BSA and IgG impossible.

3.7. Ion-exchange HPLC

Separation according to charge was performed using an anion-exchange column (Fig. 7). This resulted in the separation of the two β-Lg variants and good baseline separation of all the whey protein standards (Fig. 7a) with the exception of IgG which did not bind to the column at pH 5.5. With the acid whey and WPC samples, however (Fig. 7b and c), although the two β-Lg variants were separated the BSA peak was not very well defined, running into the leading edge of the much larger β-Lg B peak. It also co-elutes with orotic acid which made quantitation at 214 nm impossible.

The α-Lac peak in acid whey and WPC was also not as well resolved as the α-Lac standard and with the WPC the retention time increased slightly from 3.6 to 4.3 min. This was presumed to be caused by changes to the α-Lac molecular structure during processing as discussed previously.

Overall it was possible to measure both β-Lg A and B variants and α-Lac by anion-exchange

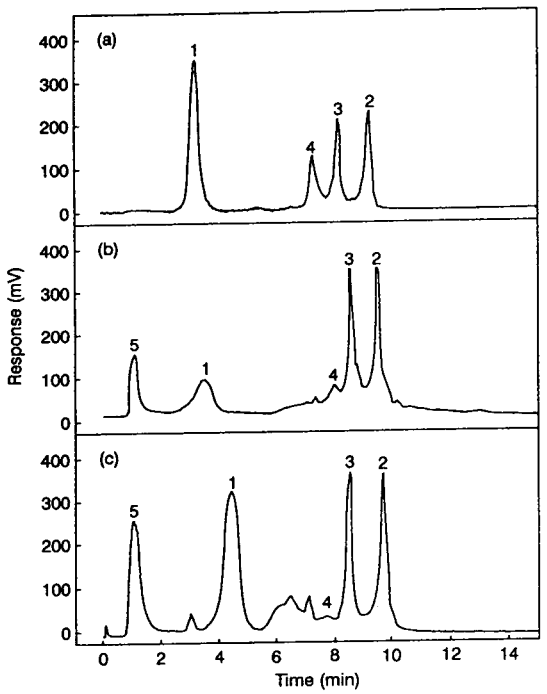

Fig. 7. Ion-exchange HPLC of (a) whey protein standards, (b) acid whey, (c) WPC, on a Pharmacia MonoQ anion exchange column. Conditions for chromatography as in Experiment. Peaks as described in Fig. 1.

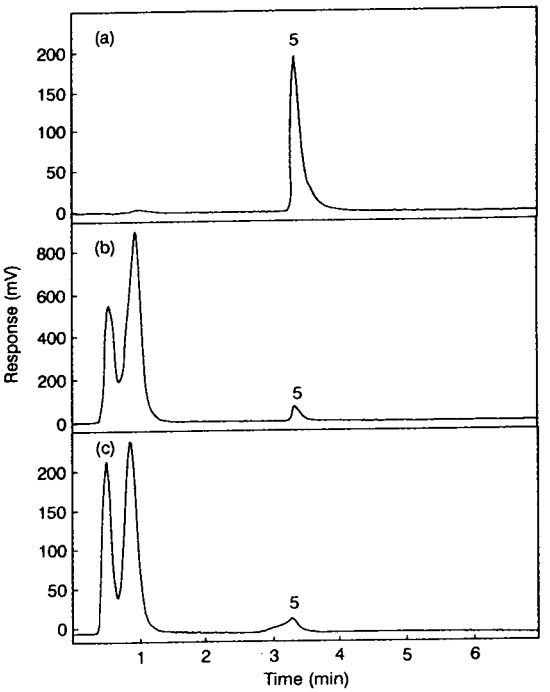

Fig. 8. Affinity HPLC of bovine IgG in (a) whey protein standards, (b) acid whey, (c) WPC, on a Pharmacia Protein G Hi-Trap column. Conditions for chromatography as in Experimental. Peaks as described in Fig. 1.

chromatography but quantification of BSA was difficult and it was not possible to quantitate IgG as it was not known what other proteins in whey besides IgG did not bind to the column.

3.8. *Affinity HPLC*

The affinity ligand protein G was used to specifically bind bovine IgG molecules (Fig. 8). All other proteins were eluted in the void volume of the column. As IgG is the predominant immunoglobulin in bovine milk [20] this matrix gave a very specific measure of the amount of bovine immunoglobulins present. It was also able to give an indication of the structural state of the IgG protein as the binding is a specific interaction between the F_c region on the immunoglobulin heavy chain and a binding site of the protein G molecule. This is demonstrated by the shapes of the IgG peak in the different samples. The standard (Fig. 8a) has a very well defined IgG peak with a sharp leading edge and only slight tailing. The IgG peak in the acid whey (Fig. 8b) is similar although with a slight loss of peak shape whilst the WPC (Fig. 8c), which has undergone more processing/denaturation by ultrafiltration, diafiltration, evaporation and drying, has a poorly defined peak shape which makes quantification more difficult.

3.9. *Quantification of acid whey and WPC*

The concentration of each whey protein in the acid whey and the WPC was determined by the different assay methods using five-point standard curves for each individual whey protein (Tables 4 and 5). As mentioned previously each analytical method had individual characteristics which resulted in variation in the results between the different assays.

Table 4
Analysis of acid whey using different methods

Separation method		Whey protein (mg/ml)			
		α-Lac	β-Lg	BSA	IgG
PAGE	Native	0.61	2.78[a]	0.26	nd[b]
	SDS	0.50	3.10	0.35	0.17[c]
HPLC	SEC	0.55	3.10	nd	0.17
	IEX	0.60	2.90	0.44	nd
	Affinity	na[d]	na	na	0.49
CE	Free zone	0.56	2.82	0.12	0.26
	Gel[e]	0.50	2.93	0.32	0.48

Sample and methods used were as described in the Experimental section. Gels, chromatograms and electropherograms are shown in Figs. 1–8.
[a] Combination of β-LgA and β-LgB.
[b] nd = Not able to be determined.
[c] Determined from IgG heavy chain.
[d] na = Not applicable.
[e] Non-reduced.

For the acid whey sample there was good agreement between the assays for both α-Lac (range 0.50 to 0.61 mg/ml) and β-Lg (range 2.78 to 3.10 mg/ml). No allowance was made for the presence of glycosylated-α-Lac which may account for the lower α-Lac levels and the higher β-Lg levels in the SDS-PAGE, size-exclusion HPLC and CGE results. The largest variation occurred amongst the BSA (range 0.12 to 0.44 mg/ml) and IgG (range 0.17 to 0.49 mg/ml) results. These variations were due principally to the low concentration of these proteins in the whey which made accurate quantitation more difficult and also to their heterogeneous nature.

In comparison to the whey sample there was wide variation in all the whey protein values of the WPC sample when they were assayed by the different methods. As mentioned previously when discussing the individual assays there were considerable problems differentiating and quantifying the individual whey proteins in the WPC, presumably because of chemical modifications to the proteins during processing. This was evident from the blurred bands for the WPC proteins on the SDS- and native-gels and from the loss of resolution with HPLC and CE.

With respect to the individual whey proteins the α-Lac and β-Lg values were between 47 to 64 mg/g and 128 to 157 mg/g respectively and the differences in the values observed between the different assays could not be as readily explained by the ability of the individual assay methods to differentiate the glyco-α-Lac moiety from the other whey proteins as was observed with the acid whey sample. As with the whey sample the BSA and IgG values in the WPC were not very consistent, again probably a reflection of the low concentration and microheterogeneity of these proteins in the WPC.

Table 5
Analysis of WPC using different methods

Separation method		Whey protein (mg/g powder)			
		α-Lac	β-Lg	BSA	IgG
PAGE	Native	52	129[a]	20	nd[b]
	SDS	47	151	26	17[c]
HPLC	SEC	51	139	14	19
	IEX	61	140	21	nd
	Affinity	na[d]	na	na	17
CE	Free zone	56	134	28	12
	Gel[e]	64	135	14	6

Sample and methods were as described in the Experimental section. Gels, chromatograms and electropherograms are shown in Figs. 1–8.
[a] Combination of β-LgA and β-LgB.
[b] nd = Not able to be determined.
[c] Determined from IgG heavy chain.
[d] na = Not applicable.
[e] Non-reduced.

3.10. Comparison of CE assays and other techniques

When comparing the CE free zone and gel results with those obtained using the other analytical techniques, the CE results were generally within the ranges of the other results and followed their trends. Thus capillary gel electrophoresis results for α-Lac and β-Lg were low and high respectively as was observed for both the PAGE-SDS and size-exclusion HPLC methods. There was also more variation in the results with both BSA and IgG. The reproducibility of the CE results was as good as those for HPLC and better than could be attained by PAGE (results not shown).

4. Conclusions

Two new CE-based methods (GCE and CZE) have been used to quantitate the four major whey proteins in both liquid whey samples and reconstituted WPC powder. These were then compared with other methods to measure the whey proteins. Overall none of the assays could provide all the results for the few major whey proteins. For liquid whey samples the main obstacles against achieving this goal appeared to be the large differences in concentration, extinction coefficients and microheterogeneity of the different whey proteins and in the ability of the different assays to measure either native or total whey protein.

Whilst the range of results for α-Lac and β-Lg was reasonably narrow over the different assays there was considerable variation between the results for BSA and IgG. The variation within the α-Lac and β-Lg results may be decreased by differentiating out and allowing for the glycosylated-α-Lac fraction. To achieve this the extinction coefficient and standard curves will need to be determined for glycosylated α-Lac. This will form the basis of future work in the area.

The large variations in the results for the BSA and IgG concentrations may be overcome by analysing samples at both a high and a low concentration and to have separation methods in which the BSA and IgG proteins are well resolved from the α-Lac and β-Lg proteins at high concentration levels. Under these constraints capillary gel electrophoresis appeared to be the most promising method for analysing whey proteins although the two β-Lg variants were not separated by this method and a sample preparation method which avoided precipitations at low whey dilutions will have to be developed.

For WPC powders, however, there also appeared to be problems with changes to the protein structure brought about by the different processing steps. More research is required on both sample preparation and on the extent of protein denaturation and how this is reflected by the different assays.

Acknowledgement

The authors would like to thank Dr. Rex Humphrey, Dr. Derek Knighton and Dr. Skelte Anema for helpful discussions.

References

[1] P.F. Fox, in P.F. Fox (Editor), *Developments in Dairy Chemistry, Vol. 4*, Elsevier Applied Science, London, 1989, p. 1.
[2] H.E. Swaisgood, in P.F. Fox (Editor), *Developments in Dairy Chemistry, Vol. 1*, Applied Science Publishers, London, 1982, p. 1.
[3] R. Jenness, in P.F. Fox (Editor), *Developments in Dairy Chemistry, Vol. 1*, Applied Science Publishers, London, 1982, p. 87.
[4] B. Ribadeau-Dumas and R. Grappin, *Lait*, 69 (1989) 357.
[5] E.D. Strange, E.L. Malin, D.L. Van Hekken and J.J. Basch, *J. Chromatogr.*, 624 (1992) 81.
[6] Z. Deyl and R. Struzinsky, *J. Chromatogr.*, 569 (1991) 63.
[7] F.-T.A. Chen and J.H. Zang, *J. Assoc. Off. Anal. Chem. Int.*, 75 (1992) 905.
[8] N. de Jong, S. Visser and C. Olieman, *J. Chromatogr.*, *A* 652 (1993) 207.
[9] A. Cifuentes, M. de Frutos and J.C. Diez-Masa, *J. Dairy Sci.*, 76 (1993) 1870.
[10] J.A.H.J. Otte, K.R. Kristiansen, M. Zakora and K.B. Quist, *Neth. Milk Dairy J.*, 48 (1994) 81.
[11] G.R. Paterson, J.P. Hill and D.E. Otter, *J. Chromatogr. A*, 700 (1995) 105.
[12] P. Mailliart and B. Ribadeau-Dumas, *J. Food Sci.*, 53 (1988) 743.
[13] R.S. Humphrey and L.J. Newsome, *New Zealand J. Dairy Sci. Technol.*, 19 (1984) 197.
[14] A.T. Andrews, *Electrophoresis*, Oxford Science Publications, 2nd ed., 1986.
[15 U.K. Laemmli, *Nature*, 2278 (1970) 680.
[16] D.R. Knighton, personal communication.
[17] K.E. Hopper and H.A. McKenzie, *Biochem. Biophys. Acta*, 295 (1973) 352.
[18] R.S. Humphrey, W.C. Thresher, N.W. Haggarty, D.E. Otter and J.P. Hill. Brief communication of the *XXIV International Dairy Congress, Melbourne, 18–22 September 1994*, Australian National Committee of the International Dairy Federation, Glen Iris, p. 99.
[19] R. Jenness, in N.P. Wong (Editor), *Fundamentals of Dairy Chemistry* Van Nostrand Reinhold Company, New York, 3rd ed., 1988, p. 1.
[20] J.E. Butler, *J. Dairy Sci.*, 52 (1969) 1895.

ELSEVIER

Journal of Chromatography A, 700 (1995) 125–136

JOURNAL OF CHROMATOGRAPHY A

Separation of transfer RNA and 5S ribosomal RNA using capillary electrophoresis

Eleftheria Katsivela*, Manfred G. Höfle

GBF–National Research Centre for Biotechnology, Division of Microbiology, Mascheroder Weg 1, D-38124 Braunschweig, Germany

Abstract

Capillary gel electrophoresis and capillary electrophoresis using entangled polymer solutions was investigated for their applicability for the separation of low-molecular-mass RNAs (transfer RNA and 5S ribosomal RNA), with a size range of 70–135 nucleotides, from bacteria. Cross-linked polyacrylamide gel-filled capillaries (3 and 5%) were used for capillary gel electrophoresis. Good resolution was obtained using gel-filled capillaries only for small tRNAs with lengths to 79 nucleotides, larger tRNAs and 5S rRNA could not be resolved using this method. Buffers containing sieving additives were employed to improve separations of RNA by capillary electrophoresis using entangled polymer solutions. The use of linear sieving polymers in buffers resolved 5S rRNA and tRNAs, even when they possessed only different secondary structure or small differences in length (1–5 nucleotides).

1. Introduction

The rapid detection, identification and classification of bacteria is a continuing, world-wide scientific goal, particularly for medical and ecological purposes. The classical methods of bacterial identification are based primarily on phenotypic and physiological characteristics (e.g., growth on different media) and do not examine directly the genotypic characteristics of bacteria. Recently, a variety of molecular and genetic techniques have been introduced for the identification and classification of bacteria. These methods include DNA/DNA hybridisation [1], 5S, 16S and 23S rRNA and rRNA gene sequencing [2,3], as well as fingerprinting of proteins and DNA [4,5]. The only direct, genotypic fingerprinting technique using RNA is the low-molecular-mass RNA (low-M_r RNA) profiling method [7]. This new RNA fingerprinting method generates one-dimensional band patterns for three groups of molecules of taxonomic significance: 5S rRNA, large tRNAs and small tRNAs (size range 70 to 135 nucleotides). These band patterns allow an identification of bacterial strains due to species- and genus-specific tRNA bands and group-specific 5S rRNA bands and can also be applied directly to analyses of environmental samples [8].

The standard technique for low-M_r RNA profiling employs slab polyacrylamide gel electrophoresis (PAGE), followed by silver stain detection [7]. While this has been accepted as a standard methodology, several drawbacks exist. Slab gel electrophoresis is time-consuming, labour intensive and difficult to automate. Capil-

* Corresponding author.

0021-9673/95/$09.50
SSDI 0021-9673(94)01091-9

lary electrophoresis (CE) provides an attractive alternative to the conventional method, because of shortened separation times, on-line detection, automated sample injection and reduced amounts of sample needed.

Separation of DNA fragments has been demonstrated using different CE techniques [9–16]. In most cases, gel-filled capillaries with different concentrations of cross-linked polyacrylamide have been used. Such separations of DNA poly- and oligonucleotides, as well as of polymerase chain reaction (PCR)-amplified DNA fragments, are well described and investigated [9–11]. Besides cross-linked polyacrylamide matrices, separation media containing agarose [12] and non-cross-linked linear polyacrylamide have been used [13]. In all cases, problems exist for the preparation of capillaries filled with such separation media (e.g., polyacrylamide, agarose), as well as in their handling. Additionally, the capillaries have a finite shelf-life as well as a low reproducibility. For example, bubbles may form within the capillaries by sudden current or temperature fluctuations, due to either a point of high resistance within the column, such as a build-up of high-molecular-mass sample residue or non-uniform temperature control, and finally gel degradation occurs. The capillaries then become useless and must be discarded.

As an alternative to gels, solutions of entangled polymers can be used as macromolecular sieving media [14–16]. These include water soluble, viscous, linear polymers such as hydroxypropylmethylcellulose (HPMC) or hydroxyethylcellulose (HEC). These polymers produce a sieving effect, can be replenished after each run, and are easy to handle. The capillaries used are coated, open tubular, and possess a long lifetime. Generally, these non-cross-linked polymer sieving systems possess separation efficiencies nearly equivalent to those obtained with gel-filled capillaries for the separation of DNA fragments [14–16].

High reproducibility, as well as potential for automation, were required for a routine application of the separation of low-M_r RNA by CE. Although, an easy transfer of low-M_r RNA profiling from conventional gel electrophoresis to capillary gel electrophoresis (CGE) was expected. This has proven to be difficult. In this paper we present the development and optimisation of a separation methodology for different, pure low-M_r RNA standards and the determination of whole low-M_r RNA profiles using polymer solutions, as well as gel-filled capillaries. Finally, we compare the resolutions of the low-M_r RNA fingerprints, as determined by conventional slab gel electrophoresis and by CE.

2. Experimental

2.1. Materials

Tris(hydroxymethyl)aminomethane (Tris), ammonium peroxodisulphate, N,N,N′,N′-tetramethylethylenediamine (TEMED) were obtained from Sigma (St. Louis, MO, USA). Acrylamide was purchased from Amresco (Solon, OH, USA) and 3-(trimethyoxysilyl)propylmethacrylate (Bind Silane) from LKB (Bromma, Sweden). Ethylenediaminetetraacetic acid (EDTA) and boric acid were obtained from Riedel–de Haen (Deelze, Germany). The ready available PCR product analysis buffer with 7 *M* urea was purchased from Bio-Rad (Richmond, CA, USA). The polymer HPMC, with a viscosity rating of 4000 cP for a 2% solution at 25°C, was obtained from Sigma.

$tRNA_{Phe}$ and $tRNA_{Tyr}$ from *Escherichia coli* MRE 600 were supplied by Sigma. Purified 5S rRNA was provided at a concentration of 0.8 $\mu g/\mu l$ and a tRNA mixture from *E. coli* MRE 600, containing 5S rRNA and tRNAs, were purchased from Boehringer Mannheim (Mannheim, Germany). This tRNA mixture was used as a standard low-M_r RNA mixture. Polydeoxyadenylic acids [$pd(A)_{25-30,\ 40-60}$] were obtained from J & W Scientific (Folsom, CA, USA).

Gel-filled capillaries, μPAGE-3 (3% T, 3% C PAGE[1]) and μPAGE-5 (5% T, 5% C PAGE), as well as open tubular, coated capillaries DB-1, were purchased from J & W Scientific.

[1] T = [g acrylamide + g N,N′-methylenebisacrylamide (Bis)]/100 ml solution; C = g Bis/T

2.2. Equipment

A Spectra Phoresis 500 CE (Spectra-Physics, Fremont, CA, USA) was used in negative polarity mode (anode at the detection side) for all separations. Temperature control was achieved with a peltier cooling system from Spectra Phoresis 500. Electrokinetic injections were always carried out and nucleic acids were detected at 260 nm using a UV detector.

2.3. Methods

RNA denaturation

A 20-μl volume of the standard low-M_r RNA mixture from *E. coli* (60 μg RNA/ml) was mixed with 40 μl formalin, 16 μl formaldehyde (37%) and 8 μl 40 m*M* Tris–HCl buffer, 1 m*M* EDTA (pH 5.0). The sample was heated for 15 min at 65°C, than cooled in ice and stored at 4°C.

Capillary gel electrophoresis

CGE was performed in gel-filled capillaries μPAGE-3 and μPAGE-5, 44 cm (36 cm effective length) × 75 μm I.D. The capillaries were conditioned daily at 25°C and 100 V/cm, negative polarity for 5 min. The applied voltage was increased stepwise to 250 V/cm over a period of 30 min. The current was stable at approximately 4–5 μA. Samples were introduced into capillaries by electromigration at −5 kV for 5 s. Separations were performed under constant voltage at 250 V/cm. The separation buffer solution contained 100 m*M* Tris–borate and 7 *M* urea at a pH 8.3.

Capillary electrophoresis using entangled polymer solutions

DB-1 open tubular capillaries, 70 cm (62 cm effective length) or 118 cm (110 cm effective length) × 100 μm I.D. with a coating of 0.1 μm dimethylpolysiloxane, were used without modification. 70 cm DB-1 capillaries were filled automatically with the appropriate polymer sieving buffer for 15 min (110 cm long capillaries required 25 min). Between runs, the capillaries were washed, in turn, with Milli-Q water and methanol twice (110 cm long capillaries three times) for 5 min. Column lifetime was determined to be in excess of 100 injections.

The first polymer sieving buffer, named "PCR product analysis buffer" from Bio-Rad, contained 267 m*M* Tris–borate, 7 *M* urea and polymer modifier (pH 8.3) and was "ready for use". The second polymer sieving buffer that was used contained 350 m*M* Tris–borate, 2 m*M* EDTA and 7 *M* urea (pH 8.6). A 10 ml volume of buffer was mixed with 0.5% (w/w) HPMC and heated for 10 min at 80°C in a closed vessel. The HPMC solution was stirred slowly at room temperature until it appeared homogeneous and transparent. The HPMC solution was used on the second day after preparation and was stable for at least one month at room temperature.

The samples were prepared at a concentration of 100 μg/ml in 40 m*M* Tris–borate–EDTA buffer (pH 5.0) and were introduced into the capillaries by electromigration. Before sample injection, the injection side of the capillary was washed with Milli-Q water twice for 0.1 min. All separations were performed at 20°C.

Conventional gel electrophoresis

Separation of low-M_r RNA was carried out under high power by denaturing PAGE [17]. Dried samples of low-M_r RNA (3 μg) were suspended in 4 μl of a loading solution [300 mg/ml sucrose, 460 mg/ml urea, 10 μl/ml 20% sodium dodecyl sulfate (SDS), 1 mg/ml bromophenol blue, 1 mg/ml xylene cyanol, all substances dissolved in TBE buffer] and loaded on polyacrylamide gels [gel size 550 × 170 × 0.4 mm, 10% acrylamide, acrylamide:N′,N-methylenebisacrylamide 28.8:1 (w/w), 7 *M* urea, in TBE buffer: 100 m*M* Tris, 83 m*M* boric acid, 1 m*M* EDTA, pH 8.5] that were bound to a carrier glass plate and run in a high-power electrophoresis unit (2010 Macrophor electrophoresis unit and 2297 Macrodrive 5 power supply, LKB–Pharmacia, Bromma, Sweden). Gels were run at 60°C and at constant power that was increased stepwise from 40 to 160 W during the 3 h run. RNA bands were visualised by a modified ammoniac silver staining procedure [7]. Gel scans were performed using a transmission

densitometer (Elscript 400, Analysentechnik Hirschmann, Taufkirchen, Germany) at a wavelength of 546 nm. A detailed description of the conventional electrophoresis of low-M_r RNA has been given previously [7].

3. Results and discussion

3.1. Capillary gel electrophoresis

Contrary to work having been carried out on the separation of DNA, there have been no reports on the separation of RNA using CGE. Although given the differences between DNA and RNA molecules, we have based our first studies with RNA on the previous work carried out on the separation of single stranded deoxyoligonucleotides with lengths of 30–160 bases. Paulus et al. [10] reported good resolution of DNA oligonucleotides over a range of 30–160 bases with 2.5–4% T and 3.3% C polyacrylamide gel-filled capillaries. Therefore, we tested, as a first approach, two types of commercially available capillaries that have the reported concentration of polyacrylamide, μPAGE-3 with 3% T, 3% C and μPAGE-5 with 5% T, 5% C PAGE. Moreover, we were able to reproduce the results of the separation of the polydeoxyadenylic acids $pd(A)_{25-30}$ and $pd(A)_{40-60}$ using these capillaries. In comparison with μPAGE-5, shorter migration times were obtained using the μPAGE-3. This result was expected due to the larger mesh size on the 3% polyacrylamide gel allowing the linear polydeoxyadenylic acids to move faster through the gel pores.

However, the results obtained for ribonucleic acids were different from those obtained for the polydeoxyadenylic acids. The separation of $tRNA_{Phe}$, using a 5% cross-linked polyacrylamide gel, is shown in Fig. 1A. Good resolution of $tRNA_{Phe}$ (76 nucleotides) was obtained using the 5% T and 5% C gel-filled capillaries, comparable to resolutions obtained using conventional polyacrylamide gels (55 cm long) (Fig. 1B).

In comparison to 5% gel-filled capillaries, the separation for tRNA was improved using 3% gel-filled capillaries and the analysis time was decreased. The separation of a mixture of three low-M_r RNA standards ($tRNA_{Phe}$, $tRNA_{Tyr}$ and 5S rRNA) using a 3% gel-filled capillary is shown in Fig. 2. The first two peaks belong to the $tRNA_{Phe}$ and the two following ones to the $tRNA_{Tyr}$. The two peaks of $tRNA_{Tyr}$ are noticeably less sharp than the peaks of $tRNA_{Phe}$. The 5S rRNA is only detectable from the increase of the baseline. Additionally, a separation of the 5S rRNA could not be achieved and the increase of baseline suggests that a build-up of the 5S rRNA degradation products was occurring. 5S rRNA is a ribosomal component and might be more sensitive to the separation conditions than are cytoplasmic tRNAs. Alternatively, degradation of the gel is also possible explanation for the baseline increase. Lalande et al. [18] described a biomolecule deformation called "trapping form". In this case, both ends of the DNA molecule are very close to each other in the field direction. The electrophoretic forces acting on the molecule are cancelled, and the mobility is zero until a new, non-compact conformation is reached. Thereby, the resistance within the capillary is high, due to gel degradation.

Results from the separation of low-M_r RNA standards (Fig. 2) demonstrate that a separation of tRNAs, with good resolution using CGE, is only effective for small molecules, for example $tRNA_{Phe}$, belonging to the class 1 tRNA (72–79 nucleotides long [6]). The resolution of tRNAs decreased with increasing nucleotide length. On the contrary, a separation of the 5S rRNA could not be achieved using 3 or 5% gel-filled capillaries. Similar results were obtained for the separation of 5S rRNA using a different type of gel-filled capillary (eCap gel U 100P, Beckman, Fullerton, CA, USA) (data not shown). Probably, the mobility of low-M_r RNA molecules is different from that of DNA, and deformation of their structure, due to electric forces within the gel network, hinders a good resolution for molecules greater than 79 nucleotides. The limited column durability and the short lifetime are additional difficulties. Therefore, another CE separation method was explored.

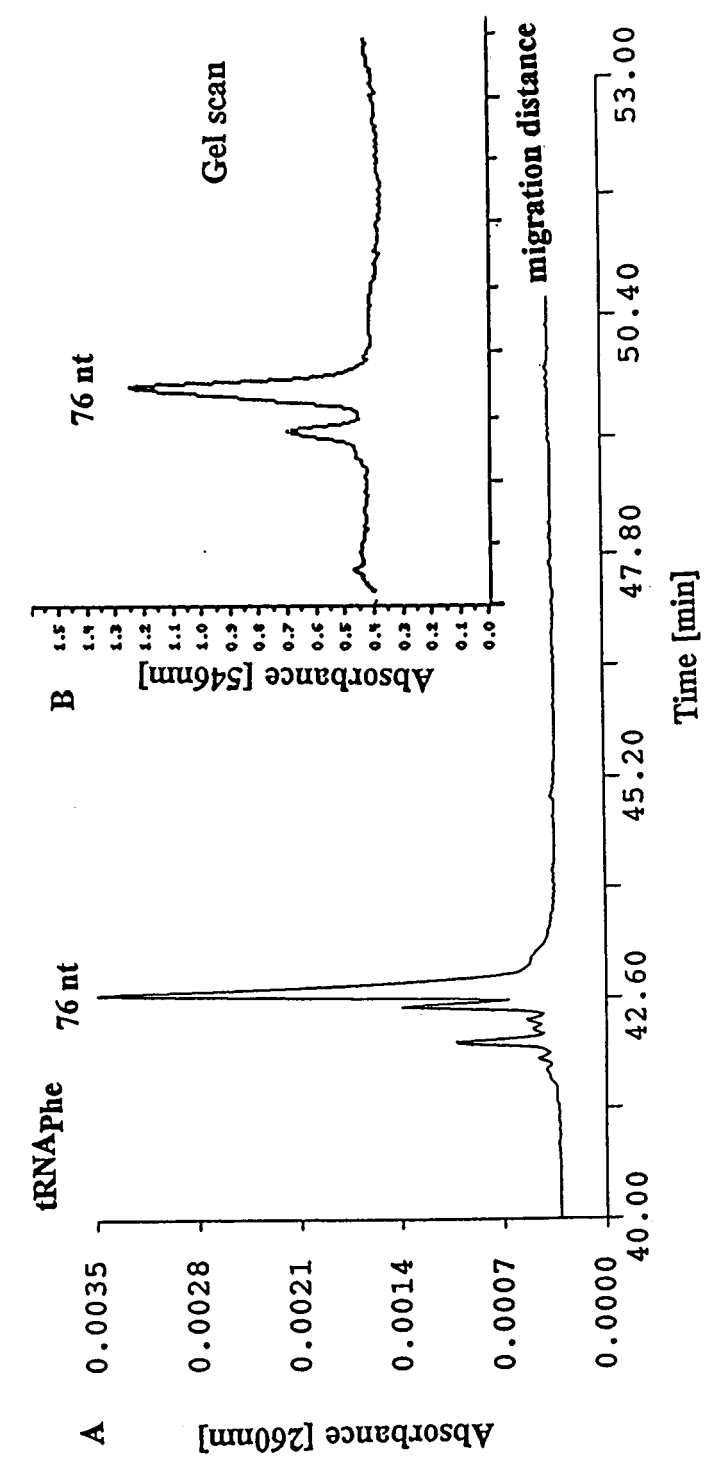

Fig. 1. (A) Gel-filled CE separation of $tRNA_{Phe}$ from *E. coli* MRE 600 using 5% cross-linked polyacrylamide gel. Buffer: 100 m*M* Tris–borate and 7 *M* urea, pH 8.3. Sample: 8 μg/ml. (B) Gel scan of $tRNA_{Phe}$ separated by conventional PAGE. nt = Nucleotides.

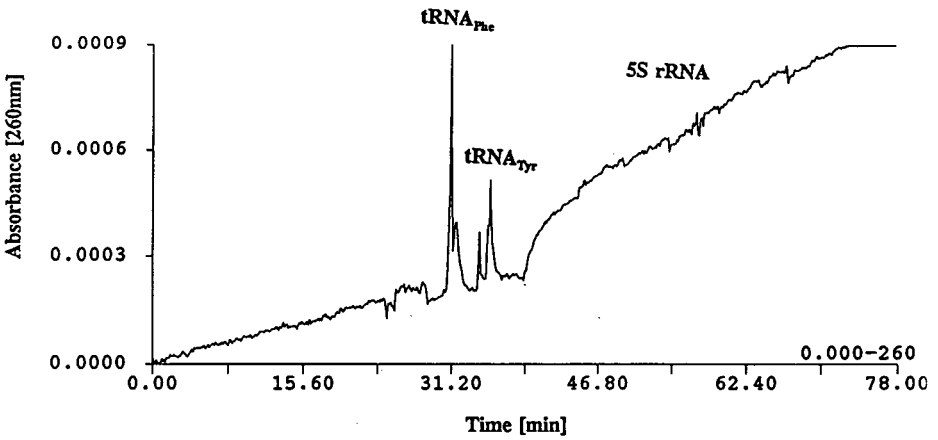

Fig. 2. Gel-filled CE separation of a mixture of three low-M_r RNA standards (tRNA$_{Phe}$, tRNA$_{Tyr}$ and 5S rRNA) from *E. coli* MRE 600 using 3% cross-linked polyacrylamide gel. Sample: 24 μg/ml.

3.2. Capillary electrophoresis using entangled polymer solutions with commercial buffer including sieving additives

Solutions of entangled polymers offer a good alternative to the CGE. This technique promises to combine the advantages of free-solution CE (automation, speed, reproducibility and accurate quantification) with the range of applications and resolving power of gel-based systems.

A dynamic, transient polymer network is formed in CE with entangled polymer solutions rather than a rigid, chemical, cross-linked gel network. These polymer solutions possess a viscosity without gel consistency. Many reports demonstrated separations of DNA restriction fragments and PCR products ranging in size from 72 to 1353 base pairs (bp), with resolutions comparable to CGE, using entangled polymer solutions [15,19–22].

Firstly, we tested, as sieving medium, a commercially available analysis buffer with sieving additives (Bio-Rad) for the separation of the low-M_r RNA molecules larger than 79 nucleotides that could not be separated by CGE. Fig. 3 shows the separation of tRNA$_{Tyr}$ (Fig. 3A) and of 5S rRNA (Fig. 3B). Both samples were separated as well by slab gel electrophoresis (gel scans, Fig. 3C and D). The 5S rRNA of *E. coli* easily separated into the characteristic two main fractions of 5S rRNA with lengths of 115 and 120 nucleotides. As demonstrated with 5S rRNA (Fig. 3B), separation of ribonucleic acids with, at least, 5 nucleotide differences are possible using this system. Moreover, we obtained high reproducibility of migration time of both separations with a relative standard deviation (R.S.D.) for 20 runs in the range 0.2–0.4%.

Fig. 4 presents the separations of a standard low-M_r RNA mixture from *E. coli* using DB-1 capillaries with a length of 70 cm (62 cm effective length) (Fig. 4A) and 118 cm (110 cm effective length) (Fig. 4B). The first six peaks (1–6) belong to the class 1 tRNAs (length of 74–79 nucleotides). The following five peaks (7–11), belong to the class 2 tRNAs (length of 83–90 nucleotides). The last peak (12) represents the 5S rRNA (120 nucleotides). The position of the 5S rRNA was determined by progressive addition of 5S rRNA to the sample. The separation profile obtained, using the 70 cm long capillary, represented a relatively poor resolution, although the three main groups of low-M_r RNA (class 1 and class 2 tRNA and 5S rRNA) could be clearly differentiated. However, no improvement was obtained through variation of running conditions (e.g., increased electric fields or temperature, longer washings and buffer filling of the capillary or use of DB-17 capillary). Finally, an increase in the length of the capillary from 70

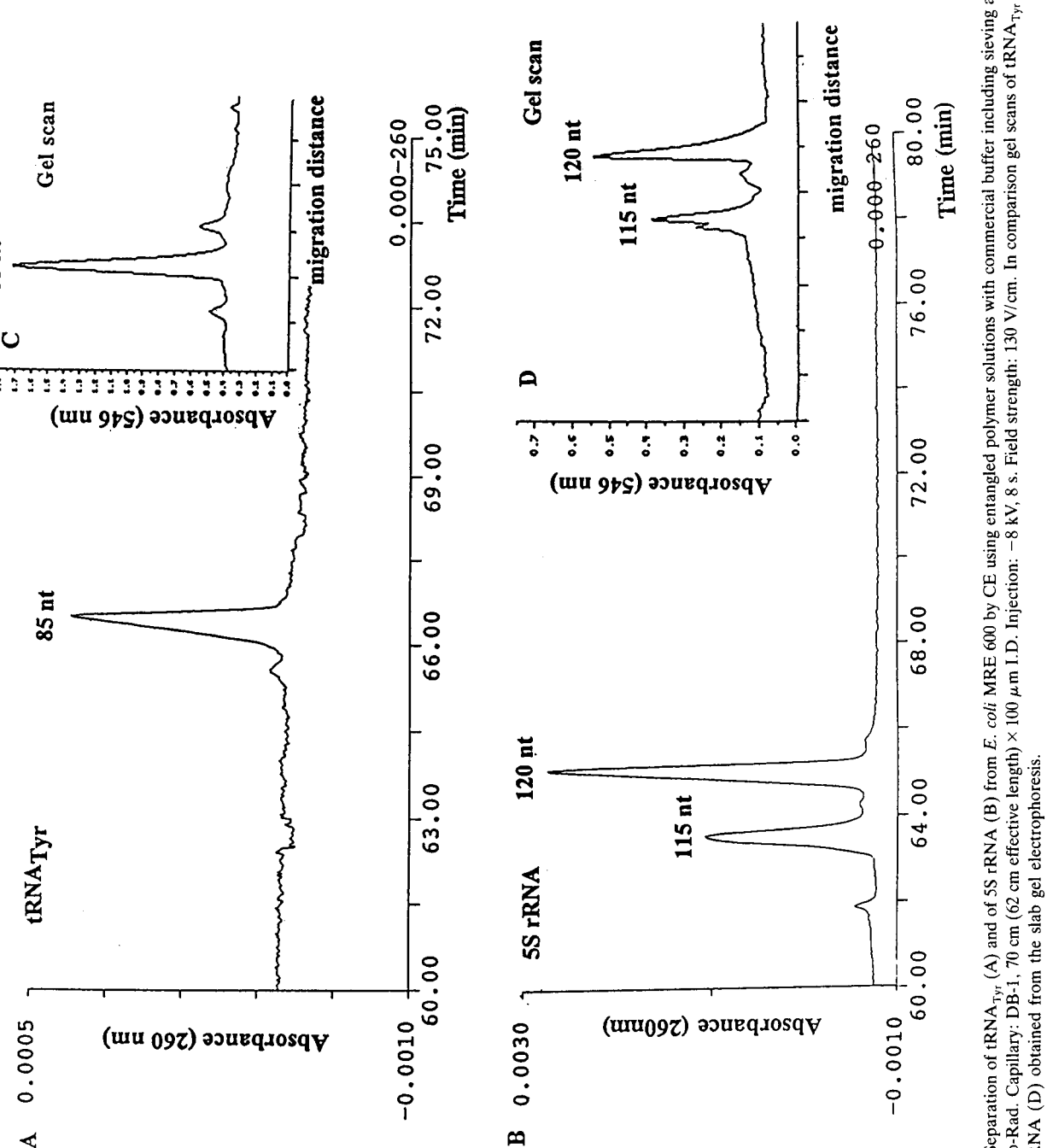

Fig. 3. Separation of $tRNA_{Tyr}$ (A) and of 5S rRNA (B) from *E. coli* MRE 600 by CE using entangled polymer solutions with commercial buffer including sieving additives from Bio-Rad. Capillary: DB-1, 70 cm (62 cm effective length) × 100 μm I.D. Injection: −8 kV, 8 s. Field strength: 130 V/cm. In comparison gel scans of $tRNA_{Tyr}$ (C) and of 5S rRNA (D) obtained from the slab gel electrophoresis.

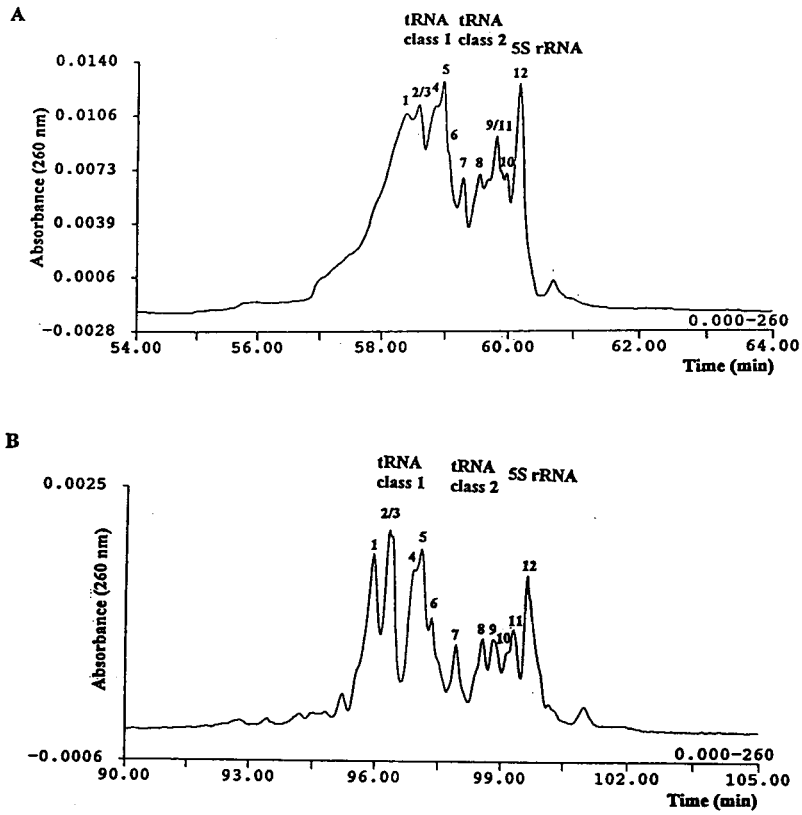

Fig. 4. Separation of standard low-M_r RNA mixture from *E. coli* MRE 600 by CE using entangled polymer solutions with commercial buffer including sieving additives from Bio-Rad. Capillary: DB-1, 70 cm (62 cm effective length) × 100 μm I.D. (A) and 118 cm (110 cm effective length) × 100 μm I.D. (B). Injection: −3 kV, 10 s. Field strength: 150 V/cm by the 70 cm capillary and 220 V/cm by the 118 cm capillary.

cm to 118 cm was observed to affect an improved resolution. The longer the capillary, the better the resolution. Thus, peaks number 1 and 2, as well as the groups of peaks 1–3 and 4–6, belonging to the class 1 tRNA, are separated from each other. A decrease of overlapping was obtained in the class 2 tRNA, the peaks 7–11 are nearly baseline separated.

In comparison to 70 cm capillaries, we observed an increase of migration time to at least 40 min using 118 cm capillaries. The separations were performed under low electric field strength (150 and 220 V/cm respectively). Although, retention times could be reduced by using higher electric fields, worse resolutions were also produced. Several reports have demonstrated the negative influence of high electric fields on the resolution of separation [23,24]. In comparison to standard gel scans of the same sample (Fig. 6B), a nearly satisfactory resolution was obtained using the 118 cm long capillary. However, the three groups of low-M_r RNA are separated better and differentiated easier using the slab PAGE.

As is shown in Fig. 4, tRNAs with small differences in length of 1–5 nucleotides (class 1 or class 2 tRNA) or with different secondary structures, were resolved by CE using entangled polymer solutions. The influence of the secondary structure in CE separations using polymer buffers was also demonstrated in the following experiment. The resolution of the low-M_r RNA mixture from *E. coli* was compared to the resolution of the same sample after denaturation

into single strands (ss). The low-M_r RNA mixture from *E. coli* was treated with formalin and formaldehyde for complete denaturation, and separated under the same conditions as the non-treated sample. Fig. 5 demonstrates the resolution of this separation. Only one broad peak was obtained instead of a resolved profile. A separation of components was not possible in the absence of secondary structures using this system. Inadequate resolution was obtained also by the separation of linear ss polydeoxyadenylic acids under the same running conditions. A minimum length difference of 10 nucleotide bases was necessary for a separation of two ss DNA oligonucleotides (data not shown).

Although, the separation by CE using entangled polymer solutions of 5S rRNA from *E. coli* appears to be size-dependent (Fig. 3B), a resolution of the low-M_r RNA mixture from *E. coli* also was obtained due to the secondary structure (Fig. 5). Probably, an interaction of the RNA molecules with the entangled polymer network exists also. An entanglement coupling interaction of biomolecules (as passing analyte), moving under the influence of an electric field, with polymer molecules in the buffer, has been reported previously [19,25].

In comparison to CGE, RNA molecules greater than 79 nucleotides can be separated by CE using entangled polymer solutions with commercial buffer including sieving additives from Bio-Rad. Low-M_r RNA profiles may be analysed, with satisfactory resolution, using this separation system. On the other hand, shorter migration times and better resolution are desired. Therefore, we employed additional polymers as sieving additives in the separation buffer.

3.3. Capillary electrophoresis using entangled polymer solutions with 0.5% HPMC as sieving additive

Zhu et al. [26] first demonstrated that electrophoresis buffers containing cellulose additives such as methyl or hydroxymethyl cellulose provide a molecular-sieving capability for the CE separation of nucleic acids (i.e. non-gel electrophoresis). Therefore, we tested separations using 70 cm long DB-1 capillaries and HPMC (0.5%, w/w) as a sieving agent in the buffer. The separation of the low-M_r RNA mixture from *E. coli* is shown in Fig. 6A. In comparison, the gel scans and the slab gel separation of the same sample are shown in Fig. 6B and C, respectively. The peak pattern obtained by the CE was different from the pattern of the conventional gel electrophoresis. Additionally, a larger separation distance was obtained between the different low-M_r RNA groups (class 1 and class 2 tRNA and 5S rRNA) using slab PAGE. High electric fields

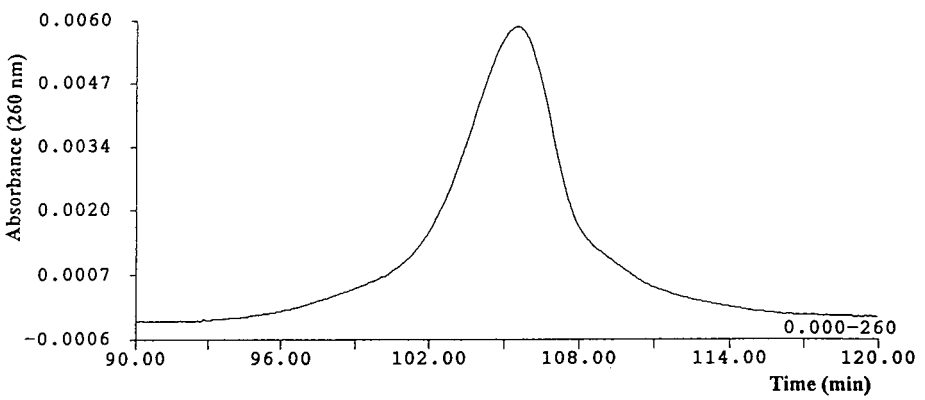

Fig. 5. Separation of denatured low-M_r RNA mixture from *E. coli* MRE 600 by CE using entangled polymer solutions with commercial buffer including sieving additives from Bio-Rad. Capillary: DB-1, 118 cm (110 cm effective length) × 100 μm I.D. Injection: −3 kV, 10 s. Field strength: 250 V/cm.

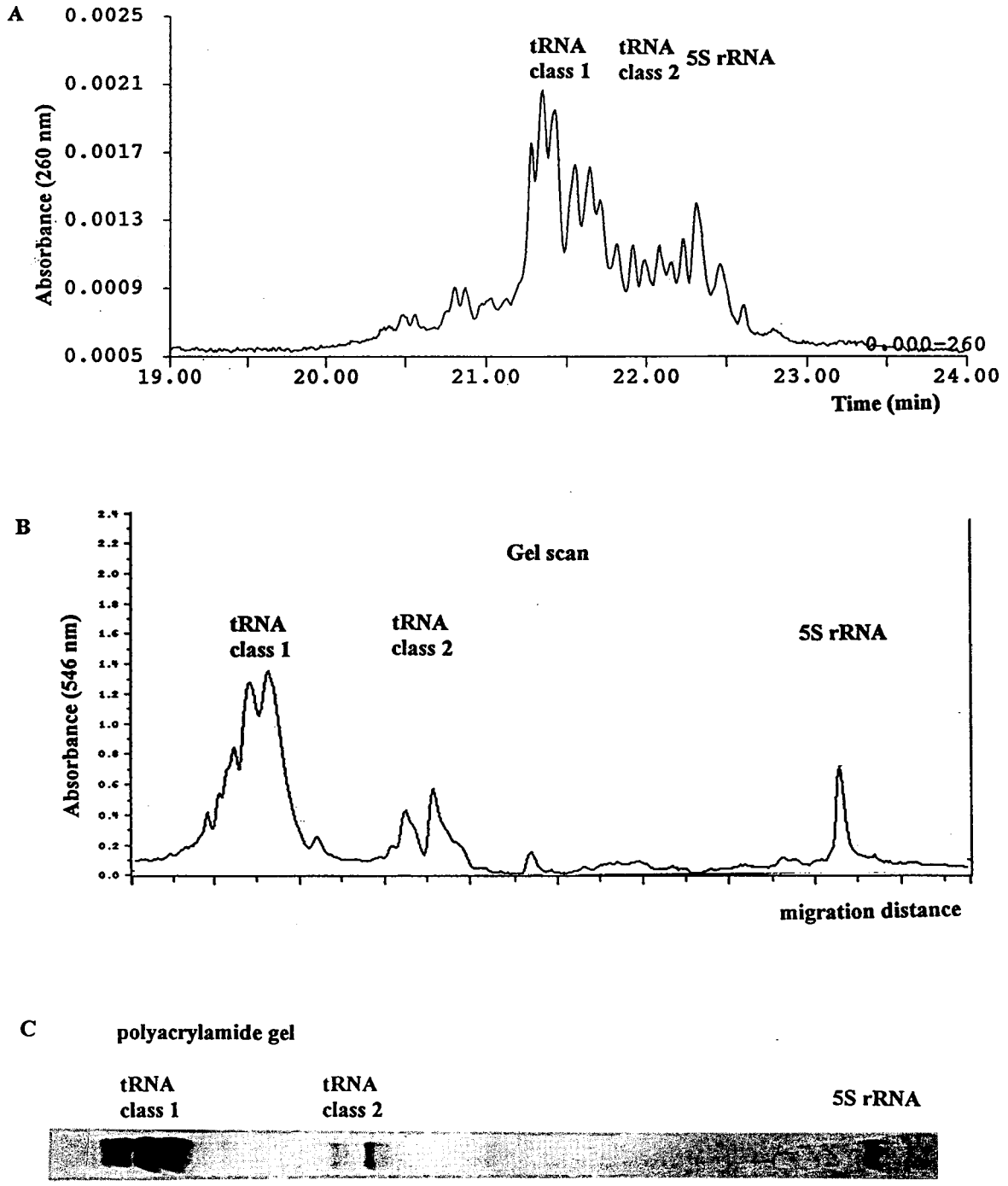

Fig. 6. (A) Separation of low-M_r RNA mixture from *E. coli* MRE 600 by CE using entangled polymer solutions with 0.5% HPMC. Capillary: DB-1, 70 cm (62 cm effective length) × 100 μm I.D., 0.1 μm thickness. Buffer: 350 m*M* Tris–borate, 2 m*M* EDTA, 7 *M* urea and 0.5% HPMC (pH 8.6). Injection: −10 kV, 15 s. Field strength: 570 V/cm. Gel scan (B) of the same sample from slab PAGE (C).

could be used (570 V/cm) by the CE using entangled polymer solutions with 0.5% HPMC, reducing the run time to 30 min and producing a very good resolution. This resolution was better than that attained by the CE using entangled polymer solutions with commercial buffers including sieving additives and 118 cm long capillaries (Fig. 4B) as well, as by the gel scans of the conventional slab gel electrophoresis (Fig. 6B). CE using entangled polymer solutions with 0.5% HPMC, therefore, becomes an attractive alternative to the slab gel electrophoresis. The shorter separation times and the potential for automation are additional advantages.

The use of 0.5% HPMC appeared to be more applicable for the separation of RNA than for separation of DNA fragments with small length differences. Comparing the separation of two double stranded (ds) DNA fragments (271 and 281 bp) under the same conditions, Schwartz et al. [20] observed that the separation of two components with a difference of 10 bp is only possible through intercalation of the ds DNA by the addition of ethidium bromide to the sample before electrophoresis. Probably the deformation of the DNA structure, by addition of ethidium bromide, leads to the separation due to interactions within the HPMC network. The deformation of the DNA was explained by the biased reptation theory wherein DNA, in solutions of entangled polymer, moves by repeated stretching, slippage, relaxation and re-extension [25]. Probably, ds DNA molecules, without addition of ethidium bromide, does not undergo all of these changes in conformation.

The different, previously reported model systems (e.g. Ogston model [27]; reptation model [28]; and biased reptation model [25]) for the moving of a passing analyte, particularly DNA, by CGE, as well as by CE using entangled polymer solutions may not be directly applicable for the CE separation of low-M_r RNA. The most important separation parameter appeared to be, besides mass and charge, the spatial structure, as well as the changes in conformation and the interaction with the appropriate separation network.

4. Conclusions

The separation of low-M_r RNA by CE using entangled polymer solutions, as well as by CGE, has shown that resolution of low-M_r RNA differs from the resolution of DNA molecules of comparable size. CE using entangled polymer solutions was reliable because of the improved resolution of low-M_r RNA molecules as well as the facility of handling. This CE method was more convenient and yielded more reproducible results than those obtained when gel-filled capillaries were used. The use of CE using entangled polymer solutions with HPMC as polymer additive was suitable for routine analysis of low-M_r RNA profiles (high resolution, reproducibility, system automation, high stability of the buffer, low cost of the capillaries). In this respect, the CE using entangled polymer solutions can represent a realistic alternative to the conventional slab gel electrophoresis. This approach can be of particular importance for future studies in molecular microbial ecology and taxonomy.

Acknowledgements

This work was supported by funds of the Commission European Communities HRAMI T-Project (BIOT CT-910294). E. Moore kindly proof read the manuscript.

References

[1] J.L. Johnson and N.J. Palleroni, *Int. J. Systematic Bacteriol.*, 39 (1989) 230.
[2] E.R.B. Moore, R.-M. Wittich, P. Fortnagel and K.N. Timmis, *Lett. Appl. Microbiol.*, 17 (1993) 115.
[3] A.K. East, D.E. Thompson and M.D. Collins, *J. Bacteriol.*, 174 (1992) 8158.
[4] M. Goodfellow and A.G. O'Donnell (Editors), *The New Bacterial Systematics*, Academic Press, London, 1993, p. 251.
[5] J.-R. Meunier and P.A.D. Grimont, *Res. Microbiol.*, 144 (1993) 373.
[6] M.G. Höfle, *Arch. Microbiol.*, 153 (1990) 299.
[7] M.G. Höfle, *J. Microbiol. Methods*, 8 (1988) 235.
[8] M.G. Höfle, *Appl. Environ. Microbiol.*, 58 (1992) 3387.

[9] D.N. Heiger, A.S. Cohen and B.L. Karger, *J. Chromatogr.*, 516 (1990) 33.
[10] A. Paulus, E. Gassmann and M.J. Field, *Electrophoresis*, 11 (1990) 702.
[11] J.A. Luckey and L.M. Smith, *Electrophoresis*, 14 (1993) 492.
[12] P. Boček and A. Chrambach, *Electrophoresis*, 13 (1992) 31.
[13] A. Paulus and D. Hüsken, *Electrophoresis*, 14 (1993) 27.
[14] P.D. Grossman and D.S. Soane, *J. Chromatogr.*, 559 (1991) 257.
[15] M.H. Kleemiss, M. Gilges and G. Schomburg, *Electrophoresis*, 14 (1993) 515.
[16] B.R. McCord, J.M. Jung and E.A. Holleran, *J. Liq. Chromatogr.*, 16 (1993) 1963.
[17] D. Rickwood and B.D. Hames (Editors), *Gel Electrophoesis of Nucleic Acids*, IRL Press, Oxford, 1982, p. 1.
[18] M. Lalande, J. Noolandi, C. Turmel, R. Brousseau, J. Rousseau and G.W. Slater, *Nucl. Acids Res.*, 16 (1988) 5427.
[19] A.E. Barron, D.S. Soane and H.W. Blanch, *J. Chromatogr. A*, 652 (1993) 3.
[20] H.E. Schwartz, K. Ulfelder, F.J. Sunzeri, M.P. Busch and R.G. Brownlee, *J. Chromatogr.*, 559 (1991) 267.
[21] D.A. McGregor and E.S. Yeung, *J. Chromatogr. A*, 652 (1993) 67.
[22] R.P. Singhal and J. Xian, *J. Chromatogr. A*, 652 (1993) 47.
[23] W.A. MacCrehan, H.T. Rasmussen and D.M. Northrop, *J. Liq. Chromatogr.*, 15 (1992) 1063.
[24] S. Nathakarnkitkool, P.J. Oefner, G. Bartsch, M.A. Chin and G.K. Bonn, *Electrophoresis*, 13 (1992) 18.
[25] Y.C. Bae and D. Soane, *J. Chromatogr. A*, 652 (1993) 17.
[26] M. Zhu, D.L. Hansen, S. Burd and F. Gannon, *J. Chromatogr.*, 480 (1989) 311.
[27] A.G. Ogston, *Trans. Faraday Soc.*, 54 (1958) 1754.
[28] P.G. de Gennes, *Scaling Concepts in Polymer Physics*, Cornell Univ. Press, Ithaca, NY, 1979.

ELSEVIER

Journal of Chromatography A, 700 (1995) 137–149

JOURNAL OF CHROMATOGRAPHY A

Sequencing of antisense DNA analogues by capillary gel electrophoresis with laser-induced fluorescence detection

Alexei Belenky, David L. Smisek, Aharon S. Cohen*

Hybridon, Inc., 1 Innovation Drive, Worcester, MA 01605, USA

Abstract

A method using capillary gel electrophoresis with laser-induced fluorescence detection is described which permits complete sequence determination of antisense DNA analogues of unknown sequence. This method, originally created as a tool to confirm the sequence of antisense oligonucleotides being developed as therapeutic drugs, utilizes data collected under a range of experimental conditions described by the Ogston model as applied to gel electrophoresis. A linear relationship independent of experimental conditions between the relative electrophoretic migration time and the oligonucleotide base number was observed and is shown to be consistent with a simplified version of this model and can be used to facilitate the sequence determination.

1. Introduction

Antisense medicine is still in its infancy, but is maturing rapidly. Several human trials have already begun or are about to begin, and sequencing that determines the target-sense as well as the antisense sequence is the key to successful anti-viral treatment. Antisense compounds under investigation are chemically modified DNA such as phosphorothioates or methylphosphonates and are in general between 15 to 50 bases in length. The chemical modification of phosphodiester DNA is normally performed to inhibit enzymatic activity. For example, phosphorothioates are much more resistant to exonucleases than unmodified DNA (phosphodiesters) [1]. The chemical properties of a modified DNA molecule can be quite different from its phosphodiester counterpart. For example, the pK_a due to charge distribution on phosphorothioates is different than the pK_a of phosphodiesters [2]; phosphorothioates are more hydrophobic than phosphodiesters and therefore exhibit more secondary structure behavior [3]. Consequently, optimization and modification of analytical methods used for phosphodiesters need to be made and protocols need to be updated to reflect this different chemistry [4].

DNA sequence determination is an important structural analysis, especially when information is needed to determine an unknown sequence of a short strand of DNA or DNA analogue or to confirm the specific sequence of a certain antisense drug. At present, two methods are used to prepare phosphodiester DNA fragments for sequencing: the chemical degradation approach of Maxam and Gilbert [5] and the chain-termination method of Sanger et al. [6]. Four separate reactions yield fragments differing in length by only a single nucleotide which terminate at adenosine (A), cytosine (C), guanosine (G) or thymidine (T) residues. These products are gen-

* Corresponding author.

0021-9673/95/$09.50
SSDI 0021-9673(94)01092-7

erally resolved by electrophoresis on a denaturing polyacrylamide gel. The method of product visualization has traditionally been autoradiography, usually ^{32}P or ^{35}S incorporated into the DNA strand; however, fluorescent detection of DNA fragments has been recently introduced. Fluorescent tags are attached either to the primer [7] or to each of the terminating dideoxynucleotides [8]. In either case, detection can be achieved using laser-induced fluorescence (LIF). Automated LIF methods bypass the normal post-electrophoresis manipulations. The fluorescently labeled fragments are detected on-line; the data are collected and sent to a computer via an analog-to-digital converter for processing and analysis.

Many different DNA sequencing protocols originating from the chain termination reaction of Sanger et al. [6] have been developed over the years. Recently, sequencing with LIF detection was used in a variety of protocols including single-dye coding of bases with four different peak heights [9–12], single-dye coding of three bases by peak height ratios plus one base coded by a gap [10,12], two-dye-binary coding of three bases with one base coded by a gap [13], two-dye coding by peak height ratios with two optical channels [14], and four-dye coding with two optical channels [15]. Although all of these methods offer different aspects of flexibility, none of them describe the complete sequencing of a short single-stranded DNA (ssDNA) from the very first to the very last base. Moreover, none of these methods were ever applied in practice for routine sequencing, and sequencing of antisense DNA analogues was not considered.

Successful sequencing depends on the separation step. A problem that is sometimes encountered during sequencing is band compression when different fragments possessing similar electrophoretic migration times are not resolved leading to an ambiguous or incorrect sequence. One cause of this phenomenon is the effect of sequence-specific secondary structure. Denaturing conditions can minimize the effects of secondary structure. Under our experimental conditions, band compression does not appear to be a problem for the short fragments under consideration.

One of the fastest growing areas in separation science today is capillary electrophoresis (CE). The method is similar to high-performance liquid chromatography (HPLC) in its instrumentation and operation, but differs in the principle of separation, CE has high resolving power, and low mass detection limits [16]. As active participants in the introduction and development of oligonucleotide separations by CE, we have utilized capillary columns both in the open-tube mode [17] and the gel-filled mode, also known as capillary gel electrophoresis (CGE) [18]. Separations with a very high resolving power of 30 million theoretical plates per meter have been achieved using CGE [19]. Based on these results, CGE potentially can be utilized in routine DNA sequencing [20]. The method is readily coupled to a variety of detection methods including LIF and mass spectrometry (MS). With the rapid development of matrix-assisted laser desorption ionization (MALDI) MS, the combination of CE and MS promises to be an important analytical tool [21,22].

Enzymatic sequencing of short DNA analogue substrates using MALDI-MS for detection has been documented very recently [23,24]. The method uses exonucleases with phosphodiester DNA as a substrate. The protocol is relatively slow; aliquots are taken every 15 min and directly analyzed by MALDI-MS [25]. When DNA analogues are to be sequenced under these conditions, exonuclease digestion is problematic because the analogues have been designed for their insusceptibility to exonucleases [1]. In any case, the development of a method, by which an antisense DNA analogue sequence can be determined from the very first to the very last base will be a major contribution to the sequencing effort. The method which we now describe is such a method and can be automated, validated, and used for routine sequence determination.

2. Experimental

2.1. Chemicals and reagents

Ultra-pure Tris base, urea, acrylamide and EDTA were purchased from Schwartz/Mann Biotech (Cleveland, OH, USA). Ammonium

persulfate and N,N,N′,N′-tetramethylethylenediamine (TEMED) were purchased from Bio-Rad (Richmond, CA, USA). Boric acid was obtained from Sigma (St. Louis, MO, USA). All phosphorothioate oligomers were synthesized in the laboratory, desalted, lyophilized, and reconstituted in sterile water for injection (Lyphomed, a division of Fujisawa USA, Deerfield, IL, USA). The fluorescently tagged primers were obtained from Applied Biosystems (Foster City, CA, USA).

2.2. CE apparatus

The CE apparatus with UV and LIF detection and the preparation of gel-filled capillaries for the separation of DNA molecules have been described previously [20]. A 30 kV, 500 μA direct-current high-voltage power supply (Model ER/DM; Glassman, Whitehouse Station, NJ, USA) was used to generate the potential across the capillary. UV detection of phosphorothioates at 270 nm was accomplished with a Spectra 100 (Spectra-Physics, San Jose, CA, USA). For LIF detection an argon ion laser (Model 543 100BS; Omnichrom, Chino, CA USA) was employed. All CE runs were performed at room temperature. The data were acquired and stored on an AcerPower 486/33 computer (Acer American, San Jose, CA, USA) through an analog-to-digital converter (Model 970; PE Nelson, Cupertino, CA, USA).

2.3. Gel-filled capillaries

Fused-silica capillary tubing (Polymicro Technologies, Phoenix, AZ, USA) with an inner diameter of 75 μm, an outer diameter of 375 μm, an effective length of 10–15 cm, and a total length of 30–60 cm was treated with (methylacryloxypropyl)trimethoxysilane (Petrarch Systems, Bristol, PA, USA) and then filled with a de-gassed solution of polymerizing acrylamide in aqueous media with formamide [1–3 × TBE buffer (1 × TBE buffer = 0.1 *M* Tris–borate, 2 m*M* EDTA), pH 8.3 containing 6–8 *M* urea]. Polymerization was achieved by adding ammonium persulfate solution and TEMED.

2.4. Sequencing method

A method was developed to determine the sequence of a short strand of DNA or DNA analogue. This method consists of 6 steps: (1) synthesis of auxiliary DNA (auxiliary DNA phosphorylated at the 5′ end was purchased from New England Biolabs, Beverly, MA, USA), (2) ligation of the auxiliary DNA to the DNA for which the sequence has to be determined by either "bridge" ligation or "blunt" ligation, (3) primer annealing (the primer is tagged with a fluorescent label), (4) sequencing using Sequenase 2.0 DNA Sequencing Kit (United States Biochemical, Cleveland, OH, USA), (5) separation of the sequencing mixture (by CGE–LIF) and (6) sequence determination.

3. Results and discussion

As mentioned earlier, antisense DNA molecules under investigation are chemically modified analogues which may possess quite different chemical properties compared to their phosphodiester counterparts and are often modified to inhibit enzymatic activity. The outcome of any pre-sequencing enzymatic preparation of these compounds is not apparent. Consequently, several different approaches were investigated.

3.1. "Bridge" ligation using T_4 DNA ligase

In developing our sequencing method, we began by using T_4 DNA ligation as the pre-sequence enzymatic preparation step. If the Sanger approach is used to sequence a short ssDNA, some base sequence information is lost at the 3′ end. This loss of information is primer-size dependent and normally 15–17 bases, i.e., sequence information will only be available right after the primer. Because we want to determine the sequence from the very first base, base 1, to the very last base, we need to protect the first base at the 3′ end by ligating a known sequence of single-stranded oligonucleotide which can hybridize to the primer. This segment of oligonucleotide is defined as the auxiliary DNA. The auxiliary DNA is composed of two identified

sequence regions. One region from the 3′ end consists of 17 bases complementary to the sequence of the primer, in our case the M13mp18(−21) primer, followed by a signaling region of nine T bases (schematically shown in Fig. 1). The function of the signaling region is to denote the beginning of the reading sequence. Base 1 of the oligomer to be sequenced is located right after the auxiliary DNA. A 12-mer bridge DNA is also used in the ligation reaction mixture to support both the antisense and the auxiliary DNA and to facilitate the ligation reaction. This 12-mer bridge consists of two regions of six bases, one complementary to the last six bases of the auxiliary DNA at the 5′ end and the other to the first six bases of the antisense DNA to be sequenced. This imposes a limitation since the first six bases from 3′ end of the antisense oligomer must be known prior to using this procedure. This limitation can be overcome using a different ligation approach as will be described later.

In Fig. 2 the electropherograms before and after ligation are shown, using CGE with UV detection. We observe in Fig. 2a the fast-migrating 12-mer bridge DNA followed by the phosphorothioate DNA analogue (GEM) to be sequenced; the last migrating peak is the 32-mer auxiliary DNA. The mixture is incubated for 30 min. at 37°C after the addition of T_4 DNA ligase and ATP and is then injected into the capillary for analysis by CGE. The ligation product of the GEM 25-mer to be sequenced and the auxiliary DNA, a 32-mer, is a 57-mer which appears as an additional peak shown in Fig. 2b. This 57-mer is then isolated and subjected to chain-termination reactions. As indicated previously, to design the appropriate helper bridge and use this procedure, the sequence of the six bases at the 3′ end of GEM or any ssDNA molecule to be sequenced must be known; however, if the six bases at the 3′ end of the ssDNA analogue to be sequenced are unknown, a bridge DNA cannot be designed and used in the ligation reaction. This disadvantage limits the technique to sequence confirmation instead of a general sequencing method.

Another problem encountered using the bridge ligation approach was an incomplete sequencing reaction. Since the bridge oligonucleotide has a complementary sequence to a site on the ligated product, it can interfere with the enzymatic sequencing reaction. Under the experimental conditions, the bridge oligonucleotide can rehybridize to the complementary site on the DNA to be sequenced right after $(T)_9$ from the 3′ end, and consequently, the sequencing reaction will be stopped before completion. Al-

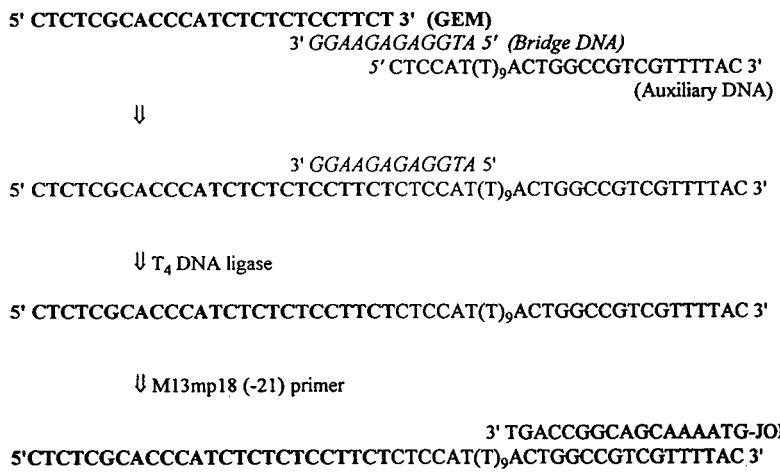

Fig. 1. Schematic representation of the "bridge" ligation protocol.

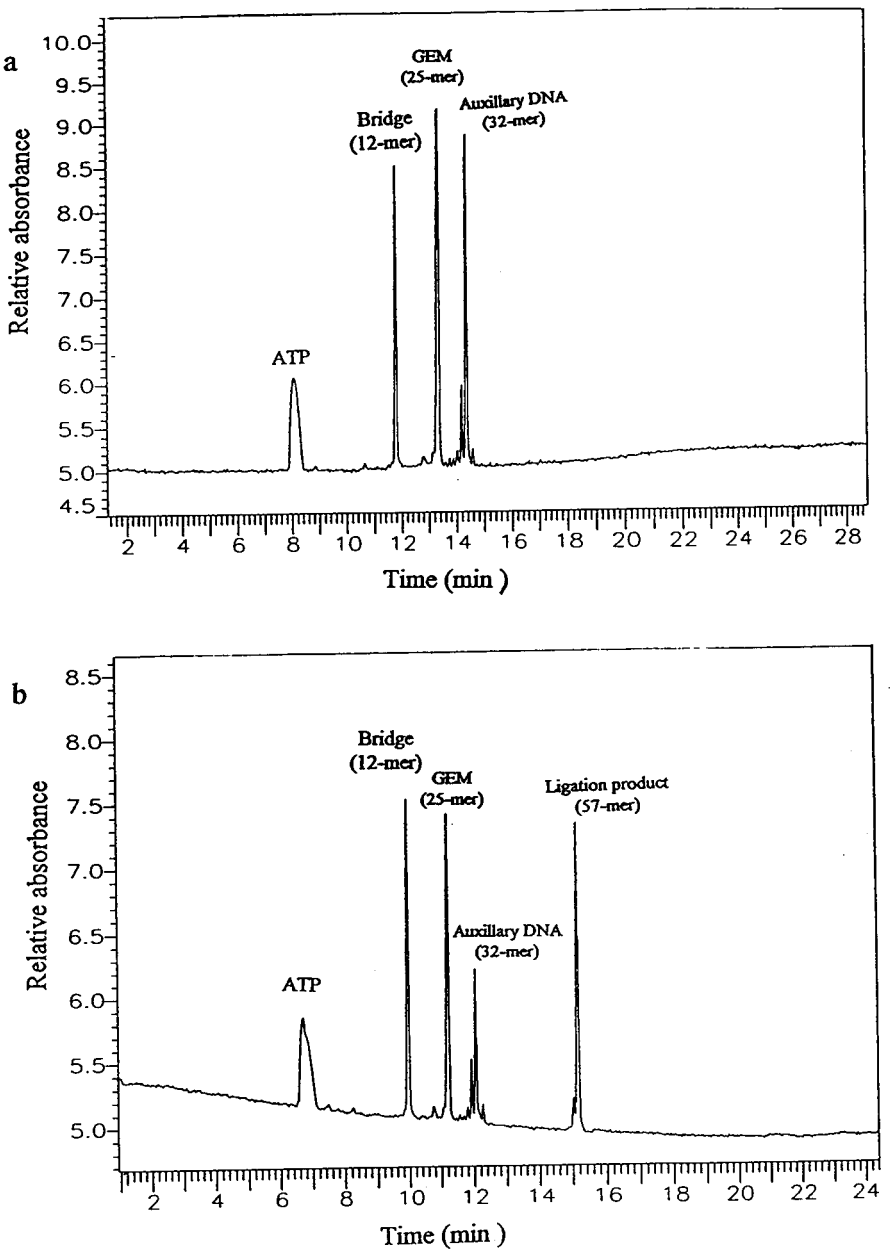

Fig. 2. UV electropherograms of the T_4 DNA ligase reaction mixture. (a) Prior to ligation. Migration order of the detected peaks: ATP, bridge DNA (12-mer), GEM (25-mer) and auxiliary DNA (32-mer). Running buffer was 1 × TBE, and the gel was 9% T polyacrylamide, 7 *M* urea. The applied electric field was 300 V/cm. (For more details, see Experimental section). (b) After the addition of T_4 DNA ligase. The slowest migrating peak is the ligation product (57-mer).

though this interference can be prevented by slab gel purification to remove the bridge DNA, the procedure is cumbersome. We have, therefore, utilized T_4 RNA ligase enzyme, which under the appropriate conditions can ligate any two unknown sequences of ssDNA [26]. Because a bridge DNA is not needed for ligation, this "blunt" ligation procedure overcomes the limitations of the bridge ligation approach.

3.2. "Blunt" ligation using T_4 RNA ligase

Experimental results in Fig. 3a show the products of the T_4 RNA ligase reaction. Because the 3′ end on the auxiliary DNA is unprotected, the enzyme forces the ligation process to proceed in cycles, and several cycles are observed. This undesirable phenomenon, which complicates the ligation procedure, can be prevented simply by having a dideoxy group or an amino group at the 3′ end of the auxiliary DNA. Results of the ligation reaction with the auxiliary DNA protected by an amino group at the 3′ end are shown in Fig. 3b. These results demonstrate that only one ligation cycle was obtained when the 3′ end of the auxiliary DNA was protected, and as with the T_4 DNA ligase procedure, ATP, GEM 25-mer, the 32-mer auxiliary DNA, and the 57-mer ligation product can be observed.

3.3. Antisense DNA analogue sequence determination

Our goal in pursuing this research was to develop an automated ssDNA sequencer for routine antisense analysis. With this in mind, we next turned to develop a working strategy to examine enzymatic sequencing of antisense DNA analogues using the T_4 RNA ligase procedure described in the previous section. Good modeling of the electrophoretic migration of the sequencing fragments is essential for automated data processing; therefore, we focused our attention on developing a better understanding of the migration behavior of the sequencing fragments under our experimental conditions.

We and others [27] have observed experimentally that over a narrow range of molecular size, a linear relationship between time and base number can be established. This relationship, which we have used to simplify the sequencing step, will be shown to be consistent with a simplified version of the Ogston model. We begin by noting that the range of experimental conditions we have selected are such that the electrophoretic mobility of the probe molecule falls within the so-called Ogston regime (see [28]). In other words, the probe molecules are small compared to the matrix mesh size and are unentangled by the polymer matrix [29]. By invoking the Ogston model, we can develop a simplified expression relating the number of bases to the migration time. We define a migration time t_n that is relative to the migration time of two internal standards, A and B. Thus,

$$t_n = \frac{t - t_B}{t_A - t_B} \tag{1}$$

where t is the migration time of the probe molecule and t_A and t_B are the migration times of standards A and B, respectively. Standards A and B are oligonucleotides of the same chemical nature as the probe molecule and possess base numbers, N_A and N_B, respectively, that bracket the probe's base number N ($N_A > N > N_B$). The selection of internal standards is facilitated by our sequencing method; one standard is the primer (N_{17}) and the other is an extra fragment created by Sequenase 2.0 terminal transferase activity after the end of the sequence (e.g., N_{58}).

Starting with the Ogston model, we can relate this relative time to the probe's base number. Ogston derived the distribution of spaces in a random network of fibers available to a spherical object [30]. This distribution was related to the electrophoretic mobility by Rodbard and Chrambach [31] and can be written in the following simplified form [32]:

$$\mu = \mu_0 \exp(-\alpha\lambda CN) \tag{2}$$

where μ is the electrophoretic mobility, μ_0 is the electrophoretic mobility in free solution, α and λ are constants, C is the matrix concentration and N is the base number. This simplified form assumes that the probe chain's radius of gyration

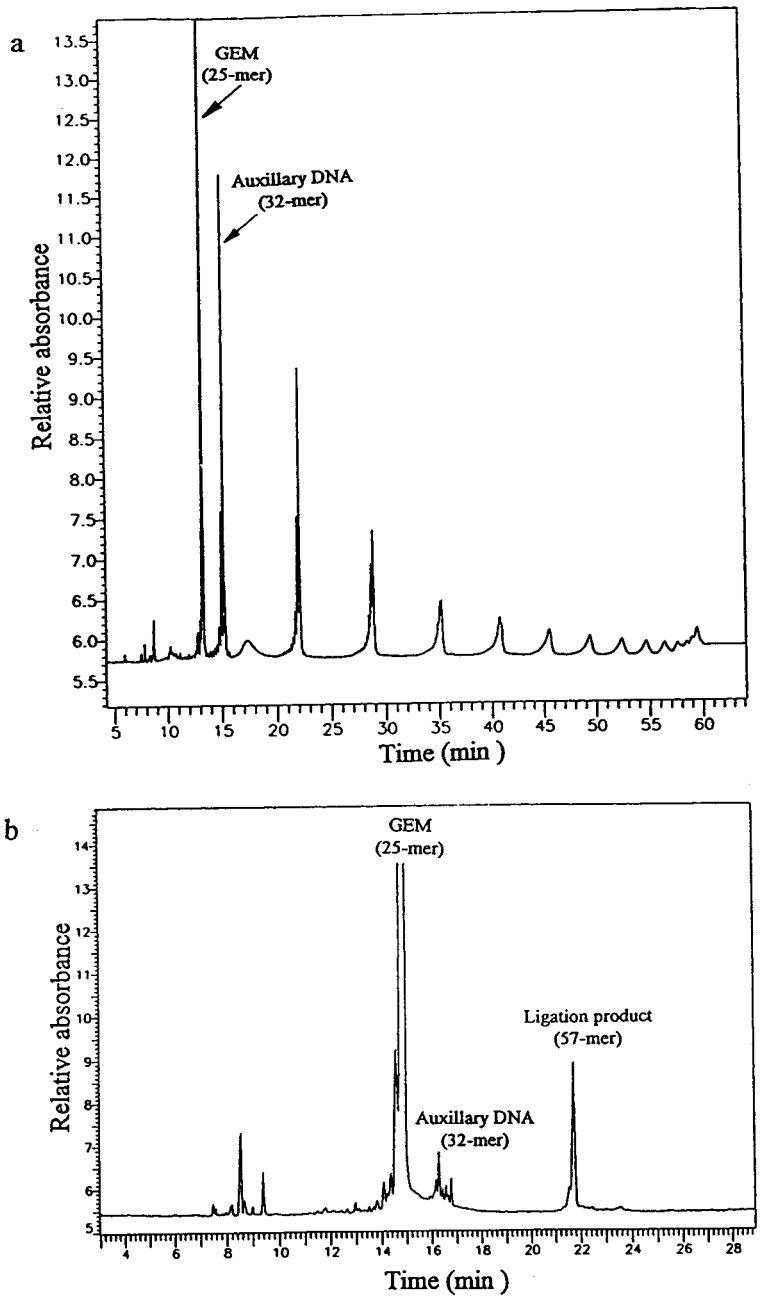

Fig. 3. UV electropherograms of T_4 RNA ligation products. (a) Several extended ligation cycles are observed. Auxiliary DNA (32-mer) with 5′ phosphate and 3′-OH was used. All other conditions as in Fig. 2. (b) Auxiliary DNA (32-mer) with 5′ phosphate and 3′ amino protection was used. No extended ligation cycles are observed.

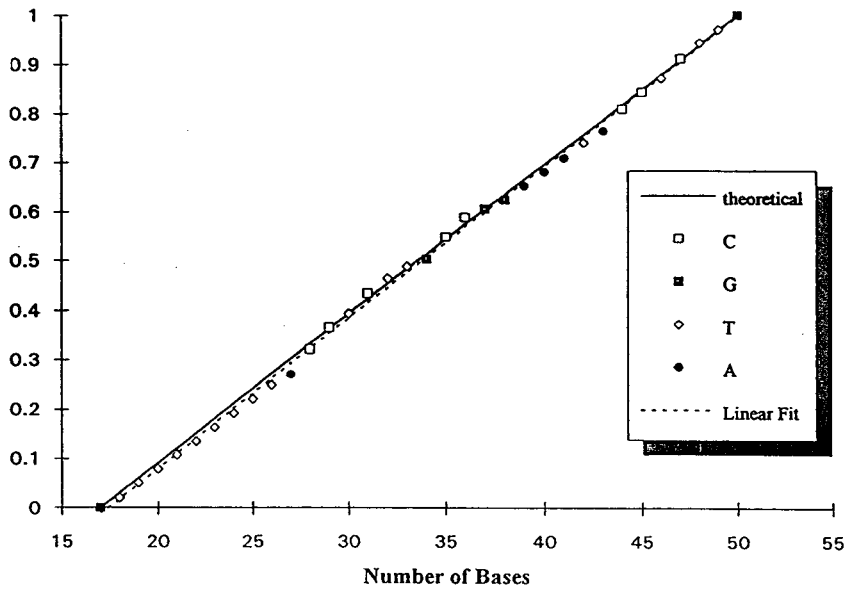

Fig. 4. Relative time (y-axis) plotted as a function of base number. Oligonucleotide standards: $N_A = 50$; $N_B = 17$. Capillary gel electrophoresis: 11% T linear polyacrylamide; 6.5 M urea, 45% formamide, 2 × TBE buffer; 400 V/cm for each sequencing reaction. Dotted line represents a linear fit with $R^2 = 0.9988$. Solid line represents the right-hand side of Eq. 6.

is much larger than the polymer matrix strand radius and that the probe chain's persistence length is small compared to its contour length (i.e., the chain should be highly flexible). For ssDNA under denaturing conditions in a polyacrylamide matrix, these assumptions appear reasonable.

From the definition of electrophoretic mobility, we can write

$$\mu = \frac{\nu}{E} = \frac{x}{tE} \tag{3}$$

where ν is the average velocity, E is the externally applied electric field strength and x is the distance traveled in time t. Using Eq. 2 and solving for t, we obtain

$$t = \left(\frac{x}{E\mu_0}\right) \cdot \exp\,(\alpha\lambda CN) \tag{4}$$

Substituting Eq. 4 into Eq. 1 and rearranging, we obtain

$$t_n = \frac{\exp\,[\alpha\lambda C(N - N_B)] - 1}{\exp\,[\alpha\lambda C(N_A - N_B)] - 1} \tag{5}$$

Using a Taylor series expansion and neglecting higher order terms, we can linearize the expression to

$$t_n = \frac{t - t_B}{t_A - t_B} = \frac{N - N_B}{N_A - N_B} \tag{6}$$

If we plot data obtained by CGE–LIF, we indeed observe this linear relationship as is illustrated in Fig. 4. A linear fit of this data closely matches the theoretical value (the right-hand side of Eq. 6) as shown in the figure. Although the data used in the figure are taken from different runs performed under identical conditions, we note that the relationship between N and t is independent of experimental parameters such as matrix concentration and electric field strength. We should be able, therefore, to use the results from several different runs under very different conditions to obtain the relative times. We have observed this independence for different electric field strengths from 200 to 400 V/cm as well as different gel concentrations ranging from 6 to 14% T[1] linear polyacrylamide and effective lengths from 6 to 15

[1] T = (g acrylamide + g N,N'-methylenebisacrylamide)/100 ml solution

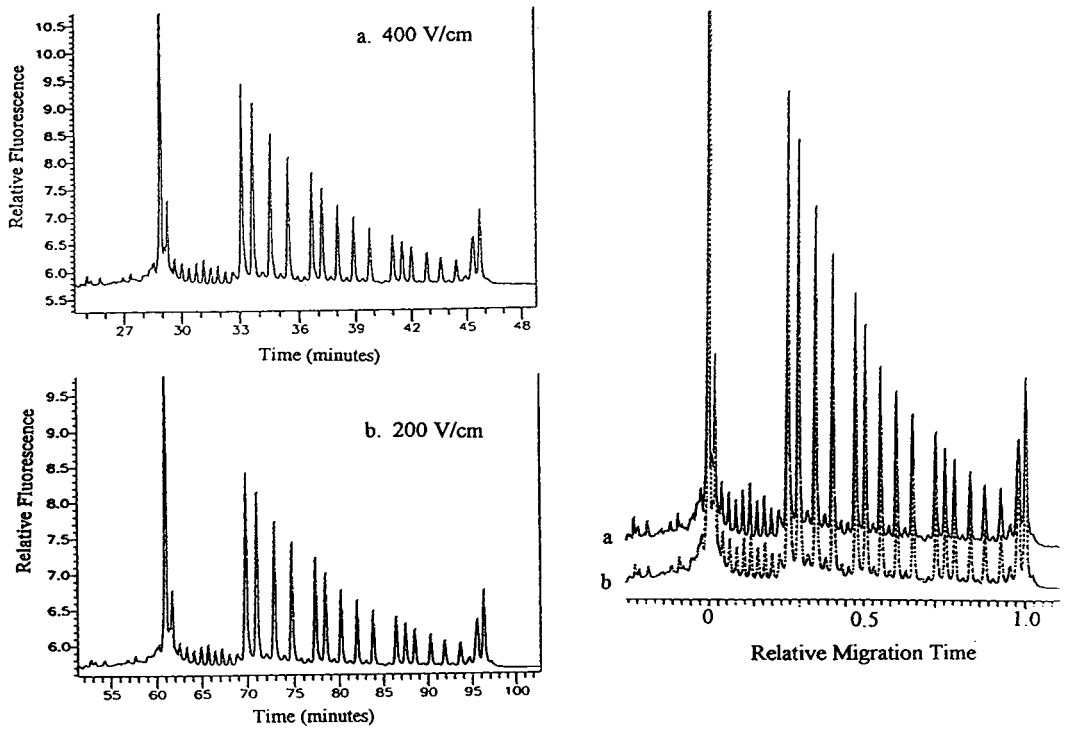

Fig. 5. Effect of electric field strength on the analysis of the ddG terminated sequencing reaction. (a) 400 V/cm, (b) 200 V/cm. Conditions: 13% T polyacrylamide, 2 × TBE buffer, 6 *M* urea, 40% formamide, effective length 12 cm.

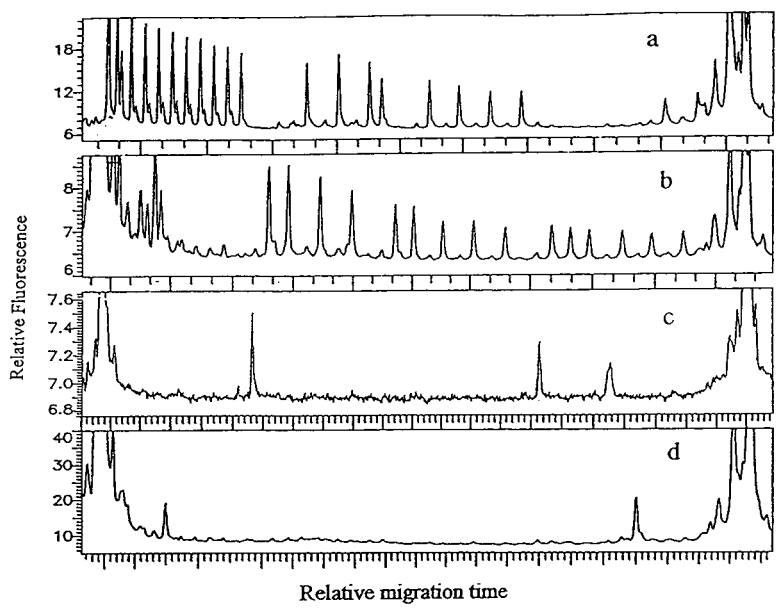

Fig. 6. LIF electropherogram of sequencing fragments from T_4 DNA ligation product (57-mer) (see Experimental section for details). Running buffer is 2 × TBE and the gel contained 14% T polyacrylamide, 7 *M* urea, 54% formamide. (a) ddA, (b) ddG, (c) ddT, (d) ddC terminated sequencing reaction. All other conditions as in Fig. 2.

cm. For example, the effect of electric field strength is shown in Fig. 5. Although the actual migration times differ by about a factor of two, when the relative migration times are used, the two runs can be readily superimposed.

By performing CGE–LIF on separate sequencing reactions for each base using the same fluorescent label to avoid potential band compression, we are able with the aid of a simple computer program to deduce the correct sequence for short oligomers using the relative time. Care should be taken in using Eq. 6 because it is related to the Ogston model only in a very limited context. Although the Ogston model may have limited applicability in a strict sense to flexible macromolecules [33], it is nevertheless a useful starting point, and we have found that the linear relationship of Eq. 6 is sufficient for the purpose of sequencing short oligomers.

Eq. 6 gives us a useful expression for t_n which is only fragment-size dependent. This expression is, of course, a conditional statement since it holds only under Ogston limitations. The best way to validate this relationship is to test this new model under experimental conditions. The ligated product (a 57-mer) was subjected to enzymatic chain termination reaction for four different bases independently (i.e., A, G, C and T). Each of the four bases ran separately as

Table 1
Relative migration time obtained from the data of Fig. 6

Fragment length (number of bases)		Relative migration time, $t_n = (t - t_B)/(t_A - t_B)$; base				Reading sequence
		A	T	C	G	
Real	GEM					
						3′
33	1		0.370			T
34	2			0.391		C
35	3		0.421			T
36	4		0.441			T
37	5			0.460		C
38	6			0.485		C
39	7		0.512			T
40	8			0.537		C
41	9		0.570			T
42	10			0.586		C
43	11		0.620			T
44	12			0.636		C
45	13		0.671			T
46	14	0.680				A
47	15			0.707		C
48	16			0.735		C
49	17			0.763		C
50	18	0.786				A
51	19			0.812		C
52	20				0.828	G
53	21			0.856		C
54	22		0.896			T
55	23			0.904		C
56	24		0.948			T
57	25			0.953		C
						5′

t = Migration time of sequencing fragment; t_B = migration time of primer; t_A = migration time of the last peak.

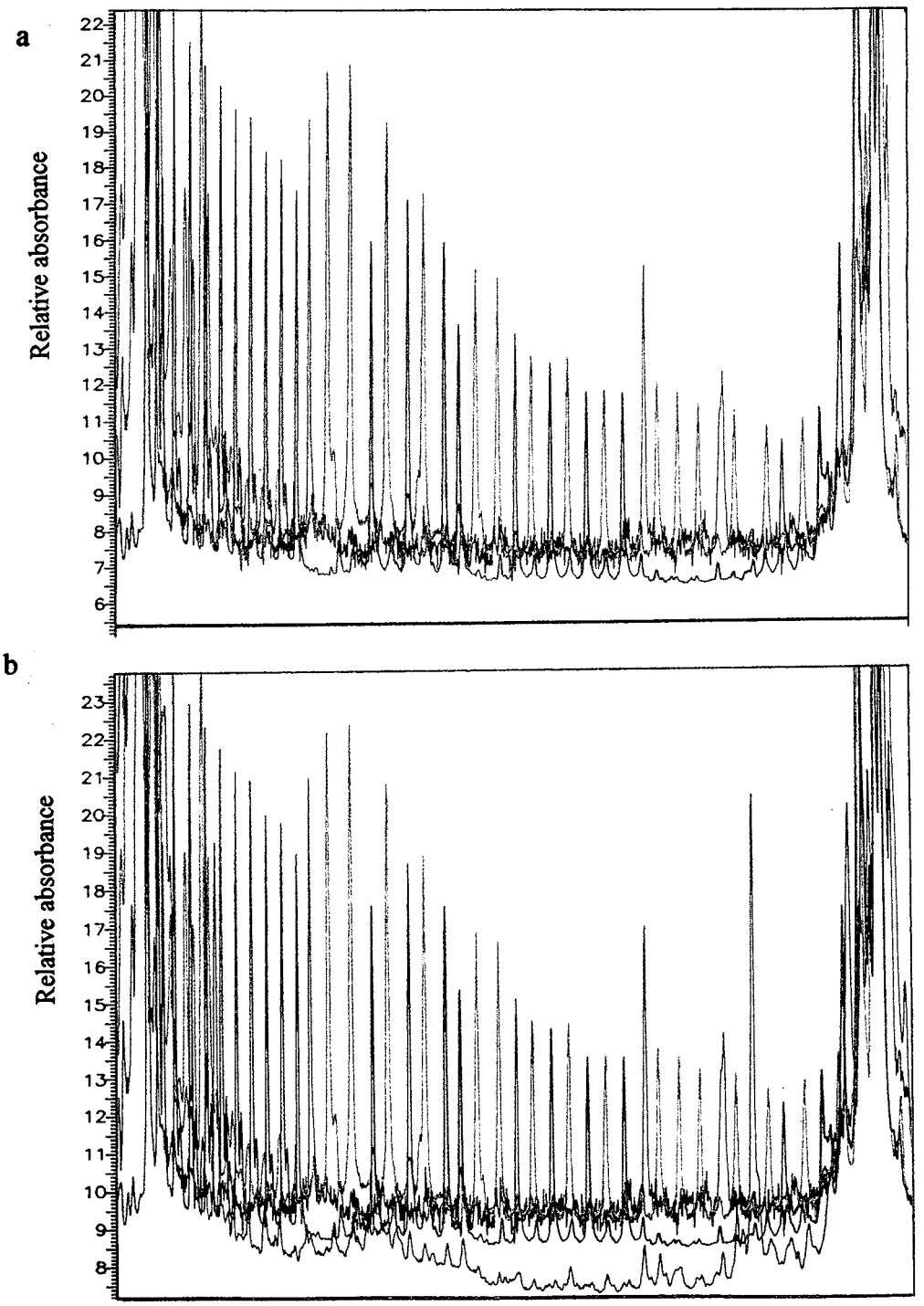

Fig. 7. Computer overlay of LIF electropherograms. (a) a, b and c electropherograms from Fig. 6 using two point re-size alignment (see text for details). Red = A bases; blue = C bases; purple = T bases. (b) a, b, c and d electropherograms from Fig. 6. Red = A bases; blue = C bases; purple = T bases; magenta = G bases. All other conditions as in Fig. 6.

illustrated in Fig. 6. The absolute migration times of the primer (N_{17}) for the A, G, T and C reactions were disperse but have been aligned in this figure as were the times for the latest migrating fragment N_{58}. The term t_n in Eq. 6 was calculated individually for each of the detected fragments between 17 and 58 bases in length. The obtained values of t_n were then rearranged in order from low to high according to the occurrence in the four different runs for the four individual bases shown in Fig. 6. The results are summarized in Table 1. Fragment 33 corresponds to fragment 1 on the GEM molecule. As indicated in this table, the sequence of GEM is determined in the right-most column from the 3′ to 5′ end. A linear relationship ($R^2 = 0.999$) is observed between the relative migration time and the base number of GEM (25-mer) for this data. Computer software capable of facilitating the sequence determining step and performing data processing was designed in the laboratory. The output of this software is in a format where the determined sequence is displayed. The software is interfaced with commercial software, Turbochrom III by PE Nelson (Cupertino, CA, USA) which can manipulate the obtained data and plot the final electropherogram of the sequencing as shown in Fig. 7.

4. Conclusions

Sequencing of antisense ssDNA analogues (phosphorothioates) using CGE interfaced with LIF is presented for the first time. As expected and published by us [4] and others [28,34], several times in the past, DNA fragments up to 100 bases in length or even longer can obey the Ogston model. Within the limitations of this model, a mathematical expression is derived and successfully used for computer-assisted antisense DNA analogue sequence determination. The strength of this expression is that t_n as defined in Eq. 6 for the relative migration of sequencing fragments is related only to the fragment length N as expressed in terms of base number. Moreover, this expression to a large extent is independent of the experimental conditions given that all sequencing fragments are separated. This latter issue was never a problem, since CGE can separate sequencing fragments with very high efficiency and resolution, as has been previously demonstrated by several laboratories [12,17,35,36]. The fact that column variance can be eliminated allows the use of high-concentration linear polyacrylamide (over 9%) and cross-linked gel columns with a fixed matrix and very high resolving power for short sequencing fragments. Under our experimental conditions we have not observed band compression for these short fragments. Finally, the sequencing method that was presented is a single-dye LIF detection approach. It is not, by any means, meant to limit the scope of application since any method described in the introduction can also be applied.

Acknowledgements

We thank Ms. Mischelle Marcel for processing the manuscript and for expert secretarial assistance.

References

[1] M. Matsukura, K. Shinozuka, G. Zon, H. Mitsuya, M. Reitz, J.S. Cohen and S. Broder, *Proc. Natl. Acad. Sci. U.S.A.*, 84 (1987) 7706–7710.
[2] P.A. Frey and R.D. Sammons, *Science*, 228 (1985) 541–545.
[3] A.J. Bourque and A.S. Cohen, *J. Chromatogr.*, 617 (1993) 43–49.
[4] A.S. Cohen, M. Vilenchik, J.L. Dudley, M.W. Gemborys and A.J. Bourque, *J. Chromatogr.*, 638 (1993) 293–301.
[5] A.M. Maxam and W. Gilbert, *Proc. Natl. Acad. Sci. U.S.A.*, 74 (1977) 560–564.
[6] F. Sanger, S. Nicklen and A.R. Coulson, *Proc. Natl. Acad. Sci. U.S.A.*, 74 (1977) 5463–5467.
[7] L.M. Smith, J.Z. Sanders, R.J. Kaiser, P. Hughes, C. Dodd, C.R. Connell, C. Heiner, S.B.H. Kent and L.E. Hood, *Nature*, 321 (1986) 674–679.
[8] J.M. Prober, G.L. Trainor, R.J. Dam, F.W. Hobbs, C.W. Robertson, R.J. Zagursky, A.J. Cocuzza, M.A. Jensen and K. Baumeister, *Science*, 238 (1987) 336–341.
[9] S. Tabor and C.C. Richardson, *J. Biol. Chem.*, 265 (1990) 8322–8328.

[10] W. Ansorge, J. Zimmermann, C. Schwager, J. Stegemann, H. Erfle and H. Voss, *Nucl. Acids Res.*, 18 (1990) 3419–3420.
[11] H. Swerdlow, J.Z. Zhang, D.Y. Chen, H.R. Harke, R. Grey, S. Wu, N.J. Dovichi and C. Fuller, *Anal. Chem.*, 63 (1991) 2835–2841.
[12] S.L. Pentoney, Jr., K.D. Konrad and W. Kaye, *Electrophoresis*, 13 (1992) 467–474.
[13] X.C. Huang, M.A. Quesada and R.A. Mathies, *Anal. Chem.*, 64 (1992) 2149–2154.
[14] D.Y. Chen, H.R. Harke and N.J. Dovichi, *Nucl. Acids Res.*, 20 (1992) 4873–4880.
[15] S. Carson, A.S. Cohen, A. Belenkii, M.C. Ruiz-Martinez, J. Berka and B.L. Karger, *Anal. Chem.*, 65 (1993) 3219–3226.
[16] Y.-F. Cheng and N.J. Dovichi, *Science*, 242 (1988) 562–564.
[17] A.S. Cohen, D. Najarian, J.A. Smith and B.L. Karger, *J. Chromatogr.*, 458 (1988) 323–333.
[18] A.S. Cohen, D. Najarian, A. Paulus, A. Guttman, J.A. Smith and B.L. Karger, *Proc. Natl. Acad. Sci. U.S.A.*, 85 (1988) 9660–9663.
[19] A. Guttman, A.S. Cohen, D.N. Heiger and B.L. Karger, *Anal. Chem.*, 62 (1990) 137–141.
[20] A.S. Cohen, D.R. Najarian and B.L. Karger, *J. Chromatogr.*, 516 (1990) 49–60.
[21] E.D. Lee, W. Muck, J.D. Henion and T.R. Covey, *J. Chromatogr.*, 458 (1988) 313–321.
[22] E. Nordhoff, A. Ingendoh, R. Cramer, A. Overberg, B. Stahl, M. Karas, F. Hillenkamp and P.F. Crain, *Rapid Commun. Mass Spectrom.*, 6 (1992) 771–776.
[23] K.J. Wu, A. Steding and C.H. Becker, *Rapid Commun. Mass Spectrom.*, 7 (1993) 142–146.
[24] T. Keough, T.R. Baker, R.L.M. Dobson, M.P. Lacey, T.A. Riley, J.A. Hasselfield and P.E. Hesselberth, *Rapid Commun. Mass Spectrom.*, 7 (1993) 195–200.
[25] U. Pieles, W. Zurcher, M. Schar and H.E. Moser, *Nucl. Acids Res.*, 21 (1993) 3191–3196.
[26] D.C. Tessier, R. Brousseau and T. Vernet, *Anal. Biochem.*, 158 (1986) 171–178.
[27] H.R. Harke, S. Bay, J.Z. Zhang, M.J. Rocheleau and N.J. Dovichi, *J. Chromatogr.*, 608 (1992) 143–150.
[28] G.W. Slater, J. Rousseau, J. Noolandi, C. Turmel and M. Lalande, *Biopolymers*, 27 (1988) 509–524.
[29] D.L. Smisek and D.A. Hoagland, *Science*, 248 (1990) 1221–1223.
[30] A.G. Ogston, *Trans. Farady Soc.*, 54 (1958) 1754–1757.
[31] D. Rodbard and A. Chrambach, *Proc. Natl. Acad. Sci. U.S.A.*, 65 (1970) 970–977.
[32] J.A. Luckey and L.M. Smith, *Electrophoresis*, 14 (1993) 492–501.
[33] E. Arvanitidou, D. Hoagland and D. Smisek, *Biopolymers*, 31 (1991) 435–447.
[34] P.D. Grossmann, S. Menchen and D. Hershey, *Gene Anal. Tech. Appl.*, 9 (1992) 9–16.
[35] H. Swerdlow and R. Gesteland, *Nucl. Acids Res.*, 18 (1990) 1415–1419.
[36] A.S. Cohen, D.L. Smisek and P. Keohavong, *Trends Anal. Chem.*, 12 (1993) 195–202.

ELSEVIER

Journal of Chromatography A, 700 (1995) 151–162

JOURNAL OF CHROMATOGRAPHY A

Analysis of internucleosomal DNA fragmentation in apoptotic thymocytes by dynamic sieving capillary electrophoresis

Mark D. Evans*[,a], James T. Wolfe[b], David Perrett[c], Joseph Lunec[a], Karl E. Herbert[a]

[a]*Division of Chemical Pathology, Centre for Mechanisms of Human Toxicity, University of Leicester, Lancaster Road, Leicester, LE1 9HN, UK*

[b]*MRC Toxicology Unit, Centre for Mechanisms of Human Toxicity, University of Leicester, Lancaster Road, Leicester, LE1 9HN, UK*

[c]*Department of Medicine, The Medical College of St. Bartholomew's Hospital, West Smithfield, London, EC1A 7BE, UK*

Abstract

The analysis, by slab gel electrophoresis, of internucleosomal DNA cleavage or laddering, characteristic of apoptosis in many cell systems, is labour intensive, difficult to automate and at best only semi-quantitative. In this report we show that CE, using dilute solutions of hydroxyethylcellulose as a replaceable sieving matrix, can be applied to the relatively rapid analysis of DNA laddering in whole digests of apoptotic rat thymocytes. Also, using the sensitivity of laser-induced fluorescence detection and the highly sensitive nucleic acid stain YO-PRO-1, the CE method reported here can use 1000–2000 fold fewer cells than needed for traditional slab gel methods.

1. Introduction

Traditionally, DNA fragments are analysed by slab gel electrophoresis using rigid, cross-linked polymers formed from agarose or polyacrylamide which serve the functions of sieving matrices to separate fragments by size and as anti-convective media to minimise the effects of Joule heating. The dissipation of Joule heat is achieved efficiently in CE by the use of very fine bore capillaries with a large surface area-to-volume ratio. Consequently, separations by CE can run at much higher field strengths allowing significantly shorter analysis times. CE has further advantages over traditional slab gel methods: automation of analysis; on-line detection; direct quantitative features, such as the ability to integrate peak areas, no staining or scanning densitometry; high mass sensitivity; analysis of minute amounts of material; and superior resolving capabilities. In contrast, slab gel electrophoresis is generally slow, labour-intensive, can suffer from poor reproducibility, uses large amounts of DNA, has limited quantitative capability and automation has proved difficult.

Although rigid cross-linked polymers, predominantly polyacrylamide, have been used in the CE format they suffer disadvantages such as problematic capillary packing procedures, expensive pre-packed capillaries, the use of chemically modified capillaries and a high probability of irreversible degradation of capillary performance. An alternative uses dilute entangled polymer solutions such as hydroxylated cellulose

* Corresponding author.

0021-9673/95/$09.50
SSDI 0021-9673(94)01263-6

derivatives [1–3] as a sieving matrix, which can be replaced between runs. Sometimes termed dynamic sieving CE, this is a relatively new technique that has primarily been applied to the analysis of polymerase chain reaction products and restriction enzyme digests [4–6].

Apoptosis and necrosis are well recognised modes of cell death in eukaryotic cells. Whereas necrosis is a response to gross cytotoxic insult, apoptosis is a more ordered, metabolically controlled cellular demise which enables the elimination of cells without the release of intracellular components and pathological consequences such as excessive inflammation [7,8]. The primary morphological and biochemical features of apoptosis are chromatin condensation, plasma membrane blebbing, loss of cell volume and DNA fragmentation. Nuclear and cytoplasmic condensation are followed by nuclear fragmentation and the appearance of apoptotic bodies, arising from cell surface blebs, containing nuclear remnants and intact organelles [7,8]. Cells which are apoptotic can therefore be quantitated by identifying their overt morphology by light microscopy. It has also been shown that apoptotic cells can be distinguished by their increased fluorescent dye uptake, which can then be detected and quantified by flow cytometry [9–11]; these cells have been shown to be apoptotic by several criteria.

Endonuclease-mediated cleavage of DNA in the linker regions between nucleosomes during the later phases of apoptosis can result in an internucleosomal or 'ladder' fragmentation pattern following gel electrophoresis. Each 'rung' of the ladder represents a multiple of the basic nucleosome unit which contains 160–240 base pairs (bp), depending on the organism. The DNA ladder is regarded as a biochemical marker of apoptosis in many systems. Several approaches have been used to measure DNA fragmentation in apoptosis ranging from crude measures of the molecular size of DNA in cell populations or individual cells, to the specific study of internucleosomal cleavage in agarose gels using electrophoresis. One commonly used measure of DNA fragmentation involves the centrifugation of a cell lysate and the determination of DNA in the pellet (high-molecular-mass) and the supernatant (fragmented); their ratio being used as an index of fragmentation [12–14]. DNA strand breakage in individual apoptotic cells has been analysed by in situ nick translation, involving the incorporation of a nucleotide analogue by DNA polymerase I followed by detection of the analogue with a fluorescently labelled antibody [15,16]. Labelled cells are examined by microscopy or flow cytometry to quantitate apoptosis. Internucleosomal cleavage is most specifically identified by slab gel electrophoresis of DNA in whole cell digests or DNA extracted from cells. Semi-quantitative assessment of 'laddering' in ethidium bromide stained gels is achieved by scanning densitometry or visual assignment of relative band intensity [17–19].

In this report the development of dynamic sieving CE for the analysis of the characteristic internucleosomal DNA fragmentation pattern observed in immature rat thymocytes is presented. This CE application combines several advantageous characteristics of existing CE methodology and slab gel sample preparation for determination of internucleosomal DNA cleavage. These are, a replaceable sieving matrix at low pH in uncoated silica capillaries and the direct analysis of whole cell digests. In addition, the use of a sensitive fluorescent nucleic acid dye, YO-PRO-1, greatly increases the sensitivity of detection of DNA 'laddering' compared to that achieved by conventional slab gel electrophoresis.

2. Experimental

2.1. Chemicals

Two standard DNA digests were used during method development, *Hae*III digest of ΦX174 DNA (Sigma, Poole, UK), which contains eleven double stranded DNA (dsDNA) fragments in the range 72–1353 bp, and a 123 bp ladder containing dsDNA fragments from 123–4182 bp (Gibco, Paisley, UK). Digests were diluted to 4.9 μg/ml for *Hae*III digest and 0.75

μg/ml for the 123 bp ladder with distilled, deionised water and stored at −20°C in aliquots. Hydroxyethylcellulose (Aldrich, Poole, UK) was used as the sieving matrix. For DNA fragment detection, YO-PRO-1 diiodide {1-(4-[3-methyl-2,3,-dihydro-(benzo-1,2-oxazole)-2-methylidene]-quinolinium)-3-trimethylammonium propane diiodide} (Molecular Probes, Eugene, OR, USA) was used, this was supplied as a 1 m*M* solution in DMSO and further diluted with DMSO to a 50 μ*M* working stock and stored at 4°C. Proteinase K (from *Tritirachium album*) and ribonuclease A (RNase A, E.C. 3.1.27.5, Type IV from bovine pancreas) obtained from Sigma were used for thymocyte digestion. Prior to use the RNase working stock (400 Kunitz units/ml in 50 m*M* Tris, 0.5 m*M* EDTA, pH 8.0) was pre-treated to eliminate DNase activity. The pH of the RNase solution was first lowered to ca. 5.0 then heated in boiling water for 15 min, the solution was then cooled to room temperature and the pH re-adjusted to ca. 8.0. The pH adjustments were made with the minimum volume of 6 *M* hydrochloric acid or 6 *M* sodium hydroxide as necessary, to avoid excessive dilution. Foetal calf serum and RPMI-1640 used in thymocyte culture were from Gibco. All other chemicals were of reagent grade and purchased from Sigma.

2.2. Equipment

Capillary electrophoresis using laser-induced fluorescence (LIF) detection was performed with a P/ACE 2050 system and a laser module 488 housing a 3 mW 488 nm (air-cooled) argon ion laser (Beckman Instruments, High Wycombe, UK).

2.3. Thymocyte isolation and treatment

Thymocytes were isolated from male Fischer 344 rats (4–5 weeks old) as described previously [20]. The resulting cell suspension was diluted in RPMI-1640 containing 10% v/v foetal calf serum and 2 m*M* L-glutamine to give a cell suspension of $15–20 \cdot 10^6$ cells/ml. Incubations were carried out for 4 h at 37°C under an atmosphere of 95% air–5% CO_2, in the presence of 0.1 μ*M* dexamethasone or 10 μ*M* etoposide (VP-16), conditions known to induce differing levels of apoptosis in rat thymocytes [9,11].

2.4. Agarose slab gel electrophoresis

Agarose gel electrophoresis to detect DNA laddering was performed essentially as described by Sorenson et al. [17].

2.5. Thymocyte digestion for CE analysis

Post exposure, thymocytes were harvested by pelleting at 200 *g* for 5 min, washed once with filter sterilised (0.22 μm Acrodisc filter unit; Gelman Sciences, Ann Arbor, MI, USA) phosphate buffered saline (PBS) and re-pelleted. The pellet was resuspended to give an appropriate cell concentration, usually $1 \cdot 10^6$/ml. The required volume of cell suspension was removed to a 500 μl Eppendorf tube and the cells pelleted at 1500 *g* for 5 min. The supernatant was removed and the thymocytes resuspended in 40 μl of digestion buffer. The digestion buffer contained 50 m*M* Tris, 0.5 m*M* EDTA, pH 8.0 (TE buffer; pH adjusted with 1 *M* hydrochloric acid) was filter-sterilised and stored at room temperature in aliquots. Immediately before use, Triton X-100 was added to the digestion buffer to a final concentration of 1% v/v. At this concentration Triton X-100 permeabilised 100% of the cells as determined by Trypan Blue inclusion. In addition to digestion buffer 5 μl of proteinase K (32 units/ml in TE buffer, pH 8.0) and 5 μl of DNase-free RNase A (400 Kunitz units/ml in TE buffer, pH 8.0) were added. The thymocyte digests were incubated for 2 h at 37°C and were either analysed immediately or stored at 4°C for up to 24 h prior to analysis, with no difference in resultant electropherograms.

2.6. Capillary electrophoresis

Hydroxyethylcellulose (HEC) was used as the sieving matrix at a final concentration of 0.5% w/v in carrier electrolyte (50 m*M* potassium dihydrogen phosphate, 0.5 m*M* EDTA, pH 5.0);

HEC was solubilised by mild heating with constant stirring. The HEC solution was filtered through a 0.45-μm filter before use and stored at 4°C for up to two weeks. Immediately before use YO-PRO-1 was added to the HEC solution to give a final concentration of 400 n*M*; HEC containing YO-PRO-1 was prepared daily.

An uncoated fused-silica capillary 57 cm × 75 μm (50 cm to detector) was used. Prior to each sample injection the capillary was flushed for 5 min at 276 kPa with the 0.5% HEC. When the resolution of standard digest peaks was diminished and/or unacceptable baseline noise apparent, the capillary was flushed at high pressure (276 kPa) with ultrapure water (5 min), 1 *M* sodium hydroxide (30 min at 50°C), ultrapure water (10 min) and 0.5% HEC (5 min). Standard restriction enzyme digests and cell digests were loaded on to the capillary hydrodynamically at 3.5 kPa for 90 s. Before injection, each sample was degassed very briefly (1 s) in a sonicator bath to minimise artifactual 'spike' formation in the electropherogram. Separations were performed at −175 V/cm and at 25°C.

3. Results

3.1. Analysis of internucleosomal DNA fragmentation in apoptotic thymocytes

A complete electropherogram for a digest of $1 \cdot 10^5$ thymocytes treated with 10 μM VP-16 is shown in Fig. 1. There are two regions to note: between 16 and 24 min the ladder fragmentation pattern was visible with the smallest fragment migrating at the start of this region; between 24 min and the end of the analysis, large DNA fragments migrated as a substantial unresolved peak. Confirmation of the base pair size of the various peaks was achieved by co-injection of thymocyte digest with *Hae*III digest of ΦX174 DNA (Fig. 2). The results indicate that the broad ladder fragmentation peaks correspond to a distribution of DNA fragments around multiples of 180–200 bp, that is nucleosomal in size. The large DNA fragments are expected to partly consist of higher multiples of nucleosomal frag-

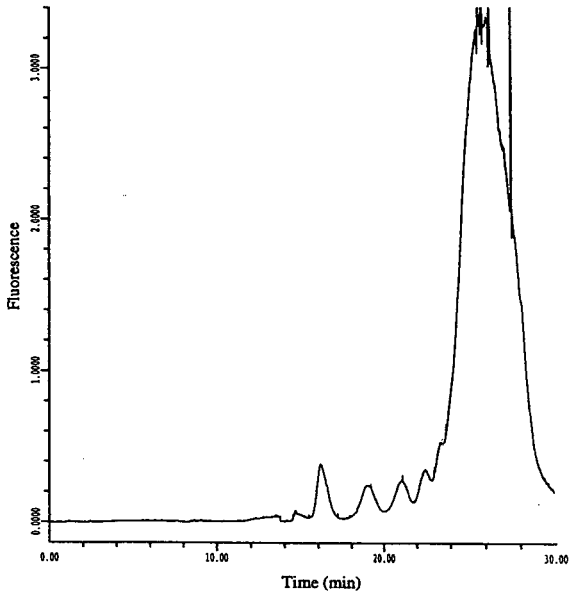

Fig. 1. A complete electropherogram for a digest of $1 \cdot 10^5$ VP-16-treated thymocytes analysed using the conditions noted in the Experimental section.

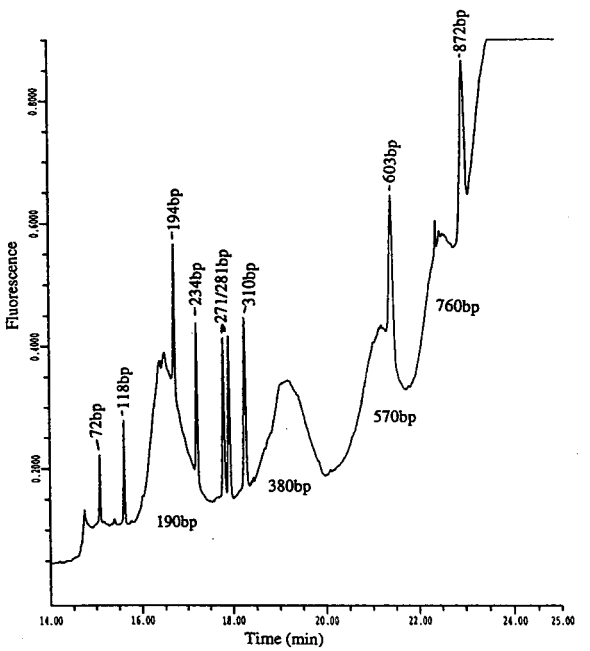

Fig. 2. Digest of $1 \cdot 10^5$ VP-16-treated thymocytes containing 98 ng/ml *Hae*III digest of ΦX174 DNA. Sizes of the ΦX174 DNA fragments and the nucleosomal fragments are indicated.

ments that remain unresolved by this CE method. A comparison of the ladder fragmentation region of electropherograms from all three types of cell exposure is shown in Fig. 3, along with slab gel data appended to Fig. 3a. A small degree of laddering was detected in control cells, consistent with faint laddering detected on the slab gel and the small percentage of apoptosis reported in the literature from flow cytometry studies [9–11]. VP-16 induced DNA laddering to a greater extent than dexamethasone, again consistent with the literature [11] and the slab gel electrophoresis data for the three thymocyte treatments showed a similar gradation of DNA laddering.

The electropherogram of a 123-bp dsDNA ladder showed up to 10 fragments with discrete, sharp peaks (Fig. 4) and a noticeable impairment of resolution above fragment 8 (984 bp). In contrast, the thymocyte nucleosomal peaks showed a Gaussian distribution, probably resulting from the inability of this CE method to resolve fragments differing in only a few base pairs and the biochemistry of the internucleosomal cleavage mechanism. The incubation of 20 μl of thymocyte digest with 2 μl of deoxyribonuclease I (E.C. 3.1.21.1, from bovine pancreas; 1012 Kunitz units/ml in deionised water) and 2 μl of phosphodiesterase I (E.C. 3.1.4.1., from *Crotalus atrox* venom; 1 unit/ml in deionised water) for 2 h at 37°C resulted in a marked attenuation of peak amplitude, further attesting to the identity of this material as nucleic acid, specifically DNA (data not shown).

The volume loaded into the capillary with the 90 s hydrodynamic load was calculated to be 134 nl. The volume of sample loaded was determined as follows: ca. 30 μM fluorescein sodium salt in cell digest was loaded into the capillary, against 0.5% w/v HEC in carrier electrolyte, at the sample loading pressure of 3.5 kPa. The time taken to reach the detector was 24.6 ± 0.5 min ($n = 3$) and the capillary volume calculated to be 2.2 μl. Therefore the capillary fill rate was 89.4 nl/s, and thus for a 90 s loading time 134.1 nl of sample was loaded. A mammalian diploid cell contains approximately 10 pg of DNA, therefore the routinely used digests of $1 \cdot 10^5$ cells/50 μl contain 20 ng DNA/μl, thus 2.7 ng of DNA is loaded per 90 s injection. Since control thymocytes are ca. 10% apoptotic after 4 h incubation, as assessed by flow cytometry, then the resultant nucleosomal fragments detected arise from ca. 270 pg of DNA. The limit of detection for nucleosomal fragments in terms of the cell number digested is dependent on the extent of apoptosis and the degree of internucleosomal cleavage occurring in the cells under study. For thymocytes treated with VP-16 for 4 h (45–50% apoptotic by flow cytometry), nucleosomal fragments were detectable by this CE method in a digest of $1 \cdot 10^3$ cells (in 25 μl digestion mixture); at least 1000-fold fewer cells than used for conventional slab gel electrophoresis (Fig. 5). This quantity of cells represents 54 pg DNA/injection. The limit of detection for *Hae*III digest of ΦX174 DNA, based on the smallest (72 bp) fragment was 70 ng/ml which corresponds to 9 pg of DNA digest injected on to the capillary with a 90-s hydrodynamic loading.

3.2. CE method development for thymocyte digests

The CE method was established using *Hae*III digest of ΦX174 DNA as the initial analyte, but method development was primarily oriented towards optimising conditions for the analysis of DNA fragments in cell digests. The effect of several variables on the migration times, total analysis time and resolution of the nucleosomal fragments was determined. The influence of parameters such as temperature, polymer concentration and field strength on the resolution of dsDNA fragments have been relatively well studied [21,22]; the final electrophoresis conditions were selected to keep analysis times below 30 min and achieve suitable resolution to allow the recognition of ladder fragmentation patterns.

Varying the concentration of YO-PRO-1 from 100 to 400 nM resulted in migration times for the nucleosomal peaks increasing by approximately 30 s with each concentration increase (Fig. 6a, b

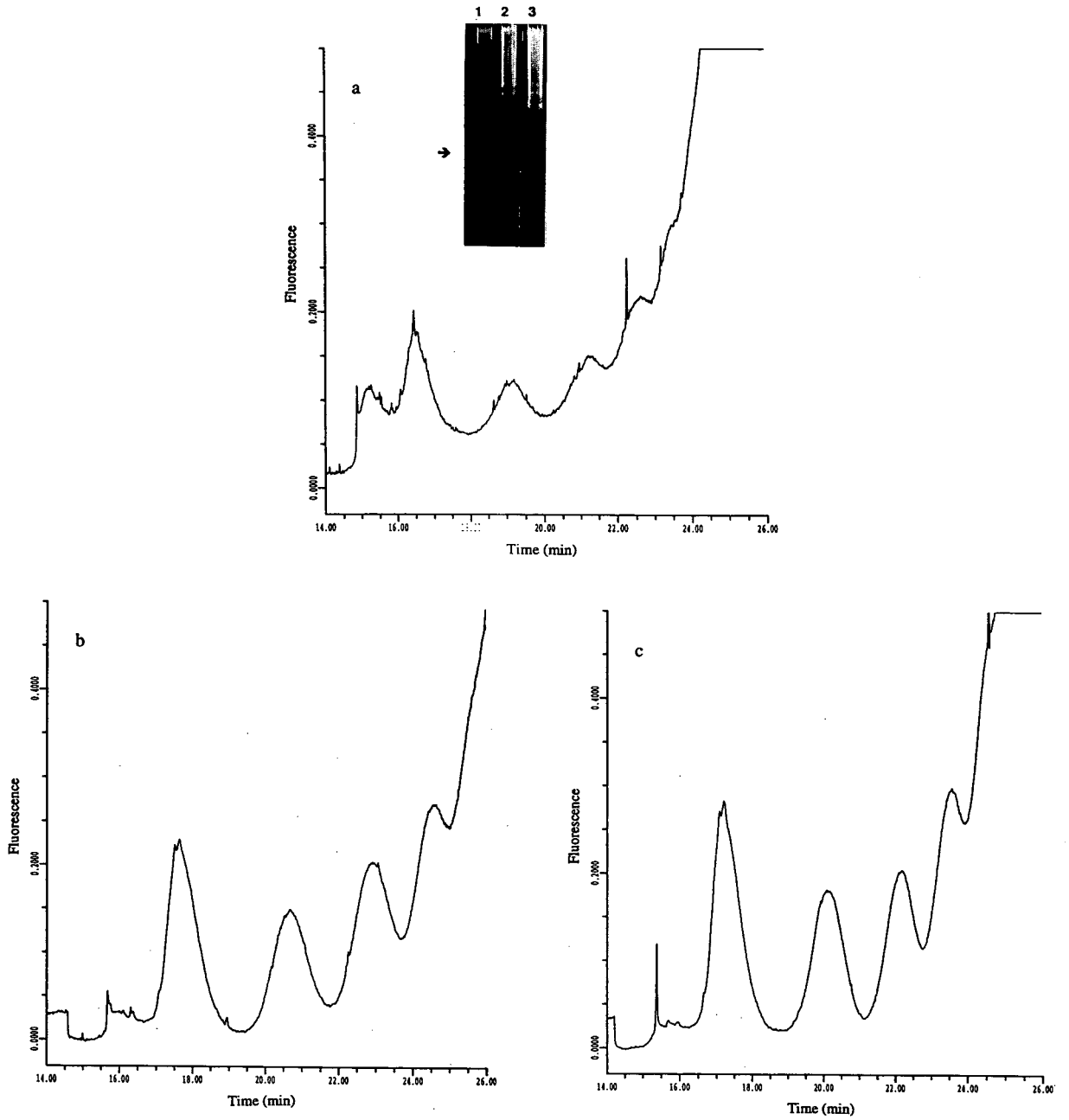

Fig. 3. DNA ladder regions for digests of $1 \cdot 10^5$ thymocytes. (a) Control; (b) dexamethasone; (c) VP-16. Appended to (a) is the agarose slab gel analysis for digests of $2 \cdot 10^6$ thymocytes. (1) Control; (2) dexamethasone; (3) VP-16. The arrow indicates the position of a 564 bp marker.

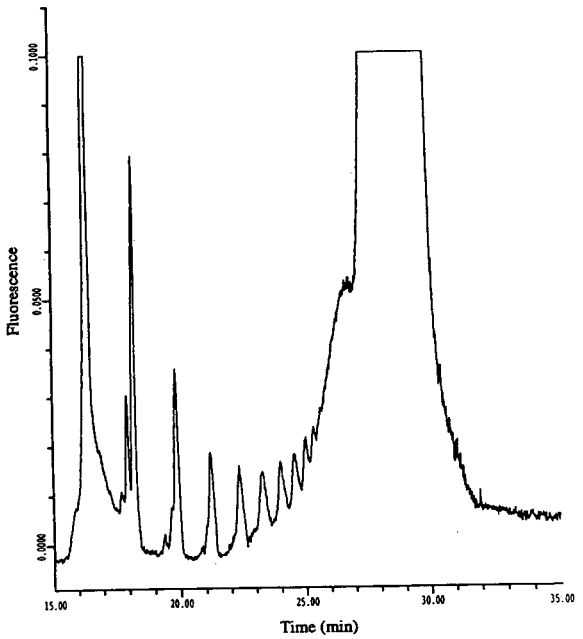

Fig. 4. 123 bp dsDNA ladder at 325 ng/ml analysed using the conditions noted in the Experimental section.

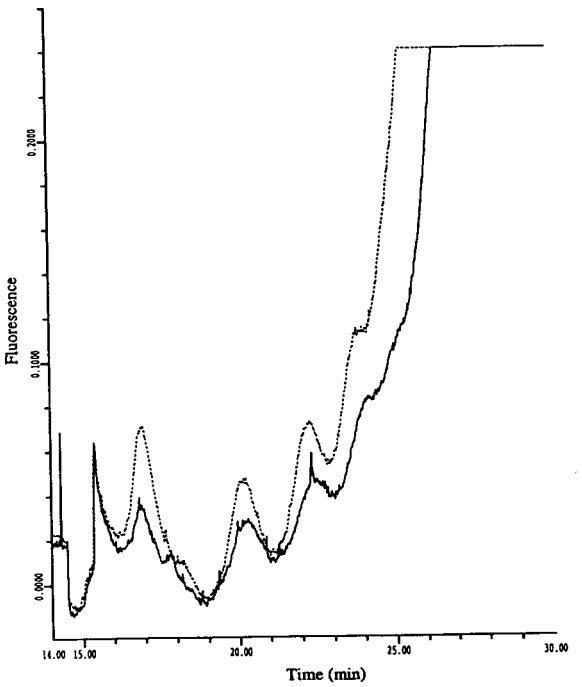

Fig. 5. Comparison of the nucleosomal fragmentation patterns from digests of $5 \cdot 10^3$ VP-16-treated thymocytes ($\cdots$) and $1 \cdot 10^3$ VP-16-treated thymocytes (—) in a 25-μl digestion volume.

and c). Increasing the YO-PRO-1 concentration from 400 to 800 n*M* resulted in only a marginal increase in migration time (Fig. 6c and d). This increase results from two influences of intercalation of YO-PRO-1 with the fragments: first, an increase in positive charge imparted by the dye; second, a decrease in the flexibility of the fragments which would then decrease fragment mobility through the sieving matrix. The latter effect is the basis for the enhancement of resolution between dsDNA fragments of similar length when adding an intercalating dye such as ethidium bromide [4]. Nucleosomal peak areas increased using 400 n*M* YO-PRO-1 compared to 100 n*M* and less so after increasing the concentration to 800 n*M*. Resolution between nucleosomal peaks was negligibly affected by increasing the YO-PRO-1 concentration from 100 to 800 n*M* (Fig. 6). Since the differences between 400 and 800 n*M* YO-PRO-1 on the analysis were relatively small, the dye was used at 400 n*M* to achieve suitable results and economise on reagent.

Initially, electrokinetic injection (-35 kV/cm for 5 s) was used for the analysis of restriction enzyme digests, since this gave sharper peaks, better resolution and a less noisy baseline compared to hydrodynamic injection. Electrokinetic injection was therefore expected to be suitable for the thymocyte digests, since small nucleic acid fragments would be preferentially loaded. However, hydrodynamic injection was found to give better electropherograms for the cell digests since the resolution of nucleosomal fragments was still achieved with less noise and more defined peak shapes. Using capillary loading times of 30 s, 60 s and 90 s gave progressively increasing peak heights and spatial areas, however, resolution did not noticeably deteriorate at longer loading times (data not shown).

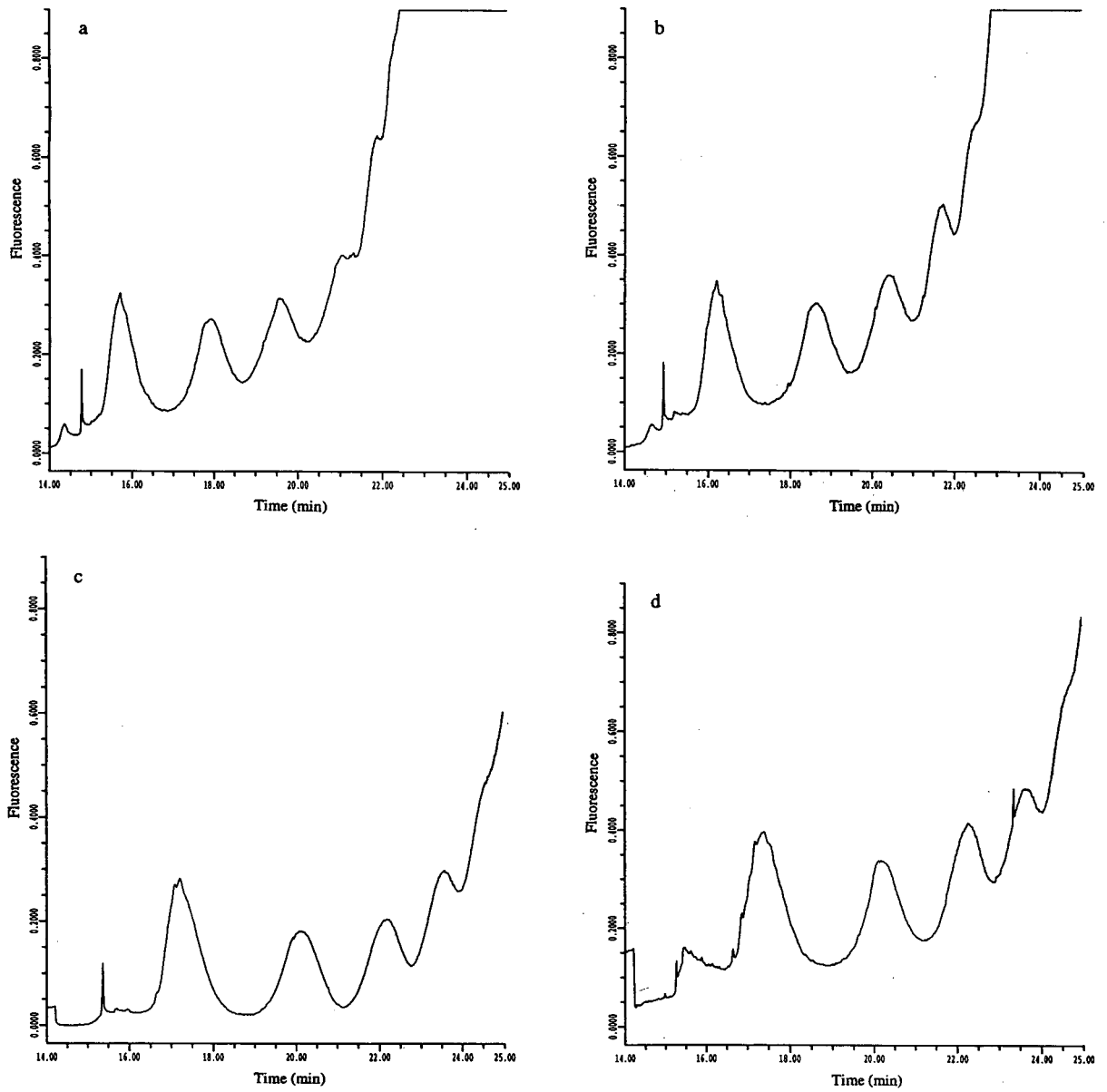

Fig. 6. DNA ladder region for a digest of $1 \cdot 10^5$ VP-16-treated thymocytes analysed using various concentrations of YO-PRO-1: (a) 100 n*M*; (b) 200 n*M*; (c) 400 n*M*; (d) 800 n*M*.

3.3. Thymocyte digestion conditions

A method similar to that first reported by Sorenson et al. [17] as an in-well digestion method on slab gels was adopted as the thymocyte digestion procedure prior to CE. The thymocytes were lysed and digested with proteinase K and RNase in a single incubation step and the whole cell digests used for CE analysis. A useful feature of this method is the elimination of a DNA extraction step prior to electrophoresis which minimises sample handling. In the

digestion procedure reported here, RNase and proteinase K are co-incubated with little detriment to the final electropherogam. The sequential incubation of RNase then proteinase K (2 h RNase, 2 h proteinase K at 37°C) or proteinase K then RNase, yields electropherograms with negligible differences compared to that for a digest obtained when to the two are co-incubated (data not shown).

The inclusion of proteinase K in the digestion mixtures was critical, since its omission resulted in a substantially depleted level of fluorescence (Fig. 7). Only a fraction of the mononucleosome fragment was detected and there was a complete absence of other fragments and high-molecular-mass DNA. Failure to remove protein from the complexes with DNA would obviously have a profound effect on the migration of DNA in this system from the perspectives of both charge and fragment (or complex) size. Conversely, although omission of RNase from the digestions had little effect on the electropherograms (Fig. 7), it was retained in the digestion mixtures to avoid possible detection of RNA by YO-PRO-1.

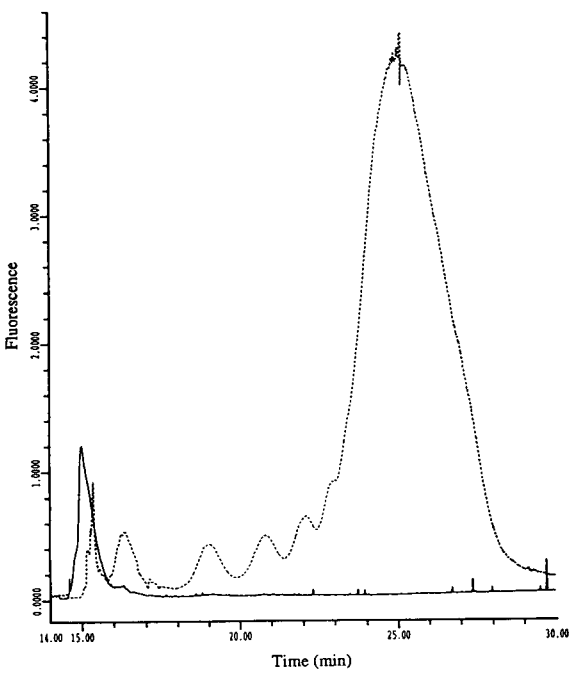

Fig. 7. The effect of excluding proteinase K or RNase from the digestion of $1 \cdot 10^5$ VP-16-treated thymocytes on the appearance of the electropherogram: (—) Proteinase K absent; (· · ·) RNase absent.

Contamination of the digestion mixture by exogenous nucleic acid was substantially eliminated by the use of filter-sterilised buffers. However, in many instances low-molecular-mass nucleic acid contamination was evident in both the RNase and proteinase K solutions which migrated just before the mononucleosome fraction with some overlap. The suitability of the incubation time of thymocytes at 37°C with RNase and proteinase K was assessed by determining the total spatial area (integrated peak area divided by migration time) for the dinucleosome to tetranucleosome peaks inclusive following incubation for 1, 2, 3 and 4 h. Over this incubation period the variation in peak spatial area was only 7%.

4. Discussion

In this study immature rat thymocytes were used since apoptosis in this cell type has been extensively studied from both morphological and biochemical perspectives [12,13,23]. Studies on DNA fragmentation in these cells are at a relatively advanced stage of characterisation and they are known to undergo internucleosomal fragmentation [9,12,13,24,25]. In addition, the conditions known to induce apoptosis in these cells are well known and this was induced to varying degrees using the synthetic glucocorticoid dexamethasone and the topoisomerase II inhibitor etoposide (VP-16). The CE method reported in this paper uses whole cell digests for the analysis of DNA laddering and enables ladder pattern recognition. In addition the data indicate that some useful quantitative information can be obtained and a preliminary comparison between apoptosis quantitated by flow cytometry and in terms of DNA laddering by CE show close agreement.

In this CE method we used the sensitive monomeric cyanine nucleic acid dye YO-PRO-1 as the DNA detection reagent for several reasons. The dye has a very high affinity for

nucleic acid, with a partition coefficient between DNA and 10% v/v aqueous ethanol of $8 \cdot 10^6$ [26]. Although YO-PRO-1 can bind to RNA and single stranded DNA, its affinity and fluorescence are much higher for dsDNA [26]. YO-PRO-1 also has excitation characteristics compatible with the 488 nm argon ion laser and has negligible intrinsic fluorescence in solution thus minimising the background fluorescence signal and increasing sensitivity [24]. The use of YO-PRO-1 as a DNA detection reagent in CE has been reported for the analysis of restriction enzyme digests and polymerase chain reaction-amplified DNA from forensic samples [6]. The high mass sensitivity of CE in combination with YO-PRO-1 means that we were able to detect DNA laddering using 1000–2000 fold fewer cells than used for slab gel electrophoresis. These very low cell numbers suggest that CE analysis of DNA ladder fragmentation can be applied to limited cell sample sizes.

The data obtained yield some useful information regarding the biochemistry of the internucleosomal DNA cleavage. The endonuclease involved in nucleosomal fragmentation during thymocyte apoptosis probably cleaves DNA at various points on the linker DNA to generate a family of nucleosomal fragments differing by only a few base pairs and hence appearing as a broad distribution on electrophoresis. A recent study using mouse thymocytes indicate that the formation of ladder fragmentation is due to the action of a single stranded rather than double stranded DNA cutting activity [27]. The apparent DNA double strand cleavage arises from the dissociation of DNA around multiple single-stranded cuts on opposite DNA strands. Besides the confirmation of fragment size, the co-injection data (Fig. 2) indicate that the nucleosomal fragments span about 50 bp either side of the estimated nucleosome size. The nucleosomal core particle contains 140 bp and species variability in nucleosome size arises from variations in the length of the linker DNA. If the endonuclease involved in ladder fragmentation in apoptosis has no sequence specificity for DNA cleavage, then the most accessible part of the DNA, the central portion of the linker region, would be the predominant cleavage point on steric accessibility grounds. The data in Fig. 2 indicate that this is likely; the least populated fragment sizes around the mononucleosomal fragment are close to the core particle (130–150 bp) and the adjacent nucleosomal particles (approximately 230–250 bp). Compared to slab gel electrophoresis, the CE method is more amenable to this type of co-injection analysis.

Cell treatment prior to analysis by electrophoresis is important to free DNA from complexes with protein and RNA and to minimise noise on the electropherograms. Several factors need to be considered when preparing the samples such as the ease and speed of preparation, the yield of DNA, and whether the handling generates artefacts. Several DNA preparation procedures have been reported in the literature for analysing low-molecular-mass DNA generated during apoptosis for which the final step is commonly analysis of the DNA in 1–2% agarose slab gels followed by ethidium bromide staining. Although there are variations in the details of the techniques the majority of workers choose one of the three main protocols. First, cell lysis in the presence of proteinase K followed by DNA extraction and RNase digestion [18,19,28]. Second, cell lysis and DNA extraction followed by sequential digestion with RNase and proteinase K [29,30]. Third, cell lysis and sequential digestion with RNase and proteinase K followed by DNA extraction [31]. Rarely are proteinase K and RNase co-incubated. It is assumed that RNase will be a substrate for the non-specific proteinase K and consequently will lose activity. The studies reported here imply this is not the case, but since whole cell digests are being used it is possible that cell-derived protein substrates for the proteinase K are in excess and thus RNase is a quantitatively minor substrate.

Although DNA ladder fragmentation patterns are frequently used as a marker of apoptosis, it is suggested to be a relatively late event and its formation is often dependent on the cell type and the stimulus used to induce apoptosis [9,16,32,33]. It is possible that in cell systems which do not show evidence of internucleosomal DNA cleavage the event is quantitatively minor

and the failure to detect DNA laddering is due to the relatively poor sensitivity of the currently used electrophoresis methods. Other criteria, related to DNA fragmentation, for detecting apoptosis have been developed, such as the application of pulsed field, or field inversion gel electrophoresis (FIGE) to examine cells for earlier, large (50–300 kbp) DNA fragments [33,34]. These larger fragments probably result from DNA strand breaks introduced via nuclease-sensitive sites arising from higher order packing of the DNA into loop (50 kbp) and rosette (300 kbp) structures [23,34]. The analysis of DNA fragments by FIGE is lengthy and the ability to detect ladder fragmentation and large DNA fragments in a single, relatively rapid, electrophoretic analysis would be of considerable use in the study of DNA fragmentation in apoptosis. The CE method described here is capable of separating a 9.4-kbp fragment from a 23.1-kbp fragment in the *Hind*III digest of λ phage within 30 min (data not shown). However, the resolution of a 23.1-kbp from a 48.5-kbp (intact λ phage DNA) fragment was not achieved. The separation of large DNA fragments in the kbp range has been reported, using polyacrylamide-coated capillaries and linear polyacrylamide as the sieving matrix and also by pulsed field CE [35,36]. We are currently developing CE methodology to analyse for internucleosomal cleavage and large DNA fragments in a single run using cellular systems undergoing apoptosis.

5. Conclusions

In this paper we have demonstrated that CE using replaceable dilute polymer solutions can be applied to the analysis of DNA ladder fragmentation in apoptotic thymocytes. The analysis can be successfully performed on whole cell digests, obviating the need for a DNA extraction step, and the resultant electropherograms allow the identification of DNA laddering. The relative degree of apoptosis based on the comparison of DNA laddering by CE agrees with that seen for slab gel electrophoresis and with flow cytometric values presented in the literature. Also, the CE method is very sensitive compared to slab gel electrophoresis, is somewhat less labour intensive, and can be automated.

Acknowledgements

The authors thank The Arthritis and Rheumatism Council for Research, UK, The Glenfield Hospital NHS Trust and the Medical Research Council, UK for financial support.

References

[1] D.N. Heiger, A.S. Cohen and B.L. Karger, *J. Chromatogr.*, 516 (1990) 33.
[2] P.D. Grossman and D.S. Soane, *J. Chromatogr.*, 559 (1991) 257.
[3] A.E. Barron, D.S. Soane and H.W. Blanch, *J. Chromatogr. A*, 652 (1993) 3.
[4] H.E. Schwartz, K. Ulfelder, F.J. Sunzeri, M.P. Busch and R.G. Brownlee, *J. Chromatogr.*, 559 (1991) 267.
[5] A.W.H.M. Kuypers, P.M.W. Willems, M.J. van der Schans, P.C.M. Linssen, H.M.C. Wessels, C.H.M.M. de Bruijn, F.M. Everaerts and E.J.B.M. Mensink, *J. Chromatogr.*, 621 (1993) 149.
[6] B.R. McCord, D.L. McClure and J.M. Jung, *J. Chromatogr. A*, 652 (1993) 75.
[7] L.E. Gerschenson and R.J. Rotello, *FASEB J.*, 6 (1992) 2450.
[8] W. Bursch, L. Kleine and M. Tenniswood, *Biochem. Cell Biol.*, 68 (1990) 1071.
[9] G.M. Cohen, X-M. Sun, R.T. Snowden, D. Dinsdale and D.N. Skilleter, *Biochem. J.*, 286 (1992) 331.
[10] C. Dive, C.D. Gregory, D.J. Phipps, D.L. Evans, A.E. Milner and A.H. Wyllie, *Biochim. Biophys. Acta*, 1133 (1992) 275.
[11] X-M. Sun, R.T. Snowden, D.N. Skilleter, D. Dinsdale, M.G. Ormerod and G.M. Cohen, *Anal. Biochem.*, 204 (1992) 351.
[12] J.J. Cohen and R.C. Duke, *J. Immunol.*, 132 (1984) 38.
[13] A.H. Wyllie and R.G. Morris, *Am. J. Pathol.*, 109 (1982) 78.
[14] D.J. McConkey, P. Nicotera, P. Hartzell, G. Bellomo, A.H. Wyllie and S. Orrenius, *Arch. Biochem. Biophys.*, 269 (1989) 365.
[15] R. Gold, G. Rothe, H. Zischler, M. Schmied, U. Tonpsch, G. Valet, H. Lassmann and H. Wekerle, *Anal. Cell. Pathol.*, 4 (1992) 159.
[16] F. Oberhammer, G. Fritsch, M. Schmied, M. Pavelka, D. Printz, T. Purchio, H. Lassmann and R. Schulte-Hermann, *J. Cell Sci.*, 104 (1993) 317.

[17] C.M. Sorenson, M.A. Barry and A. Eastman, *J. Natl. Cancer. Inst.*, 82 (1990) 749.
[18] V.J. Forrest, Y-H. Kang, D.E. McClain, D.H. Robinson and N. Ramakrishnan, *Free. Radical Biol. Med.*, 16 (1994) 675.
[19] M.M. Compton and J.A. Cidlowski, *J. Biol. Chem.*, 262 (1987) 8288.
[20] M. Raffray and G.M. Cohen, *Arch. Toxicol.*, 65 (1991) 135.
[21] R.P. Singhal and J. Xian, *J. Chromatogr. A*, 652 (1993) 47.
[22] D.A. McGregor and E.S. Yeung, *J. Chromatogr. A*, 652 (1993) 67.
[23] A.H. Wyllie, *Nature*, 284 (1980) 555.
[24] M.J. Arends, R.G. Morris and A.H. Wyllie, *Am. J. Pathol.*, 136 (1990) 593.
[25] J. Filipski, J. LeBlanc, T Youdale, M. Sikorska and P.R. Walker, *EMBO J.*, 9 (1990) 1319.
[26] R.P. Haugland, *Handbook of Fluorescent Probes and Research Chemicals*, Molecular Probes, Eugene, OR, 1992.
[27] M.C. Peitsch, C. Müller and J. Tschopp, *Nucleic Acids Res.*, 21 (1993) 4206.
[28] M. Murakami, T. Tsubata, M. Okamoto, A. Shimizu, S. Kumagai, H. Imura and T. Honjo, *Nature*, 357 (1992) 77.
[29] J. Gong, F. Traganos and Z. Darzynkiewicz, *Anal. Biochem.*, 218 (1994) 314.
[30] N. Kyprianou and J.T. Isaacs, *Endocrinology*, 122, (1988) 552.
[31] R.P. Bissonnette, F. Echeverri, A. Mahboubi and D.R. Green, *Nature*, 359 (1992) 552.
[32] R.J. Collins, B.V. Harmon, G.C. Gobe and J.F.R. Kerr, *Int. J. Radiat. Biol.*, 61 (1992) 451.
[33] F. Oberhammer, J.W. Wilson, C. Dive, I.D. Morris, J.A. Hickman, A.E. Wakeling, P.R. Walker and M. Sikorska, *EMBO J.*, 12 (1993) 3679.
[34] P.R. Walker, L. Kokileva, J. LeBlanc and M. Sikorska, *BioTechniques*, 15 (1993) 1032.
[35] T. Guszczynski, H. Pulyaeva, D. Tietz, M.M. Garner and A. Chrambach, *Electrophoresis*, 14 (1993) 523.
[36] J. Sudor and M. Novotny, *Anal. Chem.*, 66 (1994) 2446

ELSEVIER

Journal of Chromatography A, 700 (1995) 163–172

JOURNAL OF CHROMATOGRAPHY A

Determination of impurities in a novel analogue of adenosine 5′-triphosphate by capillary electrophoresis

Janet R. Dawson, Steven C. Nichols, Graham E. Taylor*

Analytical Chemistry Department, Fisons plc, Pharmaceutical Division, Research and Development Laboratories, Bakewell Road, Loughborough, Leicestershire LE11 0RH, UK

Abstract

A capillary electrophoretic method using an uncoated capillary was developed to resolve potential impurities in FPL 67085XX, a novel phosphonate analogue of adenosine 5′-triphosphate. The effects of buffers, buffer concentration, eluent pH and methanol were investigated. Optimum resolution of the impurities was achieved using an eluent consisting of 7% (v/v) methanol in 25 m*M* phosphate buffer–2 m*M* EDTA adjusted to pH 6.6.

1. Introduction

FPL 67085XX [1] (Fig. 1) is a novel phosphonate analogue of adenosine triphosphate and a potent antagonist at P_2T purinoreceptors. FPL 67085XX shows anti-thrombotic activity in animals and inhibits platelet aggregation ex vivo in man.

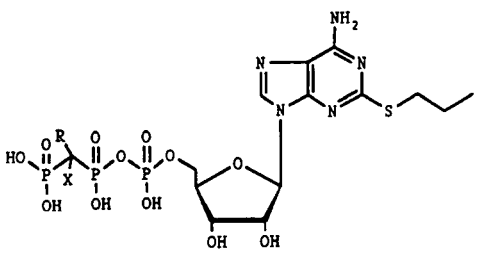

R = X = Cl, FPL 67085XX
R = Cl, X = H, FPL 69499XX
R = X = H, FPL 67933XX

Fig. 1. Structures of the compounds investigated.

FPL 69499XX and FPL 67933XX are potential impurities of FPL 67085XX. To date, it has not been possible to resolve the two impurities from FPL 67085XX using reversed-phase HPLC. Resolution was achieved using anion-exchange chromatography, with a Protein-Pak DEAE 5PW column and triethylammonium hydrogencarbonate eluent [2]. However, the peaks were too broad to allow accurate quantification of the impurities at low levels. The use of capillary electrophoresis (CE) was therefore investigated as an alternative means of resolving the two impurities from FPL 67085XX.

Although the analysis of nucleoside monophosphates by micellar electrokinetic capillary chromatography (MECC) [3–8] and by capillary zone electrophoresis (CZE) [4,9–11] is well established there are few references to the analyses of nucleoside 5′-triphosphates.

Dolnik et al. [12] and Takigiku and Schneider [13] used capillaries silylated with γ-methacryloxypropyl-trimethoxysilane to separate UTP, GTP, ATP, and CTP, and also UTP, dTTP, ITP, GTP, dGTP, dCTP, CTP, dATP and ATP from

* Corresponding author.

0021-9673/95/$09.50
SSDI 0021-9673(95)00055-0

each other. However, these capillaries have the disadvantage of not being commercially available.

Liu et al. [8] used MECC with sodium dodecyl sulphate (SDS) to partially resolve CTP, UTP, GTP and ATP. Partial baseline resolution was achieved using the cationic surfactant dodecyltrimethylammonium bromide, though the polarity of the detector had to be changed.

There have been only two reports of CZE being used for the analysis of nucleoside 5′-triphosphates and neither study involved complex sample matrixes. Pentoney et al. [14] used a 0.2 *M* borate buffer, pH 8.1, to successfully separate ^{32}P-labelled ATP and GTP. De Bruijn et al. [15] demonstrated that UTP could be separated from 5′-fluorouridine 5′-triphosphate using a 10 m*M* phosphate buffer pH 4.8.

Investigations using MECC and a simple CE method for the separation of FPL 67085XX, FPL 69499XX and FPL 67933XX using an uncoated capillary are reported below. The method may be equally applicable to other nucleoside 5′-triphosphates.

2. Experimental

The optimized conditions for separation are as follows: 25 m*M* Phosphate, 2 m*M* EDTA, 7% (v/v) methanol adjusted to pH 6.6 with sodium hydroxide. Voltage 20 kV, 67 cm × 75 μm uncoated capillary. Temperature 25°C. Wavelength 280 nm. 10 s pressure injection.

2.1. Apparatus

The CE system used was a Beckman P/ACE system 2050, controlled with System Gold version 7 software (Beckmann Instruments, Fullerton, CA, USA). The uncoated fused silica capillary, 75 μm I.D. (60 cm from injector to detector, 67 cm total length or 50 cm from injector to detector, 57 cm total length) (FSA, Loughborough, UK) was fitted into a capillary cartridge and thermostatted at 25°C. The samples were injected by pressure for 10 s (0.5 p.s.i.; 1 p.s.i. = 6894.76 Pa) and detection was by on column UV absorbance at 280 nm. The voltage supplied was +20 kV.

Before use, capillaries were preconditioned with 1 *M* phosphoric acid (20 min, pressure) followed by purified water (5 min, pressure), 1 *M* sodium hydroxide solution (20 min, pressure) and purified water (5 min, pressure).

At the start of each day, the capillary was washed with 0.1 *M* sodium hydroxide solution (25 min, pressure) followed by purified water (5 min, pressure).

Before each injection the capillary was washed with 0.1 *M* sodium hydroxide solution (2 min, pressure) and buffer solution (1 min, pressure).

2.2. Chemicals

Purified water was obtained from a Milli-Q system (Millipore, Bedford, MA, USA). Phosphoric acid, EDTA disodium salt, boric acid, borax, tris, sodium hydroxide, methanol and SDS were purchased from FSA.

FPL 67085XX, FPL 69499XX and FPL 67933XX were manufactured by Fisons Pharmaceuticals, Loughborough, UK.

Buffer system 1

Buffer system 1 consisted of 30 m*M* borate–2 m*M* EDTA pH 9.0–variable SDS concentration. The required amount of SDS was added to a solution of 30 m*M* boric acid–2 m*M* EDTA adjusted to pH 9.0 with 3 *M* sodium hydroxide.

Buffer system 2

Buffer system 2 consisted of 10 m*M* phosphate–10 m*M* Tris–100 m*M* SDS (pH 7.05). SDS (1.44 g) in a 50-ml volumetric flask which was diluted to volume with 10 m*M* Tris–10 m*M* sodium dihydrogenorthophosphate which had been previously adjusted to pH 7.05 with orthophosphoric acid (specific gravity 1.69).

Buffer system 3

Buffer system 3 consisted of a solution of 30 m*M* boric acid and 2 m*M* EDTA adjusted to the required pH with sodium hydroxide.

Buffer system 4

Buffer system 4 consisted of a solution of borax (30 m*M*s sodium tetraborate decahydrate) and 2 m*M* EDTA adjusted to the required pH with orthophosphoric acid (specific gravity 1.69).

Buffer system 5

Buffer system 5 consisted of phosphoric acid and 2 m*M* EDTA adjusted to the required pH with 0.1 *M* sodium hydroxide and the required amount of methanol added.

3. Results and discussion

3.1. MECC

Using an MECC system of 30 m*M* sodium borate–2 m*M* EDTA–100 m*M* SDS (buffer system 1 with 100 m*M* SDS the resolution of a mixture of FPL 67085 XX, nucleoside 5′-monophosphate, nucleoside and base was achieved (Fig. 2). However, migration times were short, peaks were broad and also showed some splitting. At lower pH values (<9.0), migration times

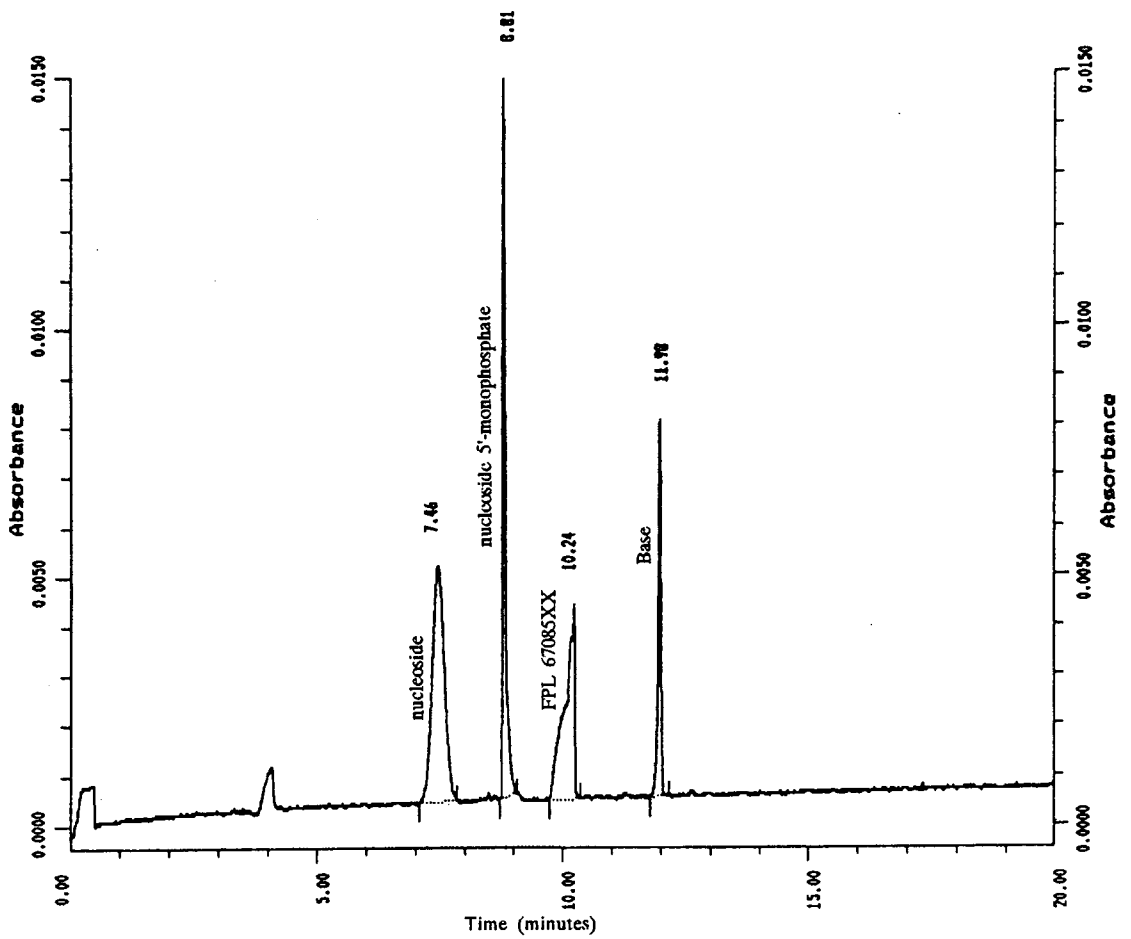

Fig. 2. Electropherogram of FPL 67085XX (0.06 mg/ml), nucleoside 5′-monophosphate (0.05 mg/ml), nucleoside (0.05 mg/ml) and base (0.03 mg/ml). 30 m*M* Borate–2 m*M* EDTA, adjusted to pH 9.0–100 m*M* SDS (system 1). Voltage 20 kV, 57 cm × 75 μm uncoated capillary. Temperature 25°C.

became very irreproducible. Different concentrations of SDS (25, 50, 75, 125, 150 m*M*) at pH 9.0 showed no significant improvement with respect to splitting of the FPL 67085XX peak. An injection of 1 mg/ml FPL 67085XX gave a very broad split peak and no resolution when a mixture of 1 mg/ml FPL 67085XX, 0.05 mg/ml FPL 69499XX and 0.16 mg/ml FPL 67933XX was chromatographed.

Using the system of Liu et al. [8] (buffer system 2), improved resolution of the components was achieved at pH 7.0 although some splitting of the FPL 67085XX peak was again observed (Fig. 3). At higher concentrations of FPL 67085XX, peak splitting increased and no resolution was achieved. Variable SDS concentrations (25, 50, 75, 125, 150 m*M*) again gave no improvement to the peak shape of FPL 67085XX, though as expected there was a dramatic change in relative migration times of the base and nucleoside to the nucleotides.

The results of the investigations suggested that

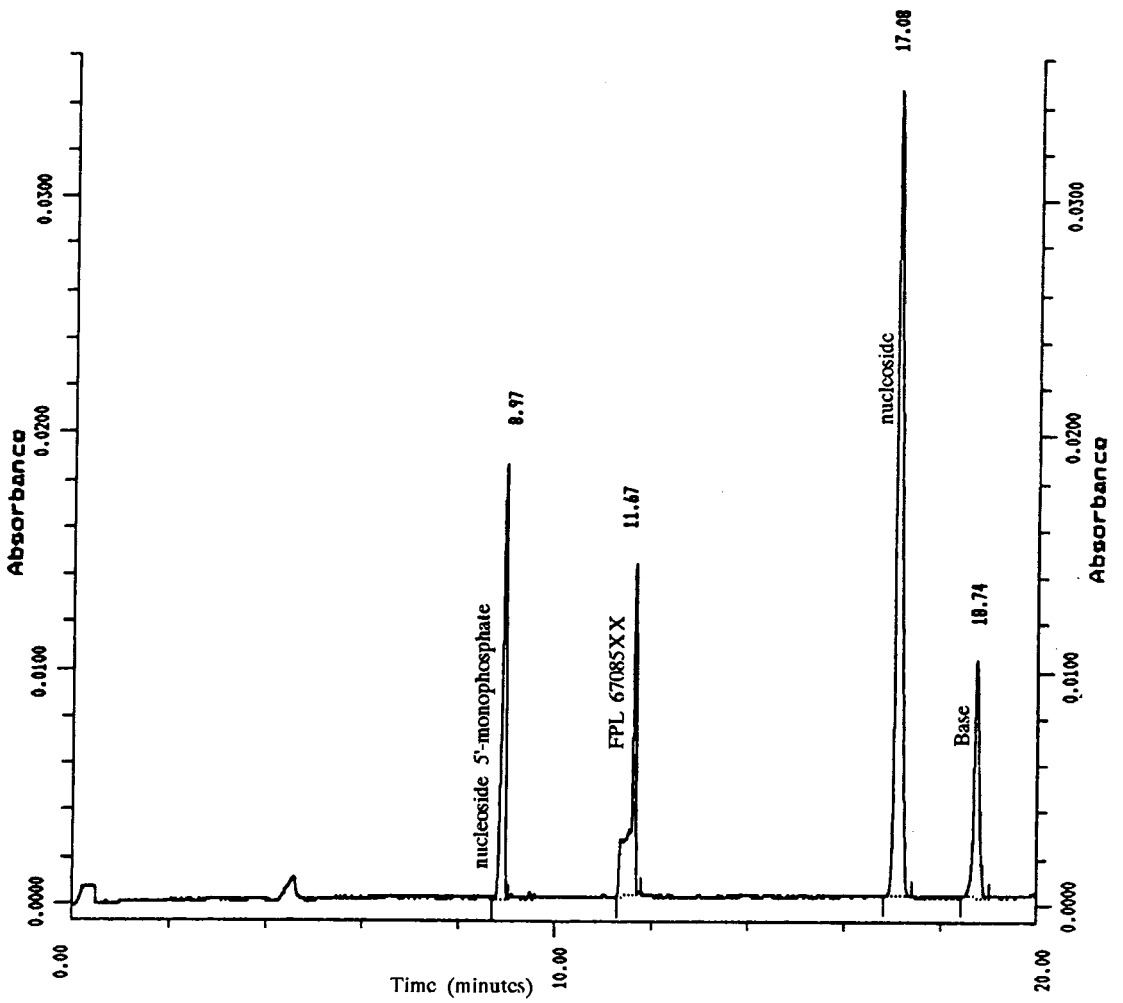

Fig. 3. Electropherogram of FPL 67085XX (0.06 mg/ml), nucleoside 5'-monophosphate (0.05 mg/ml), nucleoside (0.05 mg/ml) and base (0.03 mg/ml). 10 m*M* Tris–10 m*M* sodium dihydrogenorthophosphate, adjusted to pH 7.05–100 m*M* SDS (system 2). Voltage 20 kV, 57 cm × 75 μm uncoated capillary. Temperature 25°C.

eluents containing SDS are not suitable for the determination of the purity of FPL 67085XX. It is probable that similar problems will be encountered with other nucleoside triphosphates under similar conditions.

3.2. CZE

Borate buffer

A method similar to that of Pentoney et al. [14] was evaluated using a 30 m*M* sodium borate, 2 m*M* EDTA eluent, pH 8.0 to 9.0 (buffer system 3). The resolution of FPL 67085XX, nucleoside 5′-monophosphate, nucleoside and base was determined. Very broad and split peaks for FPL 67085XX were obtained at all pH conditions; peak shape and resolution of the other components were unaffected.

Borate–phosphate buffer

A 30 m*M* sodium borate–phosphate–2 m*M* EDTA (pH 6.0–7.8) eluent was studied (buffer system 4). In this system, the FPL 67085XX peak was sharp but the nucleoside 5′-monophosphate peak was split at eluent pHs greater than pH 6.6. The effect of pH upon the peak height and migration time of FPL 67085XX is shown in Fig. 4.

A dramatic change in peak height was observed with changes in eluent pH. The choice of pH was found to have a marked effect on sensitivity. At an eluent pH close to the pK_{a_4} of FPL 67085XX (7.1), the peak height was at a minimum. This is believed to be due to the increased electrophoretic mobility towards the anode as the charge increases from 3^- and 4^- thereby counteracting the electroosmotic flow.

The change in the migration time was explained as follows: as the pH increased from pH 6.0, the migration time decreased as the electroosmotic flow increases. However, this was counteracted by the migration time increasing as the ionisation of FPL 67085XX (pK_{a_4} 7.1) increased with increasing pH. This effectively increased the electrophoretic flow towards the anode.

The reasons for the splitting of the nucleoside 5′-monophosphate peak and not the FPL 67085XX peak are difficult to explain. Tadey and Purdey [10] suggested that nucleoside monophosphates complexed with borate which enhanced separation. It is possible that over the pH range studied, the complexation is causing split-

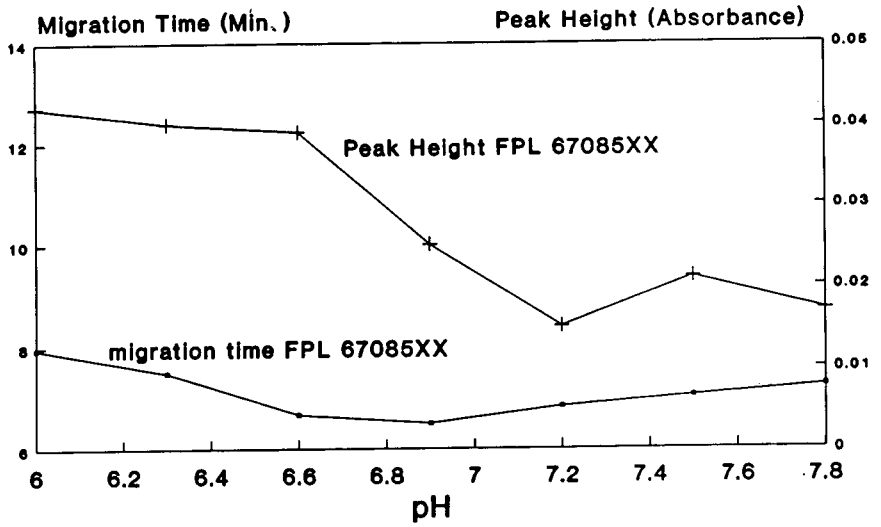

Fig. 4. The effect of pH on migration time (□) and peak height (+) of FPL 67085XX using a 30 m*M* borate–phosphate buffer–2 m*M* EDTA (system 4). Voltage 20 kV, 57 cm × 75 μm uncoated capillary. Temperature 25°C.

ting of the monophosphate peak but not of the triphosphate which carries more charge. At eluent pH values below 6.6, satisfactory peak shapes were obtained for both nucleotides. A compromise of pH 7.0 was chosen at which both the peak shape and migration times were considered to be acceptable.

Adjustment of the buffer concentration to 50 m*M* gave optimum resolution at pH 7.0. Although baseline resolution was achieved, the peak shapes were too broad to give high sensitivity (Fig. 5).

Phosphate buffer

Phosphate buffer having a pK_{a_2} of 7.1 was considered to be a potential eluent for the separation of phosphonate analogues of nucleoside triphosphates which have pK_{a_4} values of between 7.0 to 8.2 [16]. The use of phosphate

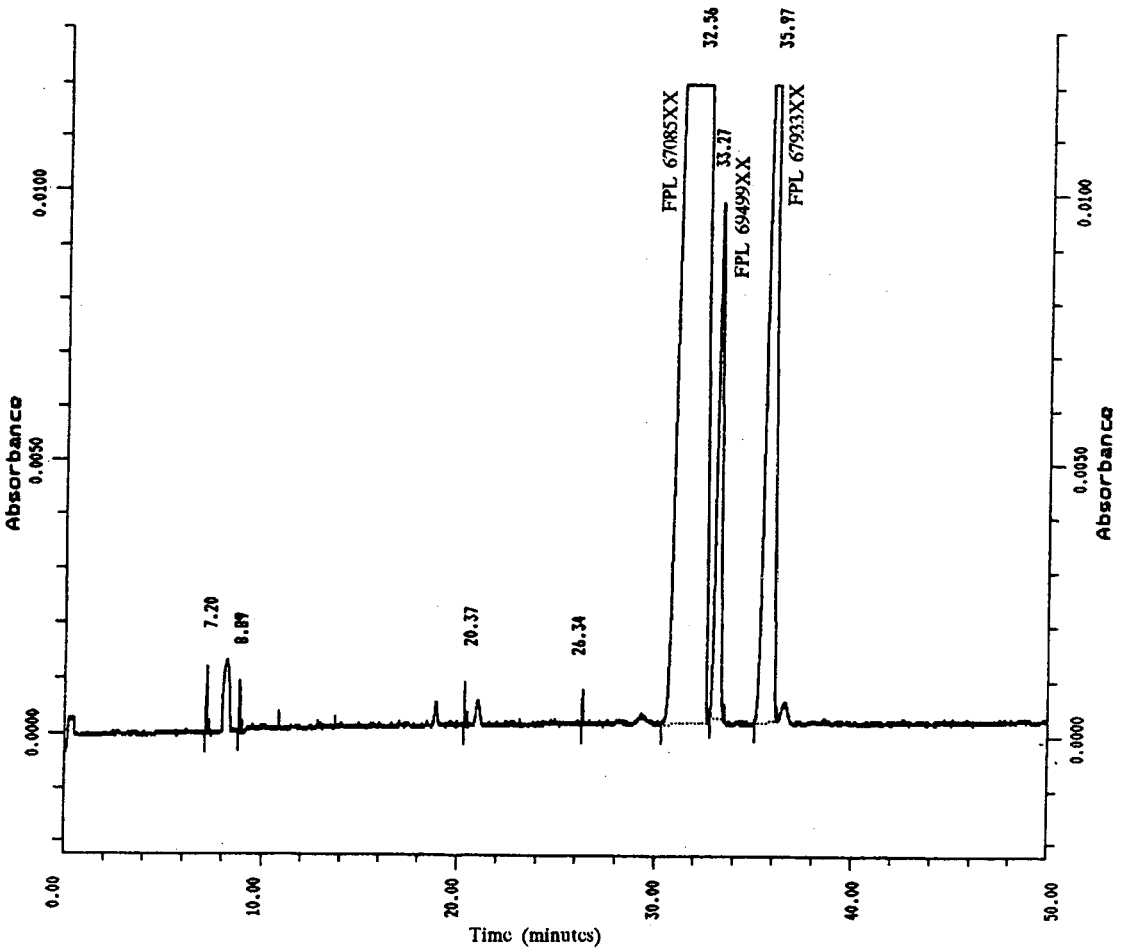

Fig. 5. Electropherogram of FPL 67085MX 1 mg/ml, FPL 69499X 0.05 mg/ml, and FPL 67933XX 0.16 mg/ml. 50 m*M* Sodium borate–2 m*M* EDTA, adjusted to pH 7.0 with phosphoric acid (system 4). Voltage 20 kV, 67 cm × 75 μm uncoated capillary. Temperature 25°C.

buffers for the resolution of the above compounds and as a means of eliminating peak splitting of the nucleoside 5'-monophosphate was thus investigated.

Effect of phosphate concentration

The effect of phosphate concentration on the migration time and peak height of FPL 67085XX at 0.25 mg/ml was studied over a sodium phosphate range of 10 to 80 m*M*. Buffers were prepared from phosphoric acid and titrated with sodium hydroxide to pH 7.0.

A dramatic change in peak height and therefore sensitivity was seen with changes in the phosphate buffer concentration. This was believed to be due to electro-dispersion caused by differences between the sample and running buffer conductivities at high and low phosphate concentrations. At high concentrations of phosphate buffer, Joule heating may also be causing band broadening. A concentration of about 30 m*M* phosphate was chosen as the optimum for further work.

Effect of pH

The effect of pH at 30 m*M* phosphate was investigated. The effect of pH on the migration times and the peak heights is shown in Fig. 6.

Major changes in the peak heights and resolution were found to occur with changes in eluent pH. Resolution between FPL 67085XX and FPL 69499XX was lost above pH 7 due to peak broadening. The poor peak shape of FPL 67085XX above pH 7 which resulted in low peak heights, cannot be attributed to a capillary wall interactions, as FPL 67085XX is highly ionised at high pH and will be repulsed from the wall.

Peak broadening may be a result of the increasing ionisation of FPL 67085XX from 3^- to 4^- state with increasing pH. This increases the electrophilic mobility towards the anode, counteracting the electroosmotic flow which will lead to an effective delay and cause band broadening. This effect may also explain why the migration times between pH 6.4 and 7.4 had remained relatively constant.

The resolution between FPL 67085XX and its analogues at eluent pH 5.8 to 6.8 was excellent.

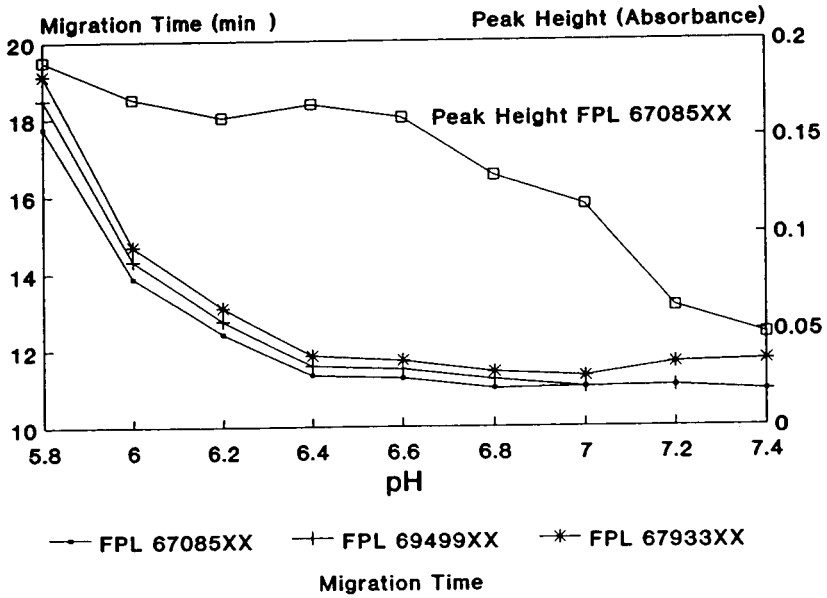

Fig. 6. The effect of pH on migration time and peak height. 30 m*M* phosphoric acid–2 m*M* EDTA, adjusted to the required pH with sodium hydroxide. Voltage 20 kV, 67 cm × 75 μm uncoated capillary. Temperature 25°C.

However, the reproducibility of the migration time was found to be very poor. This may be due to the relatively slow equilibration of the surface charge on the fused silica surface of the capillary at the above pH [17].

Effect of the organic modifier

Organic solvents are able to modify both mobility and electroosmotic force (EOF) [18], thereby leading to better resolution of components. The use of methanol was investigated as an organic modifier for the separation of FPL 67085XX and its related impurities.

Phosphate solutions, 25 m*M*, adjusted to pH 6.6 and containing between 0–12% (v/v) methanol were prepared. The effect on peak heights and variation of migration times of the compounds is shown in Fig. 7. The tailing factor and resolution between the peaks are shown in Table 1.

The migration time for all species was found to increase slightly as the methanol concentration was increased between 0 and 4% (v/v). This effect was anticipated as the EOF will have decreased. At higher methanol concentrations no further effect was seen on the migration time, however, the resolution and tailing factors showed subtle effects. Resolution of FPL 67085XX and FPL 69499XX was optimum at 4% (v/v) methanol and was effectively controlled by the width of the FPL 67085XX peak (expressed as the tailing factor). The resolution of FPL 69499XX and FPL 67933XX was optimum at 10% (v/v) methanol; this is controlled by the peak width of FPL 67933XX. A concentration of

Table 1
Effect of methanol concentration on resolution and peak tailing

Methanol (%, v/v)	Resolution FPL 67085XX/ FPL 69499XX	Resolution FPL 69499XX/ FPL 67933XX	Tailing factor
0	2.4	2.9	8.7
2	3.1	3.5	4.6
4	3.7	5.0	2.1
6	3.2	5.2	0.7
7	2.5	5.6	0.6
8	2.2	6.3	0.6
10	1.7	6.5	0.5
12	1.6	6.3	0.5

Conditions as in Fig. 7.

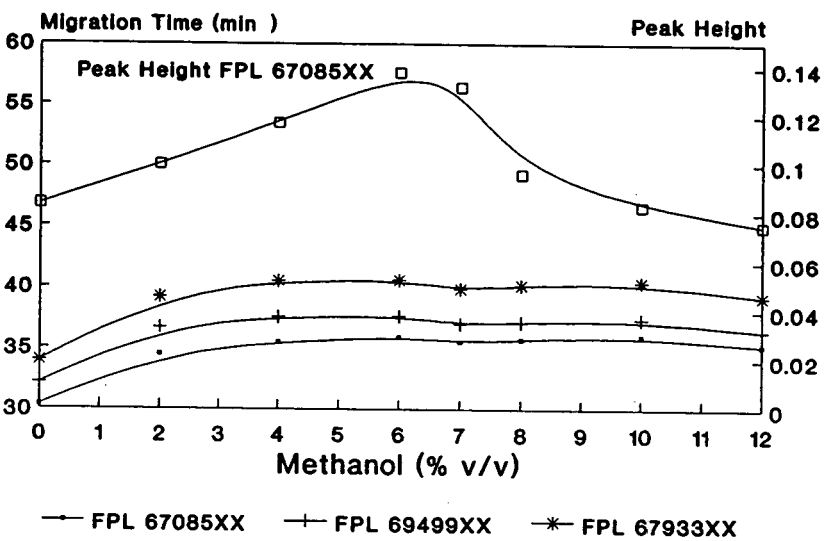

Fig. 7. The effect of methanol concentration on migration time and peak height, on FPL 67085XX using 25 m*M* sodium phosphate–2 m*M* EDTA pH 6.6–variable methanol concentration. Voltage 20 kV, 67 cm × 75 μm uncoated capillary. Temperature 25°C.

7% (v/v) methanol was chosen as optimum for the separation of all the components.

The reasons for the variation in the peak shape of FPL 67085XX with the methanol concentration are unknown. At low concentrations of methanol the peak had a tailing edge becoming symmetrical between 4 and 6% (v/v) methanol. At higher concentrations of methanol a leading edge is seen, hence tailing factors of less than 1.

An example of an electropherogram using the final conditions chosen is shown in Fig. 8. All three components are well resolved. The method gave a R.S.D. for the migration time of less than 1.0%. Using a 10 s injection of a FPL 67085XX solution the lowest detectable concentration was 0.0004 mg/ml. A linear relationship (correlation coefficient 0.9993) was established for the peak area and concentration between 0.0005 and 2.0 mg/ml (0.05–200% of the nominal concentra-

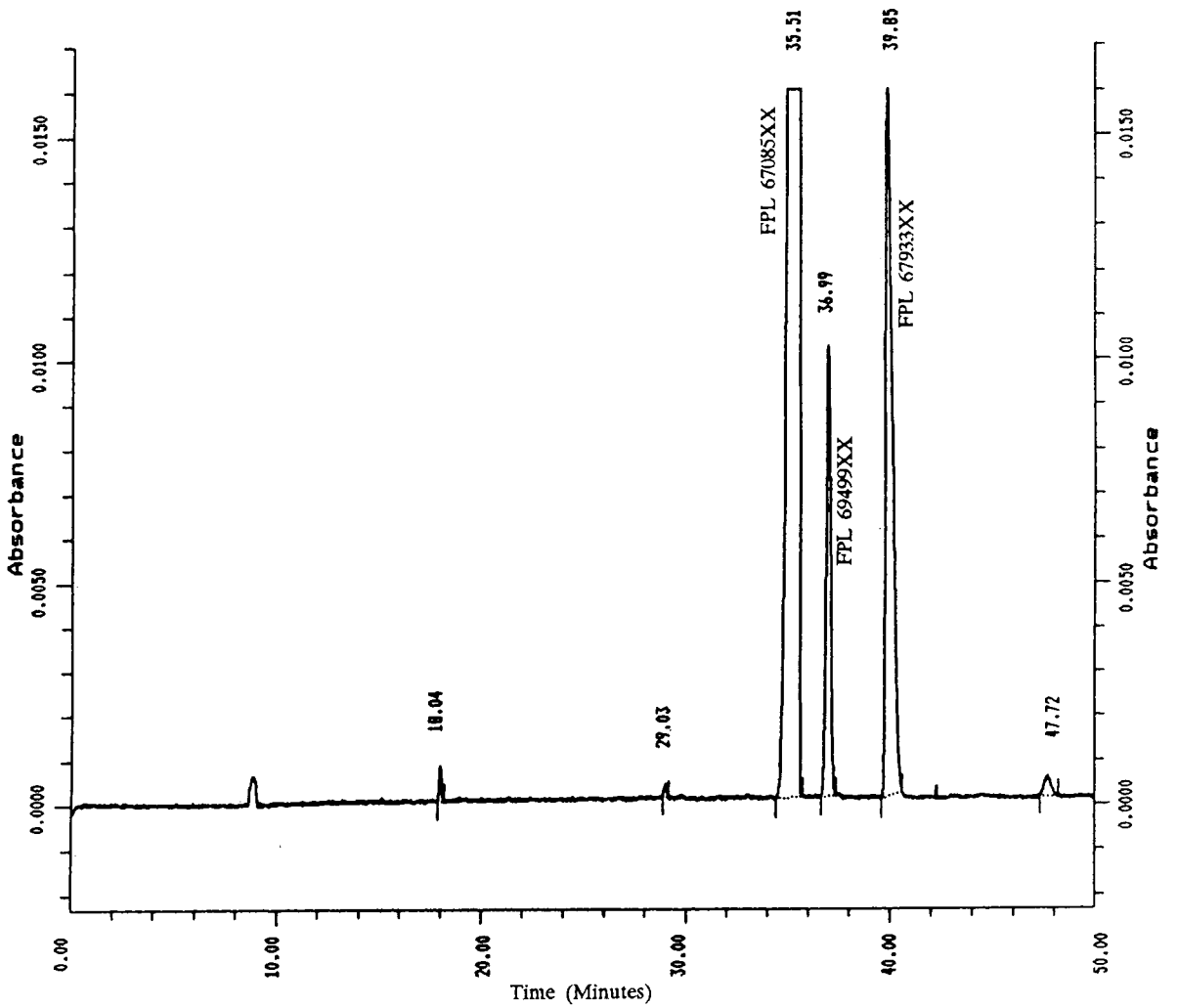

Fig. 8. Electropherogram of FPL 67085XX, FPL 69499XX and FPL 67933XX using 25 m*M* phosphate–2 m*M* EDTA–7% (v/v) methanol adjusted to pH 6.6 with sodium hydroxide. Voltage 20 kV, 67 cm × 75 μm uncoated capillary. Temperature 25°C, 10 s pressure injection.

Table 2
Reproducibility of migration time of FPL 67085MX in various buffer systems

	System 1	System 2	System 4	System 5
Number of injections	6	6	8	6
Mean migration time (min)	10.3	11.7	32.6	32.8
R.S.D. (%)	0.4	0.9	1.5	0.4

System 1: 30 m*M* borate–2 m*M* EDTA 100–m*M* SDS pH 9.0; system 2: 10 m*M* phosphate–10 m*M* Tris–100 m*M* SDS pH 7.05; system 4: 50 m*M* borax–2 m*M* EDTA adjusted to pH 7.0 with orthophosphoric acid; system 5: 25 m*M* orthophosphoric acid–2 m*M* EDTA–7% (v/v) methanol adjusted to pH 6.6 with sodium hydroxide.

tion); intercept values were less than 1% of the nominal concentration.

The reproducibility of migration times of FPL 67085XX in the above buffer systems was determined from multiple injections; data are presented in Table 2.

4. Conclusions

This work has demonstrated the major effects that buffer type, buffer concentration, pH and organic modifier can have on the resolution of a nucleoside phosphonate. By controlling all four parameters excellent resolution was obtained and variation in migration time was minimised. However, further investigations will be required to determine the robustness of the procedure, especially any day-to-day variation in the migration time.

References

[1] R.G. Humphries, *Drug Dev. Res.*, 31 (1994) 279.
[2] G.E. Taylor and S.C. Nichols, unpublished results.
[3] K.H. Row, W.H. Griest and M.P. Maskarinek, *J. Chromatogr.*, 409 (1987) 193.
[4] K.H. Row, and J.I. Raw, *Sep. Sci. Technol.*, 25 (1990) 323.
[5] T. Lee, E.S. Yeung and M. Sharma, *J. Chromatogr.*, 565 (1991) 197.
[6] A. Lecoq, C. Leuratti, E. Marfante and S. Di Biase, *J. High Resolut. Chromatogr.*, 14 (1991) 667.
[7] A. Lecoq, L. Montanarella and S. Di Biase, *J. Microcol. Sep.*, 5 (1993) 105.
[8] J. Liu, F. Banks and M. Novotny, *J. Microcol. Sep.*, 1 (1989) 136.
[9] A. Ngugen, J.H.T. Luong and C. Masson, *Anal. Chem.*, 62 (1990) 2490.
[10] T. Tadey and W.C. Purdy, *J. Chromatogr. B.*, 657 (1994) 365.
[11] W.G. Kuhr and E.S. Yeung, *Anal. Chem.*, 60 (1988) 2642.
[12] V. Dolnik, J. Liu, J.F. Banks, M.V. Novotny and P. Boček, *J. Chromatogr.*, 480 (1989) 321.
[13] R. Takigiku and R.E. Schneider, *J. Chromatogr.*, 559 (1991) 247.
[14] S.L. Pentoney, R.N. Zare and J.F. Quint, *J. Chromatogr.*, 480 (1989) 259.
[15] E.A. De Bruijn, G. Patty, F. David and P. Sandra, *J. High Resolut. Chromatogr.*, 14 (1991) 667.
[16] G.M. Blackburn, D.E. Kent and F. Kolkmann, *J. Chem. Soc., Perkin Trans. I*, (1984) 1119.
[17] W.J. Lambert and D.L. Middleton, *Anal. Chem.*, 62 (1990) 1585.
[18] C. Schwer and E. Kenndler, *Anal. Chem.*, 63 (1991) 1801.

ELSEVIER

Journal of Chromatography A, 700 (1995) 173–178

JOURNAL OF CHROMATOGRAPHY A

Investigation and optimisation of the use of micellar electrokinetic chromatography for the analysis of six cardiovascular drugs

Alison E. Bretnall*, Graham S. Clarke

Bristol-Myers Squibb Pharmaceutical Research Institute, International Development Laboratories, Reeds Lane, Moreton, Merseyside L46 1QW, UK

Abstract

A micellar electrokinetic chromatography method was optimised for the separation of the six cardiovascular drugs atenolol, nicardipine, nifedipine, diltiazem, verapamil, and amlodipine by investigating the effects of pH, sodium dodecyl sulphate (SDS) concentration, selection and concentration of organic modifier. An electrophoresis buffer of 100 m*M* borate pH 8.1 containing 50 m*M* SDS and 15% (v/v) acetone was found to provide the optimum separation with respect to resolution and migration time.

1. Introduction

Micellar electrokinetic chromatography (MEKC) is an adaptation of capillary electrophoresis originally reported by Terabe et al. [1,2]. It was originally used for the separation of electrically neutral compounds but is also effective for separating ionic compounds which because of their similar electrophoretic mobilities are not adequately resolved by capillary zone electrophoresis.

MEKC requires the addition of a charged surfactant to the background electrolyte at a level greater than its critical micelle concentration. The micelles formed have their own electrophoretic mobility which is different from the surrounding aqueous phase. Analytes may differentially partition themselves between the micellar and aqueous phases thus promoting selectivity. This selectivity can be further manipulated by the addition of an organic modifier [3] such as methanol, acetonitrile or acetone [4] to increase the elution range.

In this work, the separation of six cardiovascular drugs was optimised by the addition of an organic modifier and assessment of the effect of pH and concentration of sodium dodecyl sulphate (SDS) in the borate buffer.

2. Experimental

2.1. Reagents

Purified water was provided by a Milli-Q Plus water purification system (Millipore, Bedford, MA, USA). SDS, sodium tetraborate, boric acid and sodium hydroxide were obtained from BDH (Poole, UK). Acetone (Analar grade) and acetonitrile (Hipersolv grade) were also purchased

* Corresponding author.

0021-9673/95/$09.50
SSDI 0021-9673(95)00112-3

from BDH and methanol (HPLC grade) was purchased from Fisons Scientific Equipment (Loughborough, UK). Atenolol, nifedipine, amlodipine, diltiazem, verapamil and nicardipine were supplied from within Bristol-Myers Squibb.

2.2. Apparatus and method

A capillary electrophoresis P/ACE system 5510 (Beckman Instruments, Palo Alto, CA, USA) equipped with diode array UV detector, an automatic injector, a fluid cooled cartridge and a System Gold data station was used in this study. All electrophoresis was carried out at 30°C, with an applied voltage of +25 kV and UV detection wavelength of 200 nm. Sample introduction was performed using the pressure option for 5 s. The capillary was a 57 cm × 75 μm I.D. (50 cm to detector) fused-silica capillary tube (Beckman Instruments), and was rinsed with 0.1 *M* sodium hydroxide and the electrophoresis buffer before each electrophoretic separation

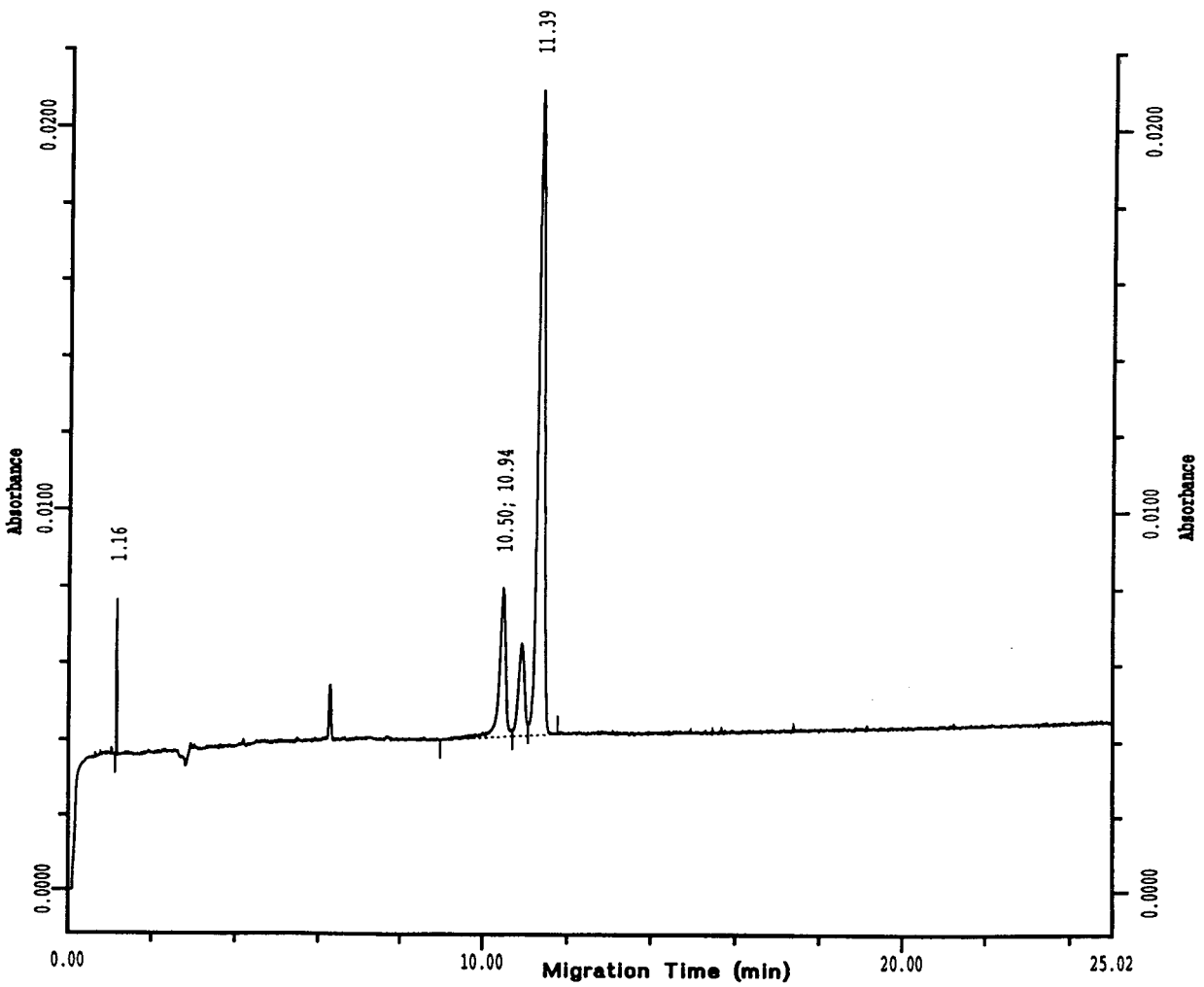

Fig. 1. Electropherogram of six cardiovascular drugs using an electrophoresis buffer of 100 m*M* borate buffer pH 8.1 containing 50 m*M* SDS. The identities of the peaks are as follows: atenolol 10.5 min, nifedipine 10.9 min and nicardipine, diltiazem, amlodipine and verapamil co-migrating at 11.4 min. Separation conditions are given under experimental.

was performed. For each separation performed for the mixture of the six cardiovascular drugs the individual standard solutions were injected under the same conditions to confirm the migration times.

2.3. Standard solutions

Stock solutions of each individual cardiovascular drug and a mixture of all six were prepared by dissolving the compounds in methanol–acetonitrile–water (1:1:2, v/v/v) at a concentration of 0.6 mg/ml. Dilution of the stock solutions was performed in 100 m*M* borate buffer pH 8.1 containing 50 m*M* SDS to give a final analyte concentration of 0.15 mg/ml.

3. Results and discussion

The separation of the six cardiovascular drugs was initially attempted using an electrophoresis buffer of 100 m*M* borate pH 8.1 containing 50 m*M* SDS. Fig. 1 shows the electropherogram, where the resolution of atenolol and nifedipine at 10.5 and 10.9 min was obtained but the remaining four compounds, nicardipine, diltiazem, amlodipine and verapamil co-migrated at 11.4 min.

In an attempt to achieve resolution of these four compounds the initial buffer of 100 m*M* borate pH 8.1 containing 50 m*M* SDS was modified by the addition of acetonitrile, methanol and acetone at concentrations of 5 and 10% (v/v). Fig. 2 shows the migration times of the six

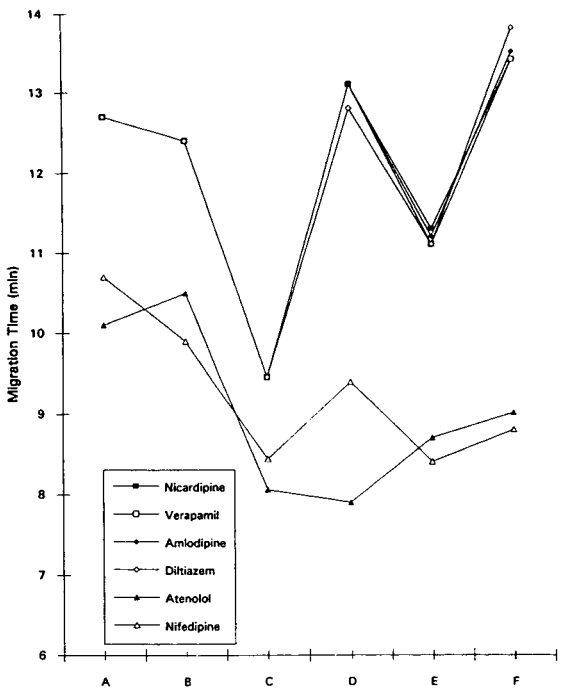

Fig. 2. The effect of organic modifiers on the migration times and separation of six cardiovascular drugs using electrophoresis buffers of 100 m*M* borate pH 8.1 containing 50 m*M* SDS with: A = 5% (v/v) methanol; B = 10% (v/v) methanol; C = 5% (v/v) acetonitrile; D = 10% (v/v) acetonitrile; E = 5% (v/v) acetone; F = 10% (v/v) acetone. All the separations were performed using the conditions described under Experimental.

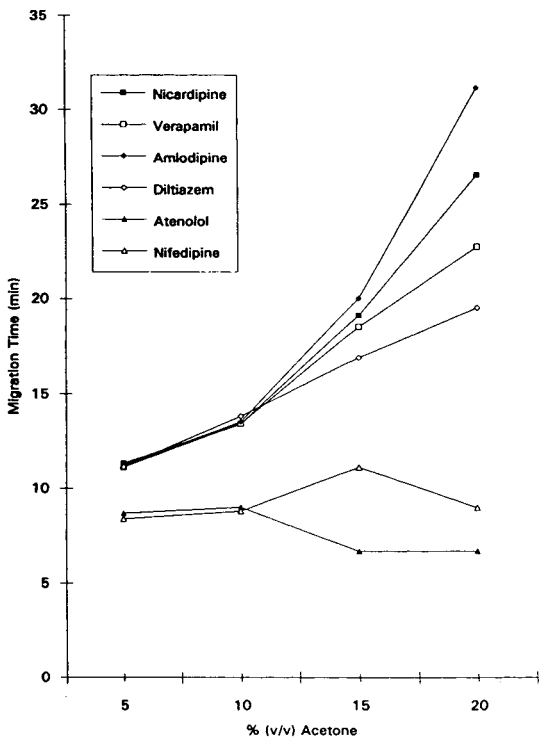

Fig. 3. Migration times of six cardiovascular drugs using electrophoresis buffers of 100 m*M* borate pH 8.1 containing 50 m*M* SDS and varying concentrations of acetone. All separations were performed using the conditions described under Experimental.

cardiovascular drugs when the buffers containing the organic modifiers were used.

Methanol has no effect on the electroosmotic flow showing migration times similar to the initial buffer system. Acetonitrile at 10% (v/v) increases the electroosmotic flow causing diltiazem to be resolved from the other three compounds. Acetone shows the greatest effect; at 5% (v/v) the electroosmotic flow has decreased but the separation capacity has increased showing resolution of amlodipine and nicardipine at 11.2 and 11.3 min but co-migration of verapamil and diltiazem at 11.1 min. At 10% (v/v) amlodipine and diltiazem at 13.5 and 13.8 min are resolved whereas the verapamil and nicardipine now co-migrate at 13.4 min.

Of the three organic modifiers acetone showed the greatest effect and so further electrophoresis buffers were prepared containing 15 and 20% (v/v) acetone.

Fig. 3 shows the effect on the migration times when increasing the acetone concentration from 5 to 20% (v/v). The optimum separation with respect to resolution and migration time was achieved with 15% (v/v) where the migration times are atenolol 6.7, nifedipine 11.1, diltiazem 16.9, verapamil 18.5, nicardipine 19.1 and amlodipine 20.0 mins.

Raising the acetone concentration to 20% (v/v) achieves increased resolution of the six drugs but with migration times in excess of 20 min for verapamil, nicardipine and amlodipine, this being considered an unacceptably long run time. The effect of varying the pH of the borate buffer and the concentration of SDS were then investigated.

Electrophoresis buffers were prepared containing 12.5, 25, 75 and 100 m*M* SDS with 100 m*M* borate buffer pH 8.1 and 15% (v/v) ace-

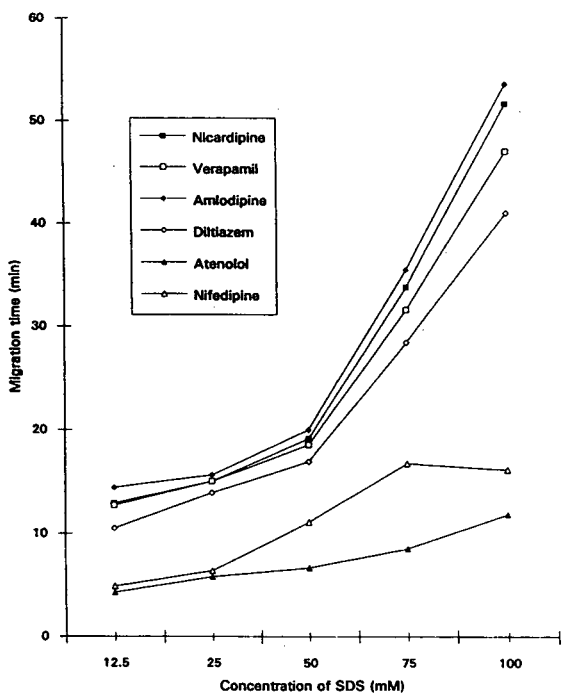

Fig. 4. The effect of varying the concentration of SDS using an electrophoresis buffer of 100 m*M* borate containing SDS and 15% (v/v) acetone. All separations were performed using the conditions described under Experimental.

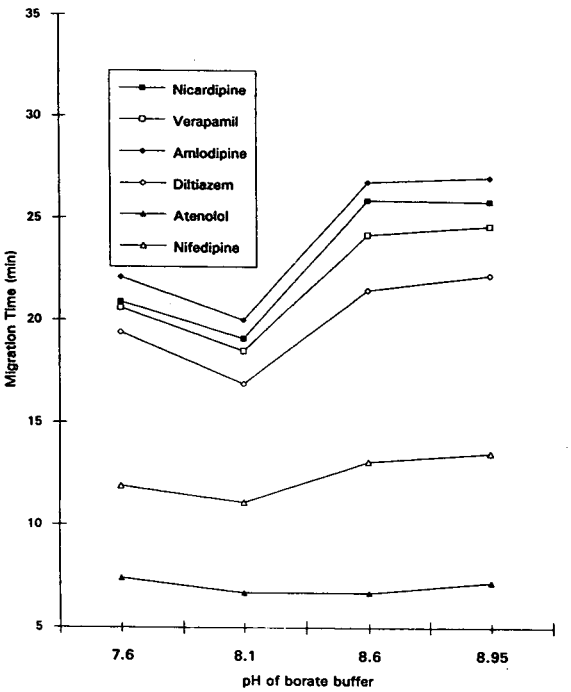

Fig. 5. Migration times of six cardiovascular drugs using an electrophoresis buffer of 100 m*M* borate buffer of varying pH containing 50 m*M* SDS and 15% (v/v) acetone. All separations were performed using the conditions described under Experimental.

tone. Fig. 4 shows the effect on the migration times of the six cardiovascular drugs. As the concentration of SDS increases the electroosmotic flow increases causing loss of peak shape due to band broadening and causing migration times to become greater than 25 min for diltiazem, nicardipine, verapamil and amlodipine.

To assess the effect of pH, electrophoresis buffers were prepared where the pH of the 100 m*M* borate buffer was 7.6, 8.1, 8.6 and 8.95 contained in 50 m*M* SDS and 15% (v/v) acetone. Fig. 5 shows the effect of pH on the migration times of the six cardiovascular drugs. As the pH of the borate buffer increases from 7.6 to 8.95, the migration times first decrease then after pH 8.1 show an increase, the separation being largely unchanged. Hence, pH 8.1 was considered to offer the optimum separation with respect to resolution and migration time.

4. Conclusions

Complete separation of the six analytes atenolol, verapamil, nifedipine, nicardipine, diltiazem and amlodipine proved difficult using MEKC with either of the commonly used organic modifiers acetonitrile or methanol. However, the use of acetone gave an increased selectivity emphasising the utility of this solvent as an organic modifier for MEKC.

By optimising the other operational parameters (the pH of the borate buffer, the SDS concentration and the concentration of organic modifier) an excellent separation of the six analytes was obtained (Fig. 6).

The separation illustrates the applicability of MEKC for the separation of a wide variety of low-molecular-mass analytes and should be considered as an alternative approach to HPLC.

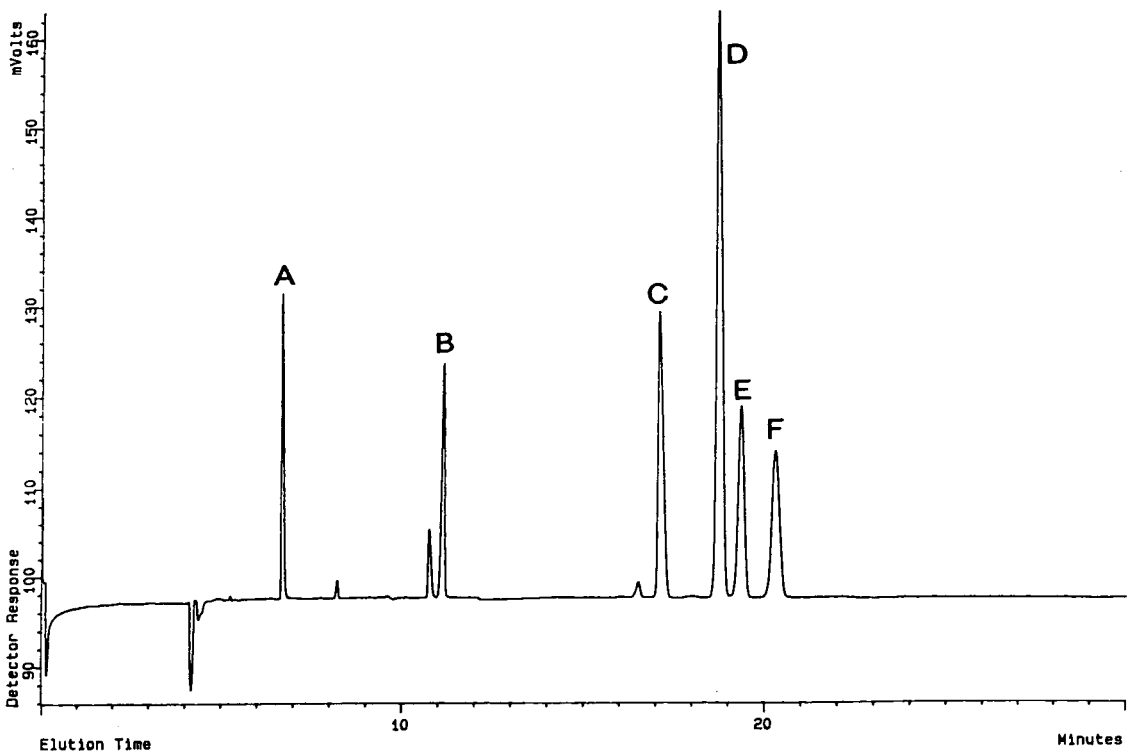

Fig. 6. An electropherogram showing the optimum separation of the six cardiovascular drugs using an electrophoresis buffer of 100 m*M* borate buffer pH 8.1 containing 50 m*M* SDS and 15% (v/v) acetone. A = atenolol; B = nifedipine; C = diltiazem; D = verapamil; E = nicardipine; F = amlodipine. The remaining separation conditions as described under Experimental.

References

[1] S. Terabe, K. Otsuka, K. Ichikava, A. Tsuchiya and T. Ando, *Anal. Chem.*, 56 (1984) 111.
[2] S. Terabe, K. Otsuka and T. Ando, *Anal. Chem.*, 57 (1985) 834.
[3] S. Terabe, *J. Pharm. Biomed. Anal.*, 10 (1992) 705.
[4] P. Lukkari, H. Vuorela and M.-L. Riekkola, *J. Chromatogr. A*, 655 (1993) 317.

ELSEVIER

Journal of Chromatography A, 700 (1995) 179–186

JOURNAL OF CHROMATOGRAPHY A

Rapid determination of drugs in biofluids by capillary electrophoresis
Measurement of antipyrine in saliva for pharmacokinetic studies

David Perrett*, Gordon A. Ross[1]

Department of Medicine, St. Bartholomew's Hospital Medical School, West Smithfield, London EC1A 7BE, UK

Abstract

A micellar electrokinetic capillary chromatography method was developed that permitted the resolution of antipyrine from endogenous compounds and its quantitation in neat saliva in as little as 1 min. Final conditions were: SpectraPhoresis 1000, 30(23) cm × 50 μm silica capillary, 50 m*M* sodium phosphate pH 9.6, 50 m*M* SDS, 10 s hydrodynamic load, detection scanning 200–300 nm or 260 nm, run 25 kV. To overcome the effects of Joule heating the capillary was cooled to 15°C. Sensitivity was < 10 μM and linearity extended to 350 μM. Comparison with an HPLC assay demonstrated that hydrodynamic injection gave a loading bias unless samples and standards were of equal viscosity. For 75 samples from five subjects the correlation of CE vs. HPLC was then $r = 0.99$.

1. Introduction

The need for quantification in therapeutic drug monitoring, pharmacokinetic and pharmacogenetic studies has generally precluded the use of electrophoretic techniques for such purposes. Such studies are currently performed using HPLC, GC or immunoassay. Additionally rapid analyses are required to deal with the large numbers of samples generated in many such clinical studies. In such instances the high efficiency and quantitation available with CE may provide an attractive alternative yet few commercial CE systems are optimised for rapid separations. Many published CE assays take as long if not longer than their HPLC equivalent.

Various options for high-speed drug analyses by CE are possible on commercial instruments without compromising sensitivity, which results from using very narrow capillaries for fast analyses. Firstly CE is capable of generating large numbers of theoretical plates but only a few thousand plates are usually required for many separations so the shortest possible capillary could be used. High pH buffers should be employed in order to generate a high and stable electroosmotic flow and if possible avoiding the need to routinely wash the capillary with alkali. High voltages can also be employed to give rapid separations but the effects of Joule heating must be avoided or compensated for. Overall analytical throughput can be increased significantly

* Corresponding author.

[1] Present address Hewlett-Packard GmbH, Waldbronn, Germany.

0021-9673/95/$09.50
SSDI 0021-9673(95)00101-8

by minimising sample preparation. Nakagawa et al. [1] introduced the concept of reducing the adverse effects of proteins from untreated biological samples on the separation by using sodium dodecyl sulphate (SDS) to solubilise proteins making it less likely that they will interact with the capillary wall.

The determination of liver function is of both clinical importance and necessary for an understanding of drug metabolism. Liver function is usually determined by the measurement of endogenous substances such as bilirubin but increasingly exogenous probes are being used. One widely used such probe substance is the analgesic antipyrine (phenazone, 1,5-dimethyl-2-phenyl-4-pyrazolin-3-one) (Fig. 1) which possesses physicochemical, biochemical and pharmacokinetic characteristics which make it ideal for probing liver function, hepatic oxidative metabolism and estimating total body water [2]. HPLC assays of antipyrine in urine [3], plasma [4] and saliva have been described. Quantifying antipyrine in plasma for pharmacokinetic work dictates either repeated venepuncture or an indwelling cannula in order to obtain samples; both these methods are uncomfortable for the patient and non-invasive sampling should be used wherever possible. Urinary measurements do not yield sufficient time points for accurate calculation of kinetics. Measuring antipyrine in saliva is considered to be the most practicable method since it is non-invasive and accurately reflects circulating antipyrine levels [5]. An HPLC assay for salivary antipyrine following extraction has been described [6].

The aims of this study were to investigate the potential of CE for high speed, high throughput analyses of biofluids by (a) developing a rapid CE assay for antipyrine suitable for use in pharmacokinetic studies using the principles outline above and (b) to compare the results from CE and HPLC analysis of antipyrine from a human study. Antipyrine had previously been separated by micellar electrokinetic capillary chromatography (MECC) since it had been used as an internal standard in assays for other compounds using 10 m*M* SDS [1,7].

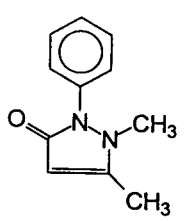

Fig. 1. Antipyrine.

2. Materials and methods

For all electrophoretic separations a SpectraPhoresis 1000 CE instrument (ThermoSeparations, Stone, UK) was used. All analyses were performed in uncoated silica capillary of either 44 (37 cm to detector) cm × 75 μm I.D. or 30 cm (23 cm to detector) × 50 μm I.D. (Polymicrotechnogies, USA). The window was located at the distances indicated from the anode. For the short capillary the capillary was passed by the shortest route from one electrode to the other in the cassette assembly. UV scanning detection over the range of 200 to 300 nm was performed. Hydrodynamic injection mode was used. The spectra of antipyrine showed a maxima at 200 nm and a plateau from 240 to 275 nm. Subsequent analyses, where identification was not critical, used fixed-wavelength detection (260 nm) for quantitation. Quantitation was based on spacial areas with multi-level external standards (see below). The separation was optimized as described below. Antipyrine was obtained from Sigma (Poole, UK)

2.1. Pharmacokinetic studies

Subjects were 11 medical students with a mean age of 23 years. After an overnight fast, 2 × 400 mg of antipyrine in gelatine capsules supplied by Pharmacy of St. Bartholomew's Hospital were administered orally. Saliva samples were obtained over the indicated time course (see for example Fig. 5). Saliva was collected by chewing on a cotton wad which was then placed in a salivary sampling tube (Salivette; Sarstedt, Leicester, UK). The tube was centrifuged for 5

min at 1000 *g* and saliva was collected at the bottom of the tube. Samples were frozen until analysis.

2.2. Final analytical conditions

MECC

Buffer: 25 m*M* sodium tetraborate, 50 m*M* SDS pH 9.6; detection: 260 nm; load: 10 s hydrodynamic; run 25 kV; 25°C. Aliquots (50 μl) of saliva were loaded onto the autosampler of the SpectraPhoresis 1000 CE instrument. The capillary was flushed for 30 s with 0.1 *M* NaOH and for 1 min with running buffer prior to each analysis.

HPLC

The reversed-phase HPLC assay was similar to that of Echizen et al. [6]. Conditions were: column 100 mm × 4.6 mm column packed with 5 μm ODS-Technosphere (HPLC Technology, Macclesfield, UK); eluent 50 m*M* sodium phosphate pH 6.0–acetonitrile (2:1, v/v) at a flow-rate of 1.5 ml/min; detection 260 nm. Injection volume was 20 μl.

Saliva samples for HPLC analysis were extracted with acetonitrile after phenacetin was added as internal standard and the mean recovery was 103.07% ($n = 47$). Maximum sensitivity was 100 n*M*.

3. Experimental

3.1. Effect of SDS concentration on antipyrine analysis

Using a 25 m*M* Na_2PO_4 pH 11 buffer in order to generate a high electroosmotic flow (EOF), the SDS concentration was varied from 5 to 50 m*M*. With 5 m*M* SDS antipyrine migrated just after the neutral marker in both water and saliva. With 10 m*M* SDS, antipyrine gave two peaks having the same spectra. At 25 and 50 m*M* SDS antipyrine appeared as a single peak in spiked saliva with efficiencies (N) of 88 800 and 78 750, respectively. Fig. 2 shows the effect of increasing SDS concentration on the relative migration time (t_m) of antipyrine to acetone (neutral marker). Although pH 11 gave good separations further work at this pH was not possible due to the considerable rise in baseline which occurred when SDS was dissolved in high-pH buffers.

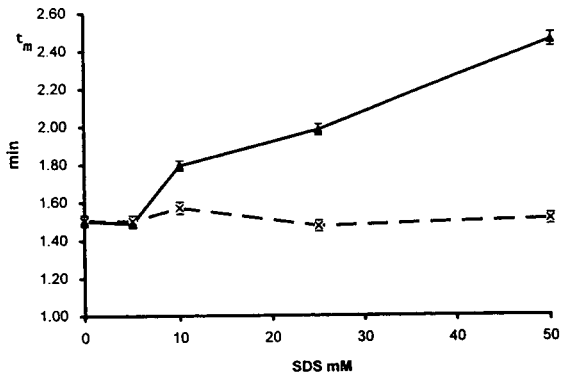

Fig. 2. Effects of increasing SDS concentration on MECC analysis of antipyrine. Conditions: buffer 25 m*M* Na_2HPO_4 pH 11.0; capillary 44 cm (37 cm to detector) × 50 μm I.D., bare fused silica; detection UV absorbance 260 nm; load 10 s hydrodynamic; run 25 kV; temperature 25°C. (——) Antipyrine; (– – –) acetone.

3.2. Effects of pH on MECC separation of antipyrine

While varying the pH it was considered prudent to maintain it at values giving a high but stable EOF. Buffers of pH 9.25, 9.4, 9.6, 9.8 and 10.1 were constructed using 25 m*M* sodium borate. Migration time, peak spatial areas and asymmetry were determined along with peak efficiencies (Table 1). The results indicated little change in the measured parameters over this pH range. The optimum pH was 9.6 which gave a rapid separation of antipyrine and reasonably efficiency. The analysis of antipyrine standards in water was linear over the range 0 to 200 μM ($r^2 = 0.998$).

3.3. MECC assay for antipyrine in saliva

Fig. 3 shows a MECC separation of saliva containing antipyrine at selected wavelengths

Table 1
Effect of pH on MECC analysis of antipyrine

pH	Efficiency (N)	Asymmetry	Migration time ($n = 3$)
9.25	44 521	1.66	3.15 (± 1.03% R.S.D.)
9.42	42 957	3.44	3.32 (± 1.10% R.S.D.)
9.60	43 346	1.44	2.54 (± 0.91% R.S.D.)
9.80	39 009	1.24	2.60 (± 0.98% R.S.D.)
10.10	45 357	1.54	2.67 (± 1.29% R.S.D.)

Analytical conditions except pH as in Fig. 3.

taken from a scanned electropherogram. Antipyrine was easily identified from its UV spectra and detection at 260 nm showed only one other peak, i.e. uric acid, which was identified by its characteristic maximum at 292 nm. It can also be seen that the saliva proteins while generally not absorbing at 260 nm had a strong absorption around 200 nm but these peaks were well resolved from antipyrine. The overall analysis time injection to injection was under 5 min.

Linearity of antipyrine assay

Calibrants were constructed using both saliva spiked with antipyrine and aqueous antipyrine standards. The assay was linear over the range 10 to 350 μM ($r = 0.96$). The limit of detection, calculated at $S/N = 2$, was 10 μM antipyrine for a 10-s injection. However on a number of occasions there were significant variations in the slope of the line e.g. 40.3 for aqueous standards and 27.1 for standards in saliva. This was apparently caused by variations in the viscosity of saliva reducing the amount injected compared to aqueous samples.

Intra-assay reproducibility

The reproducibility of the assay was investigated using saliva samples containing 21, 125 and 311 μM antipyrine. Antipyrine migration time reproducibility was 2.78 min (± 0.62% R.S.D.; $n = 6$). Spatial peak area reproducibility (R.S.D., $n = 4$) was 3.46, 2.42 and 2.47% at the three concentrations, respectively.

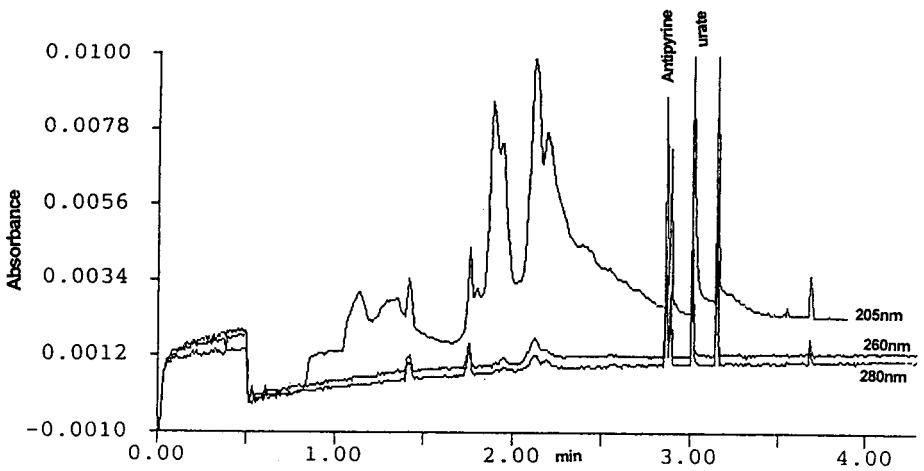

Fig. 3. UV scanning detection of antipyrine in saliva. Conditions: buffer 25 mM sodium borate, 50 mM SDS pH 9.6; capillary 44 cm (37 cm to detector) × 75 μm I.D., bare fused silica; load 10 s hydrodynamic; run 25 kV; temperature 25°C. Electropherograms displayed were selected from a 200–300 nm scan.

Recovery of antipyrine

A 10 m*M* antipyrine solution was diluted to give samples containing approximately 45, 90 and 140 μM antipyrine with water or blank saliva. All dilutions were performed by mass to avoid problems with pipetting saliva. There was no significant difference in the density of saliva compared to water. An aqueous standard curve was used to calculate the recovered concentrations. For aqueous samples there were no differences in the recoveries at the three levels and the mean recovery was 99.6% ± 4.8% R.S.D. (n = 15). The results for saliva are given in Table 2. This apparent difference in recovery compared to water was again considered to be due to the increased viscosity of saliva compared with water reducing the hydrodynamic load of the spiked saliva samples. Linear regression analysis of saliva samples gave a line with equation $y = 40.38x - 40.84$; $r^2 = 0.996$. In view of possible viscosity differences calibration curves in saliva were used for calculation of antipyrine concentrations in saliva samples.

3.4. Ultra-fast analysis of antipyrine

The analysis time may be decreased by increasing the field strength. With the 44-cm capillary, 25 kV gave a field strength of 568 V/cm; 30 kV increased this to 682 V/cm. Using a 30-cm capillary with 25 kV the field strength increases to 833 V/cm. A 30-cm capillary length is the shortest length possible with the capillary cassettes used in the SpectraPhoresis 1000. The separation length was consequently reduced to 23 cm with all other conditions unchanged.

The migration time of antipyrine decreased to 0.66 min (± 1.4% R.S.D.; n = 3). However, this was accompanied by a steadily increasing current from 100 to 250 μA, which caused an erratic baseline. Upon reducing the forced-air temperature to 15°C to counter the Joule heating these baseline irregularities disappeared, the current was stabilised and the migration time of increased to 0.72 min (± 1.13% R.S.D.; n = 3). Fig. 4 shows that the resolution of antipyrine from urate was maintained.

Table 2
Recovery of antipyrine in spiked saliva samples

Sample concentration (μM)	Calculated concentration (μM)	Recovery (%)
44.65	42.84	95.95
90.47	87.86	97.12
141.17	132.82	94.08

Analytical conditions as in Fig. 4.

4. Results

Complete antipyrine pharmacokinetic results by both MECC and HPLC analysis of saliva samples were obtained from five subjects. A typical time-course comparison in one subject is shown in Fig. 5. Correlation of results from CE and HPLC analysis for 75 samples when antipyrine was present above the limits of detection were in good agreement with a correlation of $r^2 = 0.967$ (CE = 1.05 · HPLC + 0.47) (Fig. 6).

5. Discussion

Fast analyses of suitable drugs by MECC is possible when all appropriate analytical parameters are optimised. In this study a fast assay of antipyrine using SDS-containing buffers was achieved which allowed a high throughput suitable for pharmacokinetic studies. Antipyrine had previously been separated by MECC when it was used as the internal standard in assay for cefpirimide in plasma using 10 m*M* SDS [1]. During the course of the study reported here two further assays for antipyrine have appeared. Brunner et al. [8] determined antipyrine in rat serum by MECC in a pH 8.2 buffer containing 50 m*M* SDS. Serum samples were extract prior to analysis. Wolfisberg et al. [9] measured antipyrine in human plasma without extraction using a borate/

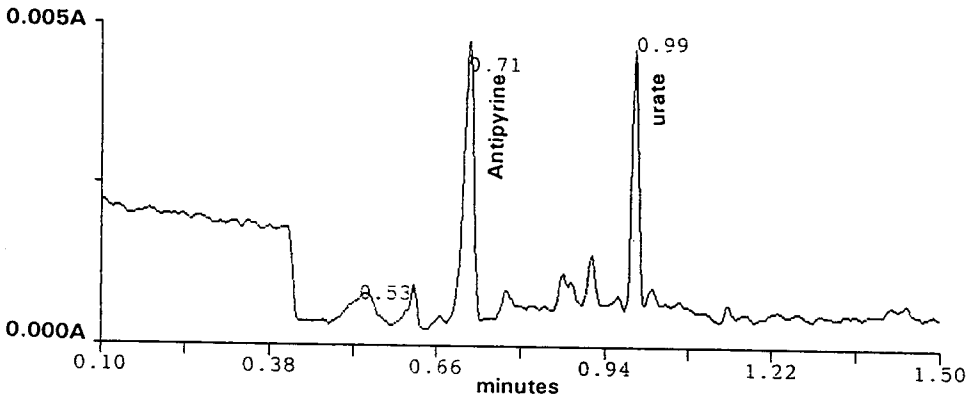

Fig. 4. Fast CE analysis of antipyrine in saliva. Conditions: buffer 25 m*M* sodium borate, 50 m*M* SDS pH 9.6; capillary 30 cm (23 cm to detector) × 50 μm I.D., bare fused silica; detection UV 200–300 nm; load 10 s hydrodynamic; run 25 kV; temperature 15°C.

phosphate buffer system pH ca. 8.1 with a run time of 6 min using a capillary configuration of 43 cm (to detector) × 75 μm with a vacuum load.

The main problems in developing this assay was the initial long term instability of the assay, either through the artefact developed from solubilising SDS in pH 11 buffer which produced an intractable baseline instability or through sample matrix effects. The final analytical conditions were selected not specifically with the analyte in mind but more with a view to minimise the effects of the sample matrix. Nishi et al. [10] reported a similar approach in the analysis of aspoxycillin in plasma using direct sample injection.

Establishing an ultra-fast separation of antipyrine using short capillaries was successful once the Joule heating effects had been compensated for. With the capillary held at nominally room temperature the power generated was 6.25 W, which would cause a calculated 38°C rise in electrolyte temperature within the capillary [11].

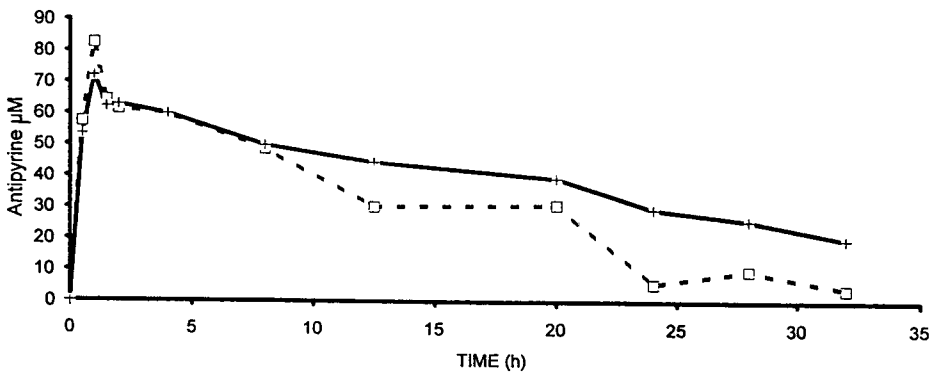

Fig. 5. Pharmacokinetic profile of antipyrine in a typical normal subject (J.R., male, 24 years). The concentrations of antipyrine shown were determined in the same saliva samples by both the rapid CE assay (broken line) and by the extracted HPLC assay (solid line).

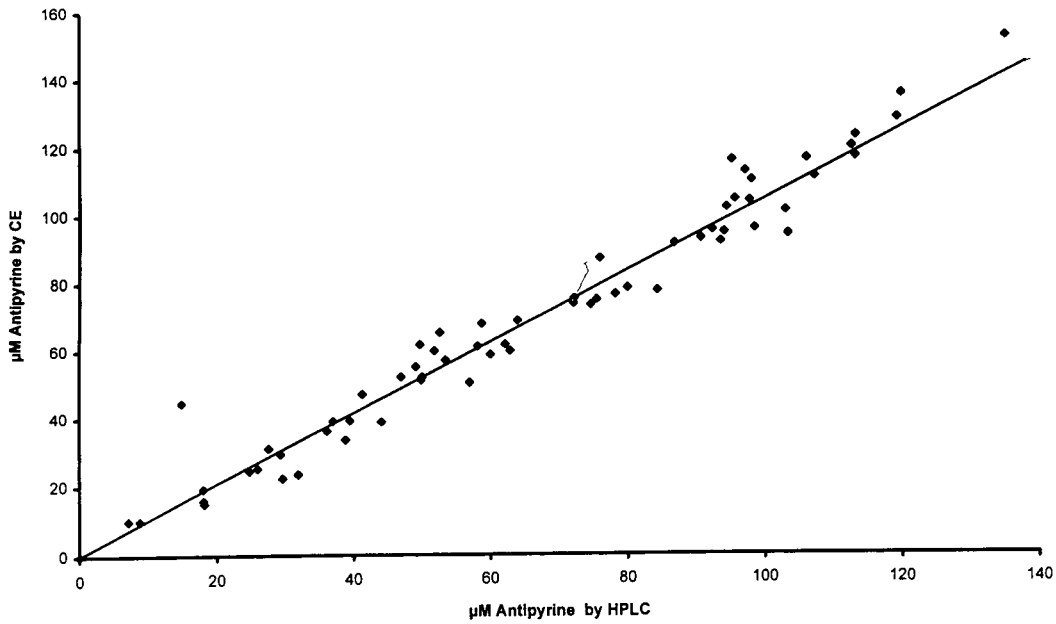

Fig. 6. Comparison of the saliva antipyrine levels as determined by CE and by HPLC in 75 samples. For assays methods see text.

Reducing the cassette temperature to 15°C by actively cooling the capillary, the current rise stabilised rapidly and the baseline was stable. Even with a cooled capillary, although the field strength had increased by 147% the velocity of antipyrine had increased by 245%, indicating that the apparent mobility of antipyrine had increased which was probably a consequence of the decreased electrolyte viscosity. A number of very fast CE assays have been demonstrated. These include the sample gating approach of Monnig and Jorgenson [12] and the separation of 30 ions in 90 s by capillary ion analysis [13]. However, few rapid assays of drugs or other analytes in biofluids have been published. With more appropriate design of instruments particularly those with cassette holders and suitable optimisation of electrolyte systems and sample preparation as reported here, it is clear that very fast routine analysis times are possible.

There appeared to be some association between SDS molecules and antipyrine since subcritical micelle concentration (CMC) some resolution of antipyrine from acetone, the neutral marker, occurred. Additionally pronounced peak splitting also occurred at SDS concentrations around the CMC (ca. 8.3 m*M*). At 25 m*M* SDS antipyrine appeared as a single peak with maximal efficiency. Peak efficiency at 50 m*M* SDS fell marginally. If the micellar concentration in the capillary was uniform no path effect would be observed and efficiency would be maximum. It may be that uniform micellar concentration was reached at 25 m*M* SDS. Most literature investigations of SDS MECC have used concentrations much greater than the CMC and the authors are aware of no other reports of peak splitting at sub- or ca. the CMC.

It is important to appreciate that possible viscosity variations between aqueous standards and neat sample when using hydrodynamic loading techniques can lead to incorrect quantitation. This was initially observed as differences between some MECC and HPLC results and confirmed by observation of differences in the slope of standard curves prepared in water and blank

saliva. Given a constant pressure difference the injected volume in hydrodynamic injection is inversely proportion to the sample viscosity of the sample [14] so less of a more viscous sample such as saliva will be injected compared to water. When using this technique it is therefore advisable to prepare standards in blank samples of the biofluid of interest. Although there was good overall agreement between the HPLC and CE assays some differences do occur, see time points above 12 h as in Fig. 5, and require comment. Firstly the analytical standards in the two assays were different since one was made up in a saliva pool. Secondly the CE assay which uses un-extracted saliva may give different data to the extracted HPLC in the presence of even weak binding to endogenous molecules.

The HPLC assay used here was twice as fast (ca. 4 min) than that of Echizen et al. [6]; however, the MECC assay was faster than either with the added benefit of having no sample preparation step. The MECC assay had a sensitivity which was adequate for the analyses being undertaken, although the HPLC assay was more sensitive with limit of detection at $S/N = 2$ of 100 nM.

6. Conclusions

A quantitative assay was established for antipyrine in saliva samples. Using MECC saliva samples could be injected directly without any prior sample extraction. This combination of minimal sample preparation and rapid analysis allowed a high sample throughput unlike many HPLC drug assays. There was an apparent association between SDS and antipyrine at an SDS concentration below the CMC. This indicated either a degree of hydrophobic interaction between antipyrine and SDS molecules or micellar formation within the capillary at concentrations below that of the CMC. MECC was used to minimise sample matrix effects rather than to effect separation of the analyte. In validating the assay attention must be given to the nature of the calibration standards especially where no internal standard is used. In comparison with an HPLC assay the CE assay was faster with the added benefit of having no sample preparation step and its sensitivity was adequate for the analyses being undertaken, although the HPLC assay was more sensitive. Sub-1 min analyses of antipyrine using short capillaries are possible if the Joule heating effects are effectively compensated for by actively cooling the capillary. Such rapid CE drug assays have the potential to rival enzyme-linked immunosorbent assay techniques in terms of overall throughput.

Acknowledgements

This work was supported by grants from the Joint Research Board of St. Bartholomew's Hospital and North East Thames Regional Health Authority (LORS Scheme).

References

[1] T. Nakagawa, Y. Oda, A. Shibukawa, H. Fukuda and H. Tanaka, *Chem. Pharm. Bull.*, 37 (1989) 707.
[2] F.F. Vickers, T.A. Bowman, B.H. Dvorchik, G.T. Passananti, D.M. Hughes and E.S. Vessell, *Drug Metab. Dispos.*, 17 (1989) 160.
[3] M.A. Sarkar, C. March and H.T. Karnes, *Biomed. Chromatogr.*, 6 (1992) 300.
[4] M.W.F. Teunissen, J.E. Meerbrug van der Torren, M.P.E. Vermeulen and D.D. Breimer, *J. Chromatogr.*, 278 (1988) 367.
[5] C.K. Svensson, *Clin. Pharmacol. Ther.*, 44 (1988) 365.
[6] H. Echizen, M. Nakura and I. Ishizaki, *J. Chromatogr.*, 526 (1990) 296.
[7] M. Miyake, A. Shiukawa and T. Nakagawa, *J. High Resolut. Chromatogr.*, 14 (1991) 180.
[8] L.J. Brunner, J.T. DiPiro and S. Feldman, *J. Chromatogr.*, 622 (1993) 98.
[9] H. Wolfisberg, A. Schmutz, R. Stotzer and W. Thormann, *J. Chromatogr. A*, 652 (1993) 407.
[10] H. Nishi, T. Fukayama and M. Matsuo, *J. Chromatogr.*, 515 (1990) 245.
[11] D.S. Burgi, K. Salomon and R.-L. Chien, *J. Liq. Chromatogr.*, 14 (1991) 847.
[12] C.A. Monnig and J.W. Jorgenson, *Anal. Chem.*, 63 (1991) 802.
[13] W.R. Jones and P. Jandik, *J. Chromatogr.*, 546 (1991) 445.
[14] R.A. Wallingford and A.G. Ewing, *Adv. Chromatogr.*, 29 (1989) 1.

ELSEVIER

Journal of Chromatography A, 700 (1995) 187–193

JOURNAL OF CHROMATOGRAPHY A

Comparison of high-performance liquid chromatography and capillary electrophoresis for the determination of some bee venom components

V. Pacáková[a,*], K. Štulík[a], Pham Thi Hau[a], I. Jelínek[a], I. Vinš[b,1], D. Sýkora[b,2]

[a]*Department of Analytical Chemistry, Charles University, Albertov 2030, 128 40 Prague 2, Czech Republic*

[b]*Tessek Ltd., Stránčická 33, 100 00 Prague 10, Czech Republic*

Abstract

HPLC and capillary electrophoretic (CE) methods were compared for the determination of phospholipase A_2 and melittin in bee venom. Size-exclusion chromatography on a Tessek Separon HEMA-BIO 40 column requires the use of a denaturing eluent (0.2% trifluoroacetic acid in 20% acetonitrile) to overcome non-specific interactions of some components, e.g., melittin. Reversed-phase HPLC on a HEMA-BIO 1000 C_{18} column with gradient elution using water–acetonitrile mobile phases containing trifluoroacetic acid and UV spectrophotometric detection at 215 nm permits the identification and determination of the main bee venom components and their preparative chromatography. CE analysis for bee venom components is optimum with electrolyte system of 150 m*M* phosphoric acid (pH 1.8) with UV spectrophotometric detection at 190 nm. In comparison with HPLC, the CE method is cheaper and faster (6 min vs. 45 min) and the separation is more efficient.

1. Introduction

The effects of bee venom have been known since prehistoric times, but its composition was established only 10–20 years ago [1,2]. It contains low-molecular-mass components, e.g., histamine (M_r 111, 0.1–1.5%), oligopeptides (M_r 200–1000), phospholipids and saccharides (about 25%), polypeptides, e.g., melittin (M_r 2840, 50% of dry venom), neurotoxic apamine (M_r 2038, 2%) and a mast cell degranulating (MCD) peptide (M_r 2593, 2%), and proteins e.g., phospholipase A_2 (M_r 19 000, 12–15%) and hyaluronidase (M_r 45 000–50 000, 1–3%). Whereas phospholipase and hyaluronidase (and also melittin, slightly) are allergens, the polypeptides are highly toxic.

Many methods have been described for characterization of bee venom, (e.g., [3–12]), including biological tests, chemical approaches based on typical protein reactions and separation techniques. Common preparative and analytical methods, such as gel filtration, ion-exchange chromatography and sodium dodecyl sulphate polyacrylamide gel electrophoresis (SDS-PAGE), are relatively time consuming and, therefore, are often replaced by high-performance liquid chromatography (HPLC) [4–11], whose principal advantages are speed of analysis (about 30 min) and high separation efficiency.

* Corresponding author.

[1] Present address: Watrex, Hošt'álkova 42, 169 00 Prague 6, Czech Republic.

[2] Present address: Department of Analytical Chemistry, Institute of Chemical Technology, Technická 5, 166 28 Prague 6, Czech Republic.

0021-9673/95/$09.50
SSDI 0021-9673(94)01170-2

Capillary electrophoresis (CE), although widely used for the separation and analysis of complex biological products, has not yet been used for this purpose. This paper deals with the identification and determination of predominant bee venom components using HPLC on new polymeric, biocompatible stationary phases and CE and critically compares these two approaches.

2. Experimental

2.1. Chemicals

Dry bee venom samples from various sources (Czech Republic, Russian Federation, Bulgaria) and fractions isolated by size-exclusion chromatography were obtained from Sevac (Prague, Czech Republic). Standard samples of phospholipase A_2 (isolated from bee venom), melittin (purity 86% by HPLC) and hyaluronidase (isolated from bovine testes) and molecular mass standards human serum albumin (HSA) (68 459), bovine serum albumin (BSA), ovalbumin (45 000), myoglobin (17 400), cytochrome *c* (13 500), ribonuclease A (13 700), aprotinin (6500), vitamin B_{12} (1355.4) and cytidine-5-monophosphate (340) were obtained from Sigma (St. Louis, MO, USA).

All other chemicals were of analytical-reagent grade from Lachema (Brno, Czech Republic) and were used as received.

2.2. Instrumentation and experimental conditions

HPLC measurements were performed using a PU 4100 LC liquid chromatograph, with a PU 4110 variable-wavelength UV–Vis detector (Philips Pye Unicam, Cambridge, UK) and a Model 7125 injector (Rheodyne, Cotati, CA, USA). The data were collected and processed using a CSW data station (DataApex, Prague, Czech Republic).

For size-exclusion chromatography (SEC), a steel column (250 mm × 8 mm I.D.) containing Separon HEMA-BIO 40, 10 μm (Tessek, Prague, Czech Republic) was used at a flow-rate of 0.5 ml/min, with UV absorbance detection at 215 nm. The mobile phases consisted of 0.1 *M* phosphate buffer (pH 7.0) or 0.2% trifluoroacetic acid (TFA) in 20% acetonitrile (ACN).

For reversed-phase chromatography (RP-HPLC) with gradient elution, a Compact Glass Cartridge (CGC) column (150 mm × 3.3 mm I.D.) packed with Separon HEMA-BIO 1000 C_{18}, 10 μm (Tessek) was used at a flow-rate of 0.5 ml/min, with UV absorbance detection at 215 nm. Eluent A was 0.22% TFA in water, eluent B was 0.2% TFA in acetonitrile. The gradient was linear from 0 to 50% B in 20 min, followed by a rise to 100% B in 5 min. After 5 min at 100% B, resetting followed to 0% B in 1 min and re-equilibration for 14 min. The column was thermostated at 37°C. Preparative separation was performed on a steel column (80 mm × 8 mm I.D.) packed with the same sorbent. The conditions were the same except for a flow-rate of 1 ml/min and a gradient time of 40 min.

Capillary electrophoresis (CE) was carried out on a Crystal CE Model 310 instrument, with a variable-wavelength UV spectrophotometric detector (ATI Unicam, Cambridge, UK). The total length of the fused-silica capillary (L_c) was 75 cm, the length to the detector (L_D) was 60 cm and the I.D. was 75 μm. A constant potential of 20 kV was applied. UV spectrophotometric detection was used at 205 or 190 nm depending on the composition of the electrolyte system. The electrolyte systems consisted of (A) 20 m*M* phosphate buffer (pH 5.0), (B) 20 m*M* Tris buffer–50 m*M* SDS (pH 9.0) and (C) 150 m*M* phosphoric acid (pH 1.8)

The calibration plots for HPLC were prepared by injecting standard mixtures of phospholipase and melittin in the running mobile phase at concentrations of 0.125, 0.20, 0.25 and 0.5 mg/ml. Solutions of Czech, Russian and Bulgarian bee venom were prepared by dissolving 5 mg of the dried material in 1 ml of mobile phase and diluting tenfold before injection. Volumes of 10 μl were injected manually with a 25-μl syringe (Hamilton, Reno, NV, USA). The standards for

the calibration plots and samples of bee venom for CE were dissolved in deionized water at a concentration of 1 mg/ml and diluted before use. Samples were injected pneumatically for 6 s at an overpressure of 30 mbar.

3. Results and discussion

3.1. Size-exclusion chromatography

One of the common methods for the separation of bee venom components, used also for preparative purposes, is size-exclusion chromatography on soft, hydrophilic gels such as Sephadex G-50 [9]. These separations are slow and have poor efficiency. Separations on rigid, macroporous sorbents suitable for high-performance size-exclusion chromatography (HP-SEC) can significantly speed up the analysis. We tried to use the HEMA-BIO 40 sorbent, an additionally hydrophilized hydroxyethyl methacrylate–ethylene dimethacrylate-based macroporous copolymer with an exclusion limit of M_r 40 000–70 000. The separation on this sorbent was found to be strongly affected by its interactions with the analytes. Under common conditions (0.1 *M* phosphate buffer, pH 7), when the standard globular proteins yielded acceptably linear calibration plots, phospholipase was eluted later than expected on the basis of its molecular mass and melittin and some other components were strongly retained (Fig. 1). Polypeptides and proteins usually have a hydrophobic interior covered by a largely hydrophilic shell. In bee venom, the strongly basic melittin has hydrophilic residues unevenly distributed and therefore such a shell cannot be formed [10]. This characteristic was probably the main cause of the strong retention of melittin. We attempted to eliminate the interactions by adding an organic solvent to the mobile phase and decreasing the pH. Finally, a mobile phase containing 20% acetonitrile and 0.2% TFA yielded a separation according to molecular mass (Fig. 2). Previous results [6,13] indicate similar problems on other polymeric HP-SEC sorbents.

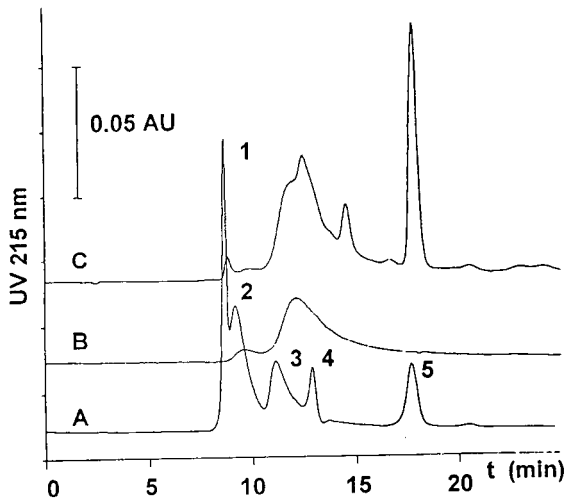

Fig. 1. HPLC separation of bee venom components by SEC. Column, 250 mm × 8 mm I.D. Separon HEMA-BIO 40 (10 μm); mobile phase, 0.1 *M* phosphate buffer (pH 7.0); detection, UV at 215 nm; injection volume, 20 μl. (A) Protein standard mixture: 1 = thyroglobulin; 2 = bovine serum albumin; 3 = cytochrome *c*; 4 = cytidine-5-monophosphate; 5 = low-molecular-mass impurity. (B) Phospholipase A, fraction V, by RP-HPLC. (C) Czech bee venom, 1.0 mg/ml.

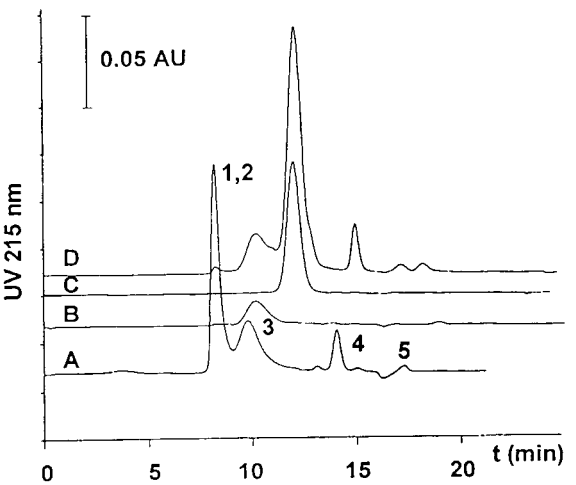

Fig. 2. HPLC separation of bee venom components by SEC. Column, 250 mm × 8 mm I.D. Separon HEMA-BIO 40 (10 μm); mobile phase, 0.2% TFA in 20% ACN; detection, UV at 215 nm; injection volume, 20 μl. (A) Protein standard mixture: 1 = thyroglobulin; 2 = bovine serum albumin; 3 = cytochrome *c*; 4 = cytidine monophosphate; 5 = low-molecular-mass impurity, 1.0 mg/ml. (B) Phospholipase A. (C) Melittin. (D) Czech bee venom.

3.2. Reversed-phase chromatography

Reversed-phase chromatography with gradient elution is usually the method of choice for separating mixtures of proteins and peptides. Melittin was not eluted from a common silica-based reversed-phase sorbent (Separon SGX C_{18}), probably owing to its interactions with residual silanol groups. A very good separation of phospholipase and melittin was achieved on a polymer-based reversed-phase sorbent, Separon HEMA-BIO 1000 C_{18} (150 mm × 3.3 mm I.D. column). Gradient elution (see Fig. 3) allowed the resolution of venom components with retention times of 14.24 min for phospholipase and 18.12 min for melittin. Owing to the lack of a suitable standard we were not able to identify hyaluronidase. The hyaluronidase standard from Sigma gave a very complex array of peaks, the reason for this apparently being its completely different origin (bovine testes).

Preparative isolation of venom components was performed on an 80 mm × 8 mm I.D. steel column packed with Separon HEMA-S 1000 C_{18} (10 μm) sorbent with 5 and 20 mg of bee venom. Seven fractions were collected and evaluated for enzyme activity (Fig. 4). Fraction V was identified as phospholipase with a high activity and fraction VI was identified as melittin. An amount of 4 mg of phospholipase was obtained after lyophilization of pooled fractions from both runs. Hyaluronidase activity was not found in any collected fraction. Probably hyaluronidase was not stable under the separation conditions used.

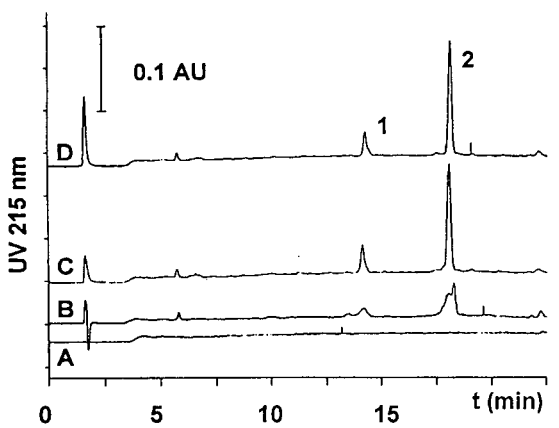

Fig. 3. HPLC separation of the components in Czech, Russian and Bulgarian bee venoms by RP-HPLC. CGC column, 150 mm × 3.3 mm I.D. HEMA-BIO 1000 C_{18} (10 μm); Eluent A, 0.22% TFA in water; eluent B, 0.2% TFA in ACN; gradient from 0 to 50% B in 20 min, from 50% to 100% B in 5 min. Detection, UV at 215 nm, 0.5 AUFS; injection volume, 10 μl of 0.5 mg/ml bee venom solution. (A) Blank run; (B) venom from Bulgaria; (C) venom from Russian Federation; (D) venom from Czech Republic. Peaks: 1 = phospholipase A_2; 2 = melittin.

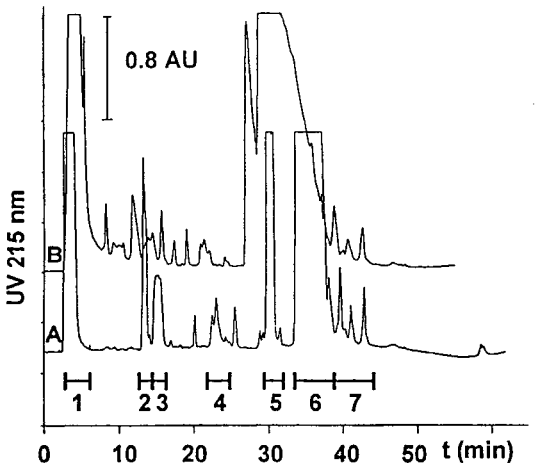

Fig. 4. Preparative HPLC separation of components in Czech bee venom by RP-HPLC. Steel column, 80 mm × 8 mm I.D. HEMA-BIO 1000 C_{18} (10 μm). Eluent A, 0.22% TFA in water; eluent B, 0.2% TFA in ACN; gradient from 0 to 50% B in 40 min, from 50% to 100% B in 5 min. Detection, UV at 215 nm, 2.0 AUFS. Injection: (A) 5 mg in 1 ml; (B) 20 mg in 2 ml.

3.3. Capillary electrophoresis

CE has been established as a very efficient and convenient method for the separation of peptides and proteins. Therefore, we tested it for the quantitative analysis of bee venom. Different electrolyte systems were evaluated (Fig. 5). First, 20 m*M* phosphate buffer (pH 5.0) was used (system A). The separation of bee venom components was satisfactory and venom samples of different origin could be distinguished, but the sensitivity of measurement gradually decreased during the analyses owing to adsorption of pro-

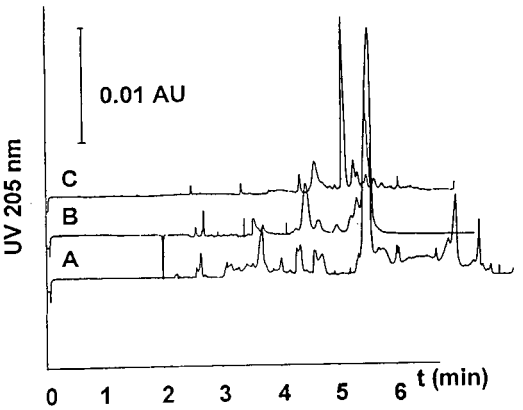

Fig. 5. Comparison of different electrolyte systems for CE separation of components in Czech bee venom. (A) 20 m*M* phosphate (pH 5.0); (B) 20 mM Tris–50 m*M* SDS (pH 9.0); (C) 150 m*M* phosphoric acid (pH 1.8). For other conditions, see Experimental.

teins on the column wall. Washing the capillary with NaOH after each injection did not improve the results.

With 20 m*M* Tris buffer–50 m*M* SDS (pH 9.0), as the electrolyte (system B), problems similar to those with phosphate buffer were encountered. The components could be distinguished but the peaks were broader.

Finally, a 150 m*M* phosphoric acid electrolyte system of pH 1.8 (system C) gave the best results. Undesirable effects of solute adsorption on the capillary wall were not observed. The precision of the measurement was very good (see Table 2). The low absorbance of this eluent even permitted the more sensitive UV detection at 190 nm. Two main components, phospholipase A_2 and melittin, were identified on the basis of peak matching with the standard solutes (Fig. 6). The resolving power of CE for phospholipase is demonstrated in Fig. 7. The standard from Sigma, apparently homogeneous with a minor impurity according to HPLC measurements, shows the presence of at least three different components, the main component amounting to only ca. 85%. Hyaluronidase could not be identified as no standard isolated from bee venom was available (cf., the analogous situation in HPLC measurements).

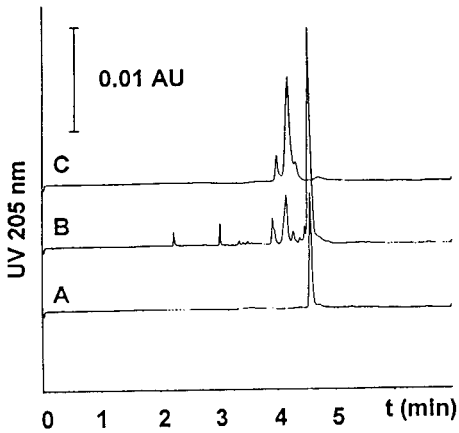

Fig. 6. CE identification of bee venom components. Electrolyte, 150 m*M* phosphoric acid (pH 1.8). (A) Melittin; (B) extract of Czech bee venom; (C) phospholipase. For other conditions, see Experimental.

3.4. Quantitative analysis

Quantitative analysis was performed using absolute calibration with standard solutions of phospholipase and melittin. The results obtained by RP-HPLC are given in Table 1. All the three bee venoms have similar contents of phospholip-

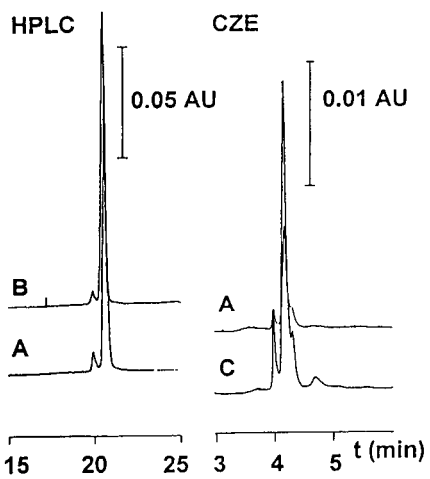

Fig. 7. Determination of phospholipase purity by RP-HPLC and CE. Conditions for RP-HPLC as in Fig. 3 and for CE as in Fig. 6. (A) Phospholipase A_2 standard (Sigma); (B) isolated by RP-HPLC; (C) isolated by SEC on Sephadex G-10.

Table 1
Comparison of determination of phospholipase A_2 and melittin in different bee venoms by RP-HPLC and CE

Bee venom	Content (%) ($n = 5$)			
	Phospholipase A_2		Melittin	
	RP-HPLC	CE[a]	RP-HPLC	CE[a]
Czech	15.4	14.5	41.6	46.5
Russian	17.1	15.8	42.9	47.3
Bulgarian	–	15.2	–	47.9

[a] CE with electrolyte system (C).

ase and melittin. The HPLC and CE analyses correlate for the Czech and Russian samples. However, the HPLC analysis of the Bulgarian sample yielded unresolved peaks and for this reason the HPLC results for Bulgarian bee venom could not be compared with those obtained by the CE method. The differences among venoms from individual honeybees were studied recently [12].

The parameters of RP-HPLC and CE analysis are given in Table 2. The lower precision of the HPLC method was probably caused by using manual injection; the use of an overfilled loop or an autosampler would probably lead to a precision comparable to that of CE. The detection limits were calculated as the ratio of three times the standard deviation of the peak-to-peak noise, s_{xy}, and the slope of the calibration plot, $3s_{xy}/S$. The concentration detection limit for the HPLC method was calculated for a 10-μl injection, however, it can be decreased to a certain extent by using larger injection volumes. The system used (gradient reversed phase of proteins) will tolerate large injection volumes (up to several ml) without an adverse effect on the resolution provided that the sample is dissolved in a low-strength eluent (aqueous TFA in this instance). The solutes are retained at the top of the column until the strength of the eluent increases sufficiently to elute them. This permits a very efficient preconcentration.

4. Conclusions

The results obtained indicate that both HPLC and CE can be readily used to differentiate bee venoms obtained from different sources. However, identification of individual components is often prevented by the lack of suitable standard compounds (standards obtained from materials other than bee venom may have completely different compositions). Size-exclusion chromatography can be used for the rough characterization of bee venom, but its separation efficiency is insufficient for quantitative purposes. Reversed-phase HPLC gives satisfactory results, using gradient elution on a polymer-based C_{18} station-

Table 2
Comparison of the parameters for Czech bee venom by RP-HPLC and CE

Analytical Parameter	RP-HPLC		CE[a]	
	Phospholipase A_2	Melittin	Phospholipase A_2	Melittin
R.S.D. (%)				
Peak area	5.2	2.8	2.1	1.5
Retention time	1.4	1.0	6.5	5.6
Detection limit:				
ng	56	30	0.4	0.15
μg/ml	5.6	3	4.5	1.6
Linear dynamic range (orders of analyte concentration)	3		2	
Analysis time (min)	45		6	

[a] CE with electrolyte system (C).

ary phase, which is suitable for the separation of strongly basic polypeptides and stable over a wide pH range.

Compared with the HPLC method, the CE analysis described is faster, the separation efficiency is better and the running costs are much lower. The precision and detection limits of the CE measurements are better than or comparable to those obtained by gradient elution in HPLC (see Table 2). The main advantage of CE over HPLC is the better resolution, permitting quantification even in cases when HPLC fails. Therefore, CE seems to be generally preferable to HPLC for bee venom analyses.

Acknowledgements

We are indebted to Dr. B. Hochová of Sevac, Prague, for the bee venom samples and the melittin, phospholipase and hyaluronidase standards. Unicam is thanked for kindly providing us with a demonstration capillary zone electrophoresis instrument.

References

[1] E. Habermann, *Science*, 177 (1972) 314.
[2] R. Mueller, *Insektenstichallergie, Klinik, Diagnostik und Therapie*, Fischer, Stuttgart, 1988.
[3] E. Habermann and K.G. Reiz, *Biochem. Z.*, 341 (1965) 451.
[4] B.E.C. Banks, C.E. Dempsey, F.L. Pearce, C.A. Vernon and T.E. Wholley, *Anal. Biochem.*, 116 (1981) 48.
[5] G.W. Shepherd, E.B. Elliott and C.E. Arbesman, *Prep. Biochem.*, 41 (1974) 71.
[6] B. Renck and R. Einarsson, *J. Chromatogr.*, 197 (1980) 278.
[7] R. Einarsson, *Acta Chem. Scand., Ser. B*, 37 (1983) 252.
[8] R. Einarsson and B. Renck, *Toxicol. (Toxicon)*, 221 (1984) 154.
[9] K. Raeder, A. Wildfeuer, F. Wintersberger, P. Bossinger and W. Muecke, *J. Chromagtogr.*, 408 (1987) 341.
[10] M.T. Tosteson, J.J. Levy, L.H. Caporale, M. Rosenblatt and D.C. Tosteson, *Biochemistry*, 26 (1987) 6627.
[11] E.M. Dotimas, K.R. Hamid, R.C. Hider and U. Ragnarsson, *Biochim. Biophys. Acta*, 911 (1987) 285.
[12] M.J. Schumacher, J.O. Schmidt, N.B. Egen and K.A. Dillon, *J. Allergy Clin. Immunol.*, 90 (1992) 59.
[13] E. Perez-Paya, L. Braco, C. Abad and J. DuFourcq, *J. Chromatogr.*, 548 (1991) 351.

ELSEVIER

Journal of Chromatography A, 700 (1995) 195–200

JOURNAL OF CHROMATOGRAPHY A

Separation of sulfonylurea metabolites in water by capillary electrophoresis

Giovanni Dinelli*, Alberto Vicari, Alessandra Bonetti

Dipartimento di Agronomia, Università di Bologna, via F. Re 6/8, I-40126 Bologna, Italy

Abstract

The potential of capillary electrophoresis (CE) for the separation and detection of the metabolites of nine sulfonylurea herbicides in aqueous solution was evaluated. A relationship between the structure of the sulfonylureas tested and the metabolites formed was found: the non-*o*-benzene-substituted sulfonylurea rimsulfuron gave only one metabolite, whereas the other eight, *o*-benzene-substituted, sulfonylureas gave 4–6 metabolites. CE was confirmed to be a very efficient separation technique, suitable for the determination of sulfonylurea herbicides and their metabolites formed during hydrolysis.

1. Introduction

Sulfonylurea herbicides are widely used to control weeds in agricultural crops such as wheat, maize, soybean, sugarbeet and rice. The first sulfonylurea, chlorsulfuron, was marketed in USA in 1982. Worldwide, nineteen sulfonylurea herbicides had been commercialized by 1994, and five more are being developed. This rapid increase is due to their activity at low application rates (2–60 g ha^{-1}) and their low mammalian toxicity [1].

In recent years, because of the increased herbicide degradation product analysis requirements for pesticide registration, considerable interest has been generated concerning the detection and separation of herbicide metabolites. The most important degradation pathways of sulfonylureas are chemical hydrolysis and microbial breakdown [2,3]. Although several experiments have shown that sulfonylureas degrade to many compounds in water and soil [4–6], not many methods for the separation of sulfonylurea metabolites have been described. Sabadie and Bastide [5,6] and Harvey et al. [7], using HPLC, separated several hydrolytic metabolites of chlorsulfuron, metsulfuron and sulfometuron. Shalaby et al. [8] described the use of LC–MS thermospray for nicosulfuron and rimsulfuron and a major metabolite of each in soil. However, little information is available on the detection and separation of metabolites formed during the hydrolysis of most sulfonylureas. Because hydrolysis is a major pathway of degradation of sulfonylureas, investigations on metabolites formed during hydrolysis should provide basic information on their general behaviour.

A simple and reproducible method was needed for the determination of sulfonylurea metabolites in water samples. In a previous paper [9], we reported the detection and separation of the hydrolytic breakdown products of metsulfuron by capillary electrophoresis (CE) and their structural identification by GC–MS.

* Corresponding author.

0021-9673/95/$09.50
SSDI 0021-9673(94)01168-0

The objectives of this study were to confirm the potential of CE for the detection and separation of the breakdown products of nine sulfonylureas in aqueous solution and to evaluate the dynamics of metabolite formation for each sulfonylurea.

2. Experimental

2.1. Reagents

Reagents for CE analysis were supplied by Sigma (St. Louis, MO, USA). All solvents used were of pesticide-free grade. The nine sulfonylureas studied were chlorsulfuron, metsulfuron, triasulfuron, ethametsulfuron, CGA 152'005, tribenuron, bensulfuron, chlorimuron and rimsulfuron. They were extracted from commercial products by Soxhlet extraction with freshly redistilled dichloromethane for 3 h. After drying with anhydrous sodium sulfate, dichloromethane was distilled off in a rotary evaporator. The residual sulfonylureas were subjected to nuclear NMR, IR and MS analyses to confirm their identity and were used in subsequent experiments without further purification, as reported by Galletti et al. [10].

2.2. Water samples fortification

The solutions were prepared using distilled water. Duplicate 50-ml water samples, each containing 25 mg l^{-1} of each sulfonylurea in 10 m*M* $NaHCO_3$, were buffered to pH 4 with 0.1 *M* HCl. The solutions were kept in the dark at 55°C in closed vials. Samples of 1 ml were taken from each vial at different times during a 10-h period and stored at −12°C until analysed.

2.3. Capillary electrophoresis

Aqueous samples were analysed directly by CE. Separation of herbicides and metabolites were performed using the micellar electrokinetic capillary chromatography with a P/ACE system from Beckman (Palo Alto, CA, USA). Separations were effected with a fused-silica capillary 50 cm long (from injection point to detector) × 75 μm I.D. at a constant temperature of 25°C. The applied voltage was 25 kV, with an injection pressure of $3.44 \cdot 10^3$ Pa for 10 s, corresponding to an injection volume of 60 nl. The electrolyte buffer was 50 m*M* sodium borate–22 m*M* sodium dodecylsulfate–10% (v/v) methanol (pH 8.0). The separation efficiency was measured by the number of theoretical plates (N) according to the equation $N = 5.54\ (t_R/w)^2$, where t_R is the retention time of a compound and w is the peak width at half-height [11]. Peak area was used for residue quantification. The degradation rate of each sulfonylurea was determined by linear regression of the natural logarithm of percentage of parent herbicide remaining against time and the slope of each line was compared with analysis of variance.

3. Results and discussion

The structures and molecular masses of the sulfonylureas studied are reported in Fig. 1. Three moieties characterize the general structure: an aryl group, the sulfonylurea bridge and a nitrogen-containing heterocycle. Chlorsulfuron, metsulfuron, triasulfuron, ethametsulfuron, CGA 152'005 and tribenuron have a triazinic heterocycle group and are *o*-benzene-substituted; bensulfuron and chlorimuron have a diazinic heterocycle group and are *o*-benzene-substituted; and rimsulfuron has a diazinic heterocycle group but is not *o*-benzene-substituted.

The electropherograms of chlorsulfuron at three sampling times (0, 2 and 10 h after incubation) are shown in Fig. 2, as an example of sulfonylurea hydrolysis. Chlorsulfuron degradation in water led to the formation of six metabolites, numbered according to their increasing retention times. The electropherograms evidence the effectiveness of the separation, as suggested by the column efficiency, ranging between 50 000 and 163 000 theoretical plates.

The retention times of each parent herbicide and their metabolites are shown in Table 1. The metabolites of each sulfonylurea were arbitrarily numbered according to their increasing retention

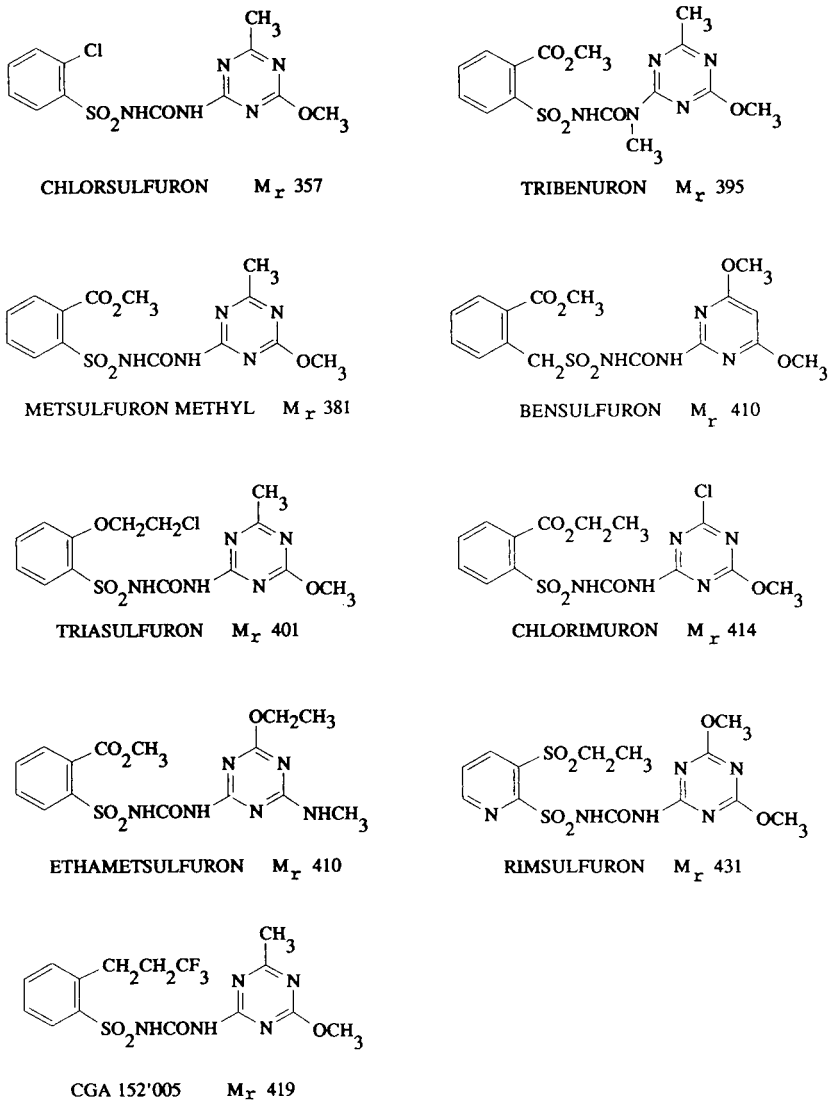

Fig. 1. Structures and molecular mass of the sulfonylureas studied.

times. The number of metabolites formed during hydrolysis appeared to be related to the structure of the sulfonylurea. The sulfonylureas characterized by a triazinic heterocycle and *o*-benzene substitution decomposed in water, leading to at least six possible degradation products, with the exception of ethametsulfuron and tribenuron, which gave five metabolites. The concentration curves of the parent herbicides and their metabolites (Fig. 3) indicate that metabolites 2 and 4 of chlorsulfuron, metsulfuron, triasulfuron and CGA 152'005 appear with a delay of 1–3 h with respect to other metabolites, suggesting that they are secondary by-products of sulfonylurea hydrolysis. The same pattern was observed for the metabolite 3 of ethametsulfuron and metabolite 2 of tribenuron. Chlorimuron and bensulfuron, sulfonylureas characterized by a diazinic

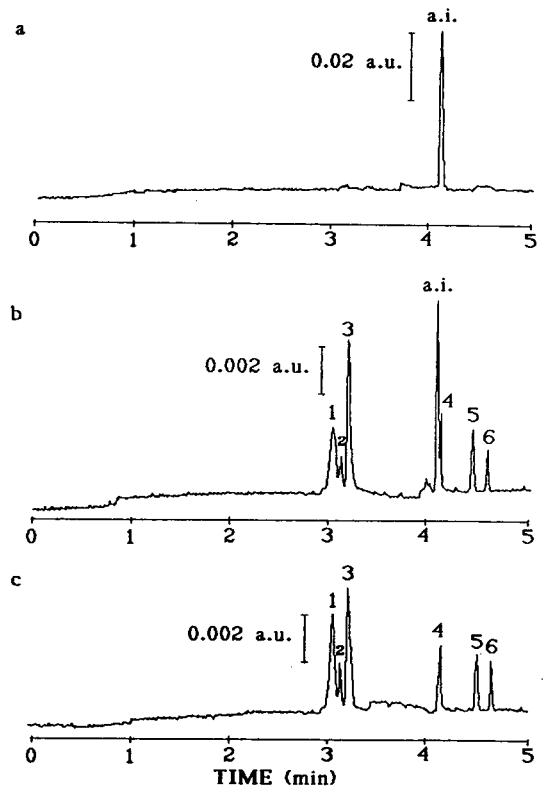

Fig. 2. Electropherograms of chlorsulfuron samples in aqueous solution. Samples in (a), (b) and (c) correspond to sampling times of 0, 2 and 10 h after incubation, respectively. The parent herbicide is indicated by a.i. and metabolites are arbitrarily numbered according to their increasing retention times. Separation conditions as reported under Experimental.

heterocycle and *o*-benzene substitution, degraded in water to form four metabolites (Fig. 3). The non-*o*-benzene-substituted sulfonylurea rimsulfuron gave only one metabolite (Fig. 3).

Hydrolysis of all the sulfonylureas followed first-order kinetics, as regression analysis of the natural logarithm of herbicide remaining yielded significant linear determination coefficients for all nine sulfonylureas (Table 2). Analysis of variance showed differences in the degradation rate constants (k) among the sulfonylureas. Tribenuron, the sulfonylurea most susceptible to hydrolysis, had a half-life of 0.37 h, whereas those for triasulfuron, ethametsulfuron and chlorimuron, the least susceptible, were >2 h. The seven times longer half-life of chlorimuron than tribenuron confirms the large differences in degradation rate within this class of herbicides, as observed in other work [1,12]. It is also clear that many sulfonylureas are extremely labile in aqueous solution and most of them undergo various transformation reactions to generate a complex mixture of decomposition products.

This study revealed that sulfonylureas and their degradation products may be simultaneously detected and separated by CE. The ease and efficiency of the method make it suitable for the analysis of large numbers of water samples for sulfonylurea metabolites and parent herbicides. However, the nature of the degradation products was not investigated in this work. Further studies are necessary to identify their structures and to

Table 1
Retention times (min ±S.D., $n = 16$) of sulfonylureas and their metabolites

Sulfonylurea	Parent herbicide	Metabolite No.					
		1	2	3	4	5	6
Chlorsulfuron	4.26 ± 0.11	3.19 ± 0.09	3.32 ± 0.08	3.55 ± 0.09	4.33 ± 0.10	4.62 ± 0.12	4.78 ± 0.11
Metsulfuron	4.45 ± 0.07	3.36 ± 0.06	3.50 ± 0.04	3.54 ± 0.06	4.50 ± 0.08	4.64 ± 0.09	4.92 ± 0.05
Triasulfuron	4.51 ± 0.09	3.36 ± 0.06	3.51 ± 0.03	3.61 ± 0.04	4.73 ± 0.06	5.01 ± 0.08	5.37 ± 0.06
CGA 512'005	4.57 ± 0.10	3.38 ± 0.06	3.55 ± 0.07	4.14 ± 0.09	4.67 ± 0.08	4.77 ± 0.11	4.95 ± 0.09
Ethametsulfuron	4.62 ± 0.05	3.26 ± 0.08	3.62 ± 0.03	4.70 ± 0.05	4.93 ± 0.06	5.20 ± 0.05	–
Tribenuron	4.31 ± 0.03	3.19 ± 0.02	3.39 ± 0.04	3.49 ± 0.05	4.68 ± 0.03	4.81 ± 0.04	–
Bensulfuron	4.39 ± 0.08	3.47 ± 0.09	3.63 ± 0.07	4.56 ± 0.08	4.82 ± 0.09	–	–
Chlorimuron	4.96 ± 0.05	3.99 ± 0.08	4.31 ± 0.02	5.53 ± 0.04	5.87 ± 0.03	–	–
Rimsulfuron	4.59 ± 0.03	6.10 ± 0.07	–	–	–	–	–

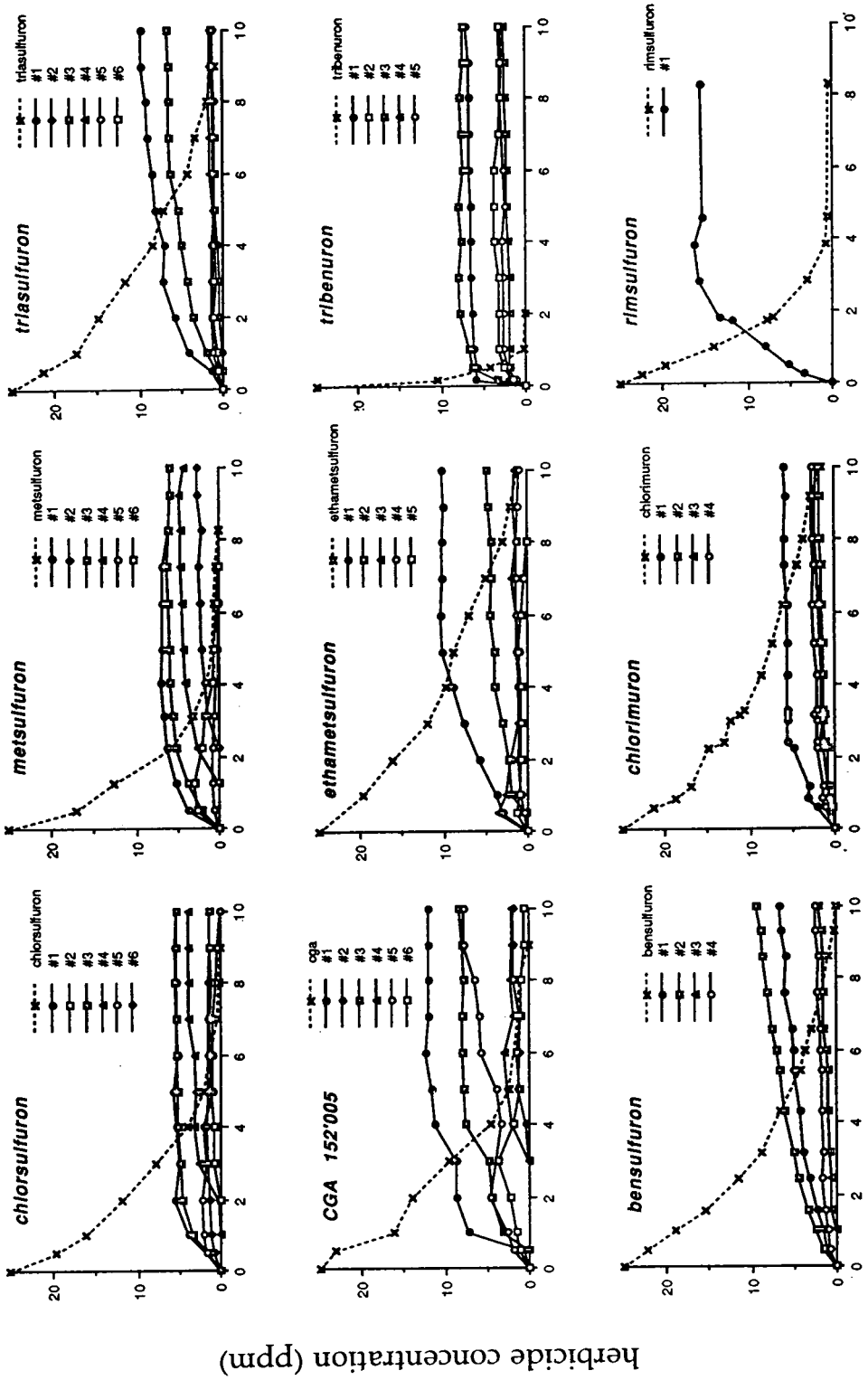

Fig. 3. Hydrolysis of the nine sulfonylureas and formation of degradation products.

Table 2
First-order rate constants (k), half-lives ($t_{1/2}$) and determination coefficients (r^2) for the sulfonylureas at pH 4 and 55°C in aqueous solution

Sulfonylurea	Rate constant[a], k	$t_{1/2}$ (h)	r^2 value[b]
Tribenuron	1.855 (a)	0.37	0.996
Rimsulfuron	0.602 (b)	1.15	0.962
Metsulfuron	0.540 (c)	1.28	0.988
CGA 152'005	0.498 (c)	1.39	0.991
Chlorsulfuron	0.463 (c)	1.50	0.993
Bensulfuron	0.356 (d)	1.95	0.975
Triasulfuron	0.299 (d)	2.32	0.987
Ethametsulfuron	0.275 (d)	2.52	0.984
Chlorimuron	0.259 (d)	2.68	0.988

[a] Means within the column followed by the same letter are not significantly different at $p \leq 0.05$ according to Fischer's protected LSD test.
[b] Linear determination coefficient describing the regression of the natural logarithm of herbicide remaining in aqueous solution over time. All values of r^2 are significant at $P \leq 0.01$.

define more accurately the degradation scheme of each sulfonylurea.

Acknowledgements

This work was financed by the European Economic Community within the project "Application and Evaluation of a New Method for the Monitoring of Pesticide Pollution in Water", contract No. AIR3-ST92-002.

References

[1] E.M. Beyer, M.J. Duffy, J.V. Hay and D.D. Schlueter, in P.C. Kearney and D.D. Kaufmann (Editors), *Herbicides: Chemistry, Degradation and Mode of Action*, Vol. 3, Marcel Dekker, New York, 1988, Ch. 3, p. 117.
[2] D.R. Fredrickson and P.J. Shea, *Weed Sci.*, 34 (1988) 328.
[3] M.M. Joshi, H.M. Brown and J.A. Romesser, *Weed Sci.*, 33 (1985) 888.
[4] A.E. Smith and A.I. Hsiao, *Weed Sci.*, 33 (1985) 555.
[5] J. Sabadie, *Weed Res.*, 30 (1990) 413.
[6] J. Sabadie and J. Bastide, *Weed Res.*, 30 (1990) 1.
[7] J. Harvey, J.J. Dulka and J.J. Anderson, *J. Agric. Food Chem.*, 33 (1985) 590.
[8] L.M. Shalaby, F.Q. Bramble and P.W. Lee, *J. Agric. Food Chem.*, 40 (1992) 513.
[9] G. Dinelli, A. Bonetti, P. Catizone and G.C. Galletti, *J. Chromatogr. B*, 656 (1994) 275.
[10] G.C. Galletti, A. Bonetti and G. Dinelli, *J. Chromatogr.*, in press.
[11] S. Fujiwara, S. Iwase and S. Honda, *J. Chromatogr.*, 447 (1988) 133.
[12] G. Dinelli, A. Vicari, A. Bonetti and P. Catizone, in A. Del Re, E. Capri, S.P. Evans, P. Natali and M. Trevisan (Editors), *Proceedings of the IX Symposium on Pesticide Chemistry, Piacenza, October 1993*, Biagini, Lucca, 1993, p. 411.

ELSEVIER

Journal of Chromatography A, 700 (1995) 201–207

JOURNAL OF CHROMATOGRAPHY A

Detection and quantitation of sulfonylurea herbicides in soil at the ppb level by capillary electrophoresis

Giovanni Dinelli[a,*], Alberto Vicari[a], Vincenzo Brandolini[b]

[a]*Dipartimento di Agronomia, Università di Bologna, Via F. Re 6/8, I-40126 Bologna, Italy*

[b]*Dipartimento di Scienze Farmaceutiche, Università di Ferrara, Via Fossato di Mortara 17/19, I-44100 Ferrara, Italy*

Abstract

A multi-residue analytical method based on solid-phase extraction enrichment combined with capillary electrophoresis (CE), using micellar electrokinetic capillary chromatography, was developed to isolate, recover and quantitate three sulfonylurea herbicides (chlorsulfuron, chlorimuron and metsulfuron) from soil samples. Optimization for CE separation was achieved using an overlapping resolution map scheme. The recovery of each herbicide was >80% and the limit of detection was 10 ppb. The capability of CE in providing quantitative analysis of sulfonylureas in soil samples at the ppb level has been demonstrated.

1. Introduction

Sulfonylurea herbicides have extremely high biochemical activity, thus enabling extremely small dosages in field crops (2–60 g/ha). However, chlorsulfuron, metsulfuron and chlorimuron have the potential to persist in soil in quantities sufficient to injure susceptible crops [1–3]. Therefore, the monitoring of their residues in soil is essential to study the persistence and the environmental behaviour.

Analytical methods for the determination of sulfonylurea residues in soil use high-performance liquid chromatography (HPLC) [4,5], gas chromatography (GC) [6–8], immunoassay [9] and bioassay [10]. In spite of the impressive versatility of capillary electrophoresis (CE) [11], the low injectable volume (usually 1–60 nl) and the poor elution power of CE with respect to other chromatography techniques restricted the use of this analytical tool in environmental analysis of agrochemicals in soil at the ppb level. Recently, CE, using micellar electrokinetic capillary chromatography (MECC), has shown good potentiality to detect herbicides in water [12,13], but had never been applied to herbicide detection in soil samples. To apply CE in analyses of herbicides in soil, particular attention has to be devoted to the optimization of separation, in order to achieve the best selectivity and resolution in such a complex matrix where many potential compounds could interfere. Different approaches have been proposed for the tuning of CE separations, i.e. the Plackett–Burman statistical design implemented by Vindevogel and Sandra [14], a theoretical approach [15], a computer simulation [16] and the overlapping resolution mapping (ORM) procedure [17].

The objectives of this study were (a) to optimize CE separation using a three-dimensional ORM scheme for the "tuning" of three interactive components [concentrations of sodium

* Corresponding author.

0021-9673/95/$09.50
SSDI 0021-9673(95)00099-2

dodecyl sulphate (SDS), methanol and isopropanol] of the electrolyte buffer and (b) to evaluate the potential applicability of CE, using MECC, combined with solid-phase extraction (SPE) enrichment for the simultaneous determination of three sulfonylureas in soil.

2. Experimental

2.1. Reagents

Reagents for SPE and CE analysis were supplied by Sigma (St. Louis, MO, USA). All solvents used were pesticide-free grade. The sample concentration column for SPE consisted in a Bakerbond (Phillipsburg, NJ, USA) C_{18} (1 g, 40-μm silica particles). Commercial formulations of chlorsulfuron [1-(2-chlorophenylsulfonyl)-3,4(methoxy-6-methyl-1,3,5-triazin-2-yl)-urea], metsulfuron [2-(4-methoxy-6-methyl-1,3,5-triazin-2-ylcarbamoylsulfamoyl) benzoic acid] and chlorimuron [2-(4-chloro-6-methoxypyrimidin-2-ylcarbamoylsulfamoyl) benzoic acid] were used. The parent herbicides were extracted from the commercial products with freshly redistilled dichloromethane in Soxhlet for 3 h. After dehydration with anhydrous sodium sulphate, dichloromethane was distilled off in rotary evaporator. The residual sulfonylureas were subjected to nuclear magnetic resonance, infrared and mass spectral analyses to confirm their identity and used for subsequent experiments without further purification, as reported by Galletti et al. [18].

2.2. ORM scheme

A three-dimensional ORM scheme to optimize the concentration of surfactant (SDS) and organic modifiers (methanol and isopropanol) was employed according to Li [17]. Briefly, eleven pre-planned experiments were carried out at strategic positions on a cubic diagram. The eleven electrolyte buffers used are reported in Table 1. Maximum and minimum concentrations of SDS tested were 80 and 30 mM, respectively, while those of methanol and isopropanol were 40–0% and 20–0% (v/v), respectively. From the experimental results of retention times, the resolution (R_s) between each pair of adjacent peaks of the electropherogram was calculated according to the following equation: $R_s = [2(t_{R1} - t_{R2})/w_2 + w_1]p$, where t_{R1} and t_{R2} are the retention times of two adjacent peaks, w_1 and w_2 are the widths of the two pairs of peaks and p is the value of penalty. In order to avoid unacceptable retention times (too short or too long), the penalty value (p) was introduced in the resolution equation. The penalty value was set at

Table 1
Pre-planned experiment conditions carried out to obtain the ORM scheme

Experiment	SDS (x_1, mM)	Methanol (x_2, %)	Isopropanol (x_3, %)	Percentage (x_1, x_2, x_3)
1	30	0	0	0, 0, 0
2	80	0	0	1, 0, 0
3	30	40	0	0, 1, 0
4	30	0	20	0, 0, 1
5	80	40	0	1, 1, 0
6	80	0	20	1, 0, 1
7	30	40	20	0, 1, 1
8	80	40	20	1, 1, 1
9	55	0	0	0.5, 0, 0
10	30	20	0	0, 0.5, 0
11	30	0	10	0, 0, 0.5

The eleven experiments were performed with 30 mM borate buffer at pH 7.0.

0.25 for retention times of metsulfuron (first peak eluted) in the range 0–5 min and 25–30 min, at 0.75 for retention times in the range 10–15 min and 20–25 min, at 1 for retention times ranging from 15 to 20 min. The calculated R_s values were then fitted in the following polynomial equation [17]:

$$R_s = a_0 + a_1x_1 + a_2x_2 + a_3x_3 + a_{11}x_1^2 + a_{22}x_2^2 + a_{33}x_3^2 + a_{12}x_1x_2 + a_{13}x_1x_3 + a_{23}x_2x_3 + a_{123}x_1x_2x_3$$

where a_i values are coefficients and x_1, x_2 and x_3 correspond to the percentage fractions at the respective axes of concentration of SDS, methanol and isopropanol in the electrolyte buffer.

2.3. Preparation of standards

A stock solution at the concentration of 100 ppm was prepared dissolving 10 mg each of the three sulfonylureas in 100 ml of methanol–water (50:50). Appropriate dilutions of this stock solution were made in methanol–water (50:50) to obtain final concentrations of 0.63, 1.25, 2.5, 3.5, 5 and 10 ppm.

2.4. Soil sample fortification and extraction

A sandy loam soil obtained from Cadriano, near Bologna, Italy, was used to prepare the soil samples for this study. The average soil composition was 27% clay, 15% silt, 58% sand, 1.3% organic matter and pH of 6.5. A stock solution containing 1 ppm of the three sulfonylureas was obtained dissolving 10 mg of each compound in 10 l of bidistilled water. From this stock solution, appropriate quantities were added to 500 g (oven-dry basis) of soil, screened through a 3-mm sieve, to give a final herbicide concentration of 10, 20 or 50 ppb. After the fortification, soil samples were mixed for 5 min in a blender and frozen at −12°C.

SPE was performed in duplicate as described by Dinelli et al. [13]. Briefly, 200 ml of sodium hydrogencarbonate solution (0.1 *M*, pH 7.8) was added to 100 g of soil (50 and 20 ppb fortifications) and to 200 g of soil for the 10 ppb level. The suspension was shaken for 1 h. The slurry was centrifuged at 13 100 *g* for 5 min. The extraction procedure was repeated twice and the liquid extracts were combined. The extracts were brought to pH 2.5 with 0.1 *M* HCl and passed, under vacuum, through a C_{18} solid-phase column. Dry residues of the 50 and 20 ppb samples were reconstituted with 1 ml of methanol–water (50:50, v/v) solution, thus obtaining an enrichment factor of 100. Dry residues of the 10 ppb samples were reconstituted with 1.5 ml of the methanol–water solution, thus obtaining an enrichment factor of 150.

2.5. CE analyses

Analyses of soil extracts were performed using the MECC technique, with the CE apparatus P/ACE System from Beckman (Palo Alto, CA, USA). Separations were made with a fused-silica capillary of 50 cm (from injection point to detector) × 75 μm I.D., thermostated at a constant temperature of 35°C. The applied voltage was 25 kV, with an injection pressure of $3.44 \cdot 10^3$ Pa for 10 s, corresponding to an injection volume of 60 nl. The electrolyte buffer, chosen according to the ORM optimization described in the Results and discussion section, was 30 m*M* sodium borate, 80 m*M* SDS, 14% methanol and 20% isopropanol (v/v), pH 7.0. The detection wavelength was set at 214 nm. The separation efficiency was measured by the number of theoretical plates (N) according to: $N = 5.54(t_R/w)^2$, where t_R is the retention time of a compound and w is the peak width at half-peak height [19]. Peak area was used for calibration curve and residue quantification of chlorsulfuron, metsulfuron and chlorimuron.

3. Results and discussion

3.1. ORM optimization

The values of R_s for the eleven pre-planned experiments (Table 1) were calculated and fitted in the polynomial equation, according to Li [17]. Resolution values for all possible combinations

of x_1 (SDS), x_2 (methanol) and x_3 (isopropanol) were calculated and represented on a three-dimensional resolution diagram, using a basic computer program. The region defining the optimum conditions for the separation of the three sulfonylureas was identified with $x_1 = 100\%$, corresponding to a concentration of SDS in the electrolyte buffer of 80 m*M*. The final overlapped resolution diagram is presented in Fig. 1. Two different zones with high response ($R_s > 1.5$) can be seen. The first partial optimum is placed at low methanol content, whereas the second is placed at low isopropanol content. It is important to note that buffers of differing compositions were able to separate the three sulfonylureas with a $R_s > 1.5$. Arbitrarily, the electrolyte buffer marked by "A" in the optimum zone at low methanol content (Fig. 1) was chosen for the subsequent analysis of soil samples, as described in the Experimental section. An electropherogram obtained with this electrolyte buffer is shown in Fig. 2a. A complete separation of the sulfonylurea peaks was achieved, with an observed R_s of 1.99 against a predicted R_s of 1.73, calculated from the polynomial equation. The column mean efficiency in the separation of the three sulfonylureas was 152 000 theoretical plates, while the asymmetry was 0.89, 0.90 and 0.78 for metsulfuron, chlorimuron and chlorsulfuron peaks, respectively. The composition of the electrolyte buffer marked by "B" in Fig. 1 was chosen from a region expected to produce poor separation. The results (Fig. 2b) confirmed the validity of the ORM scheme, as suggested by the low value of the observed R_s (0.45), against a predicted value of 0.37.

3.2. Calibration curves and sulfonylurea separation

The calibration curves demonstrate the linear response of the method with the injection of standard with concentration in the 0.6–10 ppm range. The chlorsulfuron regression equation is $y = -0.013 + 0.103x$ ($r^2 = 0.997$), that for metsulfuron $y = -0.013 + 0.171x$ ($r^2 = 0.986$) and that for chlorimuron $y = 0.008 + 0.065x$ ($r^2 = 0.993$), where y is the peak area and x is the herbicide concentration in ppm. Detection limits were calculated for a signal-to-noise ratio of 3 and were 0.63 ppm for chlorimuron and 0.5 ppm for metsulfuron and chlorsulfuron, corresponding to an injection on-column of about 10 pg of each sulfonylurea. The values of intra-day and inter-day retention times and of their relative standard deviations (R.S.D.s) for the runs made 10 times on the same day in 10 different

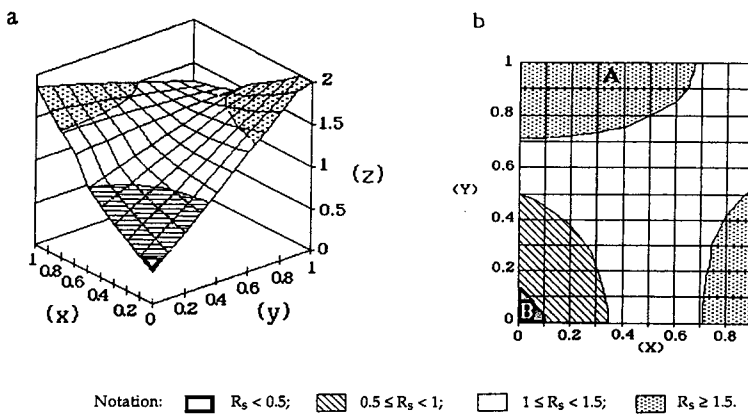

Fig. 1. Final overlapped diagrams for the separation of sulfonylureas with 80 m*M* SDS. (a) Three-dimensional view; the x-axis is the percentage proportion of methanol (1 = 40% methanol) in the electrolyte buffer; the y-axis is the percentage proportion of isopropanol (1 = 20% isopropanol) in the electrolyte buffer; the z-axis represents the resolution (R_s). (b) Two-dimensional projection; axes as in (a).

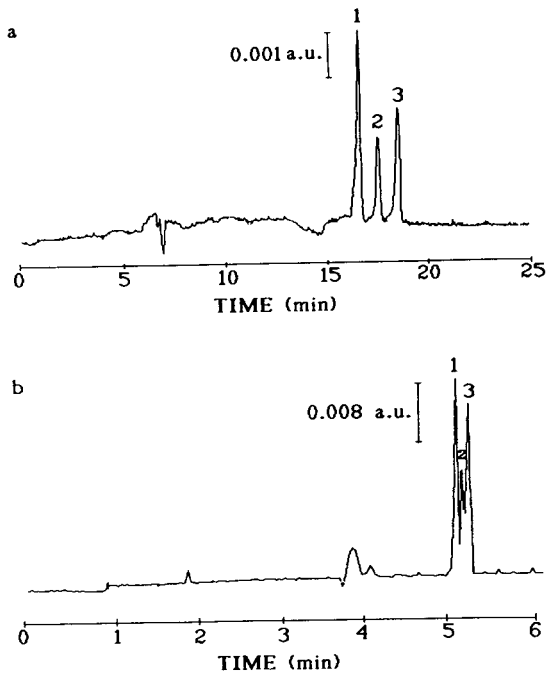

Fig. 2. Separation of sulfonylureas by CE. (a) Conditions corresponding to point "A" in Fig. 1b: 30 m*M* borate buffer pH 7; 80 m*M* SDS, 14% methanol, 20% isopropanol. Separation voltage 25 kV, pressure injection for 10 s, capillary 50 cm × 75 μm I.D., thermostated at 35°C, detection wavelenght 214 nm. (b) Conditions corresponding to point "B" in Fig. 1b: 30 m*M* borate buffer pH 7, 80 m*M* SDS, 0% methanol, 0% isopropanol. Separation parameters as in (a). Peaks: 1 = metsulfuron; 2 = chlorimuron; 3 = chlorsulfuron.

days (Table 2) indicate good repeatability. The area mean values of the peaks corresponding to injections of 3.5 ppm sulfonylurea solution and their respective R.S.D.s (Table 3) suggest good quantitative accuracy for CE.

3.3. Sulfonylurea recovery and quantitation

The electropherogram presented in Fig. 3a provides a typical profile of the soil without herbicides and shows no interferences at the retention times for the three compounds of interest. Fig. 3b displays the electropherogram of a soil sample spiked at 20 ppb with the three sulfonylureas, after SPE and a 100-fold enrichment. The identification of the sulfonylurea peaks was based on the retention time. To confirm the identification, single subsequent fortifications of the soil extract were made with each sulfonylurea at 5 ppm and reanalyzed (data not shown). The electropherogram of the soil extract after the three further fortifications corroborates the identification of peaks 1, 2 and 3 as metsulfuron, chlorimuron and chlorsulfuron, respectively (Fig. 3c). It is interesting to note that there was a surprisingly low interference caused by other constituents present in the soil samples. In fact, the peak area of the three sulfonylureas represent about the 30% of the total area of the electropherogram (Fig. 3b). In a previous research [18], samples of the same soil containing four sulfonylureas at 10 ppb were extracted by SPE and analyzed by RP-HPLC. The percent area of the sulfonylureas was about the 5% of the

Table 2
Intra-day and inter-day retention time (t_R) repeatibility (±S.D.) and R.S.D.

	Intra-day		Inter-day	
	t_R (min)	R.S.D. (%)	t_R (min)	R.S.D. (%)
Metsulfuron	16.7 ± 0.3	1.9	16.8 ± 0.4	2.5
Chlorimuron	17.5 ± 0.4	2.4	17.8 ± 0.7	4.0
Chlorsulfuron	18.2 ± 0.4	2.1	18.5 ± 0.7	3.8

Average of 10 injections of 3.5 ppm sulfonylurea solutions in the same day (intra-day), in 10 different days over one month.

Table 3
Intra-day and inter-day peak area (arbitrary units, a.u.) repeatibility (±S.D.) and R.S.D.

	Intra-day		Inter-day	
	Area (a.u.)	R.S.D. (%)	Area (a.u.)	R.S.D. (%)
Metsulfuron	0.70 ± 0.01	1.6	0.71 ± 0.04	5.0
Chlorimuron	0.19 ± 0.00	2.4	0.19 ± 0.01	6.8
Chlorsulfuron	0.37 ± 0.02	4.9	0.37 ± 0.03	7.3

Average of 10 injections of 3.5 ppm sulfonylurea solutions in the same day (intra-day), in 10 different days over one month.

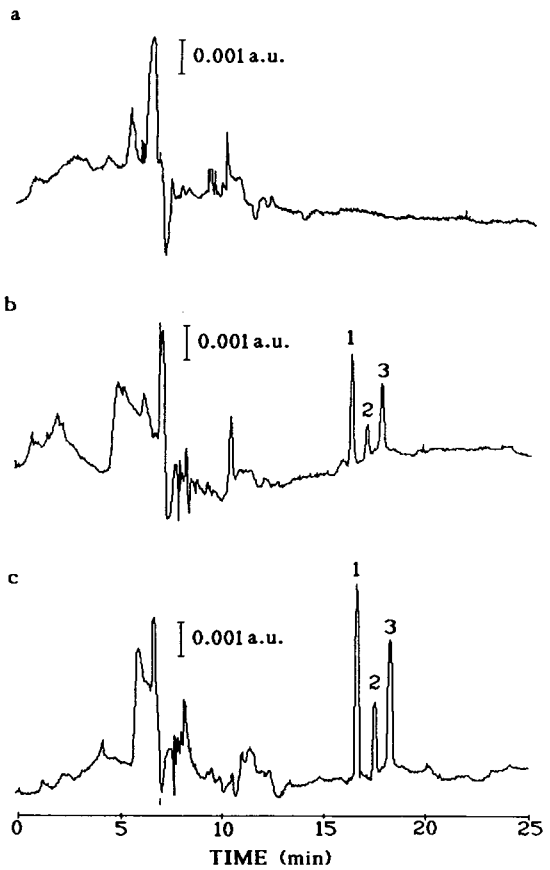

Fig. 3. Electropherograms of (a) soil sample extract without fortification; (b) soil sample extract fortified at 20 ppb; (c) soil sample extract fortified at 20 ppb with an additional fortification of each sulfonylurea at 5 ppm. Separation conditions as in Fig. 1a.

total area of the chromatogram. This suggests an on column exclusion of some soil matrix interferences during the CE separation, as shown also by Dinelli et al. [20].

The recoveries of the sulfonylureas after duplicate SPE are reported in Table 4. The mean overall recovery for the three herbicides was 95.4 ± 16.1% and the recovery was not affected by the sample concentration in the range from 10 to 50 ppb. These results confirm that SPE does not alter physicochemical traits of the three sulfonylureas and is a valid method for multiresidue analysis of sulfonylureas in CE.

Table 4
Sulfonylurea recoveries (±S.D.) after duplicate SPE from soil samples at different herbicide concentrations

	Recovery (%)		
	10 ppb	20 ppb	50 ppb
Metsulfuron	101.9 ± 16.1	91.4 ± 1.1	91.4 ± 5.7
Chlorimuron	83.0 ± 0.6	81.9 ± 3.5	82.9 ± 2.6
Chlorsulfuron	130.0 ± 6.0	104.9 ± 8.7	91.7 ± 7.9

4. Conclusions

The reported data show that CE is suitable for multiresidue detection and quantitation of sulfonylureas at the ppb level in soil. The major drawback of CE is the low system loadability, which is in the range of nanoliters. However, this drawback has been overcome by an appropriate SPE sample enrichment and an effective tuning of the separation conditions, using an ORM scheme. For soil samples with concentrations of sulfonylureas less than 10 ppb, the concentration became a limiting factor. At these concentrations, other chromatographic techniques, such as HPLC, are easier and more accurate than CE.

Acknowledgement

This work was financed by the European Economic Community within the project "Application and Evaluation of a New Method for the Monitoring of Pesticide Pollution in Water", contract No. AIR3-ST92-002.

References

[1] A. Vicari, P. Catizone and R.L. Zimdahl, *Weed Res.*, 34 (1994) 147.
[2] M.A. Peterson and W.E. Arnold, *Weed Sci.*, 34 (1985) 131.
[3] E.M. Beyer, M.J. Duffy, J.V. Hay and D.D. Schlueter, in P.C. Kearney and D.D. Kaufmann (Editors), *Herbicides: Chemistry, Degradation and Mode of Action*, Vol. 3, Marcel Dekker, New York, 1988, Ch. 3, p. 117.

[4] E.W. Zahnow, *J. Agric. Food Chem.*, 30 (1982) 854.
[5] E.W. Zahnow, *J. Agric. Food Chem.*, 33 (1985) 479.
[6] J. Ahmad, *J. Agric. Food Chem.*, 35 (1987) 745.
[7] P. Klaffenbach, P.T. Holland and D.R. Lauren, *J. Agric. Food Chem.*, 41 (1993) 388.
[8] P. Klaffenbach and P.T. Holland, *J. Agric. Food Chem.*, 41 (1993) 396.
[9] M.M. Kelley, E.W. Zahnow, W.C. Petersen and S.T. Toy, *J. Agric. Food Chem.*, 33 (1985) 962.
[10] P. Gunther, A. Rahman and W. Pestemer, *Weed Res.*, 29 (1989) 141.
[11] W.G. Kuhr, *Anal. Chem.*, 62 (1990) 403R.
[12] G. Dinelli, A. Vicari and P. Catizone, *J. Agric. Food Chem.*, 41 (1993) 742.
[13] G. Dinelli, A. Bonetti, P. Catizone and G.C. Galletti, *J. Chromatogr. B*, 656 (1994) 275.
[14] J. Vindevogel and P. Sandra, *Anal. Chem.*, 63 (1991) 1530.
[15] J.P. Foley, *Anal. Chem.*, 62 (1990) 1302.
[16] A.P. Powell and M.J. Sepaniak, *J. Microcol. Sep.*, 2 (1990) 278.
[17] S.F.Y. Li, *Capillary Electrophoresis —Principles, Practice and Applications*, Elsevier, Amsterdam, 1992.
[18] G.C. Galletti, A. Bonetti and G. Dinelli, *J. Chromatogr. A*, (1994) in press.
[19] S. Fujiwara, S. Iwase and S. Honda, *J. Chromatogr.*, 447 (1988) 133.
[20] G. Dinelli, A. Vicari, A. Bonetti and P. Catizone, *J. Agric. Food Chem.*, 43 (1995) in press.

Author Index

PUBLICATION SCHEDULE FOR THE 1995 SUBSCRIPTION

Journal of Chromatography A and *Journal of Chromatography B: Biomedical Applications*

MONTH	1994	J	F	M	A	M[a]	J	
Journal of Chromatography A	Vols. 683–688	689/1 689/2 690/1 690/2	691/1 + 2 692/1 + 2 693/1 693/2	694/1 694/2 695/1 695/2	696/1 696/2 697/1 + 2 698/1 + 2	699/1 + 2 700/1 + 2 702/1 + 2 703/1 + 2	704/1 704/2 705/1 705/2	The publication schedule for further issues will be published later.
Bibliography Section				713/1			713/2	
Journal of Chromatography B: Biomedical Applications		663/1 663/2	664/1 664/2	665/1 665/2	666/1 666/2	667/1 667/2	668/1 668/2	

[a] Vol. 701 (Cumulative Indexes Vols. 652–700) expected in October.

INFORMATION FOR AUTHORS

(Detailed *Instructions to Authors* were published in *J. Chromatogr. A*, Vol. 657, pp. 463–469. A free reprint can be obtained by application to the publisher, Elsevier Science B.V., P.O. Box 330, 1000 AH Amsterdam, Netherlands.)

Types of Contributions. The following types of papers are published: Regular research papers (full-length papers), Review articles, Short Communications and Discussions. Short Communications are usually descriptions of short investigations, or they can report minor technical improvements of previously published procedures; they reflect the same quality of research as full-length papers, but should preferably not exceed five printed pages. Discussions (one or two pages) should explain, amplify, correct or otherwise comment substantively upon an article recently published in the journal. For Review articles, see inside front cover under Submission of Papers.

Submission. Every paper must be accompanied by a letter from the senior author, stating that he/she is submitting the paper for publication in the *Journal of Chromatography A* or *B*.

Manuscripts. Manuscripts should be typed in **double spacing** on consecutively numbered pages of uniform size. The manuscript should be preceded by a sheet of manuscript paper carrying the title of the paper and the name and full postal address of the person to whom the proofs are to be sent. As a rule, papers should be divided into sections, headed by a caption (*e.g.*, Abstract, Introduction, Experimental, Results, Discussion, etc.). All illustrations, photographs, tables, etc., should be on separate sheets.

Abstract. All articles should have an abstract of 50–100 words which clearly and briefly indicates what is new, different and significant. No references should be given.

Introduction. Every paper must have a concise introduction mentioning what has been done before on the topic described, and stating clearly what is new in the paper now submitted.

Experimental conditions should preferably be given on a *separate* sheet, headed "Conditions". These conditions will, if appropriate, be printed in a block, directly following the heading "Experimental".

Illustrations. The figures should be submitted in a form suitable for reproduction, drawn in Indian ink on drawing or tracing paper. Each illustration should have a caption, all the *captions* being typed (with double spacing) together on a *separate sheet.* If structures are given in the text, the original drawings should be provided. Coloured illustrations are reproduced at the author's expense, the cost being determined by the number of pages and by the number of colours needed. The written permission of the author and publisher must be obtained for the use of any figure already published. Its source must be indicated in the legend.

References. References should be numbered in the order in which they are cited in the text, and listed in numerical sequence on a separate sheet at the end of the article. Please check a recent issue for the layout of the reference list. Abbreviations for the titles of journals should follow the system used by *Chemical Abstracts.* Articles not yet published should be given as "in press" (journal should be specified), "submitted for publication" (journal should be specified), "in preparation" or "personal communication".

Vols. 1–651 of the *Journal of Chromatography*; *Journal of Chromatography, Biomedical Applications* and *Journal of Chromatography, Symposium Volumes* should be cited as *J. Chromatogr.* From Vol. 652 on, *Journal of Chromatography A* (incl. Symposium Volumes) should be cited as *J. Chromatogr. A* and *Journal of Chromatography B: Biomedical Applications* as *J. Chromatogr. B.*

Dispatch. Before sending the manuscript to the Editor please check that the envelope contains four copies of the paper complete with references, captions and figures. One of the sets of figures must be the originals suitable for direct reproduction. Please also ensure that permission to publish has been obtained from your institute.

Proofs. One set of proofs will be sent to the author to be carefully checked for printer's errors. Corrections must be restricted to instances in which the proof is at variance with the manuscript.

Reprints. Fifty reprints will be supplied free of charge. Additional reprints can be ordered by the authors. An order form containing price quotations will be sent to the authors together with the proofs of their article.

Chromatography in the Petroleum Industry

Edited by **E.R. Adlard**

Journal of Chromatography Library, Volume 56

Petroleum mixtures consist primarily of relatively unreactive complex hydrocarbons covering a wide boiling range. Such mixtures are difficult to separate by most analytical techniques. Therefore, the petroleum industry has for many years played a leading role in the development of chromatographic methods of analysis. Since the last book specifically concerned with chromatographic analysis of petroleum appeared 15 years ago, numerous advances have been made including developments in liquid and supercritical fluid chromatography, the advent of silica capillary columns with bonded stationary phases and the commercial availability of new selective detectors.

The current book contains chapters written by experts concerning the analysis of mixtures ranging from low boiling gases to waxes and crude oils.

Although the volume is specifically aimed at the petroleum analyst, there is much information of general interest which should be of benefit to a very wide readership.

Contents:

©1995 452 pages Hardbound
Price: Dfl. 435.00 (US$ 255.75)
ISBN 0-444-89776-3

ELSEVIER
An imprint of Elsevier Science

ORDER INFORMATION

ELSEVIER SCIENCE B.V.
P.O. Box 330
1000 AH Amsterdam
The Netherlands
Fax: +31 (20) 485 2845

For USA and Canada:
P.O. Box 945, New York
NY 10159-0945
Fax: +1 (212) 633 3680

US$ prices are valid only for the USA & Canada and are subject to exchange rate fluctuations; in all other countries the Dutch guilder price (Dfl.) is definitive. Customers in the European Union should add the appropriate VAT rate applicable in their country to the price(s). Books are sent postfree if prepaid.

0021-9673(19950512)700:1:2;1-F